189(2), 2022

COMBUSTION ENGINES

EMITUJE TYLKO WODĘ. OCZYSZCZA POWIETRZE

REWOLUCJA

Toyota Mirai to technologia jutra dostępna już dziś.
To pierwszy samochód elektryczny na wodór o nadwoziu typu sedan.

MIRAI

Zużycie paliwa w Toyocie Mirai FCEV i emisja CO_2: metoda badawcza WLTP 182 KM e-CVT średnio [kg H_2/100 km] 0,84, emisja CO_2 średnio [g/km] 0. Zużycie paliwa i emisja spalin CO_2 w konkretnym pojeździe w warunkach drogowych może różnić się od podanych wyników pomiarów. Na zużycie paliwa i emisję CO_2 wpływa sposób prowadzenia pojazdu oraz inne czynniki (takie jak warunki drogowe, natężenie ruchu, stan pojazdu, ciśnienie w oponach, zainstalowane wyposażenie, obciążenie, liczba pasażerów itp.). Informacje o działaniach dotyczących odzysku i recyklingu samochodów wycofanych z eksploatacji: www.toyota.pl

COMBUSTION ENGINES

A Scientific Magazine

2022, 189(2)

Year LXI

PL ISSN 2300-9896
PL eISSN 2658-1442

Publisher:

Polish Scientific Society of Combustion Engines
60-965 Poznan, pl. M. Skłodowskiej-Curie 5, Poland
tel.: +48 61 6475966, fax: +48 61 6652204
E-mail: sekretariat@ptnss.pl
WebSite: http://www.ptnss.pl
Papers available on-line: http://combustion-engines.eu

Contents

Publisher:
Polish Scientific Society of Combustion Engines
60-965 Poznan, pl. M. Sklodowskiej-Curie 5, Poland
tel.: +48 61 6475966, fax: +48 61 6652204
E-mail: sekretariat@ptnss.pl
WebSite: http://www.ptnss.pl

Subscriptions
Send subscription requests to the Publisher's address.
Cost of a single issue PLN 40.

Preparation for print
ARS NOVA Publishing House
60-782 Poznan, ul. Grunwaldzka 17/10A

Circulation: 100 copies

Printing and binding

Zakład Poligraficzny Moś i Łuczak, sp. j.,
Poznań, ul. Piwna 1

The journal is registered and listed in the Polish and international database

BazTech
INDEX COPERNICUS INTERNATIONAL
Crossref
EBSCO
DOAJ DIRECTORY OF OPEN ACCESS JOURNALS
POL-index Polska Baza Cytowań
SHERPA/RoMEO
ROAD

Papers published in the
Combustion Engines
quarterly receive 70 points as stated by the Notification of the Minister of Science and Education dated 1 December 2021.

Declaration of the original version
The original version of the Combustion Engines journal is the printed version.

Cover
I – Toyota and Yamaha - hydrogen-fueled V8 engine *(www.yamaha-motor.eu)*;
background *(photo by Joonas-Kääriäinen from Pexels)*
IV – Kawasaki hydrogen powered Ninja H2 engine *(www.motorcycle.com)*

Article citation info:
CHOJNOWSKI, J. Safety in the use of car gas fuel installations. *Combustion Engines*. 2022, **189**(2), 3-9. https://doi.org/10.19206/CE-142172

Janusz CHOJNOWSKI

Combustion Engines
Polish Scientific Society of Combustion Engines

Safety in the use of car gas fuel installations

ARTICLE INFO

Received: 7 July 2021
Revised: 1 August 2021
Accepted: 12 September 2021
Available online: 17 September 2021

The safe use of gas fuel installations in vehicles is guaranteed by legal and technical aspects. These topics are included in this study. The regulations ensuring safety in the operation of the mentioned fuel systems serve as a solution for potentially hazardous situations. The components of propane-butane and CNG fueling systems are designed, manufactured and tested to maximize their safety of use. The regulations [6–8] define the guidelines for the arrangement and assembly method of the system components, and additionally, the assembly service itself may be performed only by an authorized workshop with granted permissions. Installations using gaseous fuels are safer than conventional fuels in the event of a collision or fire, as long as the user of the installation does not gross negligence in operation and maintenance. The article also discusses the context of the restriction in access to the car infrastructure for cars powered by gaseous fuels.

Key words: *safety, gas, fuel, LPG, CNG*

1. Introduction

The safety of use of vehicles with gas fuel supply installations is influenced by at least several factors: meticulously constructed homologation regulations [6, 7] which force constructions and manufacturers to apply solutions ensuring safe use and correct installation of the installation, as well as proper operation and maintenance, the details of which are regulated by applicable regulations [8]. The absence of tragic accidents related to the use of propane butane Liquified Petroleum Gas (LPG) and Compressed Natural Gas (CNG) as engine fuels indicates that the designed system for approving and controlling automotive gas installations is working properly. Provisions in the Regulations 67 and 110 of the United Nations Economic Commission for Europe (UNECE), according to which gas supply systems are approved, minimize the possibility of hazardous situations related to their use and minimize negative effects in emergency situations, such as a collision. A number of self-acting safety devices make the use of a gas fueled car safe and in this respect the same as with conventional fuels.

2. Installation components

A CNG and LPG supply installations are usually alternative fueling systems for spark ignition and compression ignition engines, closely cooperating with the original fuel supply system. Regardless of the type of primary power supply system used, the gas system must meet its level of original solutions, both in terms of technical advancement, as well as safety requirements and exhaust emissions [4]. Gas systems are divided into those installed in the cars at the factory, installed as an additional power supply system, somewhat "next to" the original factory system and single-fuel systems (for example city buses powered by CNG) [1, 3]. There are great structural similarities in the construction of LPG and CNG installations [1]. Different types of gas installations generally use the same set of basic components conceptually: filler, tanks, pipes and fittings, components in the engine compartment.

2.1. Gas fuel tanks

Gaseous fuel tanks as devices operating with overpressure are subject to the obligation of technical inspection, and their use in cars means that they are built on the basis of detailed requirements contained in the type-approval regulations by UNECE. The safety of the exploited tank is guaranteed by the supervision carried out from the design stage to the obligation of technical inspections [6, 7].

Automobile LPG tanks are made of steel compliant with the EN 10120 standard. They are unalloyed steels with a maximum carbon content of up to 0.2%. The materials used for LPG tanks can be successfully processed (also pressed). In the case of CNG, due to the higher operating pressure, the fuel is stored in steel cylinders manufactured by stamping from a block and hot-drawing, or composite cylinders with or without a braid. Compressed natural gas storage tanks undergo a complex test cycle, including [2, 6, 7]:

- strength of construction material,
- hydraulic pressure test,
- fire test,
- tank impact resistance test (composite),
- bullet resistance (composite).

The parent material of the tank is subjected to tensile and bending strength tests. It consists in taking samples of materials from places strictly defined in the regulations. Gas tanks must show certain behavior in a strictly defined manner [3, 6].

The tanks are also burst tested by hydraulic pressure. The pressure during the test must be suitably built up, and its changes must be recorded over time. In practice, the burst pressure of the tank has much higher limits than those imposed by the regulations by UNECE. The working pressure in the tank during normal operation does not exceed 2 MPa for LPG and in steel tanks 22 MPa, and in composite tanks 35 or even 70 MPa for CNG [3, 6]. The tank must be burst after an appropriate increase in its volume, as specified in the regulations (from 8 to 20% depending on the type of the tank). A very important regulatory requirement

is also the fact that when the tank ruptures, its fragmentation cannot occur (no fragments that could injure someone).

Each manufactured tank is subjected to a hydraulic pressure test. The test consists in filling the inside of the tank with liquid (usually water) and increasing its pressure to the value specified in the regulations. During its execution, the tank may not be permanently deformed or unsealed [2, 3, 6]. The purpose of the test is to check whether the tank with the mounted equipment will not burst as a result of the action of strictly defined fire conditions. The test is performed on a copy representing a given type of gas tank. During the test, the tank is equipped with full fittings. The tank is checked on the heat source located under the tank at a specific temperature. During the test, the temperature of the appropriate places in the mantle is measured [3, 6, 9].

The effects of the shock resistance test, consisting in dropping an empty tank at an appropriate angle to the level from a strictly defined height, are presented below in Fig. 1 [4].

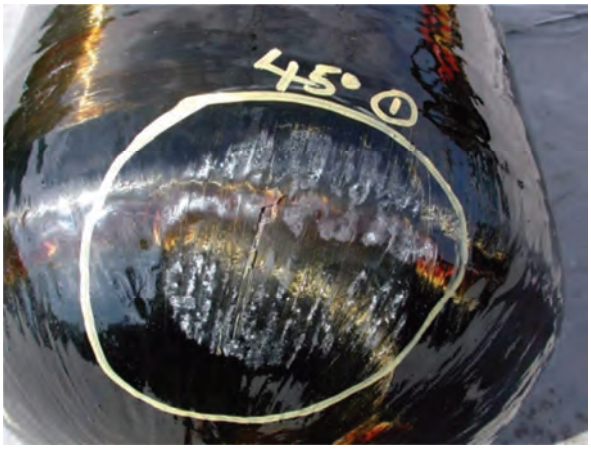

Fig. 1. The effects of the impact test of the CNG composite tank [12]

2.2. Method of mounting tanks

As the gas installation tank is its heaviest element, it is subjected to high inertia forces during a collision. During a rapid change of vehicle speed (e.g. during a collision with an obstacle), these forces try to tear the elements fastening the tank out of the place of assembly. During the collision there are very large deceleration, in the order of more than 20 g. The risk of inertia is enormous, therefore the appropriate mounting of the tanks is regulated by the provisions of UNECE. Gas tanks must be installed with the use of appropriate bolts of strength class 8.8. The fastening bolts are counted only for breaking, their shear is neglected due to the moment with which they are tightened and the resulting high friction occurring in the connection between the tank, its frame (Fig. 2) and the place of installation of the tank. If the tanks are fitted with fasteners welded to them, their welds must withstand the external forces of 30 g in all directions. The authors of the approval regulations assumed that the mounting of the tanks must withstand the load resulting from acceleration of 20 g (acting along the longitudinal axis of the car). In terms of transverse forces, the regulations say that the inertia forces resulting from acceleration of 8 g must be withstand by connecting the tank to the body. In the case of a 100 kg tank, this will correspond to a force of 8000 N acting on the tank as if its weight had increased to 800 kg. Gas tanks must not be installed in the front of the vehicle and in the engine working space. It is allowed to mount the tanks on the vehicle roof [4, 11, 12].

Fig. 2. A frame for a cylindrical LPG tank [9]

2.3. Armature securing the tank

„The 80% valve" is responsible for closing the gas supply during refueling at the fuel level corresponding to 80% of the geometric volume of the tank. This allows the space in the tank to be kept, giving the possibility of changing the LPG volume as a function of the ambient temperature. This valve is not used in CNG storage tanks. The operation of the 80% valve should be checked while refueling gaseous fuel. Overfilling the cylinder in the event of high ambient temperature may lead to activation of the safety valve [2, 6, 7].

From April 1, 2002, after introducing amendments to the regulations by the UNECE, a safety valve is installed in all valve assemblies (aka multivalve). The tank is thus protected against excessive pressure build-up. The gaseous fuel is vented through the ventilation ducts connected to the housing. The gas phase of the fuel always escapes through the valves (safety and fire valves). Liquefied gas escaping through the valves, rapidly expanding, could cause the duct diameters to shrink through frost. Approval tests of the valve verify the correctness of its operation during 10,000 opening cycles without changing the operating characteristics [3, 6, 7].

The increase in the temperature of the tank shell reduces the strength of the material from which it is made. With rapid temperature rise, the operation of the safety valve may not be sufficient to bring the pressure down to a safe level. The fire (fusible) valve opens when the tank shell reaches a certain temperature and drops it in order to avoid uncontrolled deformation or unsealing of the tank. The use of a fire valve is required if the safety valve has a capacity below 17.7 m³/min. This parameter results from and is closely related to the surface of the tank [4, 7, 12].

The overflow valve is activated if the gas flow is too intense (exceeding the engine demand of fuel), which may occur, for example, in the case of damage to the mechanical pressure line leading to the engine compartment. This valve is calibrated to operate when the differential pressure is approximately 90 kPa. The flowing gas "carries away" a mechanical element, most often a ball, which limits the gas flow to a level approximately equal to the engine's fuel requirement. In this way, the tank is protected against

a sudden outflow of gas, which poses the risk of its damage and increases the risk of explosion [2].

An indicator placed on the tank (for CNG cylinders, a similar task is performed by a mandatory pressure gauge), cooperating with a float inside the cylinder. Its indications are "approximate" and are very important in emergency situations for emergency services to assess the amount of fuel in the tank. Installed in accordance with the guidelines, the tank must be placed in such a way that its filling level can be easily read [2, 6, 7].

The operation of the working solenoid valve is determined by the operation of the engine. It closes when the engine RPM signal disappears. The necessity to use it results from the protection of gas flow in emergency situations, for example during a collision/road accident, when the engine is stopped without the will of the vehicle driver [2, 6, 7].

The gas supply from the tank to the engine compartment, when it is required to unseal the high pressure system (during service works), is closed on the cylinder with a manual valve.

The gas flow towards the gas tank only when refueling is provided by a non-return valve (Fig. 3). Its construction uses a steel ball supported by a spring. These elements are located in the refueling channel. The pressure from the fuel dispenser moves the ball away from the valve seat and deflects the support spring. After the pressure drops from the distributor side, the ball is pressed against the seat. This way, the tank is protected against fuel leakage in the event of damage to the pipe from the refueling valve [2].

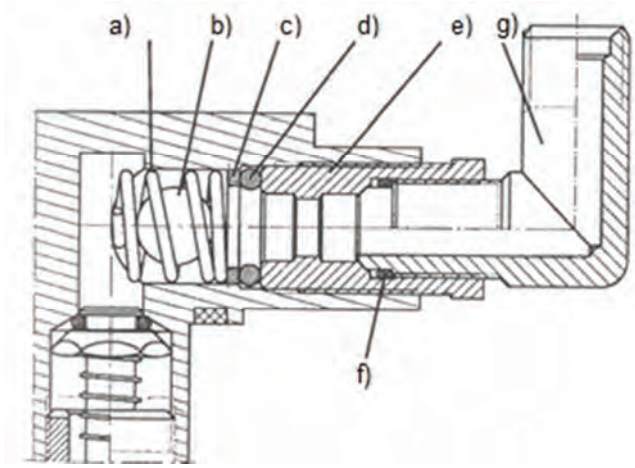

Fig. 3. Multivalve check valve [2]: a) spring, b) ball, c) washer, d) rubber sealing ring, e) reduction sleeve, f) rubber sealing ring, g) elbow fitting

The refueling valve is connected to the multivalve by a line that enables the refueling of gaseous fuel into the tank. Its construction also uses a non-return valve which prevents fuel from flowing out after refueling is finished. The LPG and CNG refueling valves are not compatible with each other (Fig. 4) [2].

All fittings of the LPG tank are placed in a gas-tight casing connected with ventilation ducts. When a leak occurs, the gas escapes through this system outside the vehicle, thus minimizing the risk of gas entering the passenger compartment of the vehicle [2, 6].

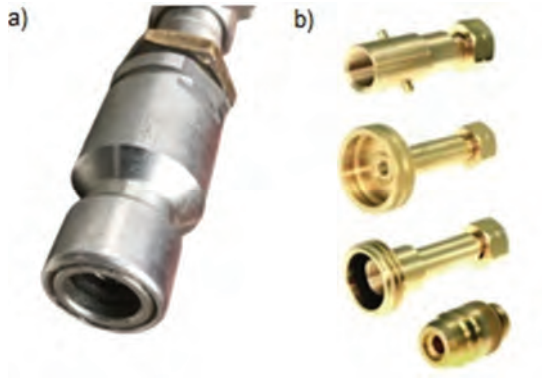

Fig. 4. Gas refueling valve: a) CNG, b) LPG – various types [11]

2.4. Gas pipes

Rigid metal or plastic pipes (also flexible) are used to connect automotive components of gas installations in which there is liquid gas. Metal pipes should be seamless, steel or copper (Fig. 5) for LPG and only steel for CNG. Steel pipes should be made of stainless steel or with additional anti-corrosion coating. Rigid pipes made of non-metallic material may be used. The copper wires should be protected with a rubber or plastic cover along their entire length. The internal diameter of the rigid pipe should not exceed 12 mm when used with gaseous fuels, and the wall thickness should be at least 0,8 mm [6, 7].

Fig. 5. Copper pipe for liquid gas fuel [11]

The requirements for flexible hose included in the regulations are very extensive and detailed. In the event of a road collision, when there is a movement of elements in the engine compartment, the priority is to avoid leakage of the gas installation, including its low-pressure part. The rubber gas pipes (Fig. 6) must consist of a smooth-walled inner tube (4) and a reinforced sheath with one or more intermediate layers (no. 1, 2, 3). If the reinforcement is made of anti-corrosion materials, the shield (1) is not required [12].

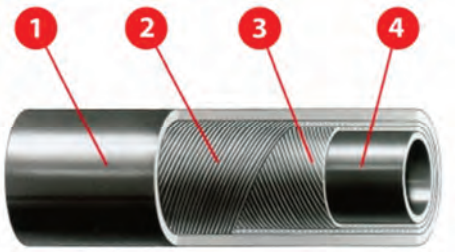

Fig. 6. Flexible fuel gas hose [12]

The inner tube is in contact with the flowing gas. The material from which it is made must be neutral in terms of the action of hydrocarbons. There is a reinforcement in the gas line to maintain the internal bending section and resistance to internal pressure. Synthetic, metal or textile fibers are used in the reinforcement. The outer layer protects the cable against the conditions in the engine compartment and protects against mechanical damage. The inner tube and the sheath must exhibit tensile strength and must be able to achieve a total elongation of at least 250%, according to ISO 37. During approval, the cables are tested for bending resistance. A length of 3500 mm of wire is considered correct when it can withstand a bend test repeated 3000 times without breaking. After the bend test, the hose must withstand the internal pressure without showing any leakage [1, 6].

The provisions of the UNECE regulations define the requirements for low-pressure rubber hoses, which must withstand a maximum working pressure of 0.45 MPa and the operating range at a temperature of –25 to 125°C. The inside of the hose is tested for chemical resistance. It is immersed in n-pentane at a temperature of 23ºC (according to ISO 1817) for 3 days. The change in the volume of the hose sample must not exceed 20%, the change in tensile strength – 25%, and the change in total elongation – 30%. Then, after the cable has been stored in air at 40ºC for 2 days, its weight is checked. The value, in comparison with the initial weight, cannot decrease by more than 5% [4, 11, 12, 18]. The cable sheath (external part) is tested for resistance to n-hexane, in which the sample is kept at 23ºC for 3 days. For sheaths, a greater tolerance of changes in mechanical parameters is allowed than for the internal part of the conduit: the maximum change in volume by 30%, the maximum change in tensile strength by 35%, and the maximum change in the total elongation by 35% [2, 3, 9]. The tightness test in accordance with the method described in ISO 4080 standard consists in connecting a 1000 mm long hose to a tank with liquid propane at a temperature of 23 ±2ºC. The gas loss in the line is monitored for 2 days. A loss greater than 95 cm³ is not allowed [1, 9]. Cables used in gas supply systems are also tested for fire resistance according to DIN 51622, DIN 12642 standards. It is required to maintain the ability to self-extinguish, and during their combustion they should not emit harmful substances [1, 9]. Gas pipes according to ISO 1431/1 must pass the ozone shield resistance test. Samples stretched to 20% elongation are exposed to air with ozone content of 50 ppm and temperature of 40°C for 5 full days. The samples should not show any cracks [2, 4, 6, 12].

The differences between the CNG and LPG lines appear in the context of the lines leading from the tank to the engine compartment. They result from the pressures at which propane-butane and CNG are stored. CNG requires stiff and more durable steel pipes (Fig. 7). The gas moving from the CNG cylinder to the engine still has a pressure several times greater than that of LPG, and any unsealing would be much more violent. Therefore, resistance to external factors as well as internal forces is important.

Fig. 7. High pressure CNG steel pipe

3. Installation assembly

3.1. Arrangement of system components in the vehicle

The provisions in the UNECE regulations, according to which gas supply systems are approved, regulate the position of the system components. In Polish law, annex 9 to the Polish ordinance of the Minister of Infrastructure on "technical conditions of vehicles and the scope of their necessary equipment" regulates the issues related to the installation of gas supply components, the operation of the vehicle with gas supply and its impact on the base fuel supply. The elements of the gas supply system should be arranged in a way that does not hinder the servicing of other car parts. The provisions of the annex concern the protection of gas system components (mechanical damage, corrosion), securing tanks against damage by cargo and that the installation should function properly and safely [2, 12].

In order to maintain the safe operation of the installation, the pipes should be arranged in a way that facilitates their inspection, so that they do not rub against the elements of the vehicle and at a distance of not less than 100 mm from the exhaust system, when a thermal screen is not used. Additionally, the cables must not run in the vicinity of the vehicle lifting points and their fixing must exclude the susceptibility of the cables to vibrations [2].

Gas pipes must not be welded, soldered or joined with snap joints. Standard self-clamping sockets are required to connect the wires, and the number of connectors should be kept to a minimum [2, 12].

Metal pipes connecting elements of the installation structure, which may be subject to a force displacing them during operation, should be shaped into loops with a radius of curvature adapted to the pipe diameter (due to the possibility of breaking) (Fig. 8) [2, 8].

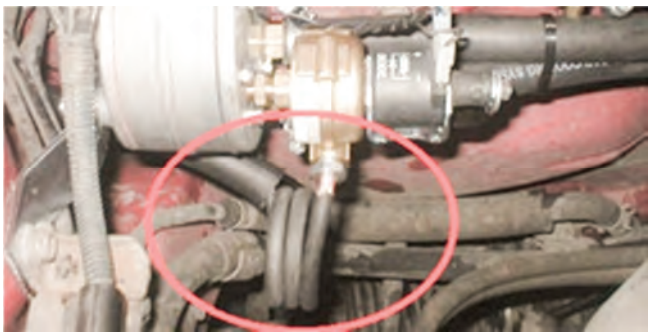

Fig. 8. The method of connecting the evaporator with a rigid copper LPG pipe

The cylindrical tanks can be mounted transversely or longitudinally with respect to the car axis (Fig. 9). The assembly rules apply to all LPG and CNG tanks installed in

cars. Gas fuel tanks cannot be installed in the front of the car or in the engine compartment. They should be installed in such a way that the effects of collisions (mainly at the front and rear of the vehicle) are minimized [2, 8].

There should be no sharp or stiff elements in the vicinity of the installed gas tanks. If the tank is installed under the chassis, its distance from the engine exhaust system (without a heat shield) must not be less than 100 mm. The ground clearance under the tank must not be less than 200 mm.

The guidelines for the installation of gas system components in the engine compartment regulate the minimum distance of the reducer from the exhaust system to 100 mm. The reducer should be installed in a place that is not exposed to temperature fluctuations (drops) while driving. In the vicinity of the reducer, in an easily accessible place, a gas solenoid valve is installed with the coil upwards. The requirement is to install the reducer in such a way that the car's movement does not affect its operation. The controller should be isolated from moisture and mounted away from strong heat sources such as the exhaust manifold or turbocharger. The installation of the gas controller and the wiring harness of the power supply system should be separated from the elements of the ignition system, as this may lead to interference [2, 2]

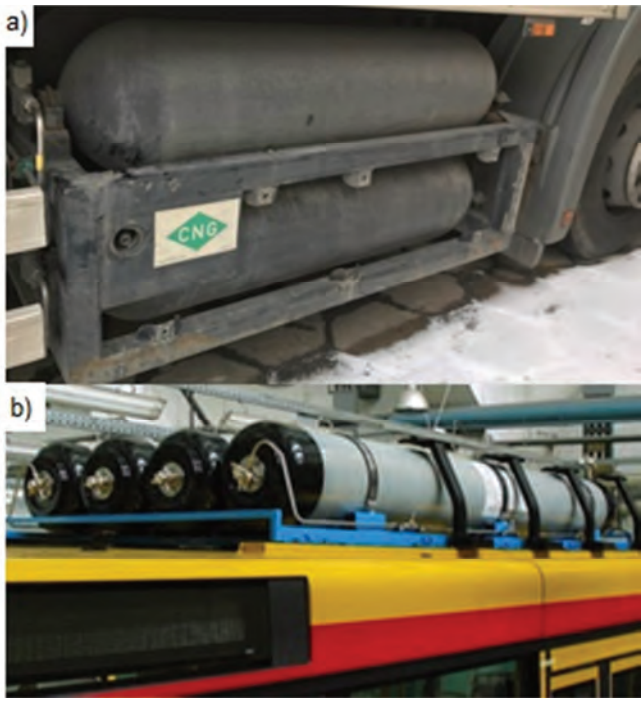

Fig. 9. Method of mounting CNG tanks: a) composite-aluminum ones on the frame of a truck; b) composite on the roof of a city bus [12]

3.2. Homologation of the method of assembly of the installation

In accordance with Polish law and the provisions of the Regulation of the Polish Minister of Infrastructure of December 24, 2003 on "the approval of the method of assembly of an installation adapting a given type of vehicle to be fed with gaseous fuel", installation services of this type of power supply may be performed by a company with a certificate of approval of the method of installation of gas supply systems it as part of the workshop dealer network. The method of fuel system assembly adapting a given type of vehicle to gas supply, which is to be performed on the territory of the Republic of Poland, should meet certain technical requirements, the fulfillment of which is confirmed in the approval procedure of the installation method adapting a given type of vehicle to gas supply. The entity performing the installation of an installation adapting a given type of vehicle to run on gas may apply for the issue or amendment of a certificate of approval for the method of mounting an installation adapting a given type of vehicle to gas supply. The document is issued by the Polish Transport Technical Inspection Director by way of an administrative decision. The list of companies with approval and cooperating workshops is kept by the Polish Motor Transport Institute [2, 8].

4. Gas installation during a road accident

The discussed construction and legal requirements minimize the negative effects of a road accident in the context of equipping the car with a gas installation. The safety of passengers is ensured by both the functionality of the control electronics and the components made in terms of the materials used. The gas tanks are constructed in a way that ensures their safety in the event of a collision. Figure 10 shows the effects of a rearward collision with an LPG-powered vehicle. Additionally, according to the law, after each collision of a vehicle, they must undergo the legalization process again [2].

Fig. 10. The rear of a vehicle with a toroidal LPG tank after collision [12]

Connectors, nozzles and couplings are made of non-sparking materials (brass), so rubbing is not able to ignite any fuel vapors [11].

The gas ECU response time to switching off the gas installation is 0.3 seconds. The control electronics of the gas systems are designed in such a way that in the event of a sudden pressure drop in the system (e.g. after the fuel supply line to the reducer is broken), the system is immediately turned off and the engine is switched to the base fuel mode. Too low pressure in the system, determined on the basis of data from the gas pressure sensor, which is part of every modern gas installation, causes the gas supply to be disconnected. Therefore, the risk of leakage of the gas system in the engine compartment, and consequently the risk of gas leakage and ignition, is minimal. If, as a result of an accident, the gas flow from the tank to the engine compartment is disturbed (the fuel line is bent or broken), restarting

the engine in gas mode will be impossible. Additionally, a solenoid valve in the engine compartment cuts off the flow of gaseous fuel when the engine (for whatever reason) is not running. The same mechanism occurs also when the fuel in the tank is exhausted – when the gas pressure drops (it stops flowing), the controller perceives it as a signal to turn off the system. Turning off the gas supply system also closes the solenoid valve on the tank, so the only gas that can leak from the vehicle is the one in the lines [4, 7, 12].

In the context of CNG, it is also worth noting its physicochemical property in the form of low density under normal conditions (the density of natural gas is lower than that of air), thanks to which all leakages caused by the collision are released into the atmosphere, where they are quickly spread in the air without reaching the lower flammability limit. This further improves safety in the event of a collision.

Thanks to the security of the gas systems, damage to the gas supply system does not adversely affect the safety of the vehicle's operation.

5. Danger during a fire in a car with a gas fuel system

The fire test of an LPG fueled vehicle [13] carried out at the Polish Military Institute of Armament Technology in Zielonka (Poland) simulated a situation where, as a result of unsealing the gasoline tank and spilling fuel, it may ignite, which is tantamount to a car fire. The fire started at the rear of the vehicle due to the location of the gasoline tank. The gas tank was also installed in the rear part. During the fire test, there were about 25 liters of fuel in the gas tank, which accounted for 73% of its geometric capacity [11]. The fire was initiated with the use of gasoline in a container placed under the vehicle. The fire engulfed the entire rear of the car. After 5 minutes and 44 seconds, the gas tank fittings were activated. The cyclical operation of the safety valve lasted up to 9 minutes of the fire. The frequency of its operation (opening and closing) was initially increasing, and then the period began to lengthen to approx. 9 seconds, while the acoustic effect decreased. After the last closing of the safety valve in 9 minutes, the fire valve opened, as evidenced by the constant stoking of the flames and the characteristic, gradually decreasing in intensity, hiss of flowing gas, which ended 11 minutes and 30 seconds after the initiation of the test [3, 13].

The test showed that the LPG tank in a car poses no greater threat than a gasoline or diesel tank, and in some respects it is superior to them because it is a high-strength component. Gas tanks are more durable than conventional fuel tanks, which are most often made of plastic. The possibility of mechanical damage to the gas tank in the event of a fire is minimal. In the extremely unfavorable case of deformation of the tank shell, it is flexible enough (required by the production technology used) that it does not become unsealed. The high durability of the tank results from its operating conditions. Nominal pressure for LPG, depending on the degree of filling and the ambient temperature, ranges from 0.6 to 1.7 MPa. During the test, the pressure in the tank reached a value that allowed the safety valve to be opened (in LPG tanks – 2.7 MPa). The pressure increase takes place at a very high temperature, which at the same time weakens the material of the tank shell and its fittings. However, even such extremely unfavorable conditions did not cause the tank to become unsealed during the test. Releasing excess gas through the safety valve eliminated the increase in internal pressure in the tank. The fire gas escaping through the safety valves and the fire was removed through the vent under the car, which minimized stoking the flame [12, 13].

6. Legal restrictions on a gas-powered vehicle

Signs visible on public roads in Europe prohibiting the entry or parking of vehicles equipped with a gas installation (Fig. 11) are not included in the state's road traffic codes or in EU regulations. Therefore, the regulations do not regulate the liability for breaking it by the driver, there is no legal basis for issuing a fine for non-compliance with this and similar signs.

Fig. 11. A sign prohibiting entry for a vehicle powered by LPG

In Polish law, the document regulating the underground parking of a vehicle equipped with gas is the regulation of the Polish Minister of Infrastructure on the ventilation of parking lots. In those where cars powered by LPG and underground gas are parked, mechanical ventilation must be used, controlled by detectors of the unacceptable level of propane-butane gas concentration (Ministry of Infrastructure Regulation of 12 April 2002 on technical conditions that should be met by buildings and their location and its amendment of March 12, 2009). The LPG entry ban sign is not a grassroots initiative by the owners of underground garages. They are obliged to do so by § 4 ust. 2 pkt. 5 of the Regulation of the Polish Minister of Interior and Administration of 7.6.2010 on fire protection of buildings, other construction facilities and areas, which says that: *"owners, managers or users of buildings, storage yards and shelters, with the exception of single-family residential buildings: place, at the entrances to closed garages with the floor below the ground level, legible information on whether or not cars powered by LPG, propane-butane, referred to in technical and construction regulations, are allowed or not to park in these garages*" The above-mentioned regulations refer to the information obligation and ventilation. The ban on entry may therefore only result from the regulations of the car park established by its owner.

Due to the lower density of natural gas than air, entry bans do not apply to vehicles powered by this type of gas fuel. CNG does not pose a fire hazard as it lies low next to the floor and in sewers.

7. Conclusion

Both legal, legalization and technical aspects guarantee the trouble-free and safe use of gaseous fuel in motor vehi-

cles, as long as the user of the installation does not lead to gross negligence in operation and service. Gaseous fuels are safer than conventional fuels, and the ongoing development of the latest generation installations with direct gas fuel injection should, in the near future, support a stable growth in their use in the automotive industry, which will translate into a further increase in the safety of vehicle operation.

Nomenclature

CNG compressed natural gas
DIN Deutsches Institut für Normung (German Institute for Standardization)
EN European Norm Standards
ISO International Organization for Standardization
LPG liquefied petroleum gas
UNECE United Nations Economic Commission for Europe

Bibliography

[1] BIENIEK, A., GRABA, M., MAMALA, J. et al. Application of biogas to supply the high compression ratio engine. *Combustion Engines*. 2019, **179**(4), 40-46. https://doi.org/10.19206/CE-2019-406
[2] GĘBUŚ, P. Niezbędnik diagnosty SKP 2020, *SIMP-AUTOMEX*. Tarnów 2020.
[3] KNEBA, Z., STEPANENKO, D. DME as alternative fuel for compression ignition engines – a review. *Combustion Engines*. 2019, **177**(2), 172-179. https://doi.org/10.19206/CE-2019-230
[4] MAJERCZYK, A., TAUBERT, S. Układy zasilania gazem propan-butan. *Wydwnictwa Komunikacji i Łączności*. Warszawa 2003.
[5] SMIL, V. Natural Gas. Fuel for the 21st Century. *Wiley*. 2015.
[6] Regulation No 67 of the Economic Commission for Europe of the United Nations.
[7] Regulation No 110 of the Economic Commission for Europe of the United Nations.
[8] Dziennik Ustaw 2016 poz. 2022 – Obwieszczenie Ministra Infrastruktury i Budownictwa z dnia 27 października 2016 r. w sprawie ogłoszenia jednolitego tekstu rozporządzenia Ministra Infrastruktury w sprawie warunków technicznych pojazdów oraz zakresu ich niezbędnego wyposażenia.
[9] Rozporządzenie Ministra Infrastruktury z 12 kwietnia 2002 r. w sprawie warunków technicznych, jakim powinny odpowiadać budynki i ich usytuowanie i jego nowelizacja z 12 marca 2009.
[10] Rozporządzenie Ministra Spraw Wewnętrznych i Administracji z 7.6.2010 r. w sprawie ochrony przeciwpożarowej budynków, innych obiektów budowlanych i terenów.
[11] AC S.A. https://www.ac.com.pl (accessed on 3.09.2021).
[12] GAZEO.PL. https://www.gazeo.pl (accessed on 3.09.2021).
[13] Military Institute of Armament Technology. https://www.witu.mil.pl/www/witu_pl.htm (accessed on 3.09.2021).

Janusz Chojnowski, MEng. – Faculty of Mechanical Engineering, Military University of Technology in Warsaw.
e-mail: *janusz.chojnowski@wat.edu.pl*

Article citation info:
KAMIŃSKA, M., KOŁODZIEJEK, D., SZYMLET, N. et al. Measurement of rail vehicles exhaust emissions. *Combustion Engines*. 2022, **189**(2), 10-17. https://doi.org/10.19206/CE-142526

Michalina KAMIŃSKA
Daniel KOŁODZIEJEK
Natalia SZYMLET
Paweł FUĆ
Rafał GRZESZCZYK

Combustion Engines
Polish Scientific Society of Combustion Engines

Measurement of rail vehicles exhaust emissions

ARTICLE INFO

Received: 6 August 2021
Revised: 20 September 2021
Accepted: 23 September 2021
Available online: 24 September 2021

The basic problem in terms of measuring exhaust emissions is the approval tests of traction vehicles, which are carried out on engine dynamometers. Therefore, it is impossible to obtain reliable results concerning their actual impact on the natural environment. It is therefore advisable to carry out the tests in real operation conditions, as is the case for road vehicles for which RDE (Real Driving Emissions) tests are carried out. The latest Stage V emission standards push for the introduction of this type of test, but no limit values for toxic exhaust gases have been established and no test guidelines have been defined for assessing actual emissions. This article describes the issues related to the legislative guidelines for non-road vehicles in force in Europe, as well as the measurement tools used, such as mobile equipment for measuring emissions of PEMS (Portable Emissions Measurement Systems) and newly developed emission gates. Additionally, the paper presents examples of locomotive exhaust emission tests in real operating conditions. The aim of the measurements was to assess the emission of toxic compounds against the relevant standards. The subject of the research was a diesel locomotive type T448.P equipped with a modernized internal combustion engine.

Key words: *exhaust emission, rail vehicles, RDE, PEMS, NRMM*

1. Introduction

Despite efforts to electrify vehicles used in road and rail traffic, vehicles with internal combustion engines still constitute a significant part of rail vehicles used in Poland (Fig. 1). The planned modernization works and purchases of new vehicles announced by Polish railway operators indicate that the future of vehicles with internal combustion engines on Polish tracks seems to be safe for the next several years or even a decade. Freight carriers have planned investments in 167 locomotives with the financial value of approximately PLN 930 million for the years 2017–2023 [19]. This situation may be influenced by the degree of electrification of the polish railway network, which has changed slightly over the years and in the years (2003–2018) increased from 59.8% to 61.8% [11–14]. This means that in 2018, 7341 km of tracks in Poland were not available for electric rolling stock.

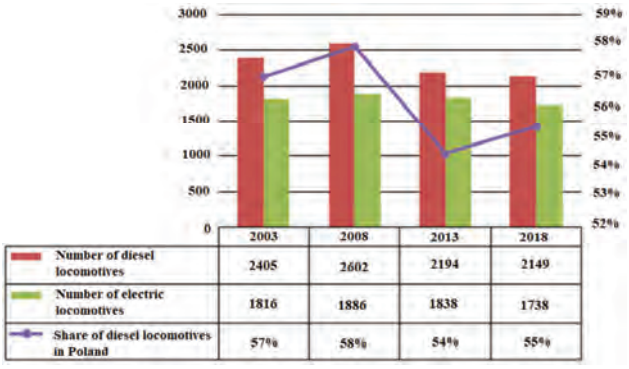

	2003	2008	2013	2018
Number of diesel locomotives	2405	2602	2194	2149
Number of electric locomotives	1816	1886	1838	1738
Share of diesel locomotives in Poland	57%	58%	54%	55%

Fig. 1. The structure of the rolling stock in Poland in 2003-2018 [11–14]

2. Exhaust emission standards for rail vehicles used in Poland

The development of measuring technology and research on the harmful effects of substances emitted in exhaust gases meant that several decades ago, increasing awareness began to appear regarding the risks associated with the emissions from internal combustion engines. As a consequence, exhaust emission standards for rail vehicle engines were developed and put into place. The ORE B13 report is the oldest form of formal recording of exhaust emission limits for vehicles used in Poland. Based on this document a twenty-nine-phase test was carried out (Fig. 2), from which four evenly distributed operating points were selected for the calculations.

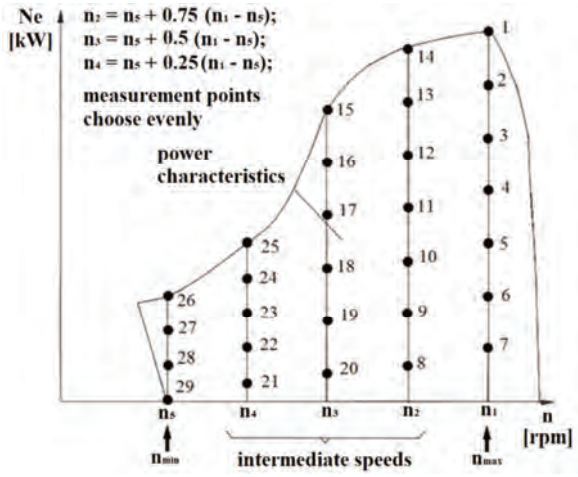

Fig. 2. The ORE B13 test measurement points [6]

Along with the above-mentioned test, emission limits for such compounds as: CO, HC and NO_x were introduced (Table 1). The standards for off-road vehicles provide the maximum value of the specific emissions for each exhaust component, i.e. expressed in the mass of substance emitted in the process of generating a unit of work. The most recent version, introduced in 1997, assumed a fourfold reduction

in carbon monoxide emissions, a fivefold reduction in hydrocarbon emissions and a twofold reduction in nitrogen oxides emissions compared to the first stage. At the same time, the opacity of the exhaust gases was to remain at the same level all the time.

Table 1. Exhaust emission limit value according to ORE B13 [1]

Applicable	CO	HC	NO_x	Opacity k
	g/kWh			m^{-1}
Until 31.12.1981	12	4.0	24	1.6–2.5
Since 01.01.1982	8	2.4	20	1.6–2.5
Since 01.02.1991	4	1.6	16	1.6–2.5
Since 01.02.1997	3	0.8	12	1.6–2.5

Poland's accession to the European Union resulted in the entry into force of the EU standards for the NRMM (Non-Road Mobile Machinery) vehicle category. On the basis of successive regulations of the European Parliament, newer and more stringent exhaust emission standards were introduced. Particular attention should be paid to the following standards: Stage IIIA (2006), Stage IIIB (2011) and Stage V (2019). Each of these stages divides the engines of off-road vehicles into categories depending on the power, type of ignition and the vehicle on which the engine is installed (Table 2). The standard provides for limits on such toxic compounds as CO, HC, NO_x, total HC and NO_x emissions, as well as PM mass (Fig. 3).

Table 2. Railway vehicle engine categories in stages: IIIA, IIIB and V [4, 18]

Norm	Stage IIIA	Stage IIIB	Stage V
Types of vehicles	Railcars RC A P < 130 kW	Railcars RC B P < 130 kW	Railcars RLR, CI/SI; P > 0 kW
	Locomotives RL A 130 kW < P < 560 kW	Locomotives R P > 130 kW	Locomotives RLL, CI/SI P > 0 kW
	Locomotives RH A P > 560 kW		
RC A – railcar engines, from 31.12 2005 RL A – locomotive engines, from 31.12 2006 RH – locomotive engines from 31.12 2008 RC B – railcar engines, from 31.12 20011 R B – locomotive engines, from 31.12 20011 RLR – railway railcars, from 31.12 20020 RLL – railway locomotives, from 31.12 20020			

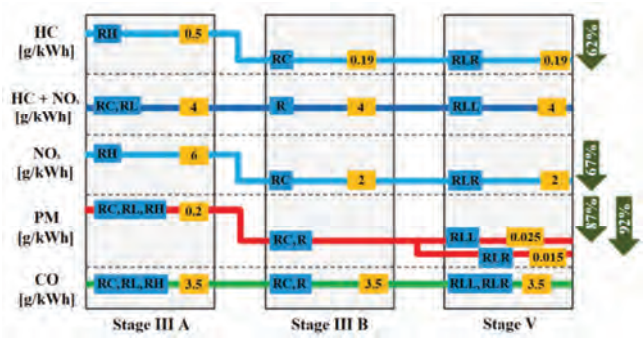

Fig. 3. Exhaust emission limits for Stages IIIA, IIIB and V [3]

As a result of these regulations, the latest designs of rail vehicle engines are equipped with modern solutions known mainly from passenger cars and trucks, such as the Common Rail injection system or the SCR (Selective Catalytic Reduction) reactor. With Stage V, there is a requirement to test NRMM vehicles under real operating conditions. However, the limit values for the individual toxic exhaust gases have not yet been defined.

3. Rail vehicle emission testing

Emission tests for NRMM category vehicles are governed by ISO 8178. The measurement cycles are carried out in the Stage I, II, IIIA, IIIB, IV and V standards for diesel engines with a net power of 19 kW ≤ P ≤ 560 kW, which run at constant or variable speed. The test procedure consists of a series of eleven measurements at different speed and torque values that characterize the typical operation of the vehicle engine. The different modes and their weighting factors are presented in Table 3. Weighting factor is the weight of the operating point for the calculation of the resulting emission. The test is performed under steady-state operating conditions, so it ignores transient conditions important from the emissivity point of the engine, when the drive unit has to adapt to the changing load.

Table 3 Test weight factors according to ISO 8178 [21]

Phase number	Torque [%]	Engine speed [rpm]	Non-road vehicles		Constant engine speed		Locomotives
			C1	C2	D1	D2	F
1	100	Rated	0.15	–	0.30	0.05	0.25
2	75		0.15	–	0.50	0.25	–
3	50		0.15	–	0.20	0.30	–
4	25	Medium range		0.06	–	0.30	–
5	10		0.10	–	–	0.10	–
6	100		0.10	0.02	–	–	–
7	75		0.10	0.05	–	–	–
8	50	Idle	0.10	0.32	–	–	0.15
9	25		–	0.30	–	–	–
10	10		–	0.10	–	–	–
11	0		0.15	0.15	–	–	0.60
C1 – test cycle for C.I. engines operated under intermittent speed C2 – test cycle for S.I. engines operated with a power > 20 kW D1 – test cycle for auxiliary engines operated under constant speed D2 – test cycle for C.I. engines operated under constant speed F – test cycle for locomotives engines							

Examination of exhaust gas composition is important in the context of engine diagnostics and its functional systems such as: catalytic converters, DPF filters (Diesel Particulate Filter) and SCR reactors [9]. Diagnostics of the wear of these elements in specific vehicles or entire series of engines may be an important step in the development of further technical solutions reducing the emission of toxic compounds. There are tests performed at the stage of research and development of structures and control tests, which are divided into:

- homologation (NTA – new type approval),
- conformity of production (tests of vehicles drawn randomly from series production to confirm compliance with approval),
- periodic tests at motor vehicle diagnostic stations.

Approval tests in accordance with ISO 8178 are a time-consuming and complicated process. They are carried out in stationary conditions, often with the use of generator brakes. Control tests, performed after installing the engine on the vehicle, are carried out after an appropriate period of operation at a diagnostic station (Fig. 4) equipped with, among others, water resistor [3].

Fig. 4. Diagnostic station for measuring operational parameters and emissions of rail vehicles [20]

The concentrations of the individual exhaust components are measured by specific exhaust gas analyzers. The exhaust gases are supplied to them thanks to the use of a probe placed in the exhaust system. Engine operating parameters, including power, are regulated from the driver's cab. Testing emissions only under steady-state conditions leads to significant discrepancies between the results of the approval tests and the emissions under real conditions [2, 15, 16]. Hence the idea of a real driving test (RDE) for road vehicles. Such measurements have already been included in the WLTP (World harmonized Light-duty vehicles) Test Procedure tests. It is possible to develop a methodology of such tests for rail vehicles and to add their results to the test according to ISO 8178 thanks to the use of PEMS devices.

4. The use of PEMS devices in the testing of the emissions of rail vehicles combustion engines

The use of PEMS equipment allows for testing vehicle emissions in real engine operating conditions (Fig. 5). Devices of this type measure the concentrations of: CO, CO_2, HC, NO_x and the mass, number and size of solid particles. The engine operating parameters are taken from the CAN (Controller Area Network) bus. In order to facilitate the comparison of RDE test results with approval tests, the CF (Conformity Factor) has been introduced.[10]:

$$CF_i = \frac{E_{r,i}}{E_{WHTC,i}} \quad (1)$$

where: i – compounds for which the concordance factor is determined, $E_{r,i}$ – emission under real operating conditions, $E_{WHTC,i}$ – emission in the WHTC test.

Determining the maximum value of the CF coefficient makes it possible to take into account the difference between the operating conditions in RDE and type-approval tests and the tolerances of the devices used. Measurements with PEMS equipment can be particularly useful when comparing emissions before and after rolling stock upgrades. The assessment of the emission change and the determination of environmental benefits may be the basis for making a decision to carry out further modernization works. In addition, tests carried out in various conditions can be the basis for the assessment of emission tests and their compliance with the actual performance of vehicles.

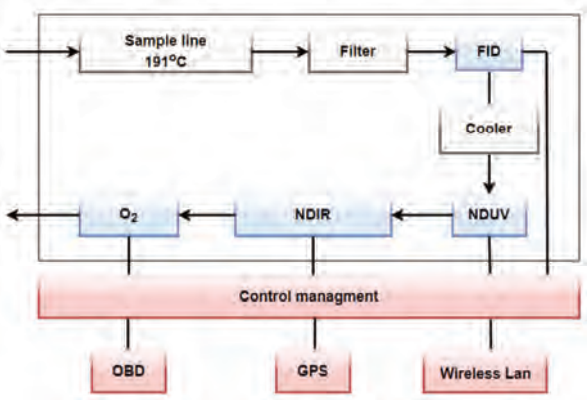

Fig. 5. Scheme of PEMS analyzer based on Semtech DS [12] FID (Flame Ionization Detector), NDUV (Non–dispersive Ultra Violet), NDIR (Non–dispersive Infrared), OBD (On-Board Diagnostics), GPS (Global Positioning System), LAN (Local Area Network)

5. Research on the emission of toxic compounds with use of remote-sensing technology

Testing in laboratory conditions and PEMS measurements do not meet all the expectations of today's exhaust emission testing. Therefore, there was a need to develop methods that would allow the measurement of vehicle emissions at a reduced cost and time-consuming research. This possibility is provided by remote-sensing technology. They are currently used to assess the emissions of road vehicles. China and the USA are the leaders in work on such solutions. The Republic of China was the first country to introduce emission standards for measurements using this method.

Two development paths can be distinguished among the developed gate solutions [7]:

– open – path, based on absorption spectroscopy to study the concentrations of harmful compounds in the exhaust gas (Fig. 6a),
– extractive, where the exhaust gas sample is collected and analyzed by laboratory analyzers (Fig. 6a).

Both methods base their results on the relation of the concentrations of toxic compounds to the concentration of carbon dioxide in the exhaust gases. In most cases, the system measures nitrogen monoxide (NO), carbon monoxide (CO), hydrocarbons (HC) and carbon dioxide (CO_2). It is also possible to determine the concentrations of nitrogen dioxide (NO_2) and ammonia (NH_3). The measurement of particulate mass (PM) is possible indirectly from the exhaust blackness. Open – path uses the laws of optics and light absorption by exhaust gas components to determine their concentrations. So far, the results of the measurements are used to select vehicles with the highest emissivity, in order to refer them to further tests, e.g. PEMS. Determining the vehicle's emissivity on the basis of such measurements

is easier for SI (Spark Ignition) engines than for CI (Compression Ignition) engines. The reason is the operation of diesel engines on lean mixtures with variable oxygen concentration. With properly operating SI engines, the CO_2 concentration is usually around 15%. In diesel engines, this value can vary from 1 to 13%, and even 15% during regeneration of cleaning systems.

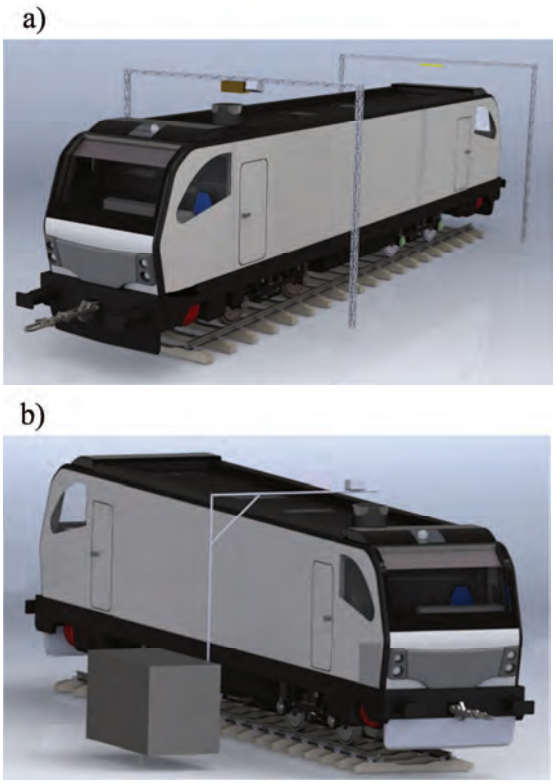

Fig. 6. Emission gate for the evaluation of type rail vehicles a) open – path, b) extractive

The issue that constitutes the greatest difficulty in the wide application of remote-sensing technology is the difficulty in unambiguously comparing their results with the maximum emission values introduced by the standards. The remote-sensing technology does not allow the measurement of the exhaust gas intensity, so it is impossible to determine the road [g/km] or specific emission [g/kWh]. Road emissions relate the mass of the pollutant to the distance traveled by the vehicle, while the specific emission relates to the useful work performed by the vehicle engine. To improve the information carrying capacity of the results, three methods of comparing the results to the maximum values were proposed. The first one is based on the estimation of CO_2 concentration on the basis of dynamic properties and characteristics. The second method is to test the amount of oxygen versus carbon dioxide in the exhaust cloud close to the end of the exhaust system. Unfortunately, there is no technology yet that would allow such measurements to be made. The third way is to define emission factors based on CO_2 emissions or fuel consumption. The assessment of the toxicity indicators, which refer individual compounds to CO_2 emissions, is presented in [17]. This approach seems to be the most developmental at present. A method of converting the concentrations of toxic compounds into road emissions has been developed, while maintaining certain dependencies.

6. Examples of tests in real operating conditions

The tests in real operating conditions were carried out on an unloaded T448.P diesel locomotive (Fig. 7, Table 4).

Table 4. Basic technical data of the research object (according to the operation and maintenance documentation [5])

Type of work	four-stroke cycle
Injection	direct
Top-up	turbocharging
Layout	V90º
Cylinder liner diameter [mm]	165
Piston stroke [mm]	185
Number of cylinders	12
Displacement volume [dm^3]	47.5
Compression ratio	13.6:1
Maximum power [kW] at rotational speed [rpm]	680 1300
Torque at 40°C coolant temperature [Nm]	560

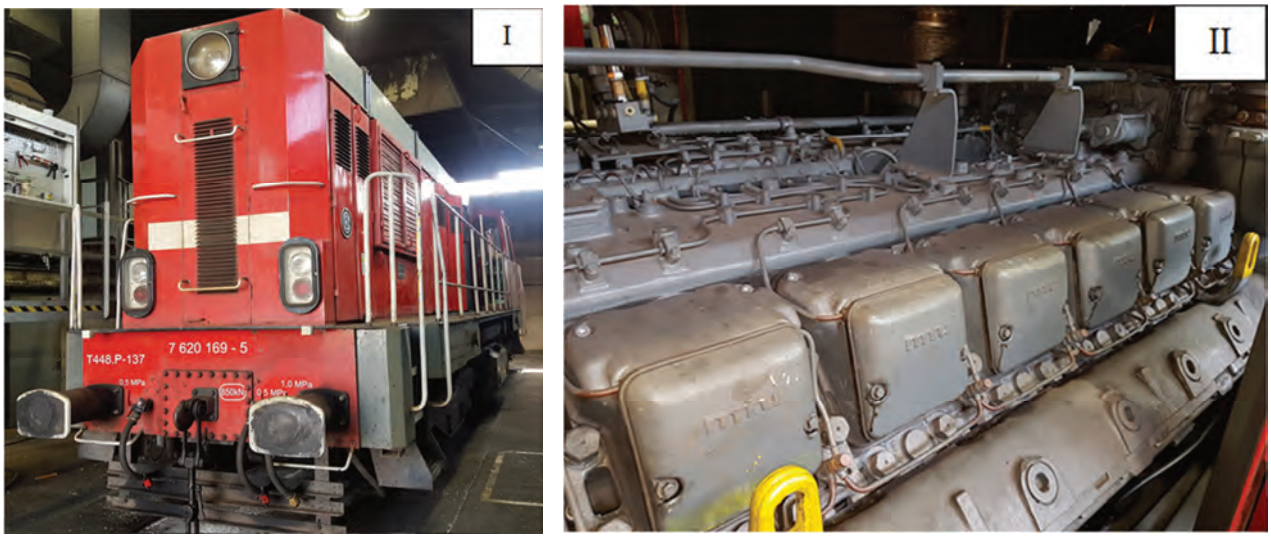

Fig. 7. General view: I – diesel locomotive T448, II – diesel engine 12V396

The aim of the measurements was to assess the emission of toxic compounds, taking into account the histograms of the load of locomotives under typical operating conditions in the light of the requirements of the relevant standards, directives and regulations [4, 6, 8, 18]. The locomotive was equipped with a 12-cylinder combustion engine with a displacement of 47.5 dm^3. It had a maximum power of 680 kW at a rotational speed of 1,300 rpm. The diagram of the performed measurements is shown in Fig. 8.

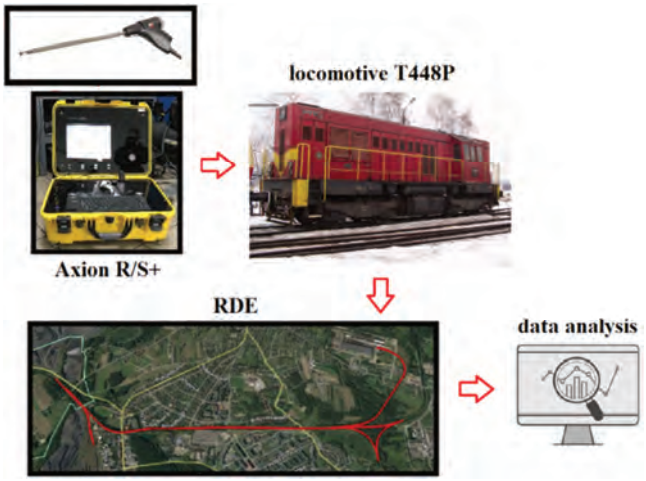

Fig. 8. Diagram of the performed tests

The tests were carried out using the Micro PEMS Axion R/S+ mobile analyzer manufactured by Global MRV. The device measures the concentration of gaseous toxic compounds with the use of: a non-dispersive infrared analyzer – NDIR (CO_2, CO, HC) and an electrochemical analyzer (NO). The equipment also allows you to measure PM concentration using a method based on Laser Scatter, in which the speed of particle movement is measured (taking into account the values assigned to PM10).

Based on the recorded parameters during the tests, the characteristics of the time density as a function of velocity – acceleration (V–a) were determined (Fig. 9). The area defined by the ranges (0 m/s; 8 m/s> and (–0.5 m/s^2; 0.5 m/s^2>) had the highest share of working time – 68%. The highest values for a single operating point (17.5%) were obtained while for speed (4 m/s; 6 m/s> and acceleration 0 m/s^2 and for idling (17.4%). It is also worth noting that the share of operating time from a run by a locomotive with zero acceleration was 61%. was 4.5 km with an average speed of 14.5 km/h, the locomotive during this test achieved a maximum speed of 54 km/h.

The intensity of CO_2 emissions (Fig. 10) of the tested object is closely related to the speed and acceleration of the vehicle, which can be seen in the entire range of vehicle operation. It is closely related to the fuel consumption of the locomotive. The highest emission intensity occurred in the following ranges (14 m/s; 16 m/s> i (0 m/s^2; 0.5 m/s^2> (117 g/s) and (12 m/s; 14 m/s> and (0 m/s^2; 0.5 m/s^2> (115 g/s). The average emission intensity remained at 34 g/s. The area with the highest values is described by the speed ranges (6 m/s; 16 m/s). > and acceleration (0 m/s^2; 1 m/s^2>. While idling, the vehicle emitted 17.4 g/s CO_2.

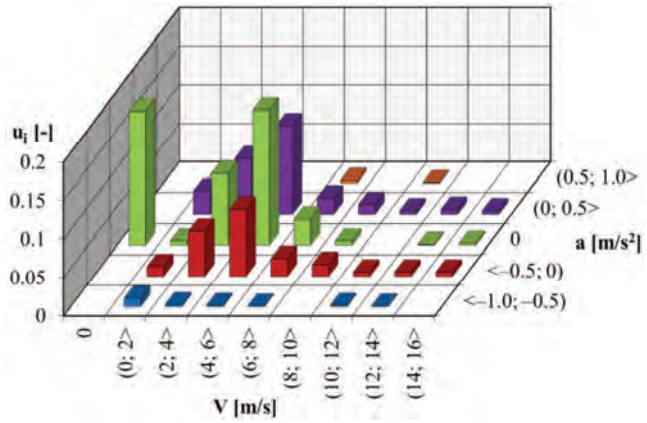

Fig. 9. Operating time density graph in real operating conditions expressed in speed and acceleration intervals

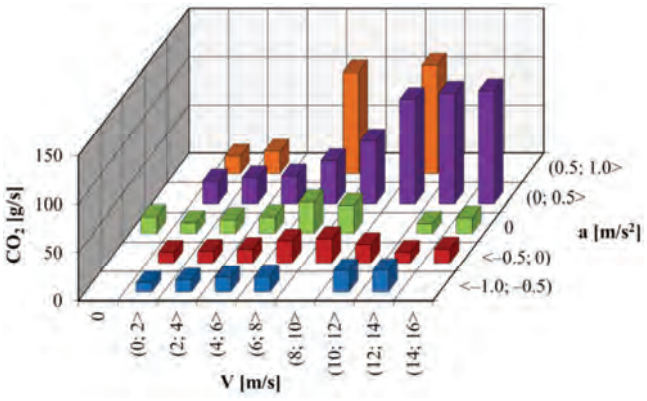

Fig. 10. CO_2 exhaust emission intensity of the tested vehicle in speed and acceleration intervals

As in the case of carbon dioxide, the obtained CO values depended on the speed and acceleration of the vehicle, but in this case their distribution was more even (Fig. 11). The highest values were obtained for the area of (6 m/s; 16 m/s> and (0 m/s^2; 1 m/s^2>), with the maximum value for a single operating point (6 m/s; 8 m/s> and (0.5 m/s^2; 1 m/s^2> was 2.44 g/s. The average value of carbon monoxide for the entire test was 0.56 g/s. At the point characterized by the lack of speed and acceleration, the vehicle was characterized by a value of 0.39 g/s.

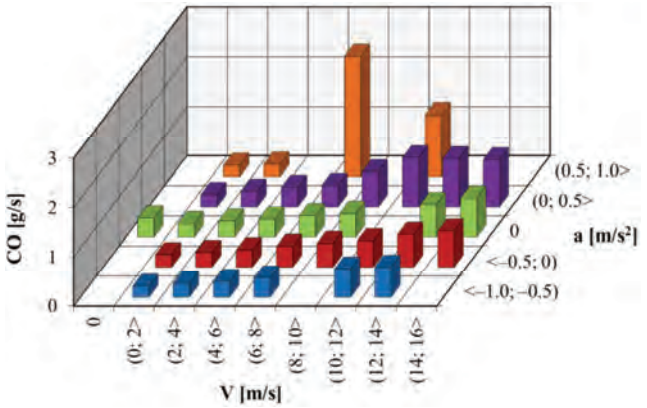

Fig. 11. CO exhaust emission intensity of the tested vehicle in speed and acceleration intervals

The values of HC emission intensity increased with increasing vehicle speed, and its average value was equal to 0.06 g/s. The highest values occurred in the area (10 m/s; 16 m/s> for the entire vehicle acceleration range. A single operating point characterized by the maximum value (0.1 g/s) occurred at the speed (14 m/s; 16 m/s> and acceleration (0 m/s^2; 0.5 m/s^2>. For idling the obtained value was close to the average value from the whole test.

The presented characteristics of the NO_x emission intensity (Fig. 13) showed that the highest values occurred in the following ranges (6 m/s; 16 m/s> and (0 m/s^2; 1 m/s^2>, where the maximum value was 2.84 g/s) was obtained at the operating point determined by the intervals (14 m/s; 16 m/s> and (0 m/s^2; 0.5 m/s^2>. The average value obtained during the tests was 0.6 g/s. For the point 0 m/s and 0 m/s^2, the emission rate was below 0.2 g/s.

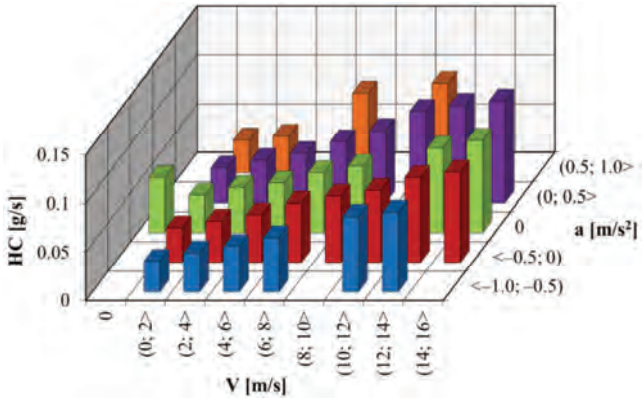

Fig. 12. HC exhaust emission intensity of the tested vehicle in speed and acceleration intervals

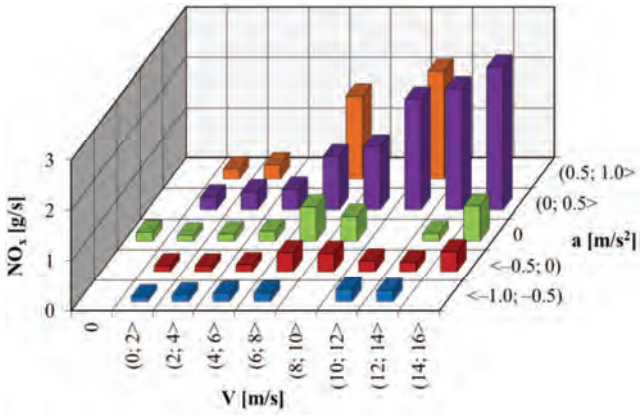

Fig. 13. NO_x exhaust emission intensity of the tested vehicle in speed and acceleration intervals

As in the case of NO_x, the PM emission intensity (Fig. 14) showed that the highest values occurred in the ranges (6 m/s; 16 m/s> and (0 m/s^2; 1 m/s^2>. Maximum value 0.34) g/s was obtained at a single operating point characterized by the speed ranges (6 m/s; 8 m/s> and acceleration (0.5 m/s^2; 1 m/s^2>). The average value of the PM emission rate was 0.04 g/s, while the value for idling did not exceed 0.01 g/s.

The next stage of the research was the measurements of the specific exhaust emissions of the tested object and comparing them with the exhaust emission standards applicable in the years of its production, included in the ORE B13 Rp 22 report, introduced in 1991. During the measurements, the locomotive obtained the specific emission of carbon monoxide at the level of 7.8 g/kWh. It was the only compound that did not meet the limits (4.0 g/kWh) established in the standard. On the other hand, the locomotive met the requirements for HC and NO_x, their values were respectively 1.12 g/kWh and 8.4 g/kWh. Tthe limit values were 1.6 g/kWh for hydrocarbon and 16 g/kWh for nitrogen oxides. However, the report did not specify any particulate limits. The favorable results result from the fact that the engine of the tested object was modernized in 1995 in order to improve its ecological indicators.

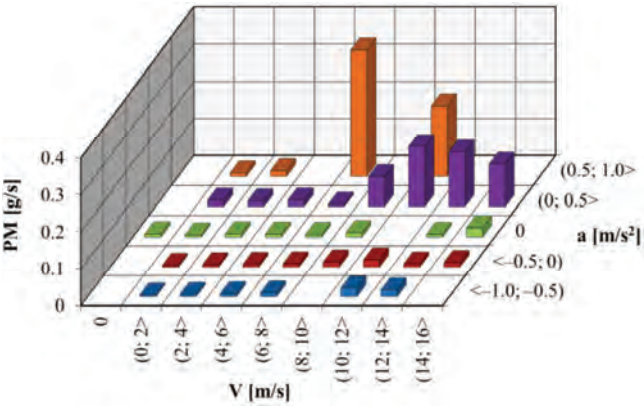

Fig. 14. PM exhaust emission intensity of the tested vehicle in speed and acceleration intervals

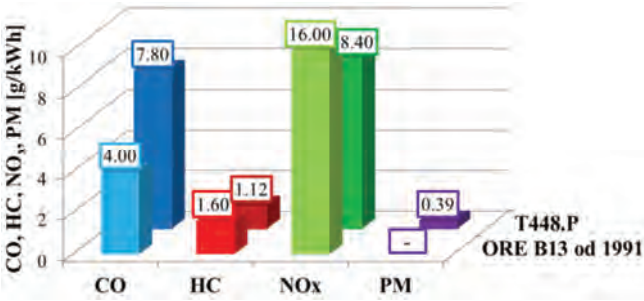

Fig. 15. Summary of test results with the limit values of harmful exhaust compounds according to ORE B13 Rp 22 in force since 1991

6. Summary

The number of diesel rail vehicles operated in Poland, their share in the rolling stock and planned investments indicate that non-electrified rolling stock will still constitute a significant part of rail vehicles in Poland. Successive exhaust emission standards for rail vehicles reduce the maximum specific emissions of toxic compounds. Tests on the emission of toxic compounds from rail vehicle engines should evolve towards combining stationary tests and measurements in real operating conditions.

The presented example of testing a rail vehicle during real operation proves that it is possible to learn more about the operating conditions of locomotives and their influence on ecological indicators. The test object had an engine in good technical condition (after renovation), thanks to which the obtained specific emission results indicate that it meets the limit according to which it was approved in addition to CO. In addition, it is not possible to emit PM as the ORE

B13 standard did not define a value for this toxic compound.

The use of PEMS equipment makes it possible to measure emissions during the normal operation of rolling stock – taking into account the limitations related to the gauge and safety. However, the introduction of the conformity factor CF may allow effective use of tests under real engine operating conditions and comparison of their results with the maximum values specified by EU standards. It should also be expected that remote sensing solutions for measuring rail vehicles will allow to identify the most environmentally harmful vehicles for further research.

Acknowledgements

The research was funded by European Union from European Regional Development Fund through the National Centre for Research and Development (Narodowe Centrum Badań i Rozwoju) – research project within the Smart Growth Programme (contract No. POIR.04.01.02-00-0002/18).

Nomenclature

CAN	controller area network
CF	conformity factor
CI	compression ignition
CO	carbon monoxide
CO_2	carbon dioxide
DPF	diesel particulate filter
FID	flame ionization detector
GPS	global positioning system
HC	hydrocarbons
ISO	international organization for standardization
LAN	local area network
NDIR	non-dispersive infrared
NDUV	non-dispersive ultra violet
NO_x	nitrogen oxides
NTA	new type approval
OBD	on-board diagnostics
ORE	centre for education development
PEMS	portable emissions measurement systems
PM	particulate matter
RDE	real driving emissions
SCR	selective catalytic reduction
SI	spark ignition
WLTP	world harmonized light-duty vehicles

Bibliography

[1] ANDRZEJEWSKI, M., DASZKIEWICZ, P., RYMANIAK, Ł. et al. Impact of modernization of locomotives operated in Poland on the emission of toxic compounds in exhaust gases. *Autobusy: Technika, Eksploatacja, Systemy transportowe*. 2018, **19**(12), 54-57. https://doi.org/10.24136/atest.2018.353

[2] ANDRZEJEWSKI, M., FUĆ, P., GALLAS, D. et al. Impact of driving style on the exhaust emission of a diesel multiple unit. *17th International Conference on Railway Engineering Design & Operation* (COMPRAIL 2020), 365-376. https://doi.org/10.2495/CR200341

[3] ANDRZEJEWSKI, M., PIELECHA, I., MERKISZ, J. et al. Legal conditions in the aspect of pollutant emissions from exhaust systems of rail vehicles engines. Journal of KONES. 2018, **25**(1), 257-264. https://doi.org/10.5604/01.3001.0012.2475

[4] Directive 2004/ 26/EC of the European Parliament and of the Council of 21 April 2004 amending Directive 97/68/EC on the approximation of the laws of the Member States relating to measures against the emission of gaseous and particulate pollutants from internal combustion engines to be installed in non-road mobile machinery. https://eur-lex.europa.eu/legal-content/EN/TXT/?uri=celex%3A32004L0026

[5] Dokumentacja techniczno-rozruchowa zmodernizowanej lokomotywy spalinowej Typu T448.P TOM II. http://www.katalogkolejowy.pl/produkty_det/3899

[6] Dyrektywa Komisji 2010/26/UE z dnia 31 marca 2010 r. zmieniająca dyrektywę 97/68/WE Parlamentu Europejskiego i Rady w sprawie zbliżenia ustawodawstw państw członkowskich odnoszących się do środków dotyczących ograniczenia emisji zanieczyszczeń gazowych i pyłowych z silników spalinowych montowanych w maszynach samojezdnych nieporuszających się po drogach. https://eur-lex.europa.eu/legal-content/PL/TXT/?uri=CELEX%3A32010L0026

[7] ICCT. Technical considerations for choosing a metric for vehicle remote-sensing regulations. November 2019. https://theicct.org/publications/china-vehicle-remote-sensing-regulations

[8] ISO/DIS 8178-1.2, 1995. Reciprocating internal combustion engines – exhaust emission measurement – Part 1: Test-bed measurement of gaseous and particulate exhaust emissions. https://www.iso.org/standard/15268.html

[9] LEWANDOWSKI, M. Silniki spalinowe pojazdów szynowych. WKŁ, Warszawa 2018.

[10] LIJEWSKI, P., MERKISZ, J., PIELECHA, J. PEMS-based investigations into exhaust emissions from non-road and rail vehicles. *Combustion Engines*. 2016, **166**(3), 46-53. https://doi.org/10.19206/CE-2016-339

[11] Mały Rocznik Statystyczny Polski. Warszawa 2004.

[12] Mały Rocznik Statystyczny Polski. Warszawa 2009.

[13] Mały Rocznik Statystyczny Polski. Warszawa 2014.

[14] Mały Rocznik Statystyczny Polski. Warszawa 2019.

[15] MERKISZ, J., LIJEWSKI, P., FUĆ, P. et al. Exhaust emission tests from non-road vehicles conducted with the use of PEMS analyzers. *Eksploatacja i Niezawodność – Maintenance and Reliability*. 2013, **15**(4), 364-368.

[16] MERKISZ, J., PIELECHA, I., ANDRZEJEWSKI, M. et al. Legal conditions in the aspect of pollutant emissions from exhaust systems of rail vehicles engines. *Journal of KONES*. 2018, **25**(1), 257-264. https://doi.org/10.5604/01.3001.0012.2475

[17] MERKISZ, J., RYMANIAK, Ł., LIJEWSKI, P. et al. Tests of ecological indicators of two-way vehicles meeting Stage IIIB and Stage IV standards in real operating conditions. *Rail Vehicles/Pojazdy Szynowe*. 2020, **1**, 1-9. https://doi.org/10.53502/RAIL-138495

[18] Regulation (EU) 2016/1628 of the European Parliament and of the Council of 14 September 2016 on requirements relating to gaseous and particulate pollutant emission limits and type-approval for internal combustion engines for non-road mobile machinery, amending Regulations (EU) No 1024/2012 and (EU) No 167/2013, and amending and repealing Directive 97/68/EC (Text with EEA relevance). https://eur-lex.europa.eu/legal-content/EN/TXT/?uri=CELEX%3A32016R1628

[19] Urząd transportu kolejowego. Tabor kolejowy przewoźników towarowych – stan obecny i plany do 2023 r. 2018.

[20] ASCO RAIL sp. z o.o. https://www.ascorail.pl (accessed on 05.2021)

[21] DieselNet. Engine & emission technology online – since 1997. https://dieselnet.com (accessed on 05.2021)

Michalina Kamińska, MEng. – Faculty of Civil and Transport Engineering, Poznan University of Technology.
e-mail: *michalina.kaminska@put.poznan.pl*

Natalia Szymlet, MEng. – Faculty of Civil and Transport Engineering, Poznan University of Technology.
e-mail: *natalia.r.szymlet@doctorate.put.poznan.pl*

Daniel Kołodziejek, MEng. – Faculty of Civil and Transport Engineering, Poznan University of Technology.
e-mail: *daniel.kolodziejek@student.put.poznan.pl*

Prof. Paweł Fuć, DSc., DEng. – Faculty of Civil and Transport Engineering, Poznan University of Technology.
e-mail: *pawel.fuc@put.poznan.pl*

Rafał Grzeszczyk, DEng. – ODIUT Automex sp. z o.o., WSB Gdańsk.
e-mail: *rafal.grzeszczyk@automex.eu*

Article citation info:
MENES, M. Program initiatives of public authorities in the field of hydrogenation of the economy in a global perspective, as of the end of 2020. *Combustion Engines.* 2022, **189**(2), 18-29. https://doi.org/10.19206/CE-142170

Maciej MENES

Combustion Engines
Polish Scientific Society of Combustion Engines

Program initiatives of public authorities in the field of hydrogenation of the economy in a global perspective, as of the end of 2020

ARTICLE INFO

Received: 14 July 2021
Revised: 20 August 2021
Accepted: 12 September 2021
Available online: 24 September 2021

In the years 2016–2020, there has been a significant acceleration in the development of technologies for the hydrogen energy use and their popularization in practice. The value of the global hydrogen market in 2018 was estimated at US $122 billion, predicted that it will increase to US $155 billion by the 2022. The appropriate policy framework has a major impact on the development of new technologies, in particular during research, prototype implementations and the initial phase of their commercialization. Of course, this also fully applies to hydrogen technologies, which was confirmed, i.a., in its study by The Hydrogen Council, a leading global organization in this field. The spearheading countries intensively involved in the development and dissemination of hydrogen technologies are primarily: Japan, China, South Korea, Germany, France, Great Britain, Scandinavian and Benelux countries, as well as Canada and the USA. A dozen more countries making up the leading group, such as: Italy, Spain, Portugal, Australia, New Zealand, Brazil, India and South Africa are making efforts to join the global hydrogen race and complete the leading group. The scale of the global development of hydrogen technologies is illustrated by the fact that at the end of 2019, vehicles with hydrogen fuel cells and the publicly accessible hydrogen refuelling stations serving them already operated in 18 countries. An effective use of the incurred expenditures undoubtedly requires the interested states to formulate an appropriate policy (strategy) for the hydrogenation of the economy, including, in addition to precisely defined long-term objectives, e.g. elements of support from public administration, assurance of: stable investment conditions and the necessary regulatory conditions. The article attempts to synthetically present the political framework, i.e. the functioning plans and programs as well as national strategies for the development of hydrogen technology and economy in 19 countries.

Key words: *greenhouse gases, hydrogen vehicles, emission measurement, directions of automotive development*

1. Introduction

In the years 2016–2020, there has been a significant acceleration in the development of technologies for the hydrogen energy use and their popularization in practice. The value of the global hydrogen market in 2018 was estimated at US $122 billion, predicted that it will increase to US $155 billion by the 2022 [1].

The appropriate policy framework has a major impact on the development of new technologies, in particular during research, prototype implementations and the initial phase of their commercialization. Of course, this also fully applies to hydrogen technologies, which was confirmed, i.a., in its study by The Hydrogen Council, a leading global organization in this field.

In the 2017 study, it clearly stated that the development of appropriate programs and strategies for the hydrogenation of the economy should be the starting point and the way to the dynamic development of hydrogen technologies, optimizing the costs of this development and achieving an adequate level of profitability as soon as possible [2].

The spearheading countries intensively involved in the development and dissemination of hydrogen technologies are primarily: Japan, China, South Korea, Germany, France, Great Britain, Scandinavian and Benelux countries, as well as Canada and the USA.

A dozen more countries making up the leading group, such as: Italy, Spain, Portugal, Australia, New Zealand, Brazil, India and South Africa are making efforts to join the global hydrogen race and complete the leading group. The scale of the global development of hydrogen technologies is illustrated by the fact that at the end of 2019, vehicles with hydrogen fuel cells and the publicly accessible hydrogen refuelling stations serving them already operated in 18 countries [3].

The article attempts to synthetically present the political framework, i.e. the functioning plans and programs as well as national strategies for the development of hydrogen technology and economy in 19 countries.

2. National strategies for the development of hydrogen technology and economy in 19 countries

Australia

Work on the hydrogen energy use was undertaken in Australia in the last years of the 20th century.

Australia is a specific country where, apart from numerous projects related to the development of hydrogen technologies, a lot is related to the production of hydrogen itself (out of 120 hydrogen projects carried out by the 2005, 55 were related to obtaining hydrogen from fossil fuels and in water electrolysis processes) [4]. This is due, on the one hand, to Australia's possession of raw materials and climate conditions, and on the other hand, to the relative proximity of the large hydrogen markets of Japan, China and South Korea.

Australia's hydrogen export potential was a precondition for undertaking work on a hydrogen economy in this country as early as the early 2000s. The export of the hydrogen produced is considered not only the most important stimulator of the development of the hydrogen economy in Australia, but also one of the basic levers of the assumed economic development of the country [5].

Transport in Australia has been adopted as the primary national area for the energy use of hydrogen, including also technological transport in mining plants or handling equipment [6].

The national roadmap for building a sustainable and effective hydrogen industry has defined the directions for the development of a clean, innovative, safe and competitive hydrogen industry prepared by the government administration, and at the same time established an expert group (Hydrogen Working Group) which was tasked with developing the National Hydrogen Strategy. The Australian Hydrogen Strategy, which includes 57 necessary measures, was published in 2019 [7].

Relevant strategies were also published by the largest Australian states, incl. South Australia [8] and Queensland [9].

The Australian central government alone allocated US $256 million to the research, feasibility studies and demonstration projects in 2015–2019.

Chile

The first country on the South American continent to prepare a strategic document for the development of the hydrogen economy is Chile. The leading element in the national hydrogen strategy published in November 2020 is "green" hydrogen, with the production of which Chile intends to conquer world markets [10].

It is supported by the country's natural conditions, which provide potentially large amounts of cheap electricity from renewable sources (highly sunny desert areas in the north of the country and windy areas in the south of the country), which exceed the domestic demand 70 times. With the cheap electricity, the cost of producing hydrogen, oscillating around 0.8–1 dollar/kg of hydrogen, is among the lowest in the world.

Cheap sources of renewable energy and the "green" hydrogen produced, on the one hand, is to ensure Chile's emission neutrality by 2050, on the other hand, by the 2030, it is to make it one of the three leading exporters of green hydrogen. According to McKinsey & Co's estimates, by the 2030 the Chilean production potential will reach 25 million tons of "green" hydrogen (5% of global demand), for which the country will export 30 billion dollars annually, ensuring 50% of supplies of this energy carrier to Japan and South Korea, and 20% to China [11].

The use of "green" hydrogen energy in the country, which is to ensure a 20% share in reducing CO_2 emissions, is to be concentrated in the gas industry and ecological refining of the mined copper ores.

The assumed development of the hydrogen sector will require investments of approximately USD 200 billion in the next 20 years, which will generate 100,000 new jobs. The Strategy assumes that by the 2025 the total capacity of electrolysers installed in the country will exceed 5 GW. The first Chilean green hydrogen plant to be built in Cabo Negro north of Punta Arenas, consisting of a 3.4 MW wind farm and a 1.25 MW electrolyser, will be commissioned in early 2022.

China

Chinese work on the use of hydrogen energy began in the mid-1950s in the space and military sector.

At the end of the 1980s, research into hydrogen technologies was also undertaken by the civilian sector, and mainly related to road transport. From the very beginning, these studies were carried out under centralized research programs, five-year economic and social development plans of the country as well as regulations and orders of public administration.

The first program with hydrogen propulsion technologies as a component – "National High Technology Research and Development Program" launched in 1987, operated until 2016 [12]. In 1997, the Basic Research Program was launched, which also ran until 2016. Since 2016, research and development work has been carried out under the National Key Research and Development Programs [13]. The directions of the conducted research result from the findings of the next five-year plans for China's socio-economic development.

In the tenth plan for 2001–2005 the issues of hydrogen vehicles were included in the "Electric Vehicle" part, in the eleventh plan for the years 2006–2010 in the "Energy saving a new energy vehicle" part, and in the twelfth plan for 2011–2015 in the "Electric vehicle critical technology "and in the thirteenth plan for 2016–2020 in the part "Energy storage and distributed energy and new energy vehicles" [14].

In May 2015, the Chinese authorities published a ten-year program "Made in China 2025" to modernize ten priority industrial sectors, including the automotive sector, with particular emphasis on the production of vehicles with alternative drives, including hydrogen one [15].

In reference to the above, in 2016 the Strategic Advisory Committee for the technological roadmap for the development of energy-saving technologies and vehicles with alternative drives published, inter alia, "Roadmap for Hydrogen Technologies" [16]. The study assumes that by the 2020, 5,000 hydrogen powered vehicles will be used in China, served by 100 hydrogen refuelling stations, and in 2030 one million vehicles served by more than 1,000 stations.

The specifics of this report, as well as other research works, resulting from the Chinese economic model, is the precise setting of not only strategic objectives, but also dozens of specific goals regarding, for example, the parameters of hydrogen-powered vehicles and their components, and even individual components.

Hydrogenization of transport, as one of the 15 development directions, was also established in the "energy technological revolution and innovative action plan for 2016-2030" published in 2016 by the Development and Reform Committee and the National Energy Agency [17].

The development of hydrogenation in the road transport achieved by the first quarter of 2020: 72 refuelling stations and 6,564 vehicles (mainly low-capacity buses and light-duty trucks) – fulfilling the assumptions of the roadmap from 2016, is a derivative of the public administration's commitment, which spent on the development of the electric car sector over USD 58 billion, including USD 12 billion alone on the development of hydrogenation of transport in 2018 [18].

In recent years in China, the issue of the development of hydrogen technologies outside the transport sector, includ-

ing in March 2019, the issue of the hydrogen energy use was included in the annual speech of the Chinese Prime Minister at the session of the 13th Chinese People's Assembly [19]. The issue of the hydrogen economy was also raised by Chinese President Xi Jinping in his speech on September 22, 2020 announcing China's intention to achieve carbon neutrality by the 2060 [19].

This does not change the fact that to date China does not have a national strategy for the hydrogenation of the economy. In June 2019, the Chinese Hydrogen Alliance (H2CN) established in 2018 by 18 different types of entities, supervised and supported primarily by the Chinese Ministry of Science and Technology, published its own version of the vision of the development of Chinese economy hydrogenation by 2050, which was not an official document [20].

The assumed vision envisages that by the 2050 the share of hydrogen in the national energy balance will increase from 2.7% in 2019 to 10%, the turnover of the hydrogen market will increase from USD 43.5 billion to USD 1.7 trillion, the number of hydrogen refuelling stations will increase 72 to 10,000, and the number of hydrogen-powered passenger cars will increase from several hundred to 5 million. In China, there will be more and more buses and trucks with fuel cells, and the number of hydrogen fuel cell installations will increase from 10,000. up to 5.5 million [19].

Denmark

Denmark is one of the countries in which work on a national strategy for the development of hydrogen economy was initiated at the earliest. As early as 1998, work began on the development of an appropriate program "The Danish hydrogen energy program" [21].

In the Danish activities, the emphasis was placed, apart from the use of hydrogen as a carrier of electricity, on its use in transport. In 2008, the first version of the relevant sectoral program – "National R&D and demostration strategy for FCH transport" was prepared [22]. Based on the above document, in 2014 the Danish transport hydrogenation program "National Implementation Plan (NIP) for hydrogen refuelling infrastructure in Denmark" was published. The program assumed significant financial reliefs both in relation to the costs of purchasing hydrogen vehicles (exemption from registration taxes amounting to 105% of the purchase price and 180% if their price exceeds 10.6 thousand euro), and also in relation to the costs of their operation (exemption from annual road tax) [23].

Exemption from the registration tax, amounting to approx. 30,000 EURO already makes the cost of purchasing a car equipped with hydrogen fuel cells competitive with respect to corresponding mid-range car with an internal combustion engine.

Hydrogen refuelling stations are co-financed up to 50% in both, the construction costs and the costs of subsequent operation. The above rules for promoting the development of hydrogenation in Danish transport are to apply according to the current regulations until 2025.

Finland

Work on the use of hydrogen energy began in Finland in the early 2000s. In 2007, a multi-annual (until 2013) hydrogen program was launched, coordinated by the Finnish Agency for Technology and Innovation (Tekes) [24].

In 2013, the Finnish research centre VTT developed the first national roadmap for the development of hydrogenation in the road transport. The above-mentioned Research Centre also prepared a roadmap for the development of hydrogen technologies in Finland in 2020, at the request of Business Finland [25].

Apart from the advantages of hydrogen as an energy carrier, the paper describes the state of development of hydrogen technologies in the country, discusses the role and costs of production, including the costs of producing "green" hydrogen (the total capacity of wind farms installed in Finland already exceeds 2.3 GW). The basis for the development of the production of "green" hydrogen is to be a well-developed potential of renewable energy production. Based on the SWOT analysis conducted, recommendations and a schedule of actions were formulated, as a result of which the energy use of hydrogen is to significantly contribute to Finland's achievement of carbon neutrality by the 2050. The material prepared by the consulting company Nordic West Office was also devoted to the issue of hydrogenation of the Finnish economy [26].

France

Work on the use of hydrogen energy begun in France at the end of the last decade of the 20th century. In 1998, public administration units, energy companies, producers of hydrogen and hydrogen installations, electrolysers, motor vehicles, scientific research centres as well as regional authorities established the AFHYPAC association (Association Francaise pour l hydrogene et les piles a combustible). In 2013, the H2Mobilite France Consortium, organisation established by the above-mentioned association, developed the first plan for the development of hydrogenation of the French economy limited to the road transport [27]. The ambitious objectives formulated in the Plan, both in terms of the fleet of hydrogen-powered vehicles and the network of hydrogen refuelling stations, have not been achieved to date.

Another, broader-spectrum Program, treating hydrogen technologies as one of the pillars of the planned transformation of the French energy system, was developed in 2018 [28].

Yet another French hydrogen program referred to the findings and even the structure of the content of the quoted report “Hydrogen scaling up. A sustainable pathway for the global Energy transition” prepared in 2017 by the Hydrogen Council.

The findings of the above Program became the basis for the 14-point plan of N. Hulot (the then minister for environmental protection), published on June 1, 2018, to popularize hydrogen as an element of the transformation of the French energy economy [29].

The plan was part of France's second multi-annual energy program covering 2018–2028. As part of the Plan, it was assumed that, starting from 2019, 100 million euro will be spent annually in public funds to support the hydrogenation of the French economy, including for the manufacture of electrolysers producing "green" hydrogen. In September 2020, the national strategy for the development and production of "green" hydrogen was published.

As part of the above strategy, it was assumed that 7 billion euro will be spent by the 2030, including 2 billion euro of the public funds in 2020-2022 for the development of production and use of "green" hydrogen (for the total amount of planned investments exceeding 32 billion euro). The three main objectives of the strategy are:

- reaching the total capacity of the electrolyser park powered by energy from renewable sources of 6.5 GW by the 2030
- development of hydrogenation of transport, in the first place: trucks, buses and railways, on a scale ensuring a reduction of CO_2 emissions by 6 million tonnes by the 2030 (with a reduction of emissions due to the use of "green" hydrogen in all applications of approx. 10 million tonnes)
- development of the research and development facilities and a modern sector of the hydrogen industry employing from 50 to 150 thousand people [30].

Spain

Spain joined the EU efforts to develop hydrogen technologies practically only in 2020. By the end of 2019, only 3 hydrogen refuelling stations were in operation, servicing approx. 35 hydrogen vehicles. In Spain, the industry has so far consumed about 0.5 Mt of hydrogen per year, mainly from the steam reforming processes of natural gas.

The basis for accelerating the activities in the field of hydrogen energy use in Spain were: the final version of the "Integrated Energy and Climate Plan" [31] adopted in January 2020 and the "Long-term strategy for the development of a modern, competitive and climate-neutral Spanish economy in the 2050 perspective" published in July 2020 (ELP), which was approved by the Spanish Council of Ministers on November 3, 2020 [32].

The document assumes that the emission of greenhouse gases by the 2050 will be reduced compared to the emissions from 2018 by 90% (from 334 Mt to 29 Mt). This will be a consequence of, on the one hand, reduction as a result of increased savings and efficiency of energy use (50% reduction in final energy consumption by the 2050), and on the other hand, the development of the renewable energy sector (42% share in final energy consumption in 2030 and 72% share in electricity production). Based on the above findings, the "Roadmap for the development of the hydrogenation of the economy based on green hydrogen", adopted by the Spanish government on October 6, 2020, was developed [33].

The document contains a plan of 60 different types of actions (regulatory, organizational, financial) to ensure that by the 2030 electrolysers with a total capacity of 4 GW (300–600 MW by 2024) will be installed in the country, 100 hydrogen refuelling stations will be built, which should service 5,000 hydrogen cars, there will be 150 buses and two railways with hydrogen train traffic. In the industry, 25% of hydrogen consumed in 2030 is to be produced based on electricity from renewable sources. The planned investments (public and private) will cost about 9 billion euro, and their implementation should ensure that as early as 2030 the national CO_2 emission will be reduced by 4.6 Mt.

The Netherlands

The Netherlands has been a European giant in the production of hydrogen for years. Most of the approximately one million tonnes of hydrogen produced primarily from natural gas is consumed by the chemical and refining industries. The issue of using hydrogen for energy purposes, primarily in the road transport, was undertaken in the early years of the 21st century. The first major transport hydrogenation program was published by the Dutch Ministry of Transport and the Environment in 2013 [34].

Another version of the Dutch transport hydrogenation development plan was presented in the Dutch hydrogen infrastructure development plan (NIP-NL) implemented in 2014/2015 as part of the EU project TEN-T-HIT (Hydrogen Infrastructure for Transport) [35].

The adopted assumptions and goals were verified and expanded in the roadmap for the development of hydrogenation in the Dutch economy, commissioned by the Dutch Ministry of Economy and Economic Policy in 2018 [36].

In the report covering 7 areas of hydrogen use, apart from quantitative projections, the directions of desired activities supporting the development and dissemination of hydrogen technologies by the public administration and other stakeholders as well as the effects in reducing greenhouse gas emissions were defined.

In April 2020, the Dutch government published a national hydrogen strategy based, among the others, on the findings of the above report as well as the findings of the National Climate Agreement, signed in 2019 with social partners [37].

Japan

Work on the use of hydrogen as an energy source began in Japan in the last years of the 20th century and initially focused on the most emissive area of heating and supplying indoor facilities (40% of total Japanese CO_2 emissions).

In 2002, the first multi-year (2002–2013) research and demonstration program "Japan Hydrogen and Fuel Cell Demonstration Project" was launched. Since 2003, the control of the program has been taken over by a specialized governmental agency "New Energy and Industrial Technology Development Organization" (NEDO).

As part of the program, the first projections of the number of hydrogen refuelling stations and hydrogen vehicles for 2010–2020–2030 were formulated.

In order to accelerate the unsatisfactory development of hydrogen technologies, in 2013 the Council for a Strategy for Hydrogen and Fuel Cell was established. In 2014, a roadmap prepared under the auspices of the Council was published, in which the objectives and schedule for the development of hydrogen technologies in various areas were specified [38].

The directions for the development of the hydrogen economy, updated and supplemented in 2016, became the basis for the official announcement by the Japanese prime minister in April 2017 of the idea of building the world's first "hydrogen society". Following the above declaration, in December 2017, a document specifying the strategy for building a "hydrogen society" was published (Basic Hydrogen Strategy) [39].

The development objectives set in the strategy are accompanied by specific recommendations, as well as the financial parametrisation of their economic conditions. Despite the state's involvement (in the years 2013–2018 alone, the Japanese administration supported the research and demonstration projects underway with USD 1.458 billion), the assumed objectives were not fully implemented [40].

The assumptions and objectives for building a "hydrogen society" formulated in the "Basic Hydrogen Strategy" based on the acquired knowledge and practical experience in the implementation of the hydrogen energy use technology have been updated in the next version of the strategic roadmap, published in March 2019 [41].

In the current modification of the assumptions and objectives of the Japanese strategy for building a "hydrogen society" it was emphasized that these goals will be subject to constant evaluation by appropriate expert groups.

Japanese activities in the field of the development of the hydrogen energy use are characterized by systematic and long-term nature and, above all, a comprehensive approach to hydrogen technologies as an instrument for transforming the country's energy system. This does not change the fact that at least the current versions of the development plans in question, in the context of the ambitious goals clashing with reality, are significantly toned down.

Canada

Work on the hydrogen energy use began in Canada in the 1980s. The research and implementation of the results made Canada one of the world leaders in the development of hydrogen technologies.

The first report on the development of hydrogen transport commissioned by the Canadian Natural Resources Agency was produced as early as 2005 [42]. In the same year, the discussions on the need to develop a strategy for the hydrogenation of the Canadian economy began [43]. The issue of hydrogen-powered vehicles was also mentioned in the directional document "Electric Vehicle Technology Roadmap for Canada"[44] published in 2010. In 2016, the Canadian administration adopted a framework for the development of a zero-emission economy, including the use of hydrogen [45].

The first strictly hydrogen oriented document defining 12 basic directions for the development of the use of hydrogen in the Canadian economy, along with relevant implementation recommendations, was published in 2019 [46]. In June 2020, the governmental agency Natural Resources Canada announced that the work on the preparation of the Canadian hydrogen strategy, which had been postulated for years, had been initiated [47]. The above initiative was supported, among the others, by the Canadian hydrogen association The Canadian Transportation Fuel Cell Association. The date of publishing the strategy has not yet been specified [48].

South Korea

Research on the hydrogen energy use began in South Korea as part of the 10-year plan – "10 Year Alternative Energy Technology Development Program" in 1988. Work continued under the next edition of the program in 1998–2007 [49].

The development of hydrogen technologies accelerated after 2000, when the Ministry of Science and Technology (MOST) launched the "High Efficient Hydrogen Program" based on which in 2003 the "21 Century Frontier Hydrogen Production Program" was formulated. At the same time, in 2004, the National DR&D Organization for Hydrogen and Fuel Cell launched a long-term implementation and demonstration program on hydrogen technologies. A year later, the first directional plan for the development of hydrogenation in the South Korean economy was announced – "Plan for hydrogen economy" [50].

As a result of the combined efforts of the public administration, which supported activities related to the development of hydrogen technologies with an amount of USD 586 million in 2004–2011 alone, and the efforts of the industrial sector in February 2013, the world's first commercial hydrogen FCEV Hyundai ix35 cars rolled off the production lines of the Ulsan factory.

In 2016, the Hydrogen Fusion Alliance associating central and local administration units, automotive companies, energy companies, and research and development centres, published a report on the development of hydrogenation of Korean car transport in 2020–2030 [51].

In order to boost the hydrogenation of the Korean economy, a working group was established in 2018, consisting of representatives of the public administration and the private sector, with the task of developing a road map for the development and dissemination of hydrogen technologies [52].

This document presenting a vision of the development of hydrogen technologies in South Korea by the 2050 was published in early 2019 [53].

Germany

In Germany, work on the hydrogen energy use was undertaken in the 1990s. This work focused primarily on the use of hydrogen in transport.

The subject theoretical studies were launched i.a. as part of the work that began in 1998 on the development of an energy strategy for transport – "Verkehrswirtschaftliche Energiestrategie" (VES). The implementation of clean energy technologies, including hydrogenation of transport, was undertaken within the framework of the Clean Energy Partnership (CEP), established in 2002 by the interested entities, on the initiative of the Federal Minister of Transport, Environment and Construction (BMVBS). In March 2006, the same Minister announced the first government plan to support the development of hydrogen technologies in 2006–2016, amounting to 500 million euro (which eventually increased to 700 million euro) [54].

The funds were used to finance the implementation of the National Innovation Program Hydrogen and Fuel Cell Technology (NIP I). In order to manage the above program, in 2008 the governmental organization National Organization Hydrogen and Fuel Cell Technology – NOW Gmbh was established. Today, this organization manages the second edition of the program (NIP II) covering the years 2016–2026 (Program for Hydrogen and Fuel Cell Technology 2016–2026 – for market preparation for competitive products). Despite the involvement of significant funds, also from public budgets, the implementation of German

transport hydrogenation development plans has been marked by significant delays from the very beginning.

The plan from 2008 assumed, inter alia, that in 2015, 100,000 hydrogen cars should be operated in Germany, served by 142–218 hydrogen refuelling stations, and in 2020 respectively 350–580 thousand hydrogen passenger cars and 56–96 thousand hydrogen vans served by 1296–2666 [55] hydrogen refuelling stations. In the next version of the plan in 2020, 150 thousand. hydrogen-powered cars served by 400 hydrogen refuelling stations [56]. In fact, at the end of 2019, there were 81 hydrogen refuelling stations in Germany serving just 679 hydrogen powered vehicles [57].

Some dynamics of the implementation of the assumed plans was brought about by the establishment in 2009, by the interested entities, primarily automotive and energy ones, with the participation of NOW GmbH, of a public-private initiative supporting the development of hydrogenation of the German H2Mobility transport.

The implementation of the German strategy for the hydrogenation of the economy published in June 2020 should bring a fundamental breakthrough [58]. The strategy defines the necessary actions to achieve the German climate objectives. The basic directions of activities are:

- increasing the competitiveness of hydrogen as an energy medium,
- development of the German market for hydrogen technologies (from 55 TWh currently to 90–110 TWh in the 2030) associated with the development of international cooperation ensuring the necessary import of "green hydrogen",
- development of knowledge and highly qualified labour resources,
- development of raw material use of hydrogen,
- increase in the share of hydrogen in the country's energy balance,
- development of infrastructure for transport and distribution of hydrogen,
- modelling and support of energy transformation processes by the public authorities,
- development of German industry and securing access to the world markets for German companies,
- participation in the creation and cooperation on the global hydrogen market,
- taking advantage of the opportunities arising from global cooperation,
- creating and ensuring a safe infrastructure for the production, transport, storage and use of hydrogen,
- improvement of the environmental protection policy.

The strategy, which is to be evaluated every 3 years [58], assumes 38 concrete activities of various nature, covering both the production of hydrogen and various areas of its use, including:

- improving the competitiveness of electricity from renewable sources (including the introduction of payments for CO_2 emissions from transport and heating), as well as limiting the taxation of electricity used to produce "green" hydrogen,
- share of public funds in the construction of electrolysers,
- strengthening financial activities under the National Innovation Program for Hydrogen and Fuel Cell Technology with funds from the Energy and Climate Found fund (3.6 billion euro by the 2023),
- financing from the above Fund for the development of production of advanced biofuels based on hydrogen (1.1 billion euro by the 2025) and the development of charging and refuelling infrastructure for alternative fuels (3.4 billion euro),
- changes to the Eurovignette Directive to make road tolls dependent on the level of CO_2 emissions.

Similar activities supporting the development of hydrogen use are also planned for aviation and water transport, as well as for other industries such as steel, chemical industry, logistics and heating [58].

For the hydrogenation of industrial production processes leading to the reduction of CO_2 emissions, over a billion euro of public funds alone have been allocated for the period 2020–2023.

The implementation of strategy is to be managed by the interministerial Hydrogen Committee composed of the heads of the ministries involved, supported by the National Hydrogen Council consisting of 26 experts [58].

On 3 June 2020, the Committee adopted a "package for the future" with a budget of an additional 7 billion euro for the development of hydrogen technologies in Germany and 2 billion euro for strengthening international cooperation in the hydrogen economy.

Norway

In Norway, the first organization supporting the development of hydrogen energy use, The Norwegian Hydrogen Forum, was established in 1996. In 2005, the Ministry of Fuel and Energy and Transport and Communications developed one of the world's first national strategies for the development of hydrogenation of the economy [59]. It was part of the measures taken in Norway since 1989 to counteract global warming. The 2005 study planned a reduction of CO_2 emissions by 30% in 2020, 40% in 2030 and 100% in 2050 in relation to the emissions from 1990 [60]. The planned activities referred primarily to the electrification, including hydrogenation, transport (road and water) which is responsible for 1/3 of total Norwegian greenhouse gas emissions. The work was continued by The Norwegian Hydrogen Council established by the above-mentioned ministries in 2005.

In 2006, the Council published the first hydrogen technology development plan to the 2020 (Action Plan 2007–2010) [61].

The adopted objectives, as in other countries supporting hydrogenation of the economy, turned out to be too ambitious and were not achieved. The next version of the plan was prepared by the Council for the years 2012–2015. In 2020, another version of the Norwegian hydrogen strategy was published [62]. It was created based on the "Green Transition Package" presented in May 2020 by the Norwegian government with a budget of over NOK 3.5 billion [63].

The 2020 strategy also focused, apart from the production and trade of hydrogen, on the development of its use in transport. The development of hydrogenation in the road

transport will result from the adoption of strict restrictions assuming that in Norway from the 2025 new passenger cars, delivery vans and city buses must be zero-emission, and from 2030 also distribution transport in the centres of large cities must be zero-emission. From 2030, 75% of the long-distance buses and 50% of trucks must be emission-free [63].

Ultimately, in 2050, all Norwegian transport is to be zero-emission.

New Zealand

New Zealand is one of the countries that returned to intensive activities in the field of hydrogen technologies after years of stagnation. The first report on the hydrogenation of the New Zealand economy was made in 2007. This year, New Zealand joined the International Partnership on Hydrogen Economy – which it does not currently belong to, and in 2005 it joined the IEA Hydrogen Implementation Agreement [64].

The modern vision of the development of the hydrogenation of the New Zealand economy was published in September 2019 [65]. The work carried out in 2017–2019 as well as the results of various pilot hydrogen projects launched in those years were used to develop the document [66].

The main assumption of the study is the development, based on the existing renewable energy sources, of the production of "green" hydrogen, which will ensure the implementation of the strategic objective of achieving carbon neutrality of the New Zealand economy by the 2050 (as early as in 2035, 100% of the electricity produced in the country is to come from renewable sources – with 85% currently) [66].

The "green" hydrogen produced is to ensure the decarbonisation of: transport, industrial processes (production of ammonia and steel and low-carbon oil refining) and the heating sector, and become the subject of export (300,000 tonnes in 2035).

Specification of the adopted goals for individual periods (until 2020, in 2020–2025, 2025–2030 and in the longer term) is included in the roadmap [66]. By the 2030, a network of approx. 200 hydrogen refuelling stations is planned (there were none by the 2020) on non-urban roads, complementing the network of stations in the large cities, as well as e.g. introduction to operation of hydrogen vessels. In addition to the national road map for the development of hydrogen technologies, a regional roadmap for the development of an integrated infrastructure for production, transmission, storage and use of hydrogen in the Taranaki port area, which is one of New Zealand's hydrogen hubs, has also been published [67].

The publication of the document, as intended, triggered a nationwide discussion in which all citizens and legal entities, until October 25, 2019, could express their opinions on the proposed directions for the development of the hydrogenation of the New Zealand economy. The results of this discussion are to be used in the future development of a national strategy for building a hydrogen economy.

Portugal

One of the first European countries, nota bene, with relatively limited achievements in the field of research and implementation of hydrogen technologies so far, which developed a national hydrogen strategy, is Portugal. The need to prepare a strategy for the development of the hydrogenation of the economy was mentioned already in 2007 [68]. Ultimately, such a strategy was published by the Portuguese Council of Ministers in May 2020 and adopted after a public debate in August 2020 [69].

The national hydrogen strategy was based on the results of a series of studies on the role and possibilities of the hydrogen energy use [70], as well as on the roadmap to achieve carbon neutrality by the 2050 developed in 2016 [71] and the National Energy and Climate Plan [72]. The main objectives of the Portuguese hydrogen strategy, similarly to the strategies of other countries, are decarbonisation of the economy and transformation of the country's energy system. This is all the more important in Portugal's Conditions because, on the one hand, 100% of the fossil fuel consumed is imported, and on the other hand, the country's natural and climatic conditions are extremely favourable for the development of cheap green hydrogen production based on electricity from renewable sources. The Strategy assumes that by the 2030, a share of renewable energy in the national balance will increase to 47% (also in the electricity production to 80%), and the total capacity of electrolysers to 1 GW. There should be 50 to 100 hydrogen refuelling stations in the country, which should service from 400 to 750 buses, 400–500 heavy-duty hydrogen-powered cars and 750–1000 hydrogen-powered vans.

Expenditures related to the hydrogenation of the economy in the perspective of 2030 alone were estimated at 7 billion euro, of which about a billion would constitute public funds.

Sweden

Work on the hydrogen energy use was started by the Swedish concern ASEA (nowadays ABB) in the 60s of the last century. The first systematic research program, Fuel Cell, financed by the Swedish Foundation for Strategies Environmental Research, was launched in 1997. As part of the program lasting until 2010, as well as subsequent initiatives, including EU initiatives, a number of research and demonstration projects devoted to the hydrogen energy use, both nationally and regionally, were carried out.

The most important examples are:

– National Hydrogen Infrastructure Development Plan for Transport [73]
– Swedish transport hydrogenation development program [74]
– or variant scenarios for the assumed development of hydrogenation in the Swedish economy [75].

The starting point for these projects are the arrangements adopted in successive versions of the Swedish energy and climate plans (NECP). Already in 2009, as part of the integrated energy and climate policy, it was assumed that by the 2050 Sweden would become an emission-neutral country (in the current version even in 2045), and an important step in this regard should be the complete independ-

ence of the Swedish transport by the 2030 from oil-derived fuels.

This does not change the fact that the long-term national strategy for the hydrogenation of the Swedish economy, including Swedish transport, has not yet been specified.

United Kingdom

The real interest in hydrogen as an energy carrier in Great Britain appeared only in the 2000s. This interest was initially focused on the use of hydrogen in the road transport, and then also in heating and powering buildings.

In 2013, The UK H2 Mobility, an organization created in 2011 by the government administration and automotive and energy entities, published the first directional plan for the implementation of hydrogen propulsion in British transport in 2015–2030 [76].

The first comprehensive vision of the potential benefits of the development of hydrogenation in the British economy was presented in a report commissioned by the government administration by the consortium: E4 Tech and Element Energy and published at the end of 2016 [77]. Already this report underlined the need for a British hydrogen strategy [77].

This does not change the fact that despite a number of achievements in the hydrogen technology and the involvement of many British players, this strategy has not been developed to date.

Postulates regarding the necessity to develop a national hydrogen strategy have intensified especially in the last several months. There were, among the others, in a report published in 2020, which presents the next version of the hydrogen road map until 2035 (with a perspective until 2050) [78]. The Business Energy and Industrial Strategy Committee also called for an urgent development of a national hydrogen strategy [79]. In the report "Renewable Hydrogen – Seizing the UK Opportunity", the implementation of the above-mentioned postulate was specified at the end of 2020 [80]. So far, a half-answer has been brought by the 10-point green plan announced by the British Prime Minister on November 17, 2020 [81]. Although the above plan includes hydrogen technologies among other technologies leading to the reduction of greenhouse gas emissions by 2035, but it differs significantly from the programming documents on hydrogenation prepared in other countries.

Italy

Work on the hydrogen energy use began in Italy in the early 2000s. In 2005, the first Italian hydrogen platform was launched under the auspices of the Ministry of the Environment. In 2016, the Mobilite H2IT Hydrogen Association (Associazione Italiana Idrogeno e Cella Combustile – Mobilita Idrogena H2IT) prepared, for the needs of the Italian Ministry of Development, the first version of the "National Development Plan for Hydrogenation in Car Transport". The provisions of the above plan were incorporated into the Italian "Alternative Fuels Infrastructure Development Plan". A modified version of the "National Road Transport Hydrogenation Development Plan" was released in 2019 [83].

In November 2020, a draft of initial guidelines for the preparation of the Italian economy hydrogenation strategy was published. The document assumes that by the 2030 10 billion euro will be invested in the hydrogenation of the Italian economy, 50% of which will be from public funds, and these investments will reduce Italian CO_2 emissions by 8 Mt, provide 200,000 new jobs and an increase in Italian GDP by 27 billion euro a year.

USA

The United States of America are a country that started the era of practical hydrogen energy use in the seventies of the last century, incl. in the Gemini and Apollo space programs.

In the Energy Act of 1992, hydrogen was already mentioned among domestic energy sources [84]. In the national energy policy of 2001, it was recommended to start work on technologies for the hydrogen energy use in various applications [85].

In February 2002, the US Ministry of Energy published precursor, on a world-scale, vision of the hydrogen economy development [86]. The first national roadmap for the development of economic hydrogenation, published in November 2002, brought the vision into reality [87]. The above studies were not implementation documents, but only information and cognitive ones. In the next EPAC energy law in 2005, an entire chapter was devoted to the hydrogen [88]. Following the provisions of EPAC from 2005, the Ministry of Energy in 2006 published an integrated plan of research and development works and demonstration activities in the field of hydrogen economy [89]. Another version of the plan was published in 2011 [90]. In 2017, a multivariant scenario for the hydrogenation of American road transport was published [91]. In June 2020, the Ministry of Energy published the preliminary assumptions of the hydrogen strategy, recognizing hydrogen as one of the basic elements of building a low-carbon economy [92]. The document summarizing the development of hydrogen technologies to date defines four priority directions, namely the development of "green hydrogen" production, the development of hydrogen infrastructure supporting transport, the development of hydrogen storage capacity and the development of the use of hydrogen for energy and fuel production.

In total, in the years 2004–2018, the Ministry of Energy and its subordinate institutions spent over USD 2.1 billion in public funds to support research and development activities [93].

Despite the American achievements, primarily in science, and support for the development of hydrogen technologies by the public administration, this country being one of the leading hydrogen countries, has not yet developed and adopted a national strategy for the hydrogenation of the economy [94].

The need for such a document specifying and coordinating both the current and future directions of activities is postulated by a number of projects implemented in various areas of hydrogenation development, especially transport [95]. The scientific response to the above demands was the preparation in 2020, under the auspices of Fuel Cell and Hydrogen Energy Association, of the American roadmap for the hydrogenation of the economy. According to the study, in 2030, hydrogen should account for 14% of all

energy consumed in the US, which should result in a 16% reduction in CO_2 emissions and a 36% reduction in NO_x emissions. The turnover of the sector with 3.4 million employees should reach USD 750 billion [96].

3. Discussion

The proper policy framework has a major impact on the development of new technologies, in particular in the research, prototype deployment and pre-dissemination phases. This fully applies to the technology of using hydrogen energy.

The survey shows that by the end of 2020, various types of documents have been developed in over 20 countries: plans, programs, road maps, national strategies for the development of hydrogen technologies. The main common points of these studies include:

- recognition of hydrogen as an important component of the transformation of national energy systems towards reducing the generated CO_2 emissions
- persistent uncertainty as to the dynamics of the decline in costs of production of hydrogen and other elements of hydrogen technologies
- focus on the energy use of hydrogen
- emergence of a group of countries with favourable conditions for cheap production of green hydrogen based on renewable energy sources.

Counteracting further global warming has become not only an absolute priority for the European Union, but also hydrogen has been widely recognised as one of the key factors in the necessary transformation. The production costs of individual components of hydrogen technologies' energy systems entered the path of their radical reduction (e.g. the costs of producing "green hydrogen" in Chile in the process of water electrolysis based on electricity from renewable sources fell to the level of 0.8–1.0 US dollars per kilogram of hydrogen). The continuous improvement of hydrogen technologies, including a significant improvement in their energy efficiency, was also of great importance. The coming years will show which direction the world energy transformation will take, but there is no doubt that the energy use of hydrogen in transport will certainly be an important element of it.

It seems that we are currently at a turning point in the development of hydrogen propulsion technology. The expansion of the network of hydrogen refuelling stations and the gradual development of the hydrogen vehicle park, undertaken primarily by public administration, also under many international programs, may break the existing development deadlock. This impasse should be overcome by the observed and expected steady decline in the costs of, first of all, the construction of hydrogen refuelling stations, which have already fallen from 1.5 million to approx. 700-800 thousand Euro at present and the production costs of hydrogen vehicles. The construction costs of a hydrogen refuelling station should drop to PLN 390–470 thousand Euro in 2030 yet. The production costs of a hydrogen passenger car should decrease from 62 thousand, in 2015 to 22.6 thousand Euro in 2030, 18.7 thousand Euro in 2040 and 18 thousand Euro in 2050. Hydrogen unit prices and the annual maintenance costs of a hydrogen vehicle should also fall.

The energy use of hydrogen in recent years in many economic sectors, among the others in transport, including especially motor transport, has finally reached the pre-commercial phase. In practice, this means that the technologies developed, e.g. hydrogen propulsion of transport means (except aviation), could already become an increasingly important element of the necessary transformation of the global energy economy towards its gradual decarbonisation.

Not only the individual countries have developed their national strategies for the development of hydrogenation, but this topic has also been taken up by the European Union. On July 8, 2020, the European Commission published the "Strategy for the development of hydrogenation of the economy as an element of building Europe's climate neutrality".

The basic premise of the EU's hydrogen strategy is the development and production of green hydrogen, i.e. the hydrogen produced with electrolysers powered by electricity from renewable sources. Although green hydrogen currently accounts for only 4% of the 8 million tons of hydrogen consumed in Europe, in the future it is to play an increasingly important role both as an integrator of individual economic sectors and as an energy carrier enabling the decarbonisation of economic processes that are difficult or impossible to electrify directly. The share of green hydrogen in the European energy mix is expected to increase from the current 2% to 13–14% in 2050.

The European Commission has unequivocally confirmed that the development of the economy hydrogenation is one of the key elements in achieving the goal of reducing the EU CO_2 emissions by 50–55% yet in 2030. To this end, in the years 2021–2024, new electrolysers with a total capacity of at least 6 GW, are yet to be built, that are expected to produce 1 Mt of green hydrogen per year.

In the published strategy, one of the priority lines of action remains the hydrogenation of transport: from the hydrogenation of buses serving local lines, through the hydrogenation of heavy long-distance road transport, rail transport operating on lines used on a scale that does not justify their electrification, the hydrogenation of inland and coastal shipping, to the hydrogenation, on the long run, of aviation and ocean shipping.

In order to implement the planned strategy along with its publication, the European Commission established an organisation called (European Clean Hydrogen Alliance). This alliance brings together representatives of industry, civil society, various levels of government and the European Investment Bank.

The publication of the strategy and the establishment of the said alliance clearly confirmed the important role of hydrogen in the transformation of the EU energy system towards its carbon neutrality, in the recovery of the economy after the collapse caused by the Covid-19 pandemic, and in building a strong, competitive position of the EU on the emerging global hydrogen market.

4. Conclusions

Only in the years 2018-2019, public authorities in 21 countries pursued a policy of direct support for the research and development of hydrogen energy technologies. These

activities were carried out under approximately 50 different initiatives (most in the transport sector: 15 for hydrogen-powered passenger cars and 10 for buses and hydrogen refuelling stations) [97].

Government spending on the research and development alone in the field of hydrogen energy technology in 2015–2018 exceeded US $ 11 billion worldwide and is constantly growing [97].

An effective use of the incurred expenditures undoubtedly requires the interested states to formulate an appropriate policy (strategy) for the hydrogenation of the economy, including, in addition to precisely defined long-term objectives, e.g. elements of support from public administration, assurance of: stable investment conditions and the necessary regulatory conditions.

In the coming months, the publication of new or updated versions of these documents is expected in other countries such as: Austria, Denmark, Italy, Great Britain, Canada, Poland, Colombia, Paraguay, Uruguay, Morocco.

Bibliography

[1] BEZDEK, H.R. The hydrogen economy and jobs of the future. *Renewable Energy and Environmental Sustainability*. 2019, **4**. https://doi.org/10.1051/rees/2018005

[2] HYDROGEN SCALING UP. A sustainable pathway for the global energy transition. *Hydrogen Council*. 2017.

[3] SAMSUN, R.C., ANTONI, L., REX, M. Mobile fuel cell application: tracking markets trends. *IEA Technology Collaboration Programme Advanced Cell*. 2020.

[4] Towards development of an Australian scientific roadmap for hydrogen economy. *Australian Academy of Science*. Canberra 2008.

[5] Opportunities for Australia from hydrogen export. *ACIL Allen Consulting*. 2018. https://www.arena.gov.au/assets/201808/Opportunities-for-Australia-from-hydrogen-eksport

[6] FLOYD, H., HIBBERT, A., AMICO, A. Hydrogen for transport. Perspective Australian use case. *Aurecon.* Melbourne 2019.

[7] Australia's National hydrogen strategy, Council of Australian Government. Energy Council Hydrogen Working Group, Department of Industry, Innovation and Science. *Commonwealth of Australia* 2019.

[8] South Australia's hydrogen action plan. Government of South Australia. 2019. https://www.renewablessa-sa.gov/en/content/uploads/2019/09/south-australia-hydrogen-action-plan

[9] Queensland hydrogen industry strategy. *Queensland Government*. May 2019. https://www.dsdmip.gld.gov.au/resources/strategy.queensland-hydrogen-industry-strategy.pdf

[10] Estrategia Nacional de Hidrogene Verde Chile, fuenta energetica para un planeta zero emisiones. *Ministerio de Energia*. Gobiermo de Chile, Santiago de Chile 2020.

[11] GORIP, P. Chile spearheads green hydrogen strategy. *Argus Media*. 20 October 2020. http://www,argusmedia.com/en/news/2150326-chile-spearheads-green-hydrogen-strategy

[12] LUN, J. Hydrogen fuel cell vehicles development in China. Pekin 2016. https://www.un.org/esa/sustdev/csd/csd14/lc/presentation/hydrogen4.pdf

[13] National key R&D programmes. http://www.chinainnovationfounding.eu/national-key-rd-programmes

[14] VERHEUL, B. Overview of hydrogen and fuel cell development in China. *Holland innovation network in China*. Pekin 2019.

[15] Made in China 2025: Mercator Institute for China Studies, 12 August 2016. http://www.mercis.org/en/report/made-in-china-2025

[16] Hydrogen fuel cell vehicle technology roadmap: strategy advisory committee of the technology roadmap for energy saving and new energy vehicles. *Society of Automotive Engineering of China* 2016.

[17] China's energy innovation action plan 2016-2030. China Energy Storage Alliance. Pekin 2016. https://www.en.cnsesa.org/featured-stories/2016/5/8/chinas-energy-innovation-action-plan

[18] Hydrogen power: China backs fuel cell technology, *Financial Times* (accessed on 2.01.2019). https://www.ft.com/../27cefc90-fa-49-11-e81of46-2022a06.02.a6e

[19] JIANJUN TU, K. Prospects of a hydrogen economy with Chinese characteristics. *Etudes de l'IFRI (The Institute francaise des relations internationale)*. Paris 2020.

[20] White paper on China hydrogen and fuel cell industry. *China Hydrogen Alliance* (H2CN). June 2019.

[21] The Danish hydrogen energy programme.

[22] National research & development and demonstration strategy for FCH transport.

[23] National implementation plan for hydrogen refuelling infrastructure in Denmark. Fuel cells programme, toward demonstration and public awarance, Tekes, Politokennot, Helsinki, 2007. https://www.eurosfires.prd.fr/7pc/documents/137414705/_ojapale_fchju_maritime_20130_14062013_public.pdf

[24] The Finnish hydrogen roadmap: Hydrogen to join electricity in the ending traffic pollution. *VTT Research Centre of Finland*. https://www.newcision.com/VTT-info/r/the-finish-hydrogen-roadmap-hydrogen-to-join-electricity-in-the-ending-traffic-pollution-c9419673

[25] LAURICO, J. Hydrogen roadmap of Finland. *VTT* June 2020. https://www.businessfinland.fi/4a828e/globalassets/finish-customers/02-bulid-your-network-bioeconomy-cleantech/alyhas-energia/hydrogen-roadmap-for-Finland2020-10-06-final-pdf-002.pdf

[26] Finland and the hydrogen economy. *Nordic West Office*. Helsinki 2020.

[27] H2Mobilite France: study for a fuel cell electric vehicle. *National Development Plan*. Mobilite Hydrogene. France 2014.

[28] Developpment l Hydrogene pour l econmie francaise, Etude prospective, Association francaise l hydrogene et les piles combustible. Paris 2018.

[29] Plan de deployement de l hydrogene pour la transition energetique, Rapport de Ministere de la Transition Ecologique et Solidaire. Paris 2018.

[30] Strategie national pour le developpment de l hydrogene decarbone en France, Ministere de la Transition Ecologique, Ministere de l Economie, les Finances et de la Relance, Ministere de l Enseigmenent Superieur, de la Recherche et de l Innovation, Secretariat general pour l investissment, Paris. September 2020.

[31] Plan Nacional Integrado de energia y clima 2021-2030, Ministerio para la Transicion Ecologica y el Reto Demografico (MITECO). Madrid 2020. https://www.ec.europa.eu/energy/sites/ener/files/documents/es/_final_necp_main_en.pdf
[32] Estrategia de decarbonization a largo plazo para una economia espanola moderna, competitiva y climaticamento neutra en 2050. Mondoa. Madrid 2020, https://www.lamondoba.gob.es/consejodemi/Paginas/enlaces/03.11.2020-enlaces-clipa-aspx
[33] Hoja de ruta del Hidrogeno: una apuesta por el hidrogeno renovable, Ministerio para la Transmision Ecologica y el Reto Demografico (MITECO). Madrid 2020. https://www.miteco.gob.es/es/prensa/ultimas-politicasel-gobierno-aprueba-la-hoja-de-ruta-del-hidrogeno-una-apuesta-por-el-hidrogeno-renovable
[34] On the way to sustainable mobility. Make room for hydrogen powered vehicles. Dutch Ministry of Infrastructure and Environment.
[35] WEEDA, M. NIP-NL, Energy research centre. (and) WEEDA, M. Economical analysis of HRS build-up in the Netherlands. *Energy Research Centre*. Petten 2015.
[36] GIGLER, J., WEEDA, M. Outlines of a hydrogen roadmap. TKI Nieuw Gas Top Sector Energie. *TKI Energie and Industry* 2018.
[37] Government strategy on hydrogen. 2020. https://www.govermental.nl.2020/04/04
[38] The strategic roadmap for hydrogen and fuel cells. *Agency for Natural Resources and Energy* 2014.
[39] Basic hydrogen strategy. Ministerial Council on Renewable Energy, *Hydrogen and Related issues* 2017.
[40] NAGASHIMA, M. Japan's hydrogen strategy and its economic and geopolitical implications. *The Institute Francaise des Relation Internationale* 2018.
[41] Formulation of a new strategic roadmap of hydrogen and fuel cells. Ministry of Economy, Trade and Industry. *Agency for Natural Resources and Energy* 2019. http://www.meti.gov.jp/english/press/2019/03/12/12.002.html
[42] Transforming the future: moving towards fuel cell power fleets in Canada urban transport system. Report for Natural Resources Canada done by Marcon DDH HIT, Montreal 2005.
[43] Towards a national hydrogen and fuel cell strategy a discussion document for Canada. Government of Canada 2005 and Canada needs a national hydrogen and fuel cell strategy. https://www.chcfa.ca/resources/chfca-blog/canada-needs-a-national-hydrogen-and-fuel-cell-strategy
[44] Electric Vehicle Technology Roadmap for Canada, electric mobility Canada. *Government of Canada* 2010.
[45] Pan-Canadian framework on clean growth and climate change: Canada's plan to address Climate Change Canada 2016. https://www.publications.gc.ca/collections_2017/eccce/En4-294-2016-eng.pdf
[46] 2019 Hydrogen pathways – enabling a clean growth future for Canadians. *Government of Canada*. https://www.hrcan.gc/ca/energy-efficiency-transportation/resources-library/2019-hydrogen-pathways-enabling-a-clean-growth-future-for-canadians/21961
[47] MOORE, A. Canada confirms it is developing national hydrogen strategy. S&P Global Platts. 9 June 2020. https://www.spglobal.com/platts/en/,mrket-insights/latest-news/metals/060820-canada-confirms-it-is-deveoping-national-hydrogen-strategy
[48] CHFCA support for the release of national hydrogen strategy. https://www.chfca.ca/wp-content/uploads/2020/10/CHFCA/Support-for-H2-Strategy-22oct2020-final.pdf
[49] LAURIKO, J. Transport related hydrogen activities in Asia. *VTT*. February 2006.
[50] LEE, C.M. Hydrogen and fuel cell activity in Korea. *IPHE*. September 2005.
[51] MEILLAUD, L. Korea strongly promotes the fuel cell cars. https://www.hydrogentoday.info, 26 August 2016.
[52] SHIN, JI-HYE. Korea takes steps towards hydrogen economy. *The Korea Herald*. 12 September 2018.
[53] Hydrogen economy roadmap of Korea. Ministry of Trade. *Industry and Energy*. Seul 2019.
[54] The German Wasserstoffspiegel, 2006, **2**. https://www.dwr-info.de/acktuelles/haupt_wspiegel.htm
[55] JOEST, S., FICHTER, M., BUNGER, U. et al. Studie zur Frage, woher kommt der Wasserstoft in Deutschalnd bis 2050. *Final report of project Germany Hy*, August 2008.
[56] LEMKE, R. Market introduction of hydrogen fuel. *Genehmitage Dissertation*. Berlin 2016.
[57] SAMSUN, R.C., ANTONI, L., REX, M. Mobile fuel cell application: trucking market trends. *IEA Technology Collaboration Programme Advanced Fuel Cell*. March 2020.
[58] The national hydrogen strategy. *Federal Ministry for Economic Affairs and Energy*. Berlin 2020.
[59] National hydrogen strategy. Norwegian Government. *Ministry of Energy and Environment and Ministry for Transport*. Oslo 2005.
[60] The Norwegian hydrogen guide. Norwegian hydrogen forum. https://www.view.hydrogen.no
[61] Fuel cells and hydrogen in Norway. FuelCellToday.
[62] The Norwegian Governments hydrogen strategy towards a low emission society. Norwegian Ministry of Petroleum and Energy. *Norwegian Ministry of Climate and Environment*. Oslo 2020.
[63] Norway to launch hydrogen strategy. Energy Global. 10 June 2020. https://www.energyglobal.com/other-renewables/10062020/norway-tolaunch-hydrogenstrategy/
[64] CLEMES, T., GARROD, M., LEVI, T. Transitioning to a hydrogen economy: issue document. CRL Energy Ltd. *Lower Hutt*. New Zealand 2007.
[65] A vision for hydrogen in New Zealand. Ministry of Business. *Innovation and Employment*. Wellington 2019.
[66] Hydrogen in New Zealand. Report 1 – Summary. *Concept Consulting Group Ltd* 2019.
[67] H2 Taranaki roadmap. How hydrogen will play a key role in our new energy future. *Tapua Rora*. New Plymouth 2019.
[68] MURRAY, M.L., SEYMOUR, E.M., PIMENTA, R. Towards a hydrogen economy in Portugal. *International Journal of Hydrogen Energy*. 2007, **32**(15), 3223-3229. https://doi.org/10.1016/j.ijhydene.2007.02.027
[69] EN-H2 estrategia nacional Para Hidrogenio Portugues, Ambiente Acao Climatico, May 2020.
[70] Integracjo Hidrogienio mas Cadeas de Walor – Sistemas energeticos integrados mais limpos e inteligentes, Direcao – Geral de Energia e Geologii, Lisbona 2018.
[71] Roadmap for carbon neutrality 2050 (RNC 2050 Long term strategy for strategy of the Portugalless economy 2050). https://www.unfccc.int/sites/defaults/files/resources/RNC2050_EN-PT20%Long%20Term%20Strategy.pdf
[72] Integrated National Energy and Climate Plan 2021-2030, December 2018. https://www.ec.europa.eu/energy/sites/ener/files/documents/ec_courtesy_translation_pt_necp.pdf

[73] EU Trans European Transport network (TEN-T) hydrogen Infrastructure for Transport Project HIT, EU 2014 and HIT-2-Corridors. EU 2015.
[74] WALMARK, G. The Swedish hydrogen report. SWECO, *HFC Nordic* 2016.
[75] Sweden – opportunities for hydrogen energy technologies considering. The National Energy and Climate Plans (NECP). *Fuel Cell & Hydrogen 2 Join Undertaking* 2020.
[76] UK H2 Mobility, Phase1 results, April 2013.
[77] HART, D., HOWES, J., MADDEN, B. et al. Hydrogen and fuel cells opportunities for growth a roadmap for the UK. E4tech. *Element Energy*. London 2016.
[78] Establishing a hydrogen economy. The Future of Energy 2035, ARUP, 2020.
[79] COMAN, Y. Can a hydrogen boom fuel a green recovery for Britain? *The Guardian*, 20 July 2020.
[80] Renewable hydrogen – seizing the UK opportunity, renewable UK, September 2020. https://cdn.ymaws.com/www.renewableuk/resource/resmgr/renewable_hydrogen_seizing.pdf.
[81] PM outlines his Ten Point Plan for green industry revolution for 250.000 jobs. *Prime minister office*, 10 Downing Street. 18 November 2020.
[82] Piano Nazionale di Sviluppo Mobilita Idrogene, Italy, October 2019. https:/www.h2it/wp-content/uploads/2019/12/Piano_Nazionale_Monilita_Idrogene_Integrale_2019_Finale.pdf
[83] Strategia Nazionale Idrogeno, Linee Guida Preliminaria, Ministerio dello Sviluppo Economico, 2020. https://www.mise.gov.it/images/stories/documenti/Strategia_Nazionale_Idrogeno_Linee_Guida_preliminari_nov20.pdf
[84] The Energy Policy Act of 1992, Public law 102-486-24, October 1992. https://www.ofdc.energy.gov/files/pdfs2527.pdf
[85] Energy innovation in the United States. Automotive Fuel Cell Applications. *OECD*. https://www.oecede.org/science/inno/31968387.pdf
[86] A national Vision of America's transition to a hydrogen economy to 2030 and beyond. *US Department of Energy*. February 2002. https://www.cere.energy.gov/hydrogenandfuelcells/vision-doc.pdf
[87] National Hydrogen Energy roadmap. U*S Department of Energy*. November 2002. https://www.cere.energy.gov/hydrogenandfuelcells/national-h2-roadmap.pdf
[88] Energy policy Act of 2005. Public Law 109-58-8 August 2005. https://www.congress.gov/109/plaws/publ/58/PLAW-109publ/58.pdf
[89] Hydrogen Posture Plan. An integrated Research Development and Demonstration Plan. *US Department of Energy. US Department of Transportation*. Washington 2006.
[90] Hydrogen and Fuel Cells Program Plan. An Integrated Strategic Plan for the Research Development and Demonstration for Hydrogen and Fuel Cells Technologies. *US Department of Energy*. Washington 2011. https://www.hydrogen.energy.gov.pdfs/program-plan2011.pdf
[91] MELAINA, M., BUSH, B., MURATORI, M. et al. National Hydrogen Scenarios. H2 US Location Roadmap Working Group. *National Renewable Energy Laboratory* 2017.
[92] Hydrogen strategy: Enabling a Low Carbon Economy. *US Department of Energy*. Washington 2020.
[93] Hydrogen Programm. https://www.hydrogen.energy.gov/budget.html
[94] MOORE, A. Feature: Canada developing national hydrogen strategy: US taking different approach. S&*P Global Platts*. 9.06.2020.
[95] MELAINA, M., BUSH, B., MURATORI, M. et al. National Hydrogen Scenarios, How many stations, where and when? H2 US Location Roadmap Working Group. *National Renewable Energy Laboratory* 2017.
[96] Road Map to US Hydrogen economy. Reduction emissions and driving growth across the nation.
[97] The Future of Hydrogen. Seizing today's opportunities. Report International Energy Agency for meeting of G20 in Osaka 2019.

Maciej Menes, MSc. – Motor Transport Institute, Warsaw, .
e-mail: *maciej.menes@its.waw.pl*

Article citation info:
ZIÓŁKOWSKI, A., FUĆ, P., JAGIELSKI, A. et al. Analysis of emissions and fuel consumption from forklifts by location of operation. *Combustion Engines*. 2022, **189**(2), 30-35. https://doi.org/10.19206/CE-141741

Andrzej ZIÓŁKOWSKI
Paweł FUĆ
Aleks JAGIELSKI
Maciej BEDNAREK

Combustion Engines
Polish Scientific Society of Combustion Engines

Analysis of emissions and fuel consumption from forklifts by location of operation

ARTICLE INFO

Received: 30 July 2021
Revised: 18 August 2021
Accepted: 30 August 2021
Available online: 20 September 2021

The share of road transport accounts for more than 85% of the total structure of freight transportation. In this process, mainly motor vehicles are used to carry out the freight work. In addition to them, forklifts are also used, whose task is to load and unload goods. These vehicles are categorized as NRMM (Non-Road Mobile Machinery). Forklift trucks have internal combustion or electric drive. The paper presents an analysis of the emission of pollutants and fuel consumption from forklift trucks equipped with diesel and LPG power. The study uses the author's test taking into account the raising/lowering of a pallet, a loaded and unloaded run. The measurements were made in the warehouse and outside the warehouse using the Portable Emission Measurement System (PEMS) equipment. The aim was to show the influence of loading conditions on the emission of pollutants and fuel consumption.

Key words: *forklifts, PEMS, exhaust emission, fuel consumption*

1. Introduction

Transport is one of the most important branches of the national economy, which directly affects its development, but at the same time it is one of the main sources of air pollution. According to the European Environment Agency, in 2016, road transport was responsible for emissions of about 39% of NO_x, 20% of CO and CO, and 10% of PM10 [4]. Although the SARS-CoV-2 pandemic caused the number of passengers transported to decrease in 2020, an increase in the amount of freight transported and the transport work performed was observed in the case of freight transported by road. According to the report "Cargo and Passenger Transport in 2020" published by the Central Statistical Office, the amount of passengers transported decreased against 2019 by more than 49%, while a 21% increase was observed in the case of freight transported by motor transport [7]. It is worth noting that the demand for freight transportation will increase in the coming years [2]. With greater vehicle transport capacity, this will result in increased emissions of pollutants into the atmosphere. As it has been shown [6], the amount of fuel consumption and CO_2 and NO_x emissions in cargo transport directly results from the amount of mass of the transported goods. Analyzing the literature, one may notice that there are many studies devoted to the issue of emission of pollutants in the process of cargo transportation by heavy vehicles [6, 13, 16]. However, there is a deficit of research works on the emission of pollutants during the performance of loading tasks, which are an indispensable element of the process of cargo transportation. These works are performed with the use of various manipulation means, including forklifts equipped with combustion engine units, the emission of which is a threat to human health, as well as negatively affect the environment causing its degradation [5, 14].

One of the most frequently used tools for loading or unloading freight are forklift trucks, discussed in this paper, which belong to the NRMM (Non-Road Mobile Machinery) vehicle category. During the approval process of non-road vehicles the emission of pollutants is measured on the basis of the stationary NRSC (Non-Road Steady-State Cycle) and dynamic NRTC (Non-Road Transient Cycle) tests. Since the operating conditions of the engines during actual operation differ significantly from the test conditions, more reliable data on engine unit emissions is provided by RDE (Real Driving Emission) tests. The possibility of obtaining reliable measurements has led to the fact that tests under real operating conditions are increasingly used to determine the emission performance of NRMM vehicles and can be complementary to tests performed under laboratory conditions [3, 9, 10, 17]. For forklift trucks, however, the method of conducting the RDE test has not yet been established. One procedure is the VDI 2198 test. However, this standardized cycle used to determine the fuel consumption of forklifts only represents the operation of the device in the warehouse, omitting, among other things, the driving of the forklift without a load. Thus, this method does not represent the emissions and energy intensity of a forklift performing loading tasks [5]. It should also be noted that the variety of ways of organizing loading processes should be taken into account when determining the test procedure of forklifts. Nowadays, forklifts have found their application in large logistics centers, closed warehouse halls and open yards. These sites vary in size, floor, weather conditions, etc. These conditions directly affect the way the forklift trucks are used, which results in a different structure of emissions and fuel consumption by devices operating in different conditions.

Currently, there are few publications on emissions from internal combustion forklifts. The topic has been covered in only a few publications [1, 8]. Determining the emission performance of forklift trucks used during loading operations is even more important as they are used in the direct vicinity of humans, contributing to the deterioration of their health. This is of particular importance when working in closed spaces.

2. Research methodology

2.1. Research objects

In order to determine the relationship in fuel consumption and emissions between forklift trucks operating in different

conditions, two machines were tested. One forklift truck was equipped with a diesel engine and the other with a LPG (liquefied petroleum gas) engine. Both units had similar empty weights and were loaded with the same payload.

The self-ignition engine vehicle had a four-cylinder unit with a capacity of 2486 cm^3 and maximum power of 36 kW at 2500 rpm. The driving unit of the second test object was a spark-ignition engine with a capacity of 2237 cm^3 and a maximum power of 38 kW. This vehicle was equipped with a TWC (Three-way catalytic converter) system. The data of each object are listed in Table 1.

Table 1. Specification of research objects

Parameter	Vehicle 1	Vehicle 2
Type of engine	CI	SI
Engine capacity	2486 cm^3	2237 cm^3
Maximum power output	36 kW at 2500 rpm	38 kW at 2100 rpm
Maximum torque	175 Nm at 2300 rpm	160 Nm at 2100 rpm
Number of cylinders	4	4
Emission standard	Stage IIIA	Stage IIIA
Aftertreatment	–	TWC
Cargo weight	1000 kg	1000 kg
Cart empty weight	3560 kg	3600 kg

Fig. 1. Research object with installed measurement equipment

2.1. Measuring instruments

The research has been carried out using the SEMTECH DS analyzer made by Sensor Inc. The instrumentation, belonging to the PEMS (Portable Emissions Measurement System) group of devices, makes it possible to measure CO, CO_2, NO_x, HC and O_2 concentrations in exhaust gases during real operating conditions. The instrumentation also enables the realization of fuel consumption and exhaust mass flow rate measurements.

The exhaust gases are taken directly from the vehicle's exhaust system. The pipe that delivers exhaust gases to the apparatus is heated up to 191°C. This procedure is done to eliminate condensation of hydrocarbons. The mass flow rate of the test gases is measured using a flow meter, which works according to the Pitot tube principle. After the gases have been purged of solids, the sample is passed to the individual analyzers where the concentration of the compound is measured. The FID (Flame Ionization Detector) analyzer measures the concentration of unburned hydrocarbons, the NDUV (Nondispersive Ultra Violet Detector) analyzer measures the sum concentration of NO and NO_2. The NDIR (Nondispersive Infrared Detector) analyzer measures the concentration of carbon monoxide and carbon dioxide.

SEMTECH DS is also equipped with electrochemical sensor enabling examination of oxygen content in the analysed exhaust gases. The data on engine operating parameters are obtained from the OBD system. Additionally, the device, thanks to the cooperation with GPS, enables to determine the location of the tested object [9, 11]. The table below summarizes the measurement characteristics of each exhaust gas compound by the analyzer (Table 2).

Table 2. Specification for measurement of exhaust gas compounds by Semtech DS [11]

Tested compound	Measuring range	Accuracy of measurement
THC	0–10000 ppm	±2.5%
NO_x	0–3000 ppm	±3%
CO	0–10%	±3%
CO_2	0–20%	±3%
O_2	0–20%	±1%

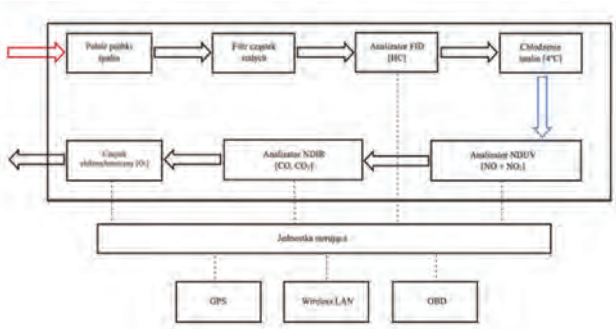

Fig. 2. Scheme of the operation of the SEMTECH DS analyzer [12]

Fig. 3. SEMTECH DS analyzer [11]

2.2. Research cycle

Forklift trucks are widely used in many industries – they are used in production halls, warehouses and distribution and logistics centers. In the case of transport processes, one of their main tasks is to carry out loading and unloading of goods from vehicles. The study of fuel consumption and emissions of forklift trucks was carried out on the basis of a modified VDI2198 (Fig. 4) test proposed by one of theauthors of the publication. The test includes the "empty run" i.e. driving the forklift truck without any load.

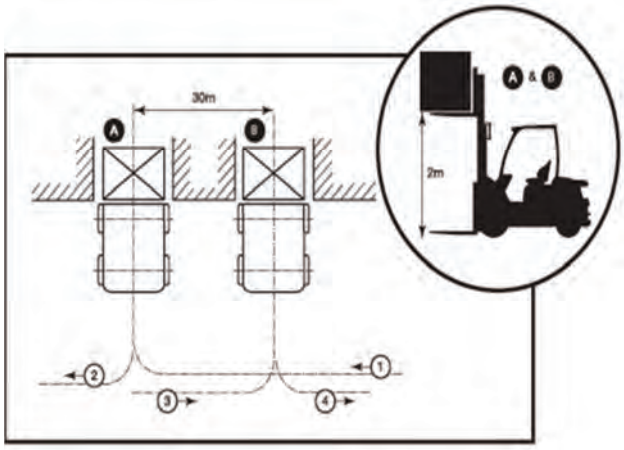

Fig. 4. The VDI2198 test [15]

The proposed test cycle (Fig. 5) consisted of the following stages:

1. loading and lifting to a height of one meter and lowering in bay A,
2. drive the cart out of bay A,
3. drive the cart to bay B (30 m),
4. lowering and unloading of the goods in bay B,
5. drive out of bay B,
6. Unloaded driving to bay A.

In order to show the influence of operating conditions on the emission structure and fuel consumption, the above cycle was carried out in two variants – at an external storage yard and inside a closed warehouse.

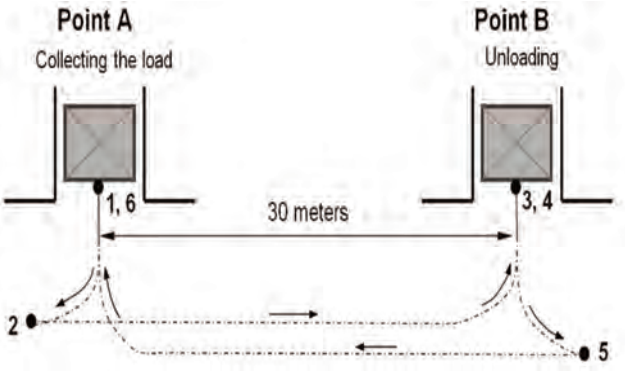

Fig. 5. Scheme of the research cycle

3. Results of the study

Tests of forklift trucks powered by diesel and LPG were performed in a developed research cycle realizing 10 repetitions for each condition – travel outside and inside the warehouse. The objects were loaded with the same mass of cargo and the runs were performed by the same operator. Outside the warehouse, the runs were made on a paved surface. In the storage hall, on the other hand, the floor was made of concrete. It was characterized by a smooth surface and the absence of possible irregularities, in contrast to the cobblestone surface. During the measurements, the exhaust gas compounds were measured: NO_x, CO, THC and CO_2. In this paper, the on-road emission values of NO_x, CO, and THC are presented for 10 measurement cycles to demonstrate the repeatability of the runs performed. Turning to the analysis of the NO_x road emission for a forklift powered by diesel, it was noticed that its values during the passage with and without the load are higher for the measurements made in the warehouse (Fig. 6). This is due to the higher dynamics of the trip, which was made possible by the quality of the substrate on which the forklift truck moved. Analyzing also the influence of the mass of the transported load on the NO_x emission values, it was shown that the average difference between the travel with and without the load was 5.2 g/km outside the hall, and 4.4 g/km in the warehouse hall. In both cases, loading the forklift with cargo resulted in a 40% increase in on-road NO_x emissions.

Carbon monoxide emissions showed a similar relationship. Driving with a load resulted in an increase in on-road emissions of over 45% for both test variants. In contrast to nitrogen oxides, higher emissions were observed for carbon dioxide during off-storage trips. This relationship was a result of the forklift driving more steadily and quietly in the outdoor storage yard (Fig. 7). The driving style was due to the fact that the operator had to adapt the driving dynamics to the unevenness of the ground when driving over paving stones, in order to ensure the safe transport of the load. The average on-road CO emissions during the work in the outdoor storage yard were almost twice as high during the load carriage and amounted to 4.2 g/km.

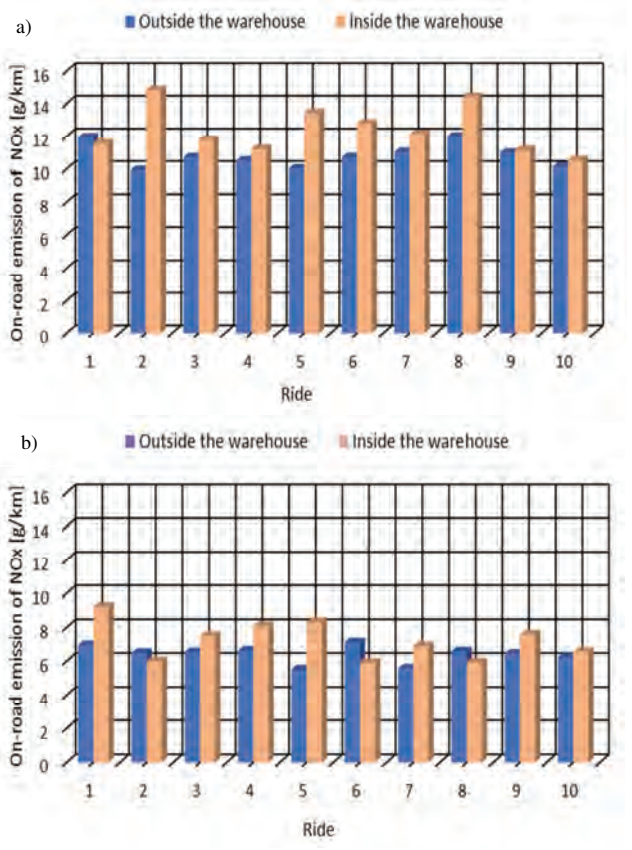

Fig. 6. On-road emissions of NO_x of a forklift truck equipped with a CI engine: a) when carrying a load, b) when driving unloaded

Tests under actual operating conditions showed significantly higher THC emissions for runs inside the warehouse (Fig. 8). On average, the value was 1.4 times higher for both loaded and unloaded runs. This trend may be due to

the direct injection of the fuel dose into the flame. When analyzing the average emission of unburned hydrocarbons, it is worth noting that loading the truck with one ton of load, resulted in an increase in emissions by 60% relative to the so-called "empty run".

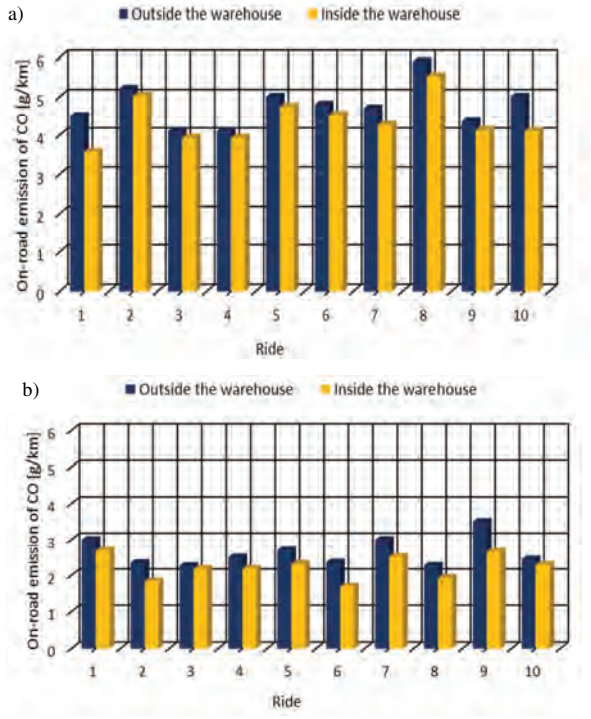

Fig. 7. On-road emissions of CO of a forklift truck equipped with a CI engine: a) when carrying a load, b) when driving unloaded

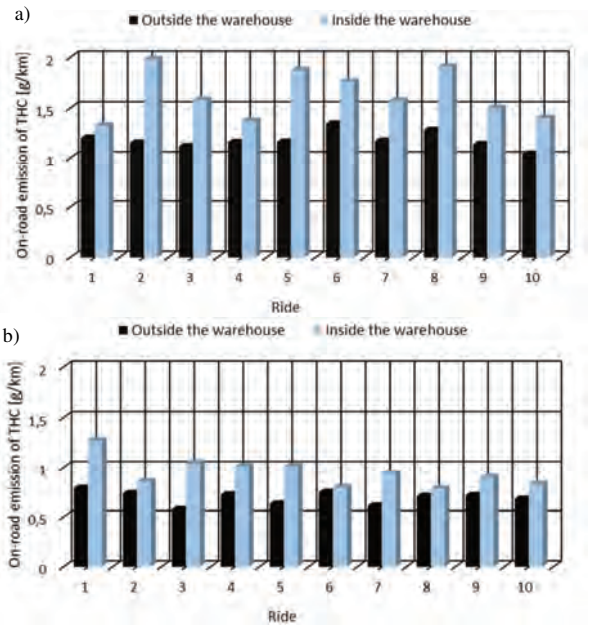

Fig. 8. On-road emissions of THC of a forklift truck equipped with a CI engine: a) when carrying a load, b) when driving unloaded

The analysis of the on-road emissions of nitrogen oxides for the LPG truck shows exactly the same trend as for the diesel truck (Fig. 9). For each trip, both for driving with and without load, the emissions were higher when the forklift was operating inside the warehouse. This is also due to the way the forklift is operated. While transporting the load, the average NO_x emission was 30.06 g/km when operating inside the warehouse and 33.76 g/km when driving outside. The difference in emissions of the previously mentioned compound is 11%.

Testing of the LPG powered forklift showed higher on-road carbon monoxide emissions during trips outside the warehouse. This trend is consistent with the diesel-powered forklift and is also due to the driving dynamics of the unit (Fig. 10).

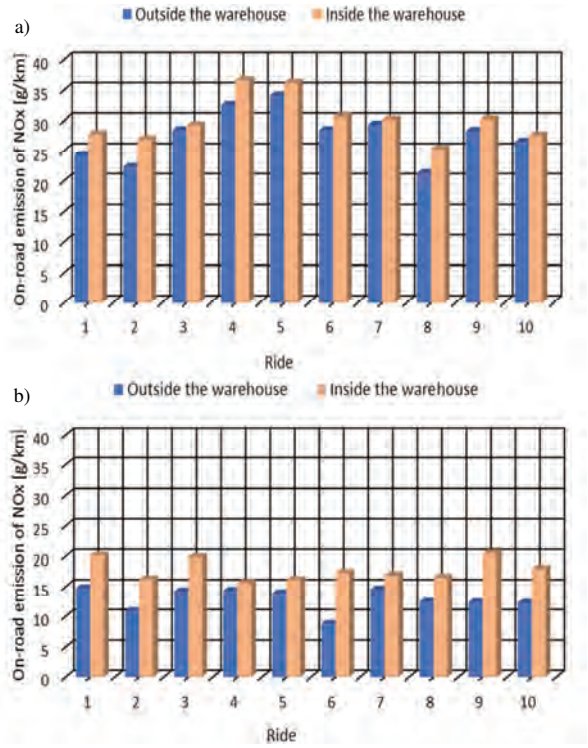

Fig. 9. On-road emission of NO_x of a forklift truck fitted with a SI LPG engine: a) when carrying a load b) when driving unloaded

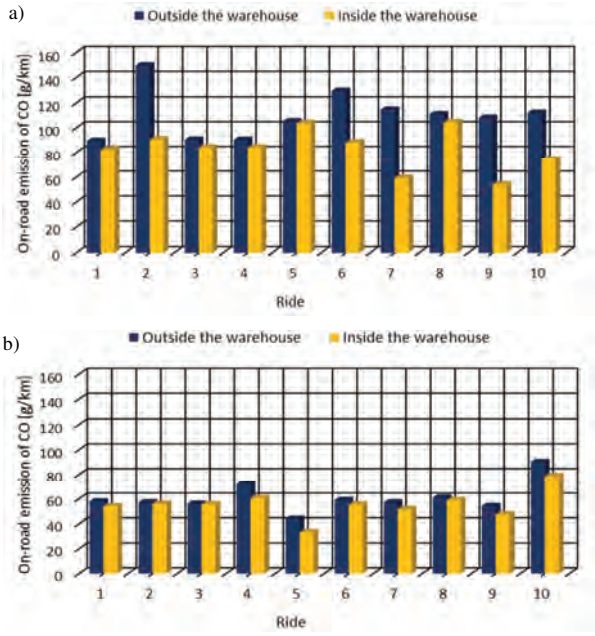

Fig. 10. On-road emission of CO of a forklift truck fitted with a SI LPG engine a) when carrying a load b) when driving unloaded

The average CO emissions for loaded trips are 88.6 g/km for the indoor test and 109 g/km for the outdoor yard trip, respectively. For the unloaded forklift test, the on-road emissions reached an average of 55.2 g/km in the indoor yard and 47.5 g/km in the outdoor yard. Such large increases relative to the compression-ignition truck are due to low-temperature mixture combustion and local and global air shortage. In addition, the reason may be due to the fact that LPG vehicles face the problem of variable composition of the fuel-air mixture, which also increases emissions. The difference in CO emissions for trips with a load inside and outside the warehouse is about 19%. Comparing this to and unloaded trip inside and outside the warehouse the difference is 5 percentage point lower at around 14%.

Turning to the analysis of THC emissions of LPG-powered trucks, increased emissions can be observed during indoor operations. This trend was maintained for each stage of the unit operation (Fig. 11). Much higher emission of the compound is a result of low efficiency of the TWC system, which did not fully oxidize propane and butane. Additionally, it is worth noting that loading the unit with cargo resulted in a more than 3-fold increase in hydrocarbon emissions relative to unloaded runs.

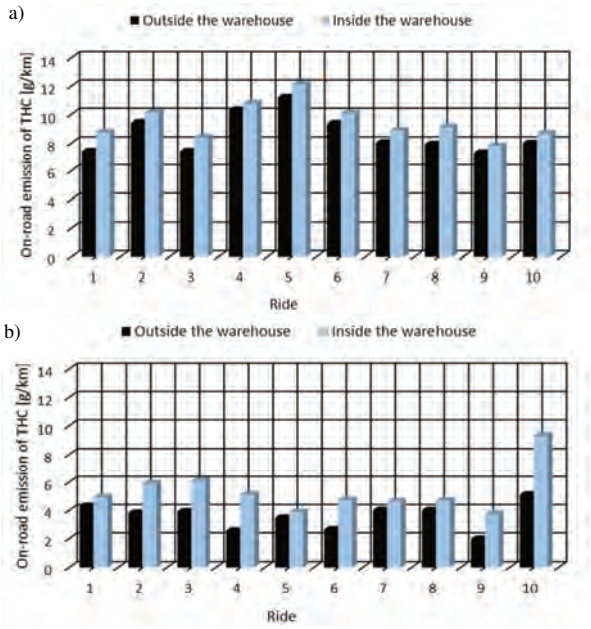

Fig. 11. On-road emission of THC of a forklift truck fitted with a SI LPG engine: a) when carrying a load b) when driving unloaded

Analyzing the recorded data of the study (Fig. 12), the average fuel consumption of the self-ignition engine from forklift was 83 dm^3/100 km when carrying a load outside the hall, while without a load it is 51 dm^3/100 km, in the case of trips inside the hall the average specific fuel consumption for carrying a load is 96 dm^3/100 km and 55 dm^3/100 km without a load. An inverse relationship was recorded in the specific fuel consumption for the LPG vehicle. For the trip with cargo outside the hall, the average specific fuel consumption is 203 dm^3/100 km, and 73 dm^3/100 km without cargo. On the other hand, in the case of recording the drive inside the hall, the measured values were 168 dm^3/100 km with load and 84 dm^3/100 km without load, respectively. Such a correlation is influenced, similar as in the case of the emission of harmful toxic compounds, by the quality of the ground on which the test objects moved and the driving technique of the driver who was responsible for driving them.

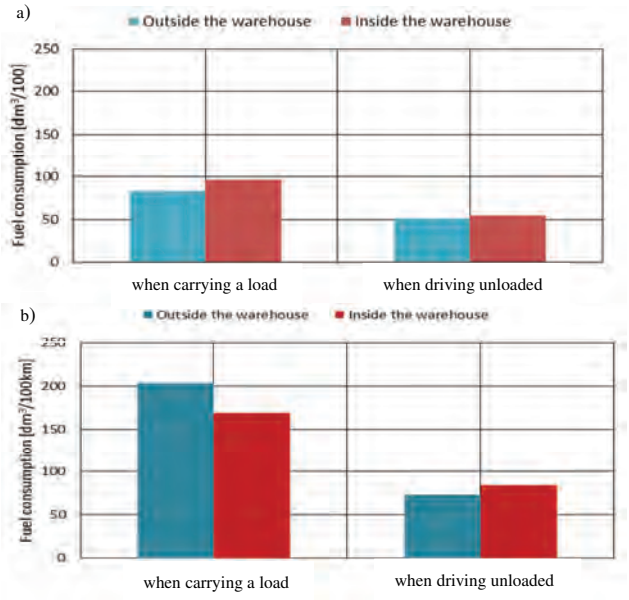

Fig. 12. Average specific fuel consumption, a) compression ignition engine vehicle, b) LPG vehicle

4. Summary

Road transport in the total structure accounts for the majority of the share compared to the other transport modes. Two forklift trucks were tested, which differed in the type of fuel used to power the internal combustion engines installed in them. In addition, the author's research test related to the testing of vehicles from the NRMM category using the PEMS apparatus for measuring harmful toxic compounds of exhaust gases was implemented. Emissions of nitrogen oxides and hydrocarbons both in the vehicle equipped with a compression-ignition engine and powered by LPG were higher during the drive inside the hall. This is due to the type of substrate, the driver's dynamics and driving style. This poses a particular threat to employees of closed warehouses who are directly exposed to these compounds. In the case of carbon monoxides, emissions were higher during off-hall trips. The authors also decided to compare the results related to the emission of harmful toxic compounds for both unloaded and loaded trips. The results were several times higher when carrying a load of 1000 kg. The average specific fuel consumption also increased when the cargo was carried. Increasing the load on the power unit through the cargo was one of the components of the increase in the previously mentioned parameter. In conclusion, both the place where the transport took place and whether the test object transported a cargo of a given mass influence the increase in emission of harmful toxic compounds of exhaust gases. The method proposed by the authors makes it possible to assess the processes of cargo loading. Conclusions from the analysis can be used to optimize logistic processes and help in designing warehouse infrastructure.

Acknowledgements

The study presented in this article was performed within the statutory research (contract No. 0415/SBAD/032).

Nomenclature

CI	compression ignition
CO	carbon monoxide
CO_2	carbon dioxide
FID	flame ionization detector
GPS	global positioning system
LPG	liquefied petroleum gas
NDIR	non-dispersive infrared
NDUV	non-dispersive ultra violet spectroscopy
NO_x	nitrogen oxides
NRMM	non-road mobile machinery
NRTC	non-road transient cycle
NRSC	non-road steady-state cycle
PEMS	portable emissions measurement system
SI	spark ignition
THC	hydrocarbons
TWC	three way catalyst

Bibliography

[1] AL.-SHAEBI, A., NOURMA, K., HUSAM, D. et al. The effect of forklift driver behavior on energy consumption and productivity. *Procedia Manufacturing*. 2017, 11, 778-786. https://doi.org/10.1016/j.promfg.2017.07.179

[2] BITTER, M., MAILÄNDER, E., PALUMBO, C. Commercial vehicle market trends. *7th AVL International Commercial Powertrain Conference*. May 22-23, Graz 2013.

[3] DEFRIES T., KISHAN S., SABISCH, M. et al. Development of emission factors, load factors, duty cycles and activity estimates from the nonroad PEMS study. *2013 PEMS Conference & Workshop*. University of California, Riverside 2013.

[4] European Environment Agency. European Union Emission Inventory Report 1990-2016. *Publications Office of the European Union*. Luxemburg 2018. https://www.eea.europa.eu/publications/european-union-emission-inventory-report-1990-2016

[5] FUĆ, P., LIJEWSKI, P., KUR□ZEWSKI, P. et al. The analysis of fuel consumption and exhaust emissions from forklifts fueled by diesel fuel and liquefied petroleum gas (LPG) obtained under real driving conditions. *Proceedings of the ASME 2017 International Mechanical Engineering Congress & Exposition*. 2017, **6**. V006T08A060. ASME. https://doi.org/10.1115/IMECE2017-70158

[6] FUĆ, P., MERKISZ, J., ZIÓŁKOWSKI, A. Impact of masses load for CO_2, NO_x emission and fuel consumption heavy duty vehicles a total mass exceeding about 12000 kg. *Postępy Nauki i Techniki*. 2012, **15**, 41-53.

[7] Główny Urząd Statystyczny. Przewozy ładunków i pasażerów w 2020 r., *Urząd Statystyczny w Szczecinie*, 2021.

[8] PANG, K., ZHANG, K., MA, S. Tailpipe emission of characterizations of diesel-fueled forklifts under real-world operations using a portable emission measurement system. *Journal of Environmental Sciences*. 2021, **100**, 34-42. https://doi.org/10.1016/j.jes.2020.07.011

[9] LIJEWSKI, P., SZYMLET, N., SOKOLNICKA, B. et al. Anali□a emisji tlenku węgla □poja□du □silnikiem o □apłonie iskrowym i be□pośrednim wtryskiem paliwa według procedury RDE. *Autobusy*. 2017, **12**, 271-275.

[10] LIJEWSKI, P., FUĆ, P., DOBRZYŃSKI, M. et al. Exhaust emission from small engines in handheld devices. *Proceedings of the Matec Web Conference*. 2017, **118**, 00016. https://doi.org/10.1051/matecconf/201711800016

[11] Press materials Sensor Inc. https://www.sensors-inc.com (accessed on 14.07.2021).

[12] MERKISZ J. et al. Development of road test to evaluate the fuel consumption in the urban cycle for city buses equipped with hybrid powertrain. *Combustion Engines*. 2015, **162**(3), 587-592.

[13] MYSŁOWSKI, J. Badania emisji spalin pojazdu ciężarowego w rzeczywistych warunkach. *Autobusy*. 2014, **6**, 199-202.

[14] RISTOVSKI, Z.D., MILJEVIC, B., SURAWSKI, N.C. et al. Respiratory health effects of diesel particulate matter. *Respirology*. 2012, **17**(2), 201-212. https://doi.org/10.1111/j.1440-1843.2011.02109.x

[15] VDI 2198. Type sheets for industrial trucks. VDI-Gesellschaft Produktion und Logistik (GPL). *Verein Deutscher Ingenieure e.V.*, Düsseldorf 2012.

[16] ZIÓŁKOWSKI, A., FUĆ, P., LIJEWSKI, P. et al. Analysis of RDE emission measurements in rural conditions from heavy-duty vehicle. *Combustion Engines*. 2020, **182**(3), 54-58. https://doi.org/10.19206/CE-2020-309

[17] Delphi Technologies. https://www.delphiautoparts.com (accessed on 14.07.2021)

Andrzej Ziółkowski, DSc., DEng. – Faculty of Civil and Transport Engineering, Poznan University of Technology.
e-mail: *andrzej.j.ziolkowski@put.poznan.pl*

Prof. Paweł Fuć, DSc., DEng. – Faculty of Civil and Transport Engineering, Poznan University of Technology.
e-mail: *pawel.fuc@put.poznan.pl*

Aleks Jagielski, MEng. – Faculty of Civil and Transport Engineering, Poznan University of Technology.
e-mail: *aleks.jagielski@doctorate.put.poznan.pl*

Maciej Bednarek, Eng. – Faculty of Civil and Transport Engineering, Poznan University of Technology.
e-mail: *maciej.bednarek@student.put.poznan.pl*

Article citation info:
SZAMREJ, G., KARCZEWSKI, M., CHOJNOWSKI, J. A review of technical solutions for RCCI engines. *Combustion Engines*. 2022, **189**(2), 36-46. https://doi.org/10.19206/CE-142551

Grzegorz SZAMREJ
Mirosław KARCZEWSKI
Janusz CHOJNOWSKI

Combustion Engines
Polish Scientific Society of Combustion Engines

A review of technical solutions for RCCI engines

ARTICLE INFO

Received: 15 July 2021
Revised: 23 September 2021
Accepted: 23 September 2021
Available online: 25 September 2021

Engines working in dual-fuel mode need special conditions to ignite air-fuel mixture without spark plug in a good moment with high combustion efficiency. To create homogenous air-fuel mixture the conditions in the cylinder are even more demanding. Many concepts of ignition was developed, but the most effective needs perfect mixing of fuel and air, which is a serious technical challenge. Technical solutions for dual-fuel engines cover the complexity of these problems thus leading to the further development of ignition systems in internal combustion engines. Fuel supply systems, the operation strategy of them, the shape of the combustion chamber are the most important elements to change and develop for correct operation of dual-fuel engines. The literature analysis showed a small amount of research carried out to optimize the operation of dual-fuel engines The variety of engines in which a dual-fuel system can be used requires much more research about them, and solutions necessary for their correctly operation.

Key words: *HCCI, RCCI, Dual-Fuel, DDFS*

1. Introduction

Internal combustion engine (IC) and the combustion process itself are constantly developing from XIX century until today. The amount of energy released in the combustion chamber and the composition of raw exhaust gases both depends of combustion. The improvement of these processes in first century of IC engines existence was mainly based by improving the shape of combustion chamber. The next century opened an opportunity for researchers to develop new solutions of the air-fuel ignition methods. These fresh solutions introduced new directions in the development of internal combustion engines.

1.1. Explication

IC engines always emit undesirable exhaust components, even if they are the most efficient, modern and equipped with, even the best exhaust gas cleaning systems. Usually systems of this type may be large and complex [9]. The typical composition of exhaust gases from marine engines are shown on Fig. 1.

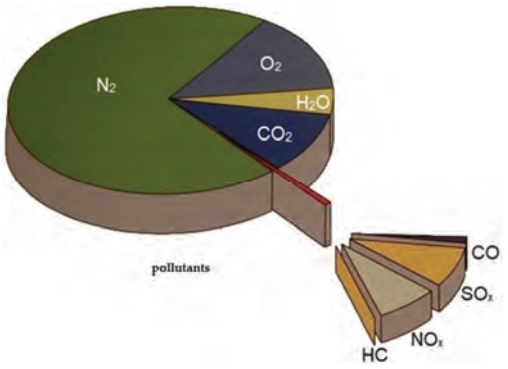

Fig. 1. The typical composition of exhaust gases from the modern, marine diesel engine (reproduced from [9])

Composition of exhaust gases is strongly dependent on what kind of fuels are used in the engine. In order to be able to use many types of fuels while maintaining a modern and well-developed combustion technology, engines have been modernized, allowing for the combustion of many fuels at the same time. This type of solution is Dual-Fuel (DF) system. DF may turn out in the future as a key point in the development of IC engines and reducing the emission of harmful exhaust components.

This work was created in order to distinguish specific solutions enabling the implementation of the most effective DF combustion systems in classic piston CI engines. A lot of works focusing on the literature review have already been done. The researchers selected engines used in various research studies, with a method of air-fuel mixture combustion similar to that one was focused for this study [22]. A very detailed review of carried out tests in analyzed studies engines performance are presented in detailed tables and summarized in the description without going into the deep technical details regarding the design of the engine and the technical solutions used in them. More detailed data on technical solutions are presented in the different studies [24, 25]. Authors decided to refine and expand with additional information from further literature analysis. Works such as [29] and [23] present a detailed description of the research carried out, and the influence of various types of fuels on engine performance, that which are not main focus in this study. The above-mentioned works also take into account the simulation results, which in this paper is limited to presenting the concept of technical solutions that may bring beneficial effects. Model simulations for the marine engine presented in the study [23] are a very important part of research on this topic due to the advantages that slow- and medium-speed engines working in the DF mode have. This study is also largely based on technical solutions used in marine engines, the development of which largely determines the future of DF engines, which is supported by many publications [18–20, 34], including technical solutions in marine engines.

The studies quoted here may constitute the core of considerations, developed with technical issues enabling the

implementation of engine operation in DF systems. Important issue which is also highlighted in this article is the flow of technology from large industrial engines to small drive units. The technical solutions presented in this work show the current state of technology and define the possibilities that arise from their widespread use and the combination of independently used technical solutions.

2. IC engines ignition systems

A simplified view of engine development through the centuries of existence of IC engines reflects the mainstream of their development. Figure 2 shows the important types of air-fuel mixture ignition systems regarding to the date of their construction.

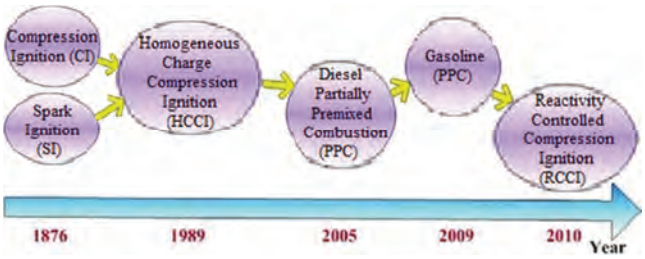

Fig. 2. Chosen ignition methods in ICE by year of construction (own graphic based on data and graphics from [25])

Ignition systems in IC engines are being developed one dependent on the other and the new design is replacing the old one. Relations between different ignition systems allow for further exploration of various IC engines concepts. Different ignition types are shown on the graph showing addiction of their use on fuel type (Fig. 3).

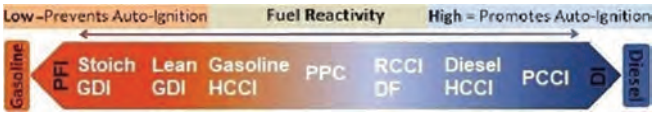

Fig. 3. The dependence of the methods of ignition of the air-fuel mixture in IC piston engines on the method of fueling the engine and the type of fuel used (own graphic based on data and graphics from [25])

Different engine ignition types are designed for use with certain fuels. The combination of some solutions may result in a significant increase in the efficiency of IC engines. Their development is possible only thanks to research on single types of ignition. DF technology is now paramount in further improving engine combustion.

2.1. IC engines ignition systems

The typical way of using fuels in IC engines is based on the use of one type of fuel that ignites either as a result of forced spark ignition (SI) or as a result of compression ignition (CI). It allows for better use of the chemical energy contained in the fuel due to the higher efficiency of this type of engines. However, the highest efficiency is currently achieved thanks to the ignition of a homogeneous air-fuel mixture, which can be ignite by spark or by compression. In Homogeneous Charge Compression Ignition (HCCI) the ignition of all the fuel in the combustion chamber occurs simultaneously. This combustion takes place at a lower temperature than in a classic diesel engine, which leads to lower heat losses and the less NO_x formation. It translates into higher thermal efficiency of engines with this type of ignition. However, in order to achieve ignition in the combustion chamber of the engine, very specific conditions are required, which are difficult to achieve [5]. Effective control of the moment at which ignition takes place in all areas of the engine operation is currently beyond the possibilities of designers. Fuel used in that type of engine must have a high octane ratio, because of its early injection. For this reason, one of the variants of engines with this type of ignition method, which has the full potential of use today, is an engine powered by two fuels by Reactivity Controlled Compression Ignition (RCCI).

RCCI is an ignition method in which high reactive fuel such as diesel fuel injected directly into the cylinder mixing with the air and self-ignites a of low reactive fuel, which is delivered to the combustion chamber earlier via indirect injection. The same way of fueling the engine characterizes a classic dual-fuel engine in which the fuel-air mixture is not homogeneous. Every modern dual-fuel engine is currently developed in the direction that allows the formation of a homogeneous air-fuel mixture [32]. Schematic of classic dual-fuel injection system is shown on Fig. 4.

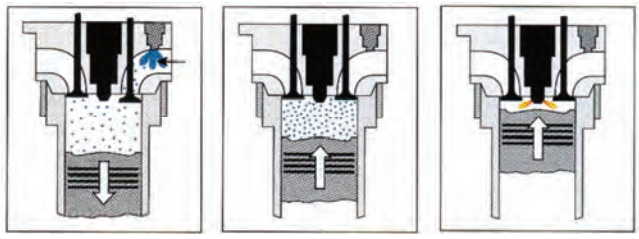

Fig. 4. Schematic drawing of direct dual-fuel injection engine work (reproduced from [9])

Before RCCI, there was a few conception which could generate better IC engines parameters. When the first engines in which a homogeneous fuel-air mixture was burned were developed, partially pre-mixed combustion (PCI) and partially premixed compression ignition (PPCI) was known. This type of ignition allows a mixture that has already been pre-mixed with air to be burned. Only when the last dose of fuel is injected into the cylinder, a fuel-air mixture is formed. In contrast to PCCI or HCCI, the name emphasizes that only a part of the fuel was mixed with air before ignition. Thanks to this method of fuel combustion, a large part of it is burned earlier than in conventional CI [12]. Gasoline Direct-injection Compression Ignition (GDCI) engine is operating basically on the same principle as PPCI or even PCCI. Difference is that the fuel used in this case is gasoline. The operation of such an engine is difficult to maintain, but since 2010 the concept of such an engine has been constantly developed [15]. HCCI ignition not possible at the current level of knowledge for use in the entire range of operation in modern piston engines. This is the basic difficulty with the widespread introduction of this type of ignition in IC engines, and it consists a number of technical problems still unsolved. Considering that these problems must be faced by HCCI and PCCI engine designers, a new concept has been introduced for a specific type of ignition: Spark (Plug) Controlled Compression Ignition (SPCCI) or Spark Assist Compression Ignition (SACI). It is self-

ignition controlled by spark plug. It is a specific method of self-ignition of a homogeneous air-fuel mixture located in the combustion chamber [30]. This type of ignition is currently in use, but mastering the ignition of a homogeneous air-fuel mixture without spark plug assist is now possible only in RCCI engines, and these kinds of ignition are the keys to introduce diesel HCCI or PCCI engine.

2.2. Dual-Fuel ignition systems

RCCI is a special type of HCCI engine that allows to use many types of fuels with high combustion efficiency and low emission of harmful exhaust components.

The low-temperature method of burning fuels in HCCI engines allows to improve the efficiency of the engine, thanks to the reduction of energy lost during combustion process. For the further development of auto-ignition engines, with increasing the range of fuels used in it, it is necessary to control the air-fuel mixture auto-ignition by using the injection of second fuel injected into the combustion chamber. The development of modern compression ignition engines is strongly dependent on engines with this type of ignition. Using two fuels with different physico-chemical properties makes it possible to control the time of compression ignition and allows to use engine in full range of operation [2].

The engine working in dual-fuel mode with diesel fuel as the reactive fuel requires only the already mentioned, pilot dose of diesel fuel to initiate the ignition. The Fig. 5 below shows a schematic view of the power supply and ignition in an RCCI engine powered by a mixture of gas fuel as the low reactive fuel and diesel as the high reactive fuel [29].

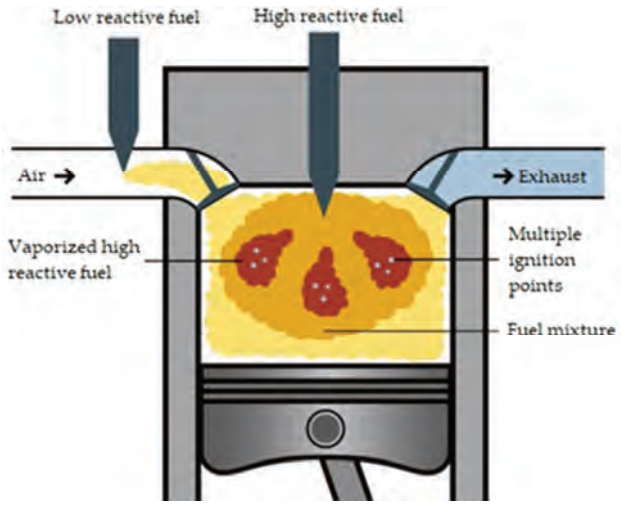

Fig. 5. Ignition and combustion in the RCCI engine (custom artwork based on [37])

In RCCI engines, low-reactive fuel, with a high octane number, is supplied to the engine along with the air through the engine's intake system. Low-reactive fuel is compressed and mixed with air to form of pre-mixed, combustible fuel-air mixture. It can be classic gasoline, alcohol, LPG, CNG or any liquid fuel with high octane ratio. Due to the high resistance to auto-ignition and knocking combustion, this mixture will not ignite despite the high temperature and pressure already in the cylinder. In the vicinity of TDC, high reactive fuel (diesel, bio-oil, GTL, CTL or HVO) is injected. This kind of fuel must be characterized by good self-ignition properties, including a low ignition temperature and the ability to large atomization of the fuel in the process of its injection. Ignition of high-reactive fuel initiates ignition of the air housing with low-reactive high-octane fuel. The essence of controlling the moment of ignition and the course of combustion of fuels used in the engine is the injection time and properties of the reactive fuel.

When using additional, low reactive fuel in DF CI engine, it's necessary to increase the amount of injected diesel fuel due to the insufficient resistance of the additional fuel to knocking combustion. Its occurrence depends on many factors, but mainly the type of fuel and the compression ratio in the engine. Knocking combustion causes the formation of uncontrolled foci of fuel self-ignition, which hinder the proper course of the combustion process and the operation of the IC engine. Its presence determines the possibility of using fuel in the engine and the degree of substitution of the basic fuel.

There is also a different fueling strategy in this type of fuel called Direct Dual Fuel Stratification (DDFS) – the difference is the use of direct injection for both fuels used in the engine [26]. Direct injection of two fuels requires the use of several injectors, or a special design injector, such as the offered product proposed by Westport corporation [34], and described in all relevant publications covering dual-fuel engine solutions [16]. Schematic show of direct dual-fuel injection work is shown on Fig. 6.

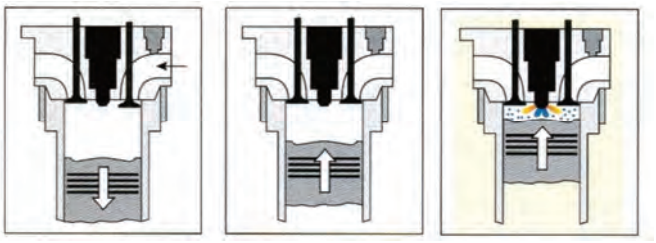

Fig. 6 Schematic drawing of direct dual-fuel injection engine work (reproduced from [9])

DDFS is a specific kind of RCCI engine, where both fuels are direct injected into the combustion chamber, where part of the low-reactive fuel is injected early enough to mix with the air, while the remaining part of the fuel can be injected in the piston's upper dead center – depending on the engine's needs [13].

There are many strategies for fueling RCCI engines and they are constantly being developed. Many solutions depend on fuels which are used in a particular RCCI engine. In the case of gaseous fuels used as low-reactive fuels, the basic parameter that is being attempted to maximize is the percentage of replacing diesel fuel with gaseous fuel. The value of this parameter strictly depends on the level of adaptation of a given engine to dual-fuel operation. Researchers want to achieve a high value of this parameter due to fuel prices and the level of emission of harmful exhaust components that can be achieved with the use of certain fuels. In most DF engines, the value of this parameter is not constant and it is not possible to maintain its high

value under high engine load. Depending on the stratification and the degree of mixing of high-octane fuel with air, the course of its combustion can be characterized in various ways, and this is often a key issue in RCCI combustion studies. The amount of fuel of a given types depends to the greatest extent on the engine load and the fuel injecting system. Figure 7 shows the chart with the dependence of the engine powered by natural gas (NG) and diesel fuel on the possibility of using both fuels in different proportions.

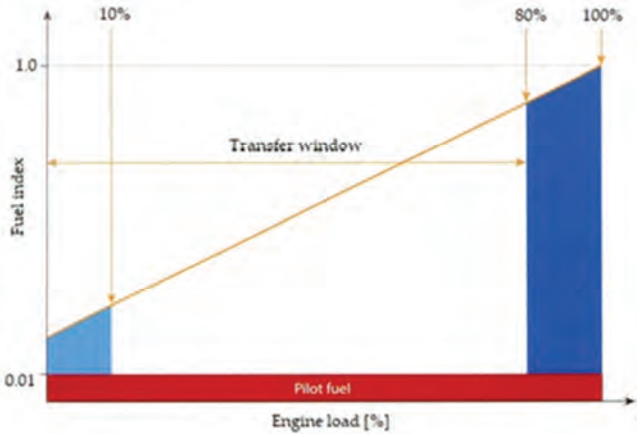

Fig. 7. The various operating conditions known as "modes" for dual-fuel engines, where horizontal is the engine load between 0–100%, and vertical is the fuel-index from 0 to 1 or 0 to 100% (reproduced from [11])

Figure above shows the DF engine fueling strategy: where the red color is pilot-fuel injection active, light blue shows that engine can be started, operated and loaded in gas mode– here engine will trip to back-up fuel after a present time, if engine load is not increased out of this area, and dark blue color means that this engine is able to run up to 100% load on either fuel, but transfers from liquid to gas are not permitted above 80% load – transfers from gas to liquid are permitted at any load. As high the fuel index is, as much liquid fuel must be used [11].

Fuels used in engines significantly influence the shape of this type of graph. Essentially all liquid and gaseous fuels of relatively high or relatively low octane numbers can be used in RCCI engines. Only those fuels that cannot be clearly classified as highly reactive or low reactive fuels would be difficult to apply in RCCI engines. If it is possible to create a homogeneous mixture of low reactivity fuel with air, this fuel may also self-ignite under the influence of pressure exerted on it by a rapidly burning highly reactive fuel, and in those option engine can be called RCCI engine. If the self-ignition occurs without forming homogeneous air-fuel mixture, the engine can be called only a DF engine. From the fuels used in those type of engines alcohols that are bio-based fuels contain in their compounds may facilitate the formation of a homogeneous mixture in the combustion chamber, so sometimes it depends on the fuel used in a given engine.

Thanks to the use of a low-reactive fuel homogeneously mixed with air, the efficiency of using the chemical energy contained in the fuel increases. Its increase is also influenced by the even temperature distribution in the combustion chamber. This reduces the total amount of heat penetrating the cylinder walls and prevents the formation of hot spots within the cylinder what is clearly visible in Fig. 8. The maximum combustion temperature in the combustion chamber is lower than in conventional compression ignition engines.

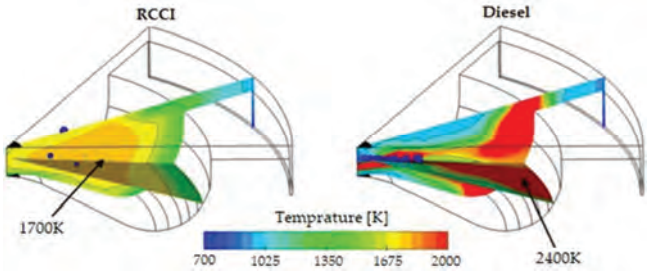

Fig. 8. Temperature distribution in the combustion chamber for a RCCI engine powered by CNG and diesel and a classic diesel engine powered only by diesel (modified graphic based on [7])

Due to the even and low-temperature course of the combustion process, the emission of nitrogen oxides, solid particles and soot is reduced, just like in the classic HCCI engine. High flame temperature is one of the main factors causing the formation of nitrogen oxides during the combustion process. Nitrogen oxides are not formed in RCCI engines as intensively as in a classic diesel engine. Due to the combustion close to the stoichiometric composition, the amount of oxygen and nitrogen in the combustion chamber during the process is therefore reduced compared to a classic diesel engine [36].

The real benefits of lowering the combustion temperature appear in large, low-speed marine engines, where the problem of cooling the combustion chamber is solved in more ambitious ways than in a small piston engines. Piston and combustion chamber cooling is more advanced, because it is possible in engines of such dimensions. Figure 9 shows the drilled holes in the large engine piston.

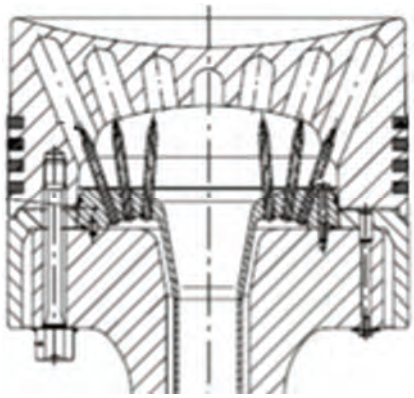

Fig. 9. Example of piston cooling drills in the Sulzer IC engine (reproduced from Pounder's Marine Diesel Engines [35] with permission from Elsevier)

Drills made in the piston enable its effective cooling with the use of engine oil. The differences in combustion temperature between conventional CI engine and HCCI or RCCI engine can potentially eliminate the need for such a solution. The lower temperature reduces the occurrence of the NO_x formation effect, which obviously allows limiting

the participation of SCR in changing the composition of exhaust gases. Low emissions that can be achieved in research engines requires significant interference in the design of the IC engine, preceded by its research and optimization of the design for the combustion of a new type of fuel. In both single-fuel diesel engines and dual-fuel diesel engines (RCCI), it is required to adapt the combustion chamber to run on a new type of fuel [7]. In the present CI engines the combustion chamber is widely profiled inside the piston. Fuel injection shape depends on to the combustion chamber shape too. Figure 10 shows the potential of injection angles for typical DI engine.

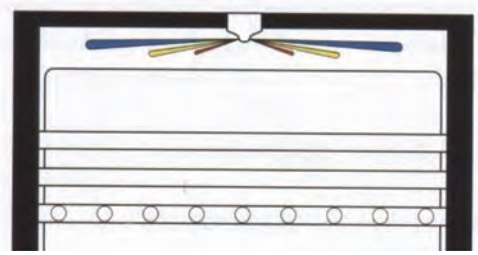

Fig. 10. Shown of the fuel injection process with various fuel-injection possibilities in example of different angles of injection (reproduced from [9])

This ability to inject fuel in different angles is greatly needed in RCCI engine. Some studies [4, 8, 29] has repeatedly shown that the shape of the combustion chamber in RCCI engines is very important for the formation of harmful chemical compounds contained in exhaust gases. Standard injection shapes in CI engines are showed in the Fig. 11. Those shapes and angles of injection in standard CI engines are not good enough for RCCI.

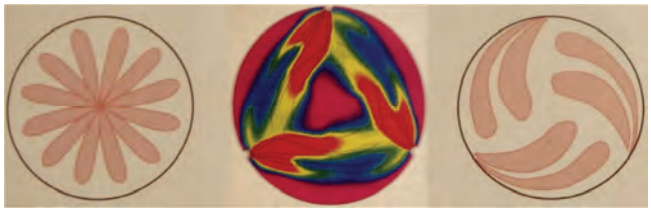

Fig. 11. Shown of the correct injection spray shapes in the injection flow of a four-stroke trunk-piston engine (left), in a large two-stroke crosshead engine with three injectors (centre), and a two-stroke crosshead engine (right) (reproduced from [9])

Those shapes and angles of injection in standard CI engines are not good enough for RCCI. While DF engines are often derived from standard CI diesel engine conversion, the limitations that result from this should be borne in mind. Defining the needs for RCCI engines reliance on such limitations, and on fact, that the most that the biggest changes involve the engine combustion chamber. Next chapter will focus on these shifts, where they can be divided into technical solutions including the construction of the piston – combustion chamber and the fuel injector.

2.3. Important RCCI technical solutions

The basic technical modification that should be carried out on an existing engine adapted to work in RCCI mode is the change of its combustion chamber and modification of the power supply system.

Important in that point is that combustion chamber space that can enable proper work of the single fuel CI engine will have a swirl ratio of low reactivity fuel problems and can have a hot spots on its surface, what which disqualifies the possibility of using low reactive fuel with an octane number that does not provide resistance to spontaneous combustion in contact with such a hot point on the surface of the combustion chamber. When dealing with this problem, designers often use additional cooling of some elements (e.g. injectors), which heat up excessively in the combustion processes [28].

The shape of the RCCI combustion chambers, with different compression ratio options, compared to the combustion chamber of a modern CI engine is shown in the Fig. 12.

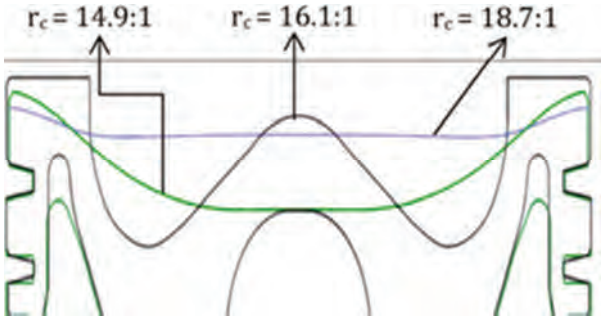

Fig. 12. Comparison of RCCI and classic CI engine piston with combustion chamber inside of it (reproduced from [31])

Form of combustion chamber in RCCI engine is fundamentally different than in classical CI diesel engine. The swirl ratio of air-fuel mixture must be higher, surface of combustion chamber can be much smaller, and the shape itself will be softer. In the Fig. 13 is shown the cross section of the piston where the sharpest edges of the combustion chamber are colored by the red circles.

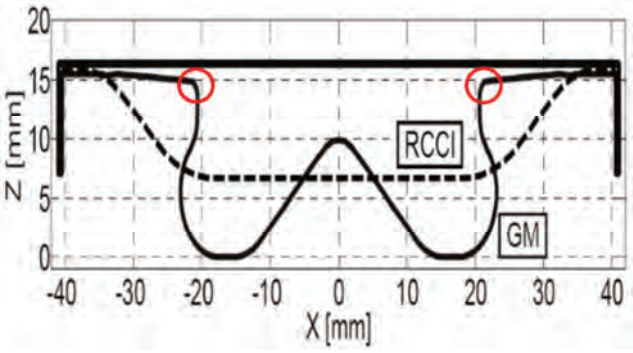

Fig. 13. Cross-section drawing of GM stock piston (solid line) and modified RCCI piston (dotted line) (reproduced from [6])

Injection of high reactivity fuel in RCCI engine takes place differently than in a classic diesel engine. Direct injection of high reactivity fuel with a centrally located injector in a classic CI engine requires the use of a combustion chamber located in the piston, the shape of which is optimal only for single-fuel engine operation. DF operation needs different combustion chamber shape. The amount of this fuel itself is many times lower in most of the engine operation area, so the space required for uniform mixing of the

injected fuel is not so great, but the places where the fuel must be delivered are extended by the area above the piston and the combustion chamber hollowed in it. Because there is already low-reactive fuel in the entire in-cylinder space over the piston, high reactive fuel must be delivered to an area already filled with this fuel. It forces a change of the place where the fuel will be injected. The changes in the injector design alone will not be enough and the researchers decided to change the factory piston into custom piston. More important is the issue of correct swirling of the air-fuel mixture [4, 8, 29]. These parameters have the greatest impact on the degree of swirling of the fuel-air mixture, which for different proportions of the fuel mixture has a different impact on the efficiency of their use. The red edges of the combustion chamber in the RCCI engine constitute a serious barrier to the proper distribution of the injected highly reactive fuel inside the combustion chamber. It is necessary in existing engines to modify them in order to improve the distribution and swirling of the air-fuel mixture. Researchers in [1] prepared project from the original GM piston to modify it into investigatory RCCI piston. Effects are shown in the Fig. 14.

Fig. 14. Photo of modified RCCI piston and stock GM 1.9 L piston (reproduced from [1])

Project of RCCI piston has been meticulously prepared and, after its construction, installed and used for further research. Researchers indicate an increase in the thermal efficiency of the engine thanks to the use of such a piston. Such scientific efforts are very much needed because there is not enough research into RCCI engines to interfere with the essential design of existing engines. In the Fig. 15 plans comparison both pistons are shown.

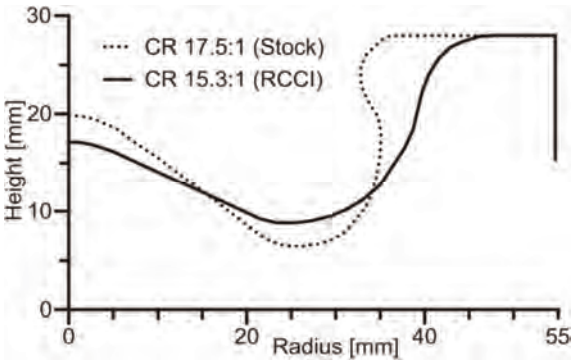

Fig. 15. Differences between piston bowl geometries in different compression ratios for RCCI engine, and classical diesel engine (reproduced from Applied Energy [22] with permission from Elsevier)

In order to adjust the combustion chamber in the piston for DF combustion, the researchers proposed an alternative shape of the combustion chamber [22], which is shown in comparative Fig. 16, containing two numerical models of combustion chambers.

Fig. 16. Potential of piston combustion chamber geometries (reproduced from [22])

Conceptions of bowl piston geometry for RCCI engines are new and different. Most of them are computer simulations concepts, but researchers [1, 7] create real piston which was showed in the Fig. 14, and prepared technical documentation for different piston shapes for testing RCCI engines, showed in the Fig. 17.

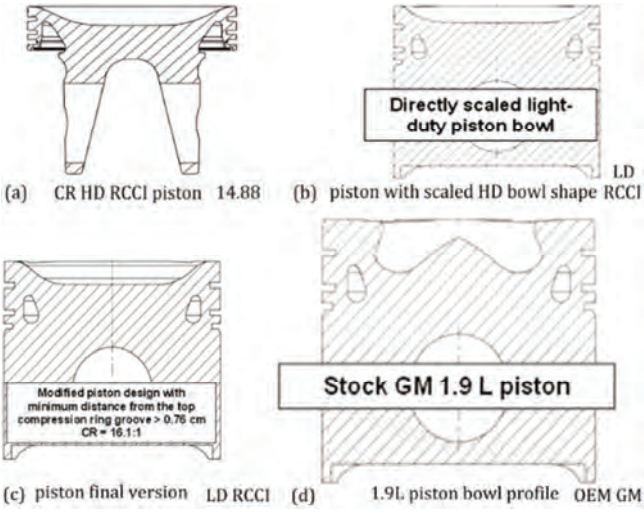

Fig. 17. Comparison of piston bowl geometries (graphic based on [6])

The geometry of RCCI piston is strongly dependent on the injector position and spray shade. There is multiple option for further research about it. The good example can be quoted in work where researchers focus on negative valve overlap (NVO) process as a promising variable valve actuation (VVA) measure to improve low-load efficiency in RCCI engines and (external) fuel reforming techniques to improve low temperature combustion (LTC) performance in those engines [19]. Was shown that low-load RCCI operation can be improved with a combination of NVO and direct diesel injection into recompressed residuals. Validating this hypothesis was the goal of their research in which they create computer simulation of the present research. In this work it's possible to find that even the fuel supply system effects on correct injection shape and piston bowl geometry what is showed in the Fig. 18.

Fig. 18. Piston bowl geometries and injection configurations in a different fuel supply systems in RCCI engines (reproduced from Applied Energy [19] with permission from Elsevier)

The way the fuel is supplied to the RCCI engine affects the geometry of the combustion chamber and the shape of injection of highly reactive fuel. On the left part on Fig. 18 the Single Point Injection (SPI) with mixer after turbocharger is showed, and on the right site is Port Fuel Injection (PFI) to individual cylinder ports. It is important to say at this stage that the generally specified methods of supplying the engine can be correlated with other engine supplying techniques. In the case of RCCI engines it can give measurable effects, as in the case of work where NVO allowed to achieve heavy exhaust gas recirculation RCCI case shows up to 75% methane emission reduction is attainable at low load through combined effect of increased mixture homogenization and elevated temperature at intake valve closing [19].

When it comes to fuel supplying RCCI engines, much depends on the size of the engine, and its construction. In smaller engines, which are commonly use in land vehicles like cars and trucks – space for using more than one fuel injector in cylinder head per cylinder is limited. Basically engines like that are equipped with fuel supply installations (Fig. 4 and 5), where low reactive fuel is supplied by PFI, and only high reactive fuel can be injected directly into cylinder. That technology is commonly used in all engines capacity, the idea of fuel delivery may be slightly different, but usage of carburetor or the gaseous fuel inlet valve in bigger engines are not fundamentally different from each other and their technical construction are well known. Figure 19 shows a scheme of a gas mixer.

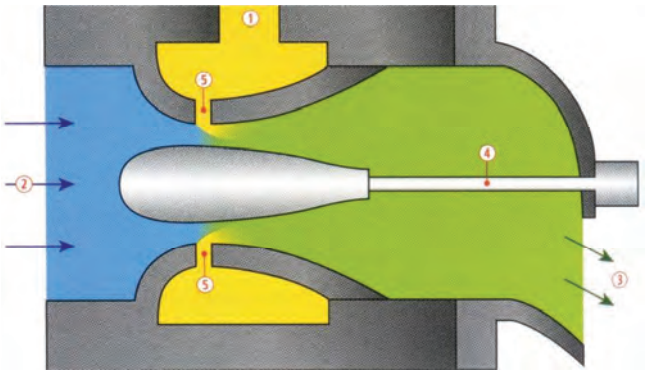

Fig. 19. A cross-sectional view of a gas mixer with an adjustable venturi insert, where 1 is the gaseous fuel supply, 2 is the air supply, 3 is the air-fuel mixture to the intake manifold of the gas- or dual-fuel engine, 4 is the adjustable venturi insert shaft connected to stepper motor, and 5 are bores for the supply of fuel-gas in the throat of the gas mixer (reproduced from [9])

The differences in the construction of such devices may differ in details but also in size, because they are used in all types of IC engines, even in the largest maritime engines. Figure 20 shows samples photos of throats intended for gas mixers mounted in the intake manifold.

When it is necessary, gas mixers working similar to carburetor are replaced by fuel injectors, localized as close to the intake valves as it is possible. It depends on the possibility of adjusting the fuel injection moment to the current demand of the engine. Those fuel injectors are not technically novelties, so their availability and knowledge of their construction is common.

Fig. 20.The examples of throat constructions from gas mixers for different engines (reproduced from [10])

The problem in further development of RCCI engines and in general of engines operating in DF mode are direct injection systems covering injection of both used fuels.

The use of two independent injectors in the cylinder head is possible, but only in sufficiently large engines. This solution allows for direct injection of two fuels, but is technically more demanding and expensive. In maritime engines exist the system of two independent injectors of diesel fuel and liquefied natural gas (LNG) in pure form [11].

The only existing mass-produced solution in small-sized engines that allows the injection of two different fuels with one injector is the dual-fuel injector technology developed by Westport. Those injectors are already available in two generations. Injector that works in high pressure direct injection (HPDI) system includes injection of both fuels at big pressure at similar time in the same engine operation moment. The scheme of that kind of injector work is shown in the Fig. 21.

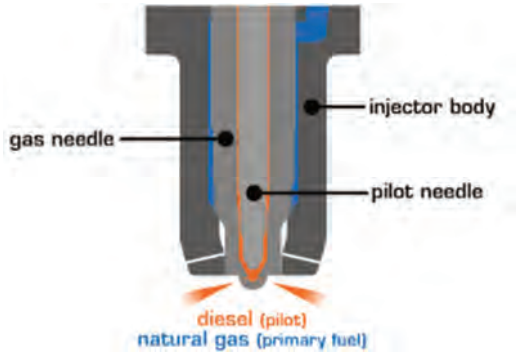

Fig. 21. Scheme of Westport company HPDI Injector Tip Assembly (reproduced from [33])

Product proposed by Westport corporation [27], and described in all relevant publications covering dual-fuel engine solutions for car and trucks [16] is only one factory-made injector available in the global market. It intended use is related to IC engines installed in heavy truck vehicles

Apart from the invention of Westport Company – and marine engines technologies with two independent injectors – DI of two fuels in small engines for passenger cars can be realized only in laboratory conditions for research purposes. In one study research team made their own handcrafted injector created for DI of CNG fuel in DF engine. Figure 19 shows the cross-section of the cylinder head with gaseous fuel injector and connection block, which is used for gaseous fuel supply for that concept DI gas injector.

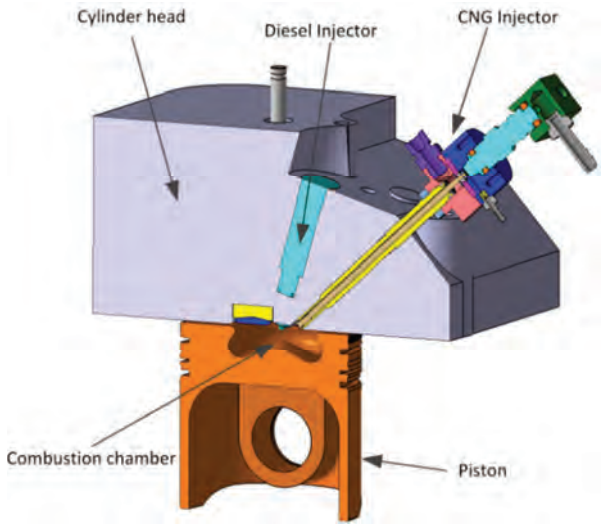

Fig. 22. The localization of the injector in CAD drawing of the cylinder head on the left and a custom gaseous-fuel injector with a parts of it on the right (reproduced from [14])

In the free market for car engines, it is hard to buy gaseous fuel direct injector, and basically impossible to buy Dual-Fuel injector – designed to inject two types of fuels simultaneously. This illustrates the early stage of development of this type of technique and its relatively low prevalence at the market. It should be borne in mind, that only DI of both fuels allows for realizing advanced fuel delivery strategies and paves the way for the development of advanced ignition techniques in IC engines, for which RCCI technique is a stop on the way to their further development.

Different group of researchers make the objective of their study to assess the potential of RCCI with direct injected low reactivity fuel in terms of thermal efficiency and methane emissions introducing gaseous fuel stratification by direct injection of it is considered to be beneficial for combustion efficiency increase [18]. Their simulation results, explanations for the observed trends are provided, and important phenomena are identified that are associated with increased low reactivity fuel stratification, which contributed to the reduction of methane emissions and an increase in NO_x emissions. Authors noted the lack of a significant amount of research on the RCCI direct injection engine. Authors of [18] noted the lack of a significant amount of research on the RCCI direct injection engine: "the improvement potential of such natural gas stratification in RCCI engines is unknown" which authors of present article can also confirm to some extent, with a few exceptions, like [21, 36] where authors introduced term DDFS, but their research is so far focused on a limited number of engines and fuels used, so that topic is still under development for the researchers

A different approach for fuel delivery can be found in the case of two-stroke engines, where fuel can be inject into the cylinder without using the injector located in the engine's head. Figure 23 shows the injection system in two stroke marine engine, where gaseous fuel is injecting direct into the cylinder when the piston starts to move upwards, to its top position. Injected gas have got much time to create air-fuel mixture, and at the top piston position secondary high reactivity fuel is injecting, starting the combustion process. This type of RCCI engine fuel supply system is only available in marine two-stroke engines.

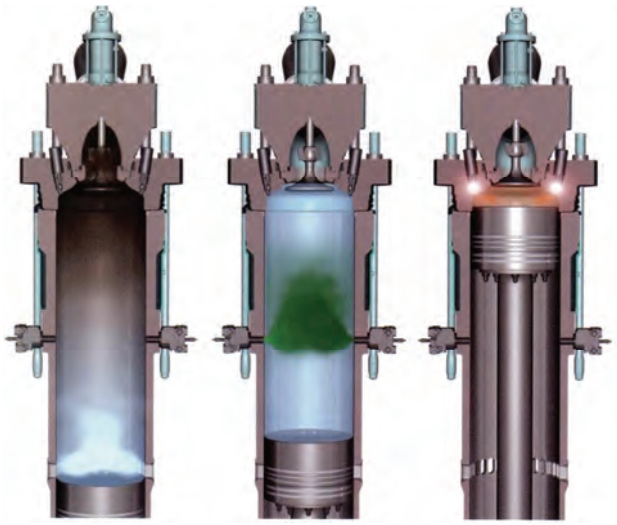

Fig. 23. Fuel injection process in two-stroke maritime engines, where the principle for the injection of low pressure gas through the cylinder liner during the upwards movement of the piston is clearly visible (reproduced from [9])

In that kind of marine engines, VVA is not a perspective technology because of two stroke engine specific construction, but researchers strongly recommend to increase knowledge and development of that technology [20]. Their experience with that technic shows that VVA makes it possible to improve combustion efficiency and thermal management (better after-treatment efficiency) and extending high load engine range. Maintaining a homogeneous mode of operation in the engine requires maintaining specific conditions. Researchers in their work create simulation concept for VVA in RCCI engine with a full load range and for two types of engine fueling: CNG-diesel and gasoline-diesel.

RCCI engines are commonly used in powerplants and marine applications, so their technology is more elaborate than in small engines. Researchers also found such potential applications for these engines, and their work show the variety of research that should be carried out on engines of this type, laying the foundations for their further work based on the stratification of low reactivity fuel and VVA [17]. The development of DF engines can be traced on the basis of gaseous engines in Wärtsilä company is shown in the Fig. 24.

It is clearly visible increase in the share of engines based on dual-fuel technology. Not all of those engines listed in that figure can work in dual-fuel mode – because a few of them was only gaseous fuel – but each of them was another important step in the development of RCCI engines.

However, development issues of small-size RCCI engines also includes external equipment, such as the engine control unit, which are currently available from only one manufacturer [3]. The difference between RCCI engine development in those different engine sizes are clearly visible and still require much more research work, especially for smaller combustion engines

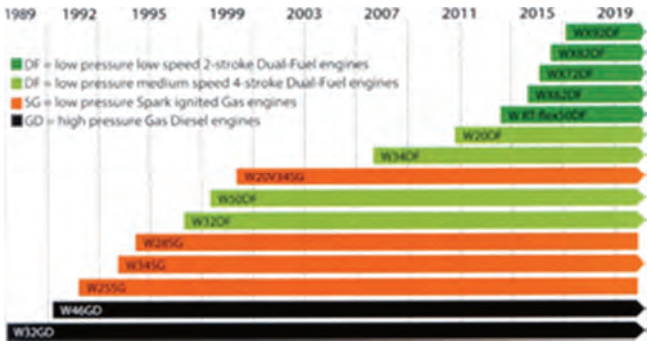

Fig. 24. Example of gaseous fuel engines development in Wärtsilä company between 1989 to 2015+ is the extensive portfolio of Wärtsilä gas- and dual-fuel engines for both two-stroke and four-stroke engine (reproduced from [9])

The last but extremely important technical challenge facing the researchers is to control the entire engine systems so it can work in the RCCI mode throughout the entire range of engine performance. No solution in this matter can be considered ready if it has not been tested in a working engine, which has so far been addressed by a small number of researchers and the publication [28]. There are not many such publications at that moment, but they are the most desirable type of publications summarizing the achievements in the field of all techniques used in RCCI engines. The correct electronic control of the engine operation will be necessary for the RCCI mode to be effectively used in the future of IC engines.

3. Conclusions

The intensive development of injection technology for both independent fuels is still needed in the context of current solutions of RCCI engines. Low reactivity fuel stratification could be the main point for future development of these engines, unfortunately there are few publications regarding DDFS topic.

There are also problems with the correct air-fuel swirl ratio and the injection angle of highly reactive fuel. It is necessary to adapt the injection shape by adapting it to the new geometry of the combustion chamber. There is some research on the subject, but much remains to be done in this subject (most studies are only computer simulations or theoretical considerations).

The combustion chamber geometry is not yet optimized for all engines where there is a need for the DF RCCI operating mode.

The most important challenge with low reactive fuel injection is the need to create a homogeneous mixture under all engine operating conditions.

In the case of highly reactive fuel injectors, the new challenge is to spray the fuel over the entire space of the combustion chamber. The RCCI combustion chamber geometry may be substantially the entire space above the piston in the cylinder space. Injection angles and injector efficiency differ significantly from that of a classic diesel injector. Basic design assumptions should be changed.

It is worth mentioning that in the future the engine industry will have to make an effort to put these types of engines into production. All the innovative technical solutions described here have only a conceptual character or were made in a single made test engine unit. The problems of mass production of new constructions are still ahead of us.

New technical solutions, especially those that are only computer simulations, definitely require further research and tests covering the use of various types of fuels, materials and test conditions.

Researchers are also faced with the challenge of combining all the technical solutions mentioned in the article in one engine and controlling its operation in a way that enables continuous operation in the RCCI mode. This challenge may be the most demanding, but its implementation requires even more detailed research into the technical solutions themselves. Especially when we are talking about small motors that are not used in industry.

Acknowledgements

This work was financed by Military University of Technology under research project UGB 880/2021.

Nomenclature

CI compression ignition
CNG compressed natural gas
DDFS direct dual fuel stratification
DI direct injection
GDI gasoline direct injection
GDCI gasoline direct-injection compression ignition
GM general motors
IC internal combustion
HCCI homogeneous charge compression ignition
HPDI high pressure direct injection
LNG liquefied natural gas
LPG liquefied petroleum gas
LTC low temperature combustion
NVO negative valve overlap
PCCI Premixed Chargé Controlled Ignition
PFI port fuel injection
PPC Partially premixed combustion
PPCI partially premixed compression ignition
RCCI reactivity-controlled compression ignition
SACI spark assist compression ignition
SCR selective catalytic reduction
SI spark ignition
SPCCI spark plug controlled compression ignition
SPI single point injection
TDC top dead center
VVA variable valve actuation

Bibliography

[1] CURAN, S., HANSON, R.M., WAGNER, R.M. et al. Efficiency and emissions mapping of RCCI in a light-duty diesel engine. *SAE Technical Paper* 2013-01-0289. https://doi.org/10.4271/2016-01-2309

[2] DAHODWALA, M., JOSHI, S., KOEHLER, E. et al. Investigation of Diesel-CNG RCCI combustion at multiple engine operating conditions. *SAE Technical Paper* 2020-01-0801. 2020. https://doi.org/10.4271/2020-01-0801

[3] DEEN SHIPPING (Mr G. Deen), ARENARED (Mr P. Nooijen), DOLDERMAN (Mr J. Been). Breakthrough LNG deployment in Inland Waterway Transport, Activity 2.3 Evaluation report pilot test MTS Argonon, LNG Binnenvaart & Deen Shipping, Rotterdam 2020.

[4] DELVESCOVO, D.A. The effects of fuel stratification and heat release rate shaping in Reactivity Controlled Compression Ignition (RCCI) combustion. *PhD Thesis*. University of Wisconsin, Madison 2016.

[5] FIRMANSYAH, A., RASHID, A.A., MORGAN, R.H. et al. Reactivity Controlled Compression Ignition (RCCI) of gasoline-CNG mixtures, improvement trends for internal combustion engines. *IntechOpen Book Series*. 2017. https://doi.org/10.5772/intechopen.72880

[6] HANSON, R.M., CURRAN, S.J., WAGNER, R.M. et al. Piston bowl optimization for RCCI combustion in a light-duty multi-cylinder engine. *SAE Technical Paper* 2012-01-0380. 2012. https://doi.org/10.4271/2012-01-0380

[7] KALSI, S.S., SUBRAMANIAN, K.A. Experimental investigations of effects of hydrogen blended CNG on performance, combustion and emissions characteristics of a biodiesel fuelled reactivity-controlled compression ignition engine (RCCI). *International Journal of Hydrogen Energy*. 2017, **42**(7), 4548-4560. https://doi.org/10.1016/j.ijhydene.2016.12.147

[8] KOKJOHN, S.L., HANSON, R.M., SPLITTER, D.A. et al. Fuel reactivity-controlled compression ignition (RCCI): A pathway to controlled high-efficiency clean combustion. *International Journal of Engine Research*. 2011, **12**(3). https://doi.org/10.1177/1468087411401548

[9] KUIKEN, K. Gas- and dual-fuel engines for ship propulsion, power plants and cogeneration. Book I: Principles, Target Global Energy Training. *PJ Onnen*. The Netherlands 2016.

[10] KUIKEN, K. Gas- and dual-fuel engines for ship propulsion, power plants and cogeneration. Book II: Engine systems and environment, Target Global Energy Training. *PJ Onnen*. The Netherlands 2016.

[11] KUIKEN, K. Gas- and dual-fuel engines for ship propulsion, power plants and cogeneration. Book III: Operation and maintenance, Target Global Energy Training. *PJ Onnen*. The Netherlands 2016.

[12] KULKARNI, A.M., STRICKER, K., BLUM, A. et al. PCCI control authority of a modern diesel engine outfitted with flexible intake valve actuation. *Journal of Dynamic Systems Measurement and Control*. 2010, **132**(5), 051009. https://doi.org/10.1115/1.4002106

[13] LUONG, M.B., SANKARAN, R., YU, G.H. et al. On the effect of injection timing on the ignition of lean PRF/air/EGR mixtures under direct dual fuel stratification conditions. *Combustion and Flame*. 2017, **183**, 309-321. https://doi.org/10.1016/j.combustflame.2017.05.023

[14] MAJCZAK, A., BARAŃSKI, G., SOCHACZEWSKI, R. et al. CNG injector research for dual fuel engine. *Advances in Science and Technology – Research Journal*. 2017, **11**(1), 212-219. https://doi.org/10.12913/22998624/68458

[15] MEISAM, A.G. History of Gasoline Direct Compression Ignition (GDCI) engine – a review. *IJRET: International Journal of Research in Engineering and Technology*. 2014, **3**(1), 335-342. https://doi.org/10.15623/IJRET.2014.0301058

[16] MELAIKA, M., HERBILLON, G., DAHLANDER, P. Spark ignition engine performance, standard emissions and particulates using GDI, PFI-CNG and DI-CNG systems. *Fuel*. 2021, **293**, 120454. https://doi.org/10.1016/j.fuel.2021.120454

[17] MIKULSKI, M., RAMESH, S., BEKDEMIR, C. Reactivity Controlled Compression Ignition for clean and efficient ship propulsion. *Energy*. 2019, **182**, 1173-1192. https://doi.org/10.1016/j.energy.2019.06.091

[18] MIKULSKI, M., BEKDEMIR, C. Understanding the role of low reactivity fuel stratification in a dual fuel RCCI engine – a simulation study. *Applied Energy*. 2017, **191**, 689-708. https://doi.org/10.1016/j.apenergy.2017.01.080

[19] MIKULSKI, M., BALAKRISHNAN, P., HUNICZ, J. Natural Gas-Diesel Reactivity Controlled Compression Ignition with negative valve overlap and in-cylinder fuel reforming. *Applied Energy*. 2019, **254**, 113638. https://doi.org/10.1016/j.apenergy.2019.113638

[20] MIKULSKI, M., BALAKRISHNAN, P., DOOSJE, E. et al. Variable valve actuation strategies for better efficiency load range and thermal management in an RCCI engine. *SAE Technical Paper* 2018-01-0254. 2018. https://doi.org/10.4271/2018-01-0254

[21] MINH, B.L., RAMANAN, S., GWANG, H.Y. et al. A DNS study of the effects of injection timing on the ignition of PRF/air mixture under direct dual fuel stratification (DDFS) conditions. *The 8th European Combustion Meeting*. Dubrovnik 2017.

[22] PACHIANNAN, T., ZHONG, W., RAJKUMAR, S. et al. A literature review of fuel effects on performance and emission characteristics of low-temperature combustion strategies. *Applied Energy*. 2019, **251**, 113380. https://doi.org/10.1016/j.apenergy.2019.113380

[23] PAYKANI, A., GARCIA, A., SHAHBAKHTI, M. et al. Reactivity controlled compression ignition engine: Pathways towards commercial viability. *Applied Energy*. 2021, **282**, 116174. https://doi.org/10.1016/j.apenergy.2020.116174

[24] PAYKANI, A., KAKAEE, A-H., RAHNAMA, P. et al. Progress and recent trends in reactivity-controlled compression ignition engines. *International Journal of Engine Research*. 2016, **17**, 481-524. https://doi.org/10.1177/1468087415593013

[25] PAYKANI, A., AMIRHASAN, K., POURYA, R. et al. Progress and recent trends in reactivity-controlled compression ignition engines. *International Journal of Engine Research*. 2015, **17**(5), 481-524. https://doi.org/10.1177/1468087415593013

[26] RAO, A., MEHRA, R.K., DUAN, H. et al. Comparative study of the NO_x prediction model of HCNG engine. *International Journal of Hydrogen Energy*. 2017, **42**(34), 22066-22081. https://doi.org/10.1016/j.ijhydene.2017.07.107

[27] Westport Fuel Systems Inc. https://wfsinc.com/

[28] Real world RCCI: reactively controlled ignition goes live. The Motorship Insight For Marine Technology Professionals. 2020. https://www.motorship.com/news101/ships-equipment/real-world-rcci-reactively-controlled-ignition-goes-live

[29] REITZ, D.R., DURAISAMY, G. Review of high efficiency and clean reactivity controlled compression ignition (RCCI) combustion in internal combustion engines. *Progress in Energy and Combustion Science*. 2015, **46**, 12-71. https://doi.org/10.1016/j.pecs.2014.05.003

[30] ROBERTSON, D., PRUCKA, R.A. Review of spark-assisted compression ignition (SACI) research in the context of realizing production control strategies. *14th International Conference on Engines & Vehicles*. 2019. https://doi.org/10.4271/2019-24-0027
[31] SPLITTER, D., WISSINK, M., DELVESCOVO, D. et al. RCCI engine operation towards 60% thermal efficiency. *SAE Technical Paper* 2013-01-0279. 2013. https://doi.org/10.4271/2013-01-0279
[32] STOREY, J.M.E., CURRAN, S.J., LEWIS, S.A. et al. Evolution and current understanding of physicochemical characterization of particulate matter from reactivity controlled compression ignition combustion on a multicylinder light-duty engine. *International Journal of Engine Research*. 2016, **18**(5-6), 505-519. https://doi.org/10.1177/1468087416661637
[33] WEICHAI, Westport secures Chinese certification for WP12 natural gas engine powered by HPDI 2.0. Green Car Congress 2020.
[34] Westport. Natural gas vehicle technologies for light, medium, heavy and high horsepower applications, 2013.
[35] WOODYARD, D. Pounder's Marine Diesel Engines (Eighth Edition) and Gas Turbines. 2004, 641-663.
[36] YAOPENG, L., MING, J., LEILEI, X. et al. Multiple-objective optimization of methanol/diesel dual-fuel engine at low loads: a comparison of reactivity controlled compression ignition (RCCI) and direct dual fuel stratification (DDFS) strategies. *Fuel*. 2020, **262**, 116673. https://doi.org/10.1016/j.fuel.2019.116673
[37] The ArenaRed performance. https://www.arenared.nl/cpbc+%7E+rcci

Grzegorz Szamrej, MSc. – Faculty of Mechanical Engineering, Military University of Technology in Warsaw.
e-mail: *grzegorz.szamrej@wat.edu.pl*

Janusz Chojnowski, MSc. – Faculty of Mechanical Engineering, Military University of Technology in Warsaw.
e-mail: *janusz.chojnowski@wat.edu.pl*

Mirosław Karczewski, DEng. – Faculty of Mechanical Engineering, Military University of Technology in Warsaw.
e-mail: *miroslaw.karczewski@wat.edu.pl*

Article citation info:
PRZYBYŁA, G., ZIÓŁKOWSKI, Ł., BUCZAK, M. et al. The tests of micro-CHP prototype with SI engine powered by LPG and natural gas. *Combustion Engines*. 2022, **189**(2), 47-53. https://doi.org/10.19206/CE-142951

Grzegorz PRZYBYŁA
Łukasz ZIÓŁKOWSKI
Mateusz BUCZAK
Zbigniew ŻMUDKA

Combustion Engines
Polish Scientific Society of Combustion Engines

The tests of micro-CHP prototype with SI engine powered by LPG and natural gas

ARTICLE INFO

Received: 11 August 2021
Revised: 4 October 2021
Accepted: 7 October 2021
Available online: 12 October 2021

This paper presents the experimental results of a Combined Heat and Power (CHP) prototype based on a SI V-twin internal combustion engine driving a synchronous generator. The paper presents the criteria that were used to select the combustion engine and the electrical generator for the prototype. The internal combustion engine has been adapted to be fuelled by natural gas or LPG, with the possibility of controlling the load in two ways, i.e. by changing the throttle position (quantitatively) and/or the value of the excess air ratio by changing the fuel dose at a constant throttle position (qualitatively). The applied method of control allows to improve the efficiency of the engine especially in the range of partial loads. The experimental tests were carried out at a constant speed of 1500 rpm. During the tests, the fuel consumption of the internal combustion engine, the composition of the exhaust gas at the outlet of the exhaust system, the electrical parameters of the synchronous generator and the temperature at selected locations of the CHP system instance were measured. According to the obtained results, there was a slight increase in the efficiency of electricity generation with the application of the developed method of control of the combustion engine. The maximum power generation efficiency for Natural Gas (NG) was higher compared to LPG by more than 2 percentage points. The exhaust gas emission level confirm that the prototype cogeneration system meets the Stage II emission standard (in accordance with Directive 2002/08/EC for small SI engines with a power below 19 kW. D2 ISO 8178).

Key words: *SI engine, efficiency, natural gas, CHP, natural gas, LPG*

1. Introduction

Small scale cogeneration units called micro-CHP driven by Internal Combustion Engine (ICE) fueled with gaseous fuels seem to be a promising solution for heat and power generation for householders. The profitability of using such system depends on firstly the investment costs and secondly the operating costs of the mCHP unit. However, an important issue in such case may be the engine lifetime. Another issue is that the electrical efficiency of mCHP units driven by ICE decreases when the electricity demands of the receivers drops. The spark-ignition engine efficiency increases by reducing the pumping loss through the throttle in the partial load range [1]. A simple solution to achieve low pump loss is that using the lean mixture for the partial engine load operation. But, the limitation of using the lean mixture is the flammability limits of the air-fuel mixture of the specific gaseous fuel.

Stirling engines, microturbines, Rankine cycle micro systems, solid-state devices, and fuel cells achieve electrical efficiencies in the range of 30–40% and total CHP efficiency of 80% for a 1 kW device. Achieving these efficiencies, however, is a difficult from both technical and economic point of view to be acceptable for the residential customer [2]. One of the best performing small-scale CHP unit is Vaillant-Honda product based on SI engine with 1.2 kW electrical power with fuel to electricity conversion efficiency of about 26.3% and the total CHP efficiency of 92% [3]. The next examples of mCHP unit that is available on the market is Yanmar mCHP systems. These are based on Miller cycle along with lean air-fuel mixture combustion. The fuel to electricity conversion efficiencies for the 5 kW (CP5WN) and 10 kW (CP10WN) systems are 28% and 31.5%, respectively, with more than 50% thermal efficiencies. Yanmar mCHP systems meet the EPA emissions standard [4, 5]. Dachs 5.5 model is another example of the small scale CHP unit from SENERTEC company. This device offer three output power levels 7.5 kW, 10.6 kW, and 14.8 kW with fuel to electricity conversion efficiencies of 26.5%, 26.5%, and 25.6% respectively which meet German TA-Luft emission standard [6, 7]. The mCHP systems based on ICE are usually available for Liquefied Petroleum Gas (LPG) or NG fuel supply.

In 2018 the natural gas was used in 55.7% of Polish households, but more than half of consumers (51.9%) used it only for cooking, and only 14.0% for space heating. In some areas of the country where have no access to NG, in-cylinders stationary LPG were more common almost 34.0%. The LPG exclusively was used for cooking by more than 99% of consumers [8, 9].

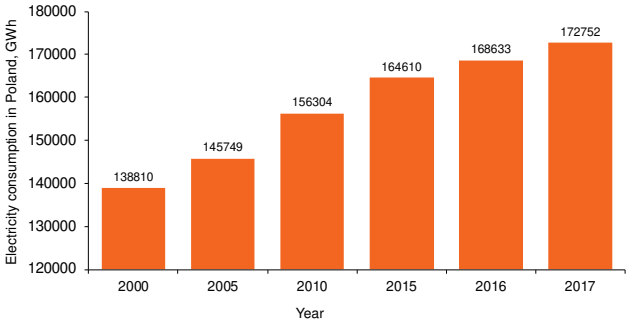

Fig. 1. Electricity consumption in Poland in the years 2000-2017

In the first decade of the 21st century, there was a significant increase in electricity consumption in Poland. In the years between 2000 to 2010, it amounted slightly more than 12%, which is an increase of over 17.4 TWh compared to the value recorded in 2000. Over the next seven years,

e.g. in the period of 2010 to 2017, there was a further increase of over 10% [10]. Electricity consumption in Poland between the years from 2010 to 2017 is shown in Fig. 1.

The demand for electricity in Poland will most likely continue to grow in the upcoming years. As mentioned before, a clear upward trend observed in recent decades, can be considered evidence of this statement. In addition, these increase of electricity consumption in the near future will be due to the growing market in sharing of electric and plug-in hybrid vehicles, as well as the growing demand for electricity in households like smart home, air conditioning, etc.

With regard to the data above, the use of local low-power cogeneration systems may be beneficial. The mCHP can be implemented on the basis of an ICE powered by NG or LPG. In the light of the Directive 2004/8/EC, micro-cogeneration refers to the combined production of electricity with a maximum electrical power of less than 50 kW.

This article presents the test results of the prototype equipped in synchronous generator, which was built by Budexpert sp. z o.o. in cooperation with a research team from the Silesian University of Technology as part of a project co-financed from the sources of the Regional Operational Program of the Silesian Voivodeship. A similar study has been conducted previously when using an asynchronous generator and the results were presented in the paper [11].

2. The prototype of mCHP with SI engine

2.1. Selection of SI engine and electric generator

One of the main assumptions for the prototype under construction was to limit the maximum electrical power to approximately 7 kW. The liquid cooled spark ignition engines with a maximum power of less than 10 kW and dedicated to long-term stationary operation are practically unavailable on the market. In the power range below 10 kW, units are available that are used, for example, to drive pumps or emergency power generators. The following criteria were used while selecting the SI engine for the prototype CHP unit:

- availability on the market and the price of the new unit, allowing it to compete in the future with cogeneration set available on the market,
- availability of spare parts,
- maximum power of about 10 kW during continuous operation at a rotational speed of 1500 rpm using standard fuel (i.e. usually gasoline),
- liquid cooling,
- the possibility of modification or replacement of the existing flywheel with a wheel with larger mass and diameter,
- the possibility of easy modification of the inlet system to run on gaseous fuel (NG/LPG),
- start from an electric starter,
- the possibility of modification of the oiling system (adapting the system to the automatic oil dosing system).

Another important aspect was also the factory (or with a slight modification) adaptation of the engine to electronic control, such as a system for determining the position and rotation of the crankshaft, sensors for coolant temperature and inlet air temperature, and a knock sensor and throttle position sensor.

Based on the technical data provided by the manufacturers of drive units, an initial selection of engines meeting the assumed requirements was made. The most important technical data of drive units with an effective power of up to 10 kW are presented in Table 1.

Table 1. Technical data of chosen SI engines

Manufacturer	Kohler			Lombardini		Toyota
Engine type	LH 640	LH 755	LH 775	LGW 523	LGW 627	1KS
Max power [kW]	17.9	20.9	23	15	14,5	21
Power @ 1500 rpm [kW]	6.5	8.5	7.5	5.5	5.4	10.5
Max torque [Nm]	52	61.5	65	37	44.5	75.2
Torque @ 1500 rpm [Nm]	50	56	54	35	39	68
Cylinders	V2	V2	V2	In2	In2	In3
Swept volume [cm^3]	624	747	747	505	611	953
Bore [mm]	77	83	83	72	72	72
Stroke [mm]	67	69	69	62	75	78
Compression ratio	8.5	8.7	8.7	8.7	9	12
Fueling system	Carb	Carb.	Inj.	Carb.	Inj.	Carb.
Weight [kg]	51.7	51.7	51.7	52	52	73.5
Dimensions H/L/W [mm]	674/ 432/ 459	674/ 432/ 459	674/ 432/ 459	484/ 538/ 372	484/ 538/ 372	651/ 488/ 402

The values of the power obtained at 1500 rpm in Table 1 are extrapolated based on the manufacturer's data. It should be noted that the manufacturer's characteristics relate to engine operation on the design fuel, i.e. 95RON gasoline. In order to determine the effective power achieved on gaseous fuels of NG and LPG by the analyzed ICE, calculations were made using the mathematical model characterized in [12]. Taking into account the economic, design, and operational aspects the KOHLER LH775 engine was selected for the prototype.

As part of the analysis of the availability of synchronous generators on the Polish market, the following companies were considered: Leroy-Somer, Mecc Alte, Linz Electric and Marelli Motori. Documentation was analyzed in search of generators with a rotational speed of 1500 rpm, capable to operate in a cogenerator with a electrical power of 7 kW. Technical data of selected generators that meet this criterion are presented in Table 2.

The comparative analysis of generators was carried out by considering minimum rated power (i.e. power for the most difficult winding cooling conditions), maximum rated power (i.e. power for good cooling conditions), maximum efficiency and power in which the generator can achieve the best efficiency. Taking into account the availability of the device and its market price, the Mecc Alte ECP282VS4 generator was selected in order to adapt for parallel operation, for example, factory-installed additional parallel oper-

ation system (PD500 + Interface). Additionally, the generator was equipped with a digital voltage regulator DER2 with a communication and programming module via USB.

Table 2. Technical data of chosen synchronous generator

Manufacturer	Leroy-Sommer	Mecc Alte	Linz Electric	Marelli Motori
Generator type	LSA40VS1	ECP282VS4	E1X13SC/4	MXB160SA4
Min rated power [kW]	7.2	7.0	7.36	9.2
Max rated power [kW]	8.8	9.0	9.12	11
Max efficiency [%]	88.85	88.5	87.8	81.2
Power @ max efficiency [kW]	8	8.8	7.5	10

2.2. The prototype characteristics

Due to the assumed two methods of controlling the power of engine, it was necessary to develop a dedicated controller to manage the elements of the fuel supply system as well as the ignition system. For this purpose, a project was developed and an prototype ECU was built toward the ability to achieve the goals. The amount of air interring to the engine was controlled by a throttle with a stepper motor. But, the stream of gaseous fuel flow was controlled by an electrically controlled valve. The amount of the excess air ratio was controlled by the signal from the broadband lambda probe installed in the exhaust duct.

The supervisory control system is based on an industrial PLC controller with a network security module. The superior control system ensures a proper operation of the electric part of the cogenerator as well as all elements are related to the heat reception from the ICE. The cogeneration device should have a safe and proper operation in the wide range of every ambient thermal. In the event of operation without heat demand, the heat reception system must ensure its proper discharge to the emergency cooler. Figure 2 shows a diagram of the high-temperature heat reception system from the exhaust gases of the engine, and low-temperature heat from the engine block cooling system and from the oil lubricating the internal of the engine. In order to ensure that system the can operate in a wide range of ambient temperature, a 30% of glycol solution was used as a circulating medium in the heat reception system of the ICE.

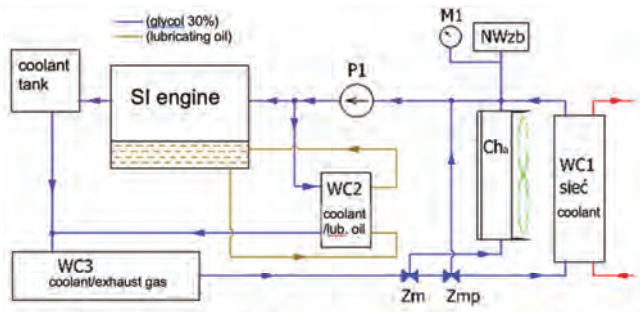

WC1, WC2, WC3 – the heat exchangers, $\mathbf{P1}_{z1}$ – coolant pump, $\mathbf{Ch}_a$ – emergency radiator, $\mathbf{Ch}_a$ – emergency radiator, **Zm** – two -state mixing valve, **Zm** – proportional mixing valve.

Fig. 2. Scheme of the heat collection system from the internal combustion engine

In this figure, the blue color represents the glycol flow in the primary circuit of the system, while the red color represents the secondary circuit (heat reception). The brown color represents the flow of lubricating oil of engine. The expansion vessel (NWzb) maintains the required glycol overpressure in the primary circuit, and its value is indicated on the pressure gauge (M1). The pump (P1) pumps glycol to the engine, which during normal operation has been previously cooled in the exchanger (WC1). The glycol stream is partially routed to the heat exchanger (WC2) where it receives heat from the lubricating oil. The remainder of the glycol stream flows through the engine indirectly cooling its internal components by absorbing heat. Then both streams combine and flow into the high-temperature flue gas-glycol exchanger, where the heat is given off as a result of the flue gas enthalpy drop. Then, the glycol flows to the mixing valve (Zm), where enables it redirect to the emergency cooler (Cha) if it is necessary. In the case that when the system works on the heat reception network (Zm), it enables the flow of glycol to the proportional mixing valve (Zmp). This valve distributes the flow between the exchanger (WC1) and the inlet of engine. The valve position depends on the temperature of the glycol at the exit of the engine.

By considering long-term operation of the cogeneration unit, a special engine oil refilling system is provided. Figure 3 shows a diagram of the system of replacement and periodic dosing of engine lubricating oil from an additional reservoir. By default, the bowl of piston holds approximately 3 dm^3 of oil, therefore the constructed reservoir has additional oil of 7 dm^3. The additional volume of oil is refilled from the reservoir. It will allow to the extend the oil change interval also it should increase the durability of the internal components of the engine during operation.

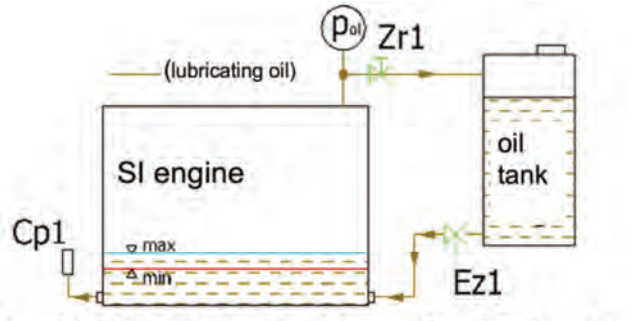

$\mathbf{p_{ol}}$ – lubricating oil pressure transducer, $\mathbf{Z_{r1}}$ – throttle valve, $\mathbf{E_{z1}}$ – solenoid valve (supply oil circuit), $\mathbf{C_{p1}}$ – oil level sensor

Fig. 3. Scheme of the engine lubricating oil refilling system

The prototype engine oil pan is a part of the engine block cast, there are two stub pipes with factory-blinded screws on its opposite side surfaces. The mentioned stub pipes were used to connect the oil dosing system. The measurement of the engine oil level system is mounted to the stub on the drive side of the engine. In turn, an oil reservoir is connected to the stub on the other side of the engine.

The engine lubricating oil is coming from the oil pan and pumped into the lubricating channels and then sprayed onto the internal parts of the engine. There is an oil pressure

sensor connected to the channel in the upper part of the engine head. A tee joint is connected to this channel, to which, on one side, a specially selected orifice is connected through the engine lubricating oil (with a very small stream) is directed to the reservoir. The other end of the tee joint is connected to the oil pressure sensor.

During operation, the oil is cycling between the engine and the reservoir. The flow of oil through the orifice, showed in the figure as the throttle valve Zr1, causes loss from the oil pan. After reaching the minimum value which is a safe value for the correct operation of the engine, the oil level sensor system (Cp1) signals the control system, which in turn activates the valve supply circuit (Ez1) and oil is supplied from the reservoir to the engine oil pan. Oil is topped up until the maximum oil level in the oil pan is reached. This state is signaled by the level sensor system then causes the Ez1 valve to close.

3. The research object and methods

The research on the prototype cogeneration unit was carried out while fuelling the engine with NG and LPG. During the testing, the engine was driving a synchronous generator specified in section 2.1. The photos of selected elements tested prototype has been shown on Fig. 4.

1 – SI engine, **2** – Lubricating oil tank, **3** – Pressure reducer, **4** – Low temperature heat exchanger, **5** – High temperature heat exchanger, **6** – Control cabinet.

Fig. 4. Image of selected elements of the prototype

To provide an electrical load, the system had been connected to the power grid. Correct operation of the electric generator with a power grid was only possible at synchronous speed, i.e. 1500 rpm. When the ICE was operated at 1500 rpm with fitted factory flywheel, there were significant changes in the instantaneous angular velocity of the crankshaft. These changes caused the generator to fall out of synchronous speed. For this reason, an additional flywheel was designed and fitted to the engine crankshaft. This method ensured that the engine was able to run at the speed that the generator can work properly.

The heat generated by the system was transferred to the radiator with a variable cooling capacity. The electric power of the cogeneration system was modulated by changing the throttle position and/or gas fuel actuator thus influencing indirectly by increasing or decreasing the torque generated on the shaft of the engine.

The tests were carried out for an optimised value of ignition advance angle and two different mixture compositions. Therefore, results carried out for five different loads of the engine during the combustion of a stoichiometric mixture. In addition, tests were conducted for each of the five mentioned loads of the engine while burning a lean mixture (λ = 1.3). The CHP prototype operating points during the laboratory tests along with selected system operating parameters (average values maintained during test trials) are presented in table 3.

Table 3. CHP system prototype points during the tests and selected system operating parameters

Test trial	1	2	3	4	5
Engine speed, [rpm]	1500				
Electric output power [W], (±2%)	1000	2000	3000	4000	5000
Time of constant work for each trial, [h]	12	12	12	12	12
Air-fuel mixture temperature [°C], (±3°C)	35	35	35	35	35
Excess air ratio [-]*, (±0.02; 0.04)	1; 1.3	1; 1.3	1; 1.3	1; 1.3	1; 1.3
Engine oil sump temperature [°C], (±2°C)	80	82	83	85	85
Engine coolant temperature [°C], (±2°C)	82	84	85	87	87
* The test trial has been performed separately for each excess air ratios and fuel					

During the experiment, the electric power was measured by the Fluke Norma 5000 power analyser. In turn, the mass stream of fuel consumed by the engine was measured using a Sartorius weight. Also, the composition of dry exhaust gases at the outlet of the engine was measured using the Capelec CAP 3000 flue gas analyser. The temperature at selected points in the system was measured using k-type thermocouples. The engine after treatment system has been equipped in three-way catalyst converter.

On the basis of the conducted research, the specific emission of exhaust compounds, electrical efficiency and total efficiency of the CHP system has been determined in a range of electrical power output changes.

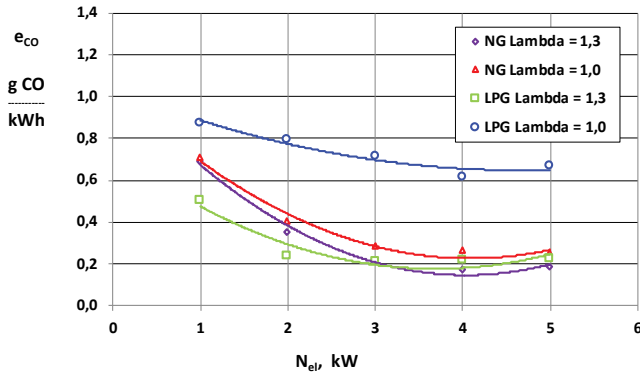

Fig. 5. Specific emission of CO vs mCHP unit output electric power

Figure 5 to 8 shows the influence of mCHP electric power output and ICE air excess ratio value on exhaust gas specific emissions. The specific emission is calculated to the value of electricity generated by the mCHP unit.

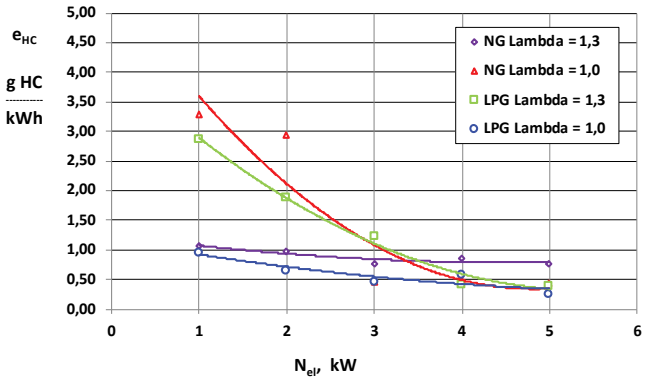

Fig. 6. Specific emission of HC vs mCHP unit output electric power

As can be seen in Figs 5 and 6, by increasing load, the unit value of CO and HC emissions decreases, which is caused by the higher temperature of the charge in the cylinder and favorable conditions for fuel oxidation.

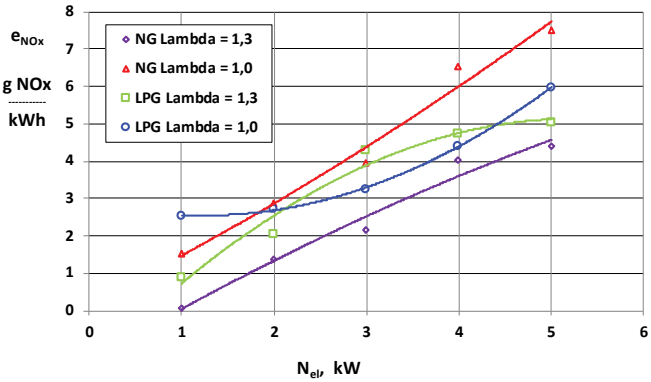

Fig. 7. Specific emission of NO_x vs mCHP unit output electric power

The specific NO_x emission (Fig. 7) increases with the increase in the load of the cogeneration system, which is related to the higher value of local temperature peaks in the combustion chamber. The main mechanism responsible for the formation of nitrogen oxides during combustion in an SI engine is the thermal mechanism.

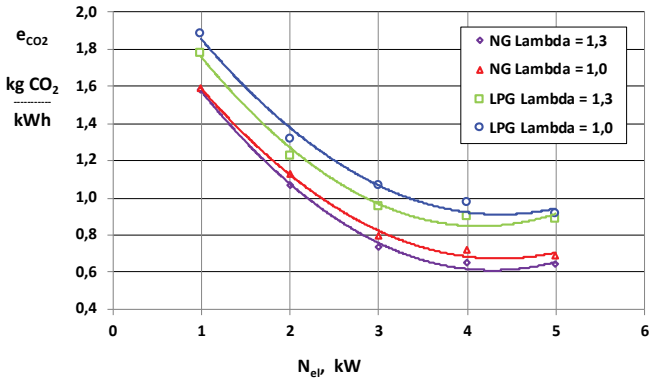

Fig. 8. Specific emission of CO2 vs mCHP unit output electric power

As can be seen in Fig. 8, the specific emission of CO_2 decreases with increasing load for both tested fuels, which is due to the fact that by increasing load of the engine, its energy efficiency increases, therefore the efficiency of electricity generation by the cogenerator (Fig. 9).

The obtained values of emission factors for harmful substances, the results of which are presented in Figs 5 to 8, confirm that the prototype cogeneration system meets the Stage II emission standard (in accordance with Directive 2002/08/EC) for small SI engines with a power below 19 kW. D2 ISO 8178.

Figure 9 shows the results of the electricity generation efficiency. The obtained results indicate that the applied method of internal combustion engine control (mixed qualitative and quantitative control) brings the expected results. The maximum efficiency of electric power when fueled by NG with the excess air ratio of λ = 1.3 is 30.7% and is higher than the value obtained for the same amount of the excess air ratio during LPG supply by 2.7 percentage points.

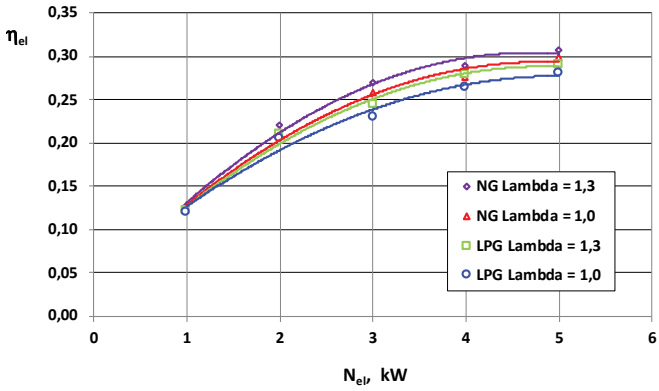

Fig. 9. Electrical efficiency of mCHP unit vs output electric power

Figure 10 shows the results of the total efficiency of the prototype for two products electricity and useful heat. The obtained results show that the applied method of controlling the allows to obtain the total efficiency of the cogeneration system at an average level of 91%.

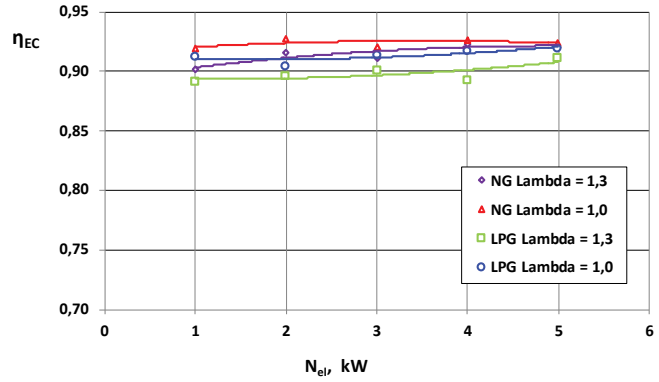

Fig. 10. Total efficiency of mCHP unit vs output electric power

It should be emphasized that the heat flux received from the system was determined in the conditions of periodic switching of heat reception, which led to fluctuations in the

temperature difference at the inlet and outlet of the plate exchanger. In addition, depending on the capabilities of the reception system, i.e. in particular on the return temperature of the heat reception medium, it is possible to use an additional condensation exchanger, that will increase the efficiency of heat generation by the cogeneration system.

4. Conclusions

From the tests of the prototype micro cogeneration system based on SI engine and synchronous generator the following conclusions can be drawn:

1. For booth used fuels, the smooth work of prototype was possible during operation the SI engine with lean air fuel mixture and amount of air excess ratio up to 1.3. It is necessary to modify ether the engine combustion chamber or use spark plugs dedicated for lean combustion for leaner mixture necessary.
2. It was essential to use an additional flywheel for the engine to obtain the same synchronization of the electric generator with the power grid.
3. The maximum electricity generation efficiency for natural gas was more than 1 percentage point higher compare to LPG. The reason of it can be the low in-cylinder temperature using NG (for each of fuel the ignition timing has been optimised taking in to account the efficiency).
4. The exhaust gas emission level confirm that the prototype cogeneration system meets the Stage II emission standard (in accordance with Directive 2002/08/EC) for small SI engines with a power below 19 kW. D2 ISO 8178).
5. The lower value of CO2 emissions when the mCHP unit is fuelled with natural gas results from the lower content of the carbon in the fuel and due to the higher value of the engine efficiency achieved for natural gas.
6. The intake valve guides was the weakest part of the engine. After approximately 800 mth of prototype work under various load (1–6 kWel), there was a lubricating oil leak in to the combustion chamber on the valve guide of cylinder No. 2.

Acknowledgements

This work was partially supported by:

– the project: Research and development work focused on the development of a micro cogenerator with an electrical output of less than 40kW together with an innovative control system for the internal combustion engine and the possibility to run on natural gas or LPG in order to exploit innovation potential and create a sustainable competitive advantage" implemented as part of the Regional Operational Program of the Silesian Region for the years 2014-2020 (European Regional Development Fund)
– the statutory research of Institute of Thermal Technology SUT

Nomenclature

e_{CO}	specific emission of carbon monoxide
e_{HC}	specific emission of hydrocarbons
e_{NOx}	specific emission of nitrogen oxides
η_{el}	electrical efficiency of mCHP unit
η_{EC}	total efficiency of mCHP unit
LPG	liquified petrolum gas
NG	natural gas
SI	spark ignition
mCHP	micro Combined Heat and Power

Bibliography

[1] SUN, T., CHANG, Y., XIE, Z. et al. Experimental research on pumping losses and combustion performance in an unthrottled spark ignition engine. *Proceedings of the Institution of Mechanical Engineers, Part A: Journal of Power and Energy*. 2018, **232**(7), 888-897. https://doi.org/10.1177/0957650918754684

[2] VISHWANATHANA, G., SCULLEYA, J.P., FISCHERA, A. et al. Techno-economic analysis of high-efficiency natural-gas generators for residential combined heat and power. *Applied Energy*. 2018, **226**, 1064-1075. https://doi.org/10.1016/j.apenergy.2018.06.013

[3] Vaillant and Honda present micro-combined heat and power system for home use. https://global.honda/newsroom/worldnews/2011/c110203Micro-Combined-Heat-Power-System.html (accessed on 16.09.2021)

[4] Yanmar. CP5WN. https://www.yanmarenergysystems.com/webres/File/CP5WN-Spec-Sheet.pdf (accessed on 16.09.2021)

[5] Yanmar. CP10WN. https://www.yanmarenergysystems.com/webres/File/CP10WN-Spec-Sheet.pdf (accessed on 16.09.2021)

[6] TAIE, Z., HAGEN, C. Experimental thermodynamic first and second law analysis of a variable T output 1–4.5 kWe, ICE-driven, natural-gas fueled micro-CHP generator. *Energy Conversion and Management*. 2019, **180**, 292-301. https://doi.org/10.1016/J.ENCONMAN.2018.10.075

[7] Dachs G/F Gen2. Technical data. https://senertec.com/wp-content/uploads/2018/12/Technical-Data-Dachs-Gen2.pdf

[8] KRYZIA, D., KUTA, M., MATUSZEWSKA, D. et al. Analysis of the potential for gas micro-cogeneration development in Poland using the Monte Carlo method. *Energies*. 2020, **13**, 3140. https://doi.org/10.3390/en13123140

[9] Central Statistical Office. Energy consumption in households in 2018; Central Statistical Office of Poland: Warsaw 2019.

[10] Energy in Poland, Ministry of Energy, Agencja Rynku Energii S.A. Warsaw 2018.

[11] PRZYBYŁA, G., RUTCZYK, B., ZIÓŁKOWSKI, Ł. Performance of micro CHP unit based on SI engine with quantitative-qualitative load control. *Combustion Engines*. 2019, **178**(3), 82-87. https://doi.org/10.19206/CE-2019-315

[12] NOCOŃ, A., NIESTRÓJ, R., KRUCZEK, G. et al. Simulation of micro co-generator transient states coupled with mathematical model of internal combustion engine. *2018 International Symposium on Electrical Machines (SME)*. 2018, 1-5. Andrychów, Poland. 10-13.06.2018. https://doi.org/10.1109/ISEM.2018.8442574

Grzegorz Przybyła, DSc. DEng. – Faculty of Energy and Environmental Engineering, Silesian University of Technology.
e-mail: *gprzybyla@polsl.pl*

Mateusz Buczak, BEng. – Faculty of Energy and Environmental Engineering, Silesian University of Technology.
e-mail: *matebuc802@student.polsl.pl*

Łukasz Ziółkowski, MEng. – Faculty of Energy and Environmental Engineering, Silesian University of Technology.
e-mail: *lziolkowski@polsl.pl*

Zbigniew Żmudka, DSc., DEng. – Faculty of Energy and Environmental Engineering, Silesian University of Technology, Poland.
e-mail: *zbigniew.zmudka@polsl.pl*

Article citation info:
NOWAK, M. Calibration of micro-simulation model in assessment of passenger car exhaust emission during acceleration. *Combustion Engines*. 2022, **189**(2), 54-59. https://doi.org/10.19206/CE-142554

Mateusz NOWAK

Combustion Engines
Polish Scientific Society of Combustion Engines

Calibration of micro-simulation model in assessment of passenger car exhaust emission during acceleration

ARTICLE INFO

Received: 27 August 2021
Revised: 21 September 2021
Accepted: 23 September 2022
Available online: 4 October 2022

In terms of simulation research, it is important to simulate real conditions as precisely as possible. This type of approach makes it possible to minimize the error in the obtained results. The dynamics of acceleration is one of the most important factors having a direct impact on fuel consumption and exhaust emissions from vehicles. The work was carried out with the use of PTV Vissim microscopic vehicle motion simulation software. The considerations were carried out on theoretical acceleration profiles with different dynamics values and the actual character of acceleration, recorded during road tests. The simulations were carried out for a car powered by spark-ignition and compression-ignition engines. The research showed that the calibration of the acceleration character of the vehicle in simulation tests may result in significant differences in obtained results of exhaust emissions.

Key words: *exhaust emission, simulation, vehicle acceleration, model calibration, acceleration dynamics*

1. Introduction

Operating conditions have a direct impact on fuel consumption and the emission of harmful exhaust compounds. Different operating conditions of propulsion systems in vehicles during type-approval measurements and during actual operation lead to over 90% difference in the average fuel consumption [8, 11]. Also, the results of measurements taken under real-life conditions differ significantly depending on the driving style [1, 4, 7]. In other works, apart from the driving style of the driver, the differences in fuel consumption or energy consumption refer to the intensity of vehicle traffic and the road congestion [3, 5]. The road congestion and in particular traffic jams, are the domain of cities with a large number of inhabitants [2, 13]. In such a situation, vehicles emit pollutants in the immediate vicinity of large numbers of people. Some publications consider the influence of the acceleration dynamics on the emission of harmful exhaust compounds, but these works are conducted in real driving conditions [12]. The traffic simulation software could be used also to solve some infrastructure problems. An example is a research, which describes the influence of rai-road level crossing on the road traffic flow [a9]. Such approach to transport engineering could result in obtaining some low cost quantitative data, which could be helpful in future infrastructure development or could give a positive feedback, which will result in further, more expensive research work.

In simulation works the traffic model should be calibrated properly, e.g. in terms of the acceleration characteristics of a single vehicle (could be also adopted to different vehicle categories), number of vehicles driving on selected roads, etc. Lack of proper calibration in terms of simulation model may contribute to significant discrepancies of obtained results in relation to the real values [10]. This study focuses on the assessment of the impact of the acceleration dynamics of a passenger vehicle up to a speed of approx. 50 km/h on the results of exhaust emissions. For this purpose, the vehicle acceleration curve was adapted to the model of the actual vehicle acceleration recorded during the road test.

2. Research methodology

The simulation tests were performed with the use of Vissim software, version 5.40, which was developed by the German company PTV. This software is commonly used by companies working in the field of traffic engineering and road managers. The tool is used to simulate vehicle traffic on a microscopic scale, which means that the best results can be obtained by analyzing small areas, including, for example, a certain road section, intersection or a small traffic area. Another type of software (eg PTV Visum) is used to analyze larger areas, eg a whole city. The advantage of the software used is the implemented vehicle traffic models, including cars, trucks, buses and trams. The analyzes can also take into account the pedestrians or cyclists. With use of an additional modules, it is possible to perform different analyzes related to, for example, exhaust emissions from vehicles moving in the modeled part of the road infrastructure.

As a part of the performed simulations, the emissivity of passenger cars representing the Euro 3 emission standard for various acceleration scenarios was assessed. Modeling included tests of accelerating a vehicle to approx. 50 km/h. For this purpose, a road section was modeled, mapping a fragment of Kornicka Street in Poznan (Fig. 1). In order to simplify the model, the traffic of vehicles was mapped only on Kornicka Street in the analyzed direction. Only vehicles taking off from a standstill were taken into account (initial speed V_0 = 0 km/h). As the vehicles entering the model have an initial speed greater than 0 km/h, they were forced to stop with use of traffic lights. Some of the vehicles entering the model stopped at the aforementioned traffic lights located along the analyzed street, which made it possible to obtain data for further analysis.

In the first order, the acceleration of passenger cars was simulated, using the acceleration values implemented in the simulation software, using the levels 1.0 m/s^2, 1.2 m/s^2 and

2.5 m/s^2. The obtained acceleration curves in function of simulation time were characterized by nearly rectangular shapes (Fig. 2). Because the obtained characteristics to a small extent reflect the nature of the actual acceleration of the vehicle, driven by a human, during which it is almost impossible to obtain such simple shapes of acceleration character. This is all the more justified as in most acceleration situations to around 50 km/h, when also the gear shifting must be taken into account. For comparison, the character of selected acceleration of a light passenger-goods vehicle recorded during a road test is presented (Fig. 3). The next step was to adapt the acceleration curve of the vehicle so that its course during the simulation was similar to the characteristics recorded during the actual tests.

Fig. 1. Section of Kornicka Street in Poznan, used in this work for vehicles acceleration modeling [6]

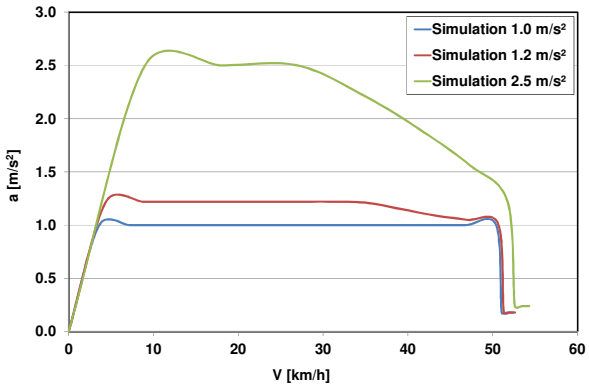

Fig. 2. Vehicle acceleration characteristics, obtained in the PTV Vissim software, obtained on the basis of the implemented data (1.0 m/s^2, 2.0 m/s^2, 2.5 m/s^2)

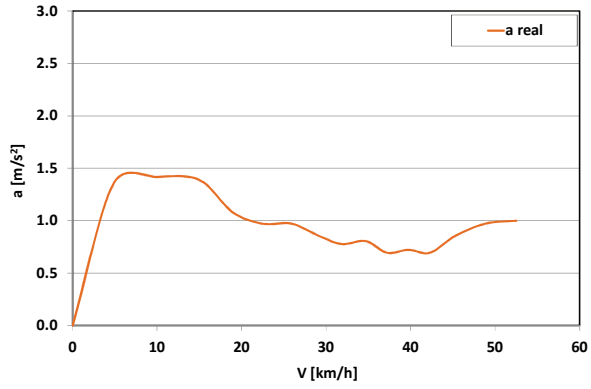

Fig. 3. The acceleration characteristics of the vehicle recorded during the actual acceleration test

The adaptation of the simulation in order to make the acceleration curve similar to the curve recorded during the real drive was carried out in many stages. During early attempts, the vehicle acceleration values were not sufficiently high immediately after starting (the acceleration curve was more inclined than during the actual measurement). In the next stage, the acceleration of some vehicles was disturbed by the slower accelerating vehicles in front. Some examples of the mentioned situations are shown in Fig. 4. The situation related to the influence of the preceding vehicles on the acceleration of the analyzed vehicle is related to the use of traffic lights in order to force the vehicle to accelerate from standstill. In the described situation, it happens that several vehicles accumulates at the red light because the vehicles are directed to the model at the intensity specified by the author. The above-mentioned model imperfections do not occur in the analyzed acceleration cases. The obtained acceleration waveforms are also not the same, which reflects the stochastic nature of the actual vehicle acceleration process and the lack of full repeatability during acceleration by the real driver in real traffic conditions.

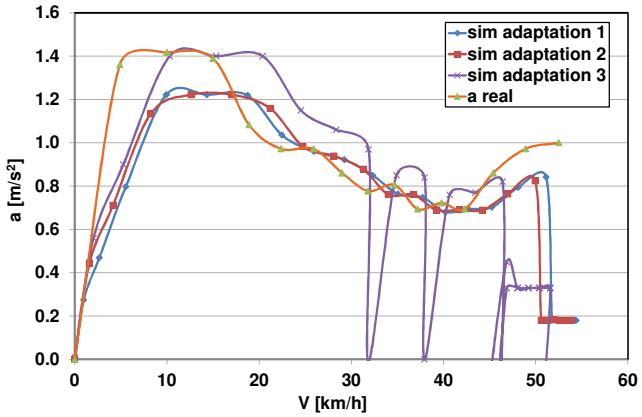

Fig. 4. The process of adaptation characteristics of acceleration of the vehicle in PTV Vissim

3. Research results

During the simulation, two types of data were collected: the speed and acceleration profiles of the vehicle during acceleration and the changes in the intensity of emissions of individual exhaust components depending on the time of simulated acceleration.

Examples of the characteristics of speed and acceleration in time for the given vehicle acceleration conditions are shown in Fig. 5–8. The acceleration generated by the Vissim software is characterized by a waveform with a shape similar to a rectangle, which especially applies to the acceleration values of 1.0 m/s^2 and 1.2 m/s^2 (Fig. 5–6). The nature of acceleration also translates into a change in speed over time, which for the two cases discussed above has the shape of a straight line. The acceleration with a maximum value of 2.5 m/s^2 (Fig. 7) is of a nature that to a greater extent reflects the acceleration modeled on the real test (Fig. 8), obtaining only higher values. During the analyzed case of real acceleration, it is characteristic that the maximum value of the vehicle acceleration is approx. 1.2 m/s^2. Moreover, the course of the acceleration value as a function

of the vehicle speed is much more complicated than in the previous cases. This is due to circumstances such as gear changes or the characteristics of the engine used.

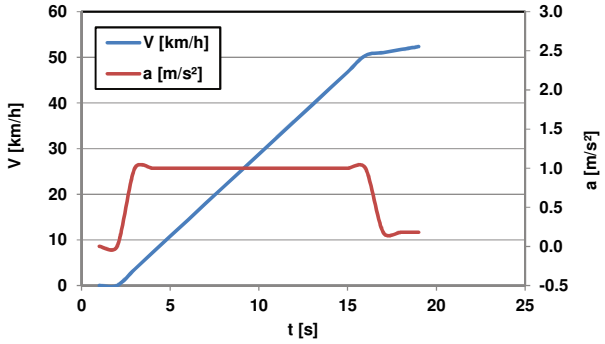

Fig. 5. Characteristics of speed and acceleration of the vehicle as a function of simulation time; a = 1.0 m/s^2

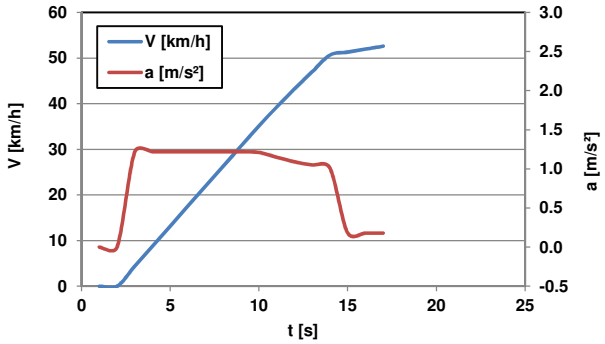

Fig. 6. Characteristics of speed and acceleration of the vehicle as a function of simulation time; a = 1.2 m/s^2

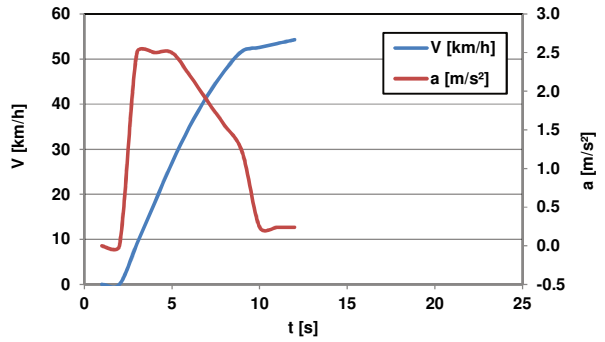

Fig. 7. Characteristics of speed and acceleration of the vehicle as a function of simulation time; a = 2.5 m/s^2

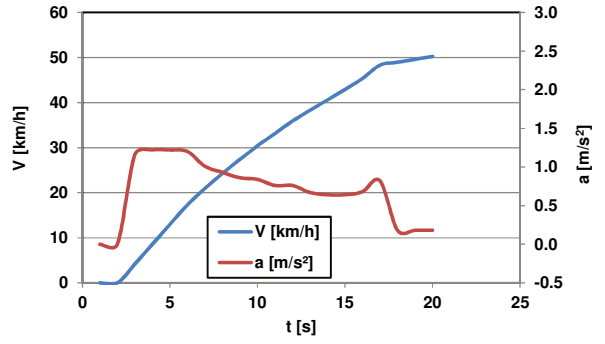

Fig. 8. Characteristics of speed and acceleration of the vehicle as a function of simulation time; mapped on the basis of a real acceleration test

The exhaust emission intensity as a function of time during the acceleration of the vehicle is shown in Fig. 9–12. The presented data was obtained during a simulated acceleration of a passenger car, compliant with the Euro 3 emission standard, while the variable parameter was the acceleration, the course of which for considered cases was presented in Fig. 5–8. The trends that can be observed in the presented graphs of the emission intensity of individual exhaust gas components are predictable and are consistent with the general relationships concerning the formation of toxic compounds in combustion engines. The greater the acceleration value, the greater the exhaust emission rate, expressed in grams per second. The greatest differences between analyzed acceleration scenarios can be observed for the NO_x and CO_2 emission rates. The greater the acceleration value, the greater the load on the drive unit, which results in higher pressure and temperature values in the combustion chamber. Increasing these two parameters promotes the formation of NO_x. The highest intensity of NO_x emission occurs during acceleration with the highest acceleration value (2.5 m/s^2) and it reaches the maximum value at the level of approx. 40 mg/s, which is almost 100% more than during acceleration with the acceleration value of 1.0 m/s^2. The lowest maximum value of the instantaneous NO_x emission intensity was recorded for the acceleration modeled on the real test. It is certainly related to the course of the acceleration curve as a function of time. The maximum value of acceleration for the case shown in Fig. 12 is kept in the vehicle speed range at the level of approx. 5–18 km/h, while at higher values of the vehicle speed, the acceleration value decreases. The rate of CO_2 emissions relates directly to the instantaneous fuel consumption. Therefore, for this benchmark, similar trends can be observed as for NO_x. For example, the maximum rate of CO_2 emission for an acceleration of 1.0 m/s^2 is approx. 5.3 g/s, while for 2.5 m/s^2, this parameter reaches the value of approx. 7 g/s, which increases the value of this parameter by over 30%. Similar trends can be observed in the case of CO and HC emissions, but the differences in this case are not so significant. This is probably related to the improvement of the combustion quality at higher engine load, which results in a lower concentration of incomplete combustion products, however, it is compensated by the higher exhaust gas flow caused by the higher engine load and/or higher rotational speed.

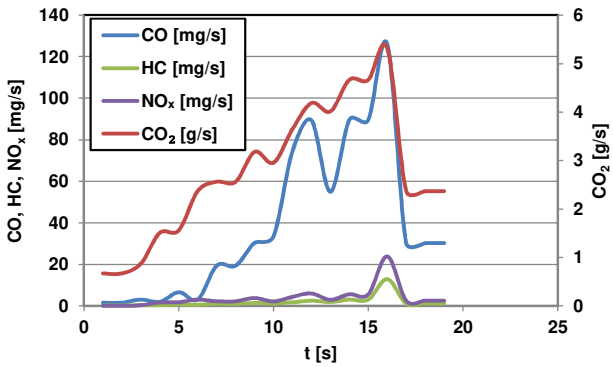

Fig. 9. Emission rates of individual exhaust gas components as a function of simulation time for: a = 1.0 m/s^2

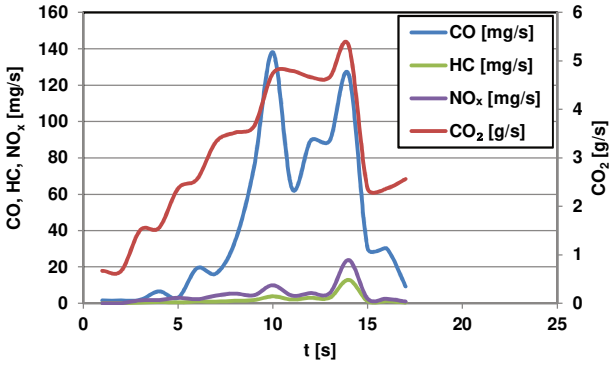

Fig. 10. Emission rates of individual exhaust gas components as a function of simulation time for: a = 1.2 m/s^2

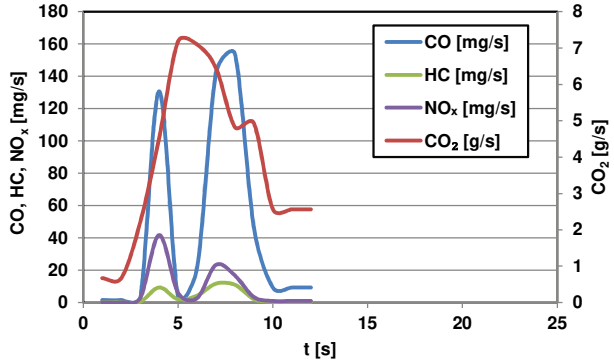

Fig. 11. Emission rates of individual exhaust gas components as a function of simulation time for: a = 2.5 m/s^2

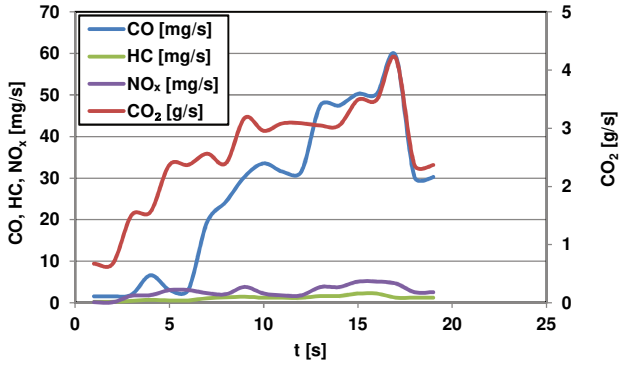

Fig. 12. Emission intensities of individual exhaust gas components as a function of simulation time for the acceleration mapped on the basis of the actual acceleration test

The influence of the value and course of the vehicle acceleration on the emission of the analyzed exhaust gas components is shown in Fig. 13–20. In this case, the cumulative mass of individual exhaust gas compounds was presented for the entire acceleration phase from a standing start to approx. 50 km/h. The figures have been grouped by two, consecutively for CO, HC, NO_x and CO_2, with the first data for vehicles powered by SI engines, followed by the data for cars with CI engines. The above-mentioned drawings were prepared based on the simulation results for cars with engines meeting the Euro 3 emission standard, which is still popular among vehicles traveling on the roads in Poland.

Higher acceleration means a higher temperature in the combustion chamber, which contributes to the improvement of combustion conditions, and therefore the concentration of incomplete combustion products (e.g. CO) is reduced. In the graphs, it is difficult to notice a significant reduction in the CO emission between an acceleration of 1.0 m/s^2 and 2.5 m/s^2. This is related to a greater exhaust gas flow during a more dynamic acceleration of the vehicle. For the analyzed case (Euro 3 emission standard), a vehicle powered by a compression ignition engine emitted more than 10 times less CO than a vehicle powered by a spark ignition engine.

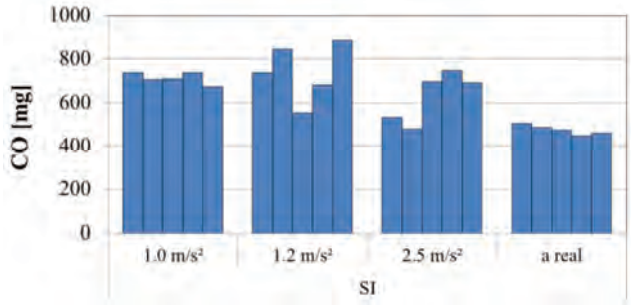

Fig. 13. CO emissions for different acceleration characteristics of a vehicle propelled with SI Euro 3 engine obtained during simulation using PTV Vissim software

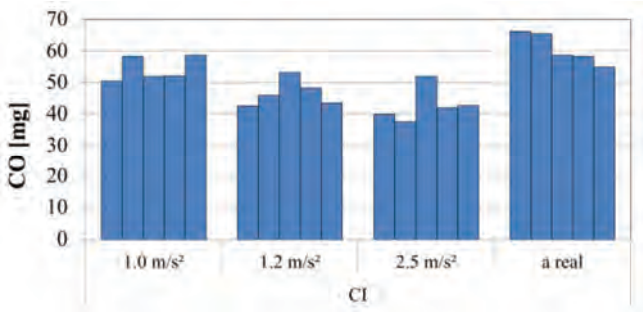

Fig. 14. CO emissions for different acceleration characteristics of a vehicle propelled with SI Euro 3 engine obtained during simulation using PTV Vissim software

As in the case of CO, the concentration of HC in the exhaust gas should be lower under the conditions of more dynamic acceleration of the vehicle. HC emission during the analyzed cases of acceleration of vehicles with SI engines, ranges from approx. 20–70 mg, while values exceeding 40 mg were obtained in individual cases and could be caused by a temporary change in the acceleration value of the vehicle. The lowest values of HC emissions were obtained for the acceleration selected on the basis of the actual test, which is certainly related to the different characteristics of the vehicle acceleration – in this case, the acceleration value of the vehicle decreases with the increase in its speed, which is a natural situation. The dependencies related to the influence of the vehicle acceleration dynamics on the HC emission from cars powered by CI engines are slightly different than those observed in the case of vehicles powered by SI engines. In this case, there is a slight reduction in HC emission as a function of the acceleration value of the vehicle, and the obtained values are several times lower than during the acceleration of the vehicle with the SI engine.

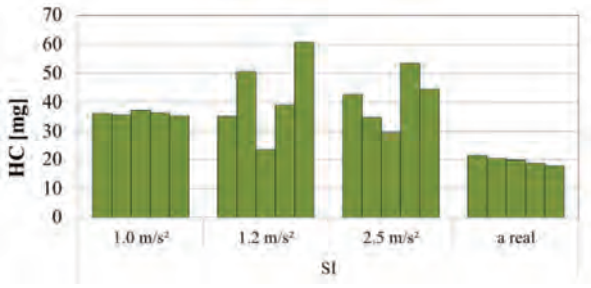

Fig. 15. HC emission for different acceleration characteristics of a vehicle propelled with SI Euro 3 engine obtained during simulation using PTV Vissim software

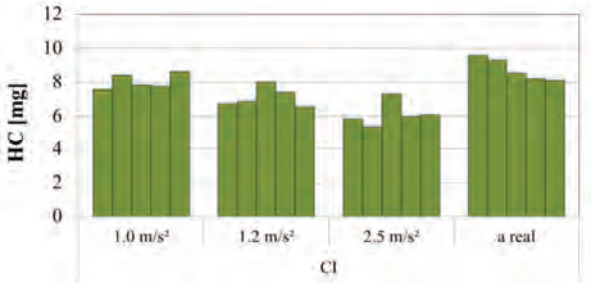

Fig. 16. HC emission for different acceleration characteristics of a vehicle propelled with CI Euro 3 engine obtained during simulation using PTV Vissim software

As the load on the drive unit increases, so does the NO_x emission during the acceleration of the car with the SI engine. However, the observed differences amount to approx. 20–30%. Much larger differences can be observed between the simulation of the highest acceleration dynamics and the acceleration recorded for the real test, when the NO_x emission is lower by up to 60%.

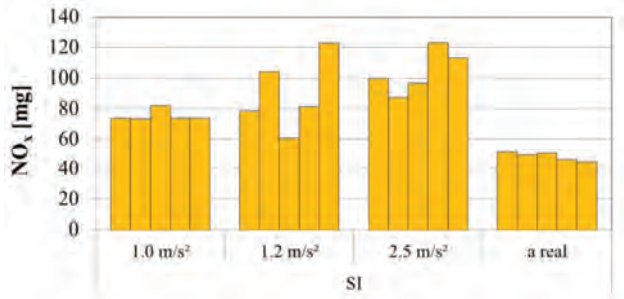

Fig. 17. NO_x emission for different acceleration characteristics of a vehicle propelled with SI Euro 3 engine obtained during simulation using PTV Vissim software

During the simulation of vehicles acceleration propelled with diesel engines, a reduction in NO_x emissions was observed as a function of the acceleration dynamics. The implementation of the actual vehicle acceleration curve contributed to a further reduction of the obtained results by approx. 10–15% compared to the acceleration value of 2.5 m/s^2. Comparing the NO_x emission registered for vehicles powered by CI engines with the emission obtained by vehicles with SI engines, it can be stated that the mass of this compound is 2–3 times higher during the acceleration of cars powered by CI engines. For example, in the case of acceleration modeled on the real test, cars powered by CI engines emitted approx. 42–50 mg of NO_x, while the mass of NO_x from cars powered by diesel engines was approx. 110–145 mg. This is caused by using the three-way catalyst, which reduces the amount of NO_x in exhaust gases.

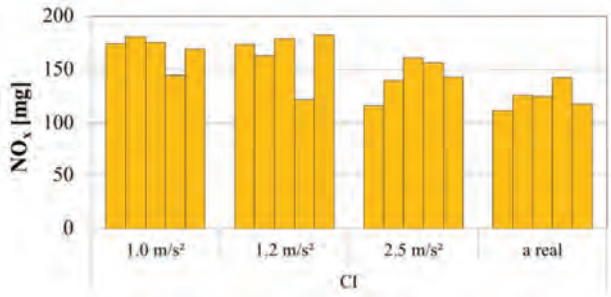

Fig. 18. NO_x emission for different acceleration characteristics of a vehicle propelled with CI Euro 3 engine obtained during simulation using PTV Vissim software

The change in the acceleration dynamics did not significantly change the CO_2 emissions from vehicles powered by SI engines. The differences between the values obtained with the acceleration value of 1.0 m/s^2 and the values with the real acceleration dynamics reach values of 5–10% in favor of the actual acceleration course. The same trends can be observed in the case of acceleration of cars with diesel engines, with the indication that the differences are slightly greater, and the minimum values were obtained during the most dynamic acceleration of the vehicle. Comparing the emission of CO_2 according to the type of the used drive system, it can be stated that during the analyzed acceleration, cars powered by CI engines emit approx. 20–30% less CO_2 than cars powered by SI engines.

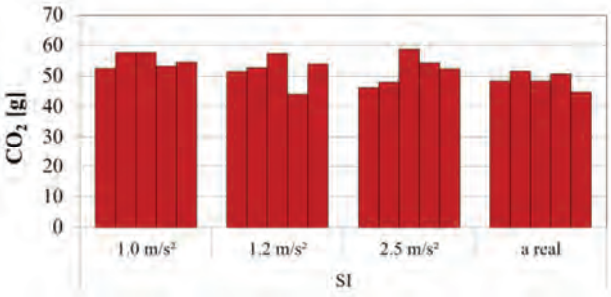

Fig. 19. CO_2 emission for different acceleration characteristics of a vehicle propelled with SI Euro 3 engine obtained during simulation using PTV Vissim software

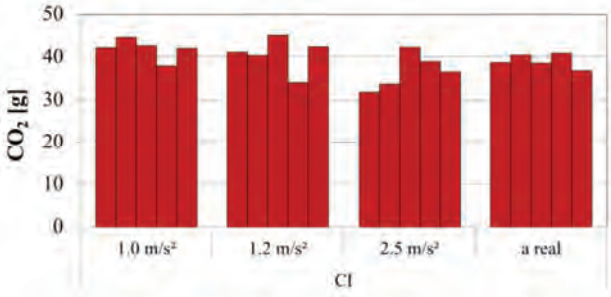

Fig. 20. CO_2 emission for different acceleration characteristics of a vehicle propelled with CI Euro 3 engine obtained during simulation using PTV Vissim software

4. Conclusions

Based on the simulation results, it can be concluded that the acceleration dynamics has a noticeable effect on the exhaust emissions from passenger cars during acceleration to 50 km/h. In the case of CO, increasing the acceleration dynamics from 1.0 to 2.5 m/s^2 resulted in the reduction of the emission of this compound by even 20%. The application of the acceleration dynamics based on real acceleration values, the results were ambiguous, because in the case of cars with SI engines, a reduction in CO emissions was recorded, reaching almost 30%, while the use of a modified acceleration curve in cars with diesel engines resulted in an increase in CO emissions by approx. 20% compared to an acceleration of 1.0 m/s^2. Almost identical trends were observed during the analysis of the influence of the acceleration dynamics on HC emission. In the case of NO_x emissions, increasing the acceleration dynamics also leads to inconclusive results, because for cars powered by SI engines there is even a 50% increase in the emission of this compound, while for cars with diesel engines, increasing the acceleration dynamics allows to reduce the emissions of this compound by even 15–20%. The lowest emission values were obtained for both types of drive systems for the actual acceleration process. The smallest differences in the vehicle acceleration dynamics function during the simulations were recorded for CO_2 emissions (approx. 5–10%).

The applied methodology is useful, for example, to assess the impact of vehicle acceleration dynamics or to compare the differences between different types of propulsion systems. Subsequent work should include the comparison of the vehicle acceleration emission values obtained during the simulation with the values obtained during the actual measurements. The measurements during road tests could give the possibility of verifying the concentrations of different exhaust compounds in exhaust gases.

Acknowledgements

The research was funded by European Union from European Regional Development Fund through the National Centre for Research and Development (Narodowe Centrum Badań i Rozwoju) – research project within the Smart Growth Programme (contract No. POIR.04.01.02-00-0002/18).

Nomenclature

CI	compression ignition
CO	carbon monoxide
CO_2	carbon dioxide
HC	hydrocarbons
NO_x	nitrogen oxides (NO + NO_2)
SI	spark ignition

Bibliography

[1] ANDRZEJEWSKI, M. The influence of the driving style on the fuel consumption and exhaust emissions. *Doctoral thesis*. Poznan University of Technology. Poznan 2013.

[2] BULL, A. Traffic congestion: The problem and how to deal with it. United Nations, Economic *Commission for Latin America and the Caribbean*. Chile 2003.

[3] DONG, Y., XU, J., LIU, X. et al. Carbon emissions and expressway traffic flow patterns in China. *Sustainability*. 2019, **11**, 2824. https://doi.org/10.3390/su11102824

[4] KURTYKA, K., PIELECHA, J. The evaluation of exhaust emission in RDE tests including dynamic driving conditions. *Transportation Research Procedia*. 2019, **40**, 338-345. https://doi.org/10.1016/j.trpro.2019.07.050

[5] KREICBERGS, J., GAILIS, M., ZALCMANIS, G. et al. Traction energy and fuel consumption evaluation methodology in urban traffic. *Proceedings of 23rd International Scientific Conference. Transport Means*. 2019, Part I.

[6] Goolge Maps. maps.google.pl

[7] MERKISZ, J., ANDRZEJEWSKI, M., MERKISZ-GURANOWSKA, A. et al. The influence of the driving style on the CO_2 emissions from a passenger car. *Journal of KONES Powertrain and Transport*. 2014, **21**(3), 219-226. https://doi.org/10.5604/12314005.1133212

[8] MERKISZ, J., ANDRZEJEWSKI, M., PIELECHA, J. Comparison of carbon dioxide emissions in real traffic conditions of the vehicle with the values obtained in the certification test on the background of European standards. *Combustion Engines*. 2011, **3**.

[9] NOWAK, M., ANDRZEJEWSKI, M., GALANT, M. et al. Simulation assessment of the selected combination of road and rail infrastructure in the aspect of choosing the route of road transport means. *AIP Conference Proceedings Computational Technologies in Engineering* (TKI'2018), 2019, **2078**, 020055. https://doi.org/10.1063/1.5092058

[10] NOWAK, M., PIELECHA, J. Comparison of exhaust emission on the basis of real driving emissions measurements and simulations. *MATEC Web of Conferences*. 2017, **118**, 00026. https://doi.org/10.1051/matecconf/201711800026

[11] Real world fuel economy measurements: technical insights from 400 tests of Peugeot, Citroen and DS cars. https://www.transportenvironment.org/

[12] SHRINDHAR BOKARE, P., KUMAR MAURYA, A. Study of effect of speed, acceleration and deceleration of small petrol car on its tail pipe emission. *International Journal for Traffic and Transport Engineering*. 2013, **3**(**4**), 465-478. https://doi.org/10.7708/ijtte.2013.3(4).09

[13] Traffic congestion: three big questions, three short answers. https://www.its.ucla.edu/for-the-press/traffic-congestion/

Mateusz Nowak, DEng. – Faculty of Civil and Transport Engineering, Poznan University of Technology.
e-mail: *mateusz.s.nowak@put.poznan.pl*

Article citation info:
JAWORSKI, A., LEJDA, K., BILSKI, M. Effect of driving resistances on energy demand and exhaust emission in motor vehicles. *Combustion Engines*. 2022, **189**(2), 60-67. https://doi.org/10.19206/CE-142949

Artur JAWORSKI
Kazimierz LEJDA
Maciej BILSKI

Combustion Engines
Polish Scientific Society of Combustion Engines

Effect of driving resistances on energy demand and exhaust emission in motor vehicles

ARTICLE INFO

Received: 15 July 2021
Revised: 6 October
Accepted: 7 October 2021
Available online: 29 October 2021

Among the fundamental factors affecting the emissions of internal combustion engines is the resistance to motion acting on the car. This is an important factor to be taken into account when testing cars in conditions simulated on a chassis dynamometer. The dependence of the driving resistance function on vehicle speed is determined on the basis of various methods, the most frequently used of which is the so-called alternative method specified in procedures for the type approval of motor vehicles with respect to the emission of pollutants in exhaust gases. The values adopted in accordance with the alternative method differ from the actual resistance acting on the car in road conditions. This is one of the reasons why the emission of pollutants and the fuel consumption of an engine in real road conditions differs from the values given by the car manufacturer, including the emission limits specified in the standards. This paper presents an evaluation of the influence of driving resistance on the energy demand and emission of pollutants in the exhaust gases by sample passenger car with SI engine fuelled by petrol and LPG.

Key words: *driving resistance, exhaust emission, vehicles, emission tests, energy demand*

1. Introduction

The emission of pollutants in vehicle exhaust gases is a fundamental problem related to vehicle operation. Increased population awareness exerts pressure on manufacturers manifesting itself in increasingly lower emission limits expressed in successive editions of vehicle type approval standards.

Tests of pollutant emissions in vehicle exhaust are carried out in laboratory driving cycles [4] and in tests conducted in real road conditions [9, 25, 27, 29, 30, 33]. The results of the actual emission tests are used in the studies conducted by the simulation method. [19]. Tests performed on a chassis dynamometer are characterized by high repeatability[17]. Tests on a chassis dynamometer, carried out as part of type approval tests, are intended to evaluate the emission of exhaust pollutants from vehicles and fuel (energy) consumption [5, 7, 8, 14, 28, 42]. However, often the results of tests on exhaust emissions obtained on a chassis dynamometer turn out to be lower than in real driving emissions (RDE) road tests [10, 16, 22, 26, 32, 41].

During laboratory testing, the aim is to approximate as closely as possible the test conditions relating to vehicle drag on the road. This is very difficult due to many factors occurring in real traffic, such as ambient temperature, driver's driving style, road gradient and wind effects [1, 6, 20, 21, 31, 38, 44]. Additionally, the problem relates to the real-time representation of drag forces by the chassis dynamometer, which involves not only the basic resistance to motion, i.e., air and rolling, but also inertia resistance. The steady-state load values on the chassis dynamometer affect the results of exhaust emissions and fuel (energy) consumption [15, 24, 35, 39, 40]. The vehicle drag force, F_o, for a horizontal road is described by the equation:

$$F_o = F_t + F_b + F_p \ [N] \tag{1}$$

where: F_t – rolling resistance force [N], F_p – drag force [N], F_b – inertia resistance force [N].

For tests on a chassis dynamometer, it is necessary to introduce the resistance force function, the so-called dynamometer characteristic curve, which includes the forces acting on the car in steady state motion on a horizontal road. These are the air and rolling resistance, which are usually expressed as a second-degree polynomial [2]:

$$F_{t,p} = F_t + F_p = m \cdot g \cdot f_o \cdot (1 + 5 \cdot 10^{-5} \cdot v^2) + 0.047 \cdot A \cdot c_x \cdot v^2 \tag{2}$$

where: m – weight of the car [kg], f_0 – rolling resistance coefficient for low travel speed close to zero, g – acceleration due to gravity [m/s^2], v – speed [km/h], A – frontal area of the car [m^2], c_x – aerodynamic drag coefficient in the longitudinal direction.

The inertia drag force is calculated from the formula:

$$F_b = m \cdot \delta \cdot a \ [N] \tag{3}$$

where: δ – rotating mass factor, a – acceleration [m/s^2].

The values of the motion resistance force functions as a function of travel speed are entered into the control software through coefficients determined by various methods [6, 12, 13, 23, 24, 35, 43]. Due to the fact that the dynamometer reproduces the resistances acting on the car in real conditions, the most advantageous method is the one based on road coast-down tests [18, 24, 35], on the basis of which the values of coefficients of the equation X_0, X_1 and X_2:

$$F_{t,p} = X_0 + X_1 \cdot v + X_2 \cdot v^2 \ [N] \tag{4}$$

With the vehicle manufacturer's consent, the so-called alternative method may be used, which consists in determining the brake load for absorbing the force F_c of the resistance depending on the mass of the vehicle by selecting the coefficients A_0 and B_0 from the table of Regulations

[43]. In this case, the motion resistance function is expressed by the formula:

$$F_c = A_0 + B_0 \cdot v^2 \text{ [N]} \quad (5)$$

2. Materials and methods

The tests were carried out on an AVL-Zoellner ROADSIM 48" chassis dynamometer installed in a climatic chamber at the Automotive Ecology Centre of the Rzeszow University of Technology (Fig. 1). The basic technical data of AVL ROADSIM 48″ Chassis Dynamometer are presented in Table 1. The tested vehicle was a passenger car equipped with an SI internal combustion engine. The basic technical data of the tested car are presented in Table 2. The tested car is representative of the average age of cars in Poland [37]. During the NEDC tests, the values of brake forces and power were recorded for two dynamometer settings using the AVL MMI software. The tests were carried out for the resistance force $F_{t,p}$ determined by the road coast-down test, and for the force determined by the alternative method. The values of the coefficients determined by the road coast-down test and by the alternative method are shown in Table 3. The characteristics of the theoretical changes of the calculated values of both forces as a function of the driving speed are shown in Fig. 2. Figure 3 shows an example of the changes in the recorded actual values of the resistance forces on the chassis dynamometer during the tests, including the inertia resistance. In addition, this graph shows the values of power and cumulative energy demand for example tests performed for the analyzed dynamometer settings. It can be seen that during the execution of the driving cycle, the actual values of speed and acceleration differ from the theoretical values of the cycle. This also affects the actual values of the motion resistance forces acting on the wheels of the car.

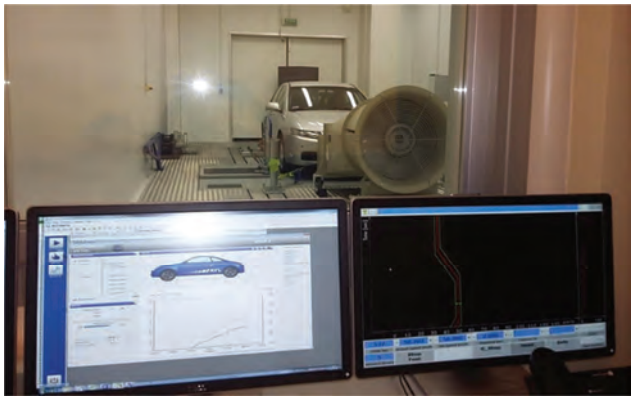

Fig. 1. View of the car on the test stand

Measurements of gaseous emissions: CO_2, CO, THC, CH_4, NMHC and NOx were carried out using AVL AMA i60 system. Specification of accuracy of AMA i60 analyzers is presented in Table 4. Due to comparative tests carried out on cars fuelled with petrol and LPG, the tests were conducted from a hot start. In the case of cold start tests, with LPG powering, the initial phase (about 100 s) started with petrol powering the engine [13]. For tests from hot start, before the test, the engine coolant temperature was 90±2°C. In this case, switching to LPG fuel took place immediately after starting the engine. The tests were conducted at ambient temperature of 23±1°C.

Table 1. Basic technical data of AVL ROADSIM 48″ Chassis Dynamometer [36]

Parameter	Value
Dimensions (Length/Width/Height)	3,600 mm/1,600 mm/1,300 mm
Roller diameter	1,219 mm
Roller mass	765 kg
Rated power	153 kW
Instantaneous power	258 kW
Maximum speed	200 km/h
Inertia simulation range	454 kg … 2,722 kg
Maximum continuous tractive force	5,987 N
Maximum instantaneous tractive force	10,096 N
Tractive force measurement error	≤ 0.1%
Speed measurement error	≤0.02 km/h
Distance measurement error	0.001%/m
Maximum axle load	2,000 kg

Table 2. Technical data of the vehicle

Parameter	Value
Length/Width/Height	4,665 mm/1,760 mm/1,445 mm
Wheelbase	2,670 mm
Weight	1,430 kg
Engine type	Petrol (gasoline)
Fuel System	Multi-point injection
Engine displacement	1998 cm^3
Engine power	115 kW@6,000 rpm
Engine torque	190 Nm@4,500 rpm
Number of cylinders	4
Number of valves	16
Wheel drive	Front
Number of gears (manual transmission)	5
Tire size	205/55 R16
Car mileage	130,000 km
Exhaust purification system	Three-way catalytic converter
Emission standard	Euro 3

Table 3. Coefficients of resistance

Coefficient	Road method	Alternative method
X_0 [N]	155.11	–
X_1 [N/(km/h)]	–0.3429	–
X_2 [N/(km/h)^2]	0.0361	–
A_0 [N]	–	7.6
B_0 [N/(km/h)^2]	–	0.0515
Equivalent inertia [kg]	1590	1590

Table 4. Specification of accuracy of AMA i60 analyzers [3]

Parameter\ Analyzer	CLD i60 LD	FID i60 LCD	IRD i60 CO_{2L}	IRD i60 L
Measured components	NO and NO_x	THC and CH_4	CO_2	CO
Reproducibility	≤ 0.5% of range full scale	≤ 0.5% of range full scale	≤ 0.5% of range full scale	≤ 0.5% of range full scale
Linearity	≤ 2% of measured value (10–100% of range full scale) ≤ 1% of range full scale whichever is smaller	≤ 2% of measured value (10–100% of range full scale) ≤ 1% of range full scale whichever is smaller	≤ 2% of measured value (10–100% of range full scale) ≤ 1% of range full scale whichever is smaller	≤ 2% of measured value (10–100% of range full scale) ≤ 1% of range full scale whichever is smaller

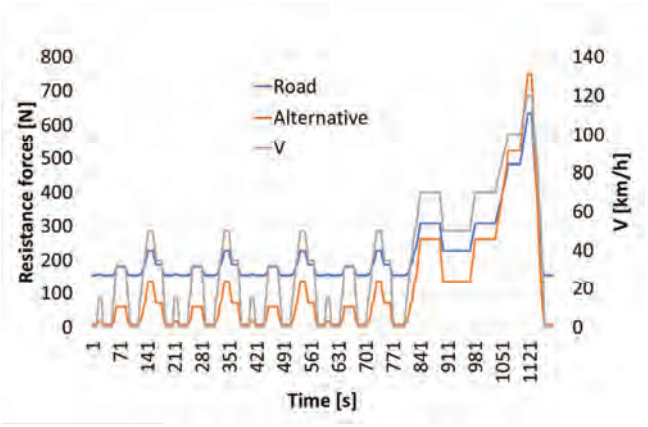

Fig. 2. Calculated resistance forces $F_{t,p}$ and F_c for road and alternative methods

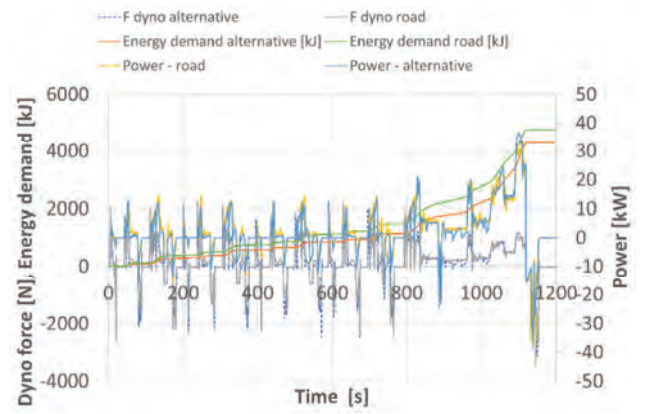

Fig. 3. Sample of measured dyno forces, dyno power and energy demand for road and alternative resistance functions

On the basis of performed tests of exhaust emissions, the EC energy consumption was calculated with the carbon balance method. The values of energy consumption for the gasoline fueling were determined from equation (6), while for the LPG fueling – from equation (7) [34]:

$$EC_{Petrol} = \frac{0.1154}{3.6 \cdot LHV_{Petrol}} (0.866 \cdot HC + 0.429 \cdot CO + 0.273 \cdot CO_2) \left[\frac{kWh}{100\ km}\right] \quad (6)$$

$$EC_{LPG} = \frac{0.1212}{3.6 \cdot LHV_{LPG}} (0.825 \cdot HC + 0.429 \cdot CO + 0.273 \cdot CO_2) \left[\frac{kWh}{100\ km}\right] \quad (7)$$

where: HC – hydrocarbons mass emission [g/km], CO – carbon monoxide mass emission [g/km], CO_2 – carbon dioxide mass emission [g/km], LHV_{Petrol} – lower heating value of petrol [MJ/kg], LHV_{LPG} – lower heating value of LPG [MJ/kg].

Fuel economy values for petrol fuelling were determined from equation (8), while for LPG fuelling – from equation (9) [34]:

$$FE_{Petrol} = \frac{100 \cdot \rho_{Petrol}}{0.1154 \cdot (0.866 \cdot HC + 0.429 \cdot CO + 0.273 \cdot CO_2)} \left[\frac{km}{l}\right] \quad (8)$$

$$FE_{LPG} = \frac{100 \cdot \rho_{LPG}}{0.1212 \cdot (0.825 \cdot HC + 0.429 \cdot CO + 0.273 \cdot CO_2)} \left[\frac{km}{l}\right] \quad (9)$$

where: HC – hydrocarbons mass emission factor [g/km], CO – carbon monoxide mass emission factor [g/km], CO_2 – carbon dioxide mass emission factor [g/km], ρ_{Petrol} – petrol density [kg/dm^3], ρ_{LPG} – LPG density [kg/dm^3].

Then the theoretical values of motor efficiency were determined from equation (10):

$$\eta_{o,j} = \frac{ER_j}{G_{pal,j} \cdot LHV_{pal,k} \cdot \eta_{un}} \quad (10)$$

where: $\eta_{o,j}$ – average overall engine efficiency in phase j (UDC, EUDC) and in the NEDC test, $G_{pal,j}$ – engine mass fuel consumption in phase j (UDC, EUDC) and the NEDC test [kg], $LHV_{pal,k}$ – lower calorific value of k_{th} fuel [kJ/kg], ER_j – total energy demand of car movement in phase j (UDC, EUDC) and for the NEDC test [kJ], η_{un} – average efficiency of the car transmission system.

The value of energy consumption of traffic for individual sections of the test cycle was calculated according to equation (11):

$$ER_j = F_{oj} \cdot s_j \quad [J] \quad (11)$$

where: ER_j – the energy demand of the car movement for the j-th test phase [J], F_{oj} – resistance force in the car motion for the j-th test phase [N], s_j – distance of the j-th test phase [m].

3. Results and discussion

The results of tests on the emission of the analysed pollutants in exhaust gases of the tested vehicle have been presented in Figs 4 to 15. The presented average values of emission factors for two test, for petrol and LPG fuels have been presented for two function of the traffic resistance forces, which were determined using the road method and the alternative method.

The influence of traffic resistance is particularly evident for CO_2 emissions (Fig. 4 to 6). The values of CO_2 emission factors are higher for tests with dynamometer load determined from road coast-down tests in relation to the load determined from the alternative method. In the case of the UDC phase (Fig. 4), the CO_2 emission rate values for the gasoline-fueled road load were about 7% higher than the value obtained for the load according to the alternative method.

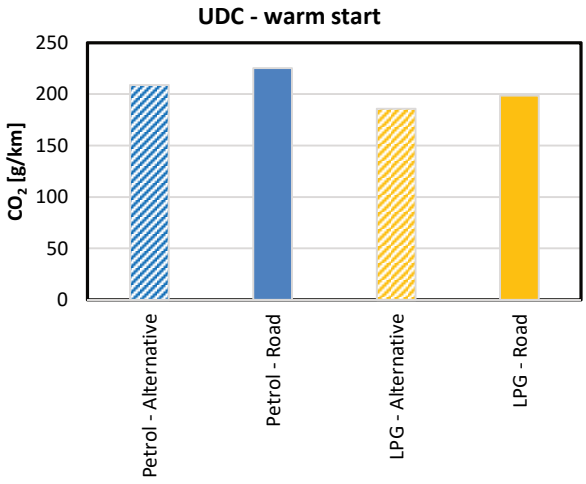

Fig. 4. Impact of resistance forces on CO_2 emissions for UDC phase

For LPG fueling, the difference was about 6%. For the EUDC phase (Fig. 5), the difference of the CO_2 emission factor was about 1%, while for the whole test (Fig. 6) it was about 4% when powered by gasoline and LPG. For the remaining pollutants analyzed (THC, CO, NO_x), no clear correlations were obtained between the dynamometer loading according to the established road and alternative methods on their emissions. In the case of gasoline fueling, the average THC emission for the road load was higher than for the alternative load (Fig. 7 and 9), while for LPG the relationship was the opposite. For the EUDC phase (Fig. 8), the average THC emissions for both tested fuels were higher for the dynamometer load by the alternative method than by the road method.

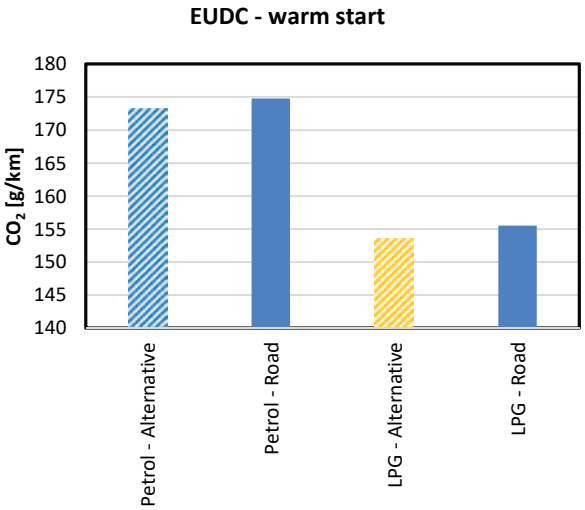

Fig. 5. Impact of resistance forces on CO_2 emissions for EUDC phase

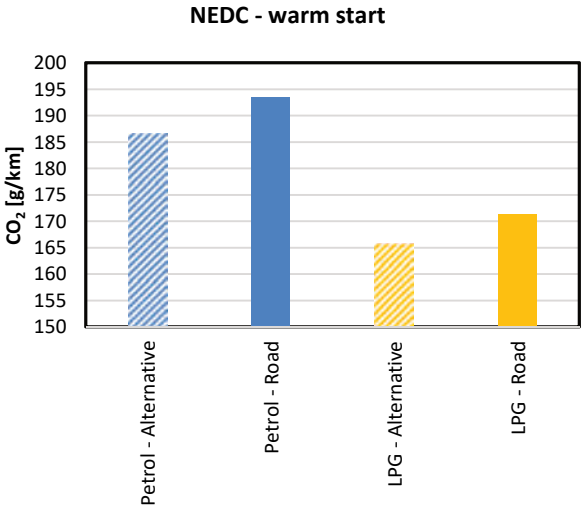

Fig. 6. Impact of resistance forces on CO_2 emissions for NEDC tests

Similar relationships were obtained for CO (Fig. 10 to 12) and NO_x emission rates (Fig. 13 to15). In the case of CO when fuelled with gasoline, higher emission factor values were obtained at the road load of the dynamometer (Fig. 10 to Fig. 12) than at the alternative load. When running on LPG, the results were the opposite, i.e. higher CO emission index values were obtained for the alternative load, both for the urban (Fig. 10), extra-urban phase (Fig. 11) and the entire NEDC cycle (Fig. 12). As with THC, NO_x emission rates from the gasoline-fueled engine were higher during the urban phase (Fig. 13) and entire cycle (Fig. 15) for the dynamometer road load, compared to the values obtained for the alternative dynamometer load. For the EUDC phase (Fig. 14), the relationships were reversed. For the EUDC phase, higher values of NO_x emission rate with LPG fuelling were obtained for the road load (Fig. 14), while in the UDC phase (Fig. 13) and throughout the test (Fig. 15) higher emission rates NO_x were obtained for the dynamometer alternative load. In the tests carried out in the papers [24], for the drag forces determined by the road method, the results of CO_2 emission indices were higher than for the drag forces determined by the coefficients specified by the manufacturer. For the other pollutants, similar to the results presented in this paper, higher or lower values were obtained.

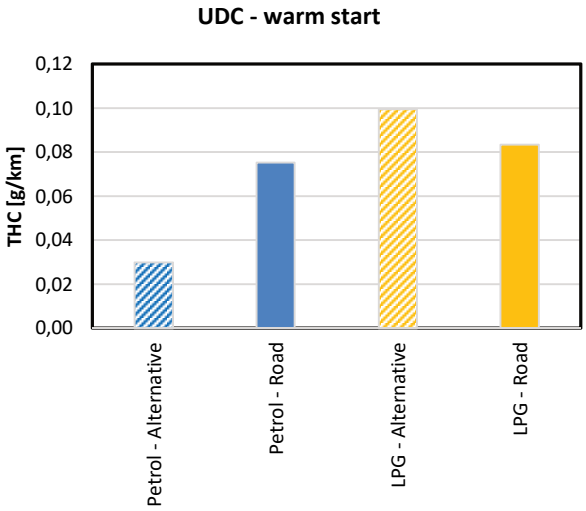

Fig. 7. Impact of resistance forces on THC emissions for UDC phase

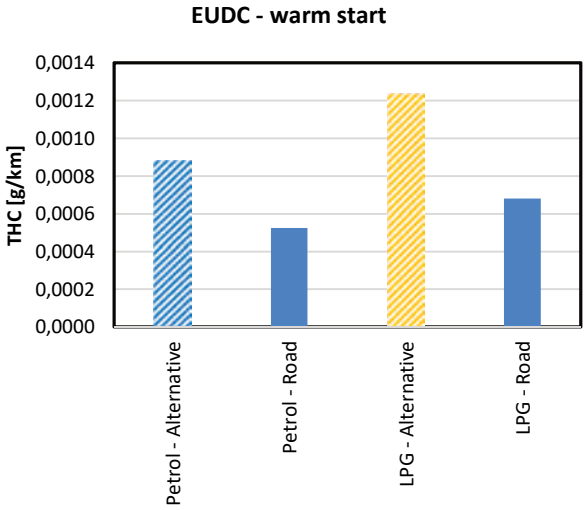

Fig. 8. Impact of resistance forces on THC emissions for EUDC phase

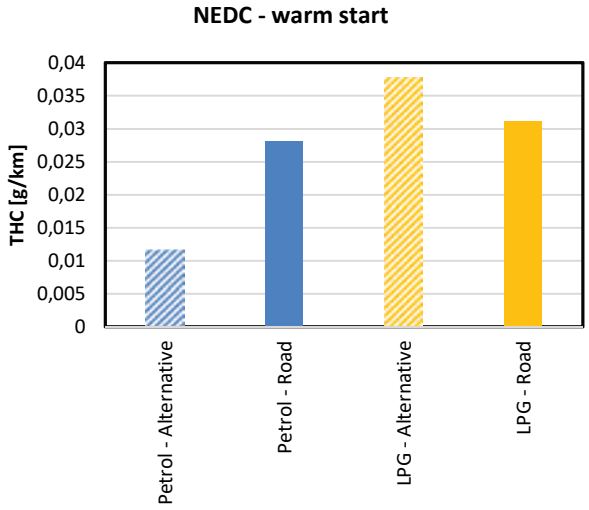

Fig. 9. Impact of resistance forces on THC emissions for NEDC test

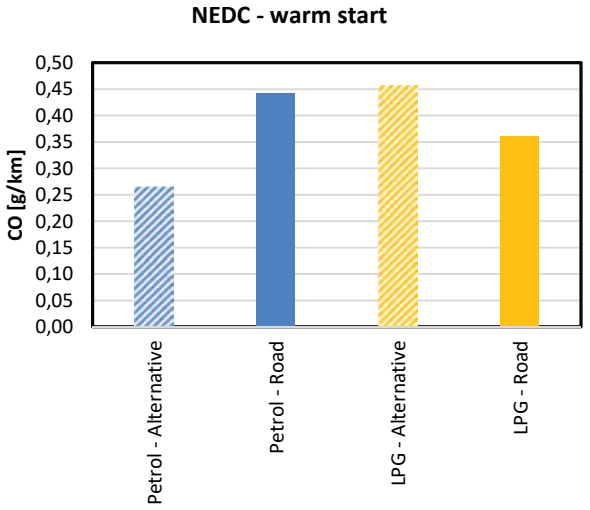

Fig. 12. Impact of resistance forces on CO emissions for NEDC tests

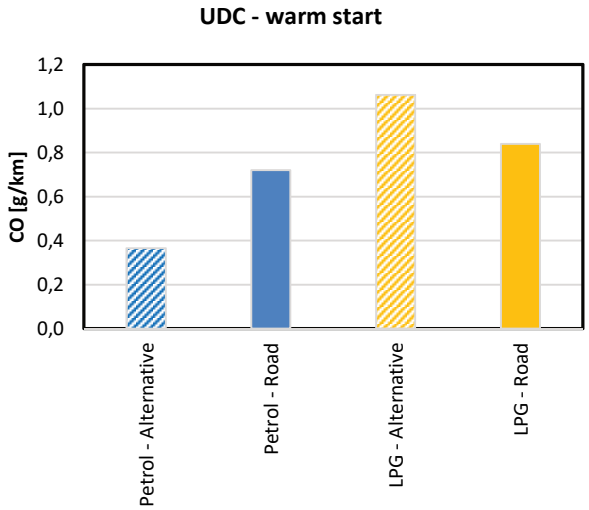

Fig. 10. Impact of resistance forces on CO emissions for UDC phase

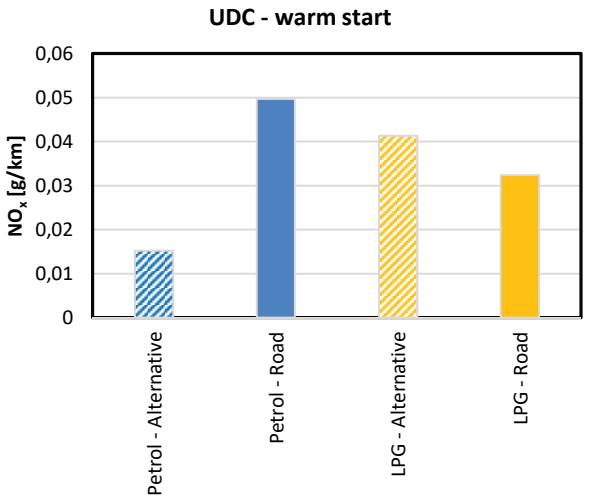

Fig. 13. Impact of resistance forces on NO_x emissions for UDC phase

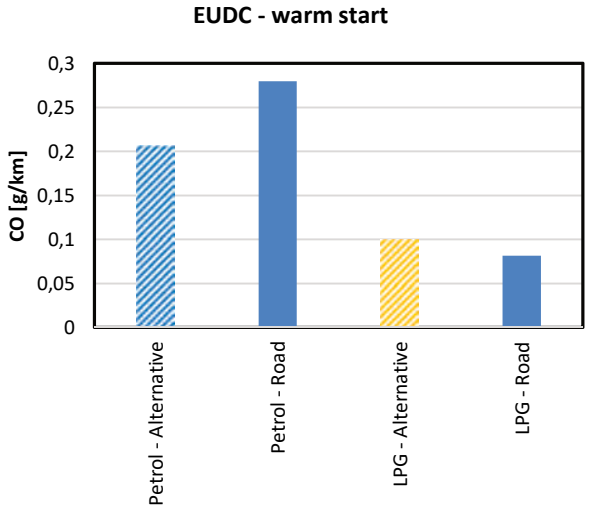

Fig. 11. Impact of resistance forces on CO emissions for EUDC phase

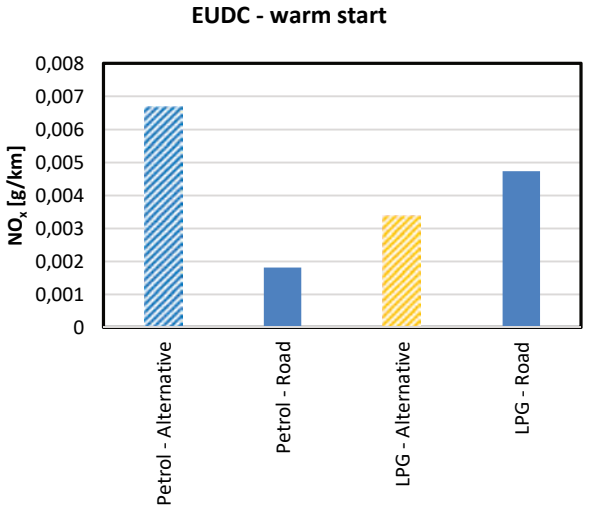

Fig. 14. Impact of resistance forces on NO_x emissions for EUDC phase

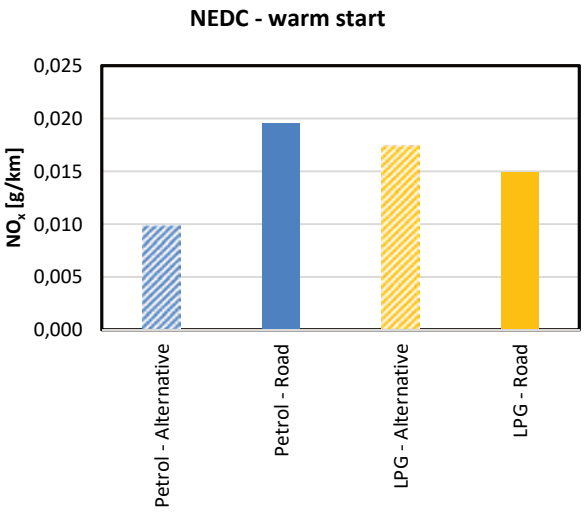

Fig. 15. Impact of resistance forces on NO_x emissions for NEDC tests

Figure 16 shows a comparison of the energy consumption for the car under test, depending on the resistance-to-motion function adopted in the tests, for petrol and LPG fuels. It can be seen that, similarly to higher CO_2 emission for tests with dynamometer load determined on the basis of road tests, the values of energy consumption are also higher. In comparison with the LPG fuel supply, the energy consumption for the gasoline fuel supply was higher.

Figure 17 shows the fuel economy values obtained in the tests for the analyzed car. The distance travelled per unit fuel volume is higher for petrol than for LPG. This is due to the higher energy value of one liter of gasoline in relation to one liter of LPG. However, the values of the distance travelled are lower for the dynamometer load according to the road method.

Taking into account the values of energy demand and the value of fuel consumed, the average values of engine efficiency were determined for the petrol and LPG fuels for the resistance forces analysed (Fig. 18). An increase in the efficiency of the engine operating under a higher load, for the resistance of motion determined by the road method, is clearly seen.

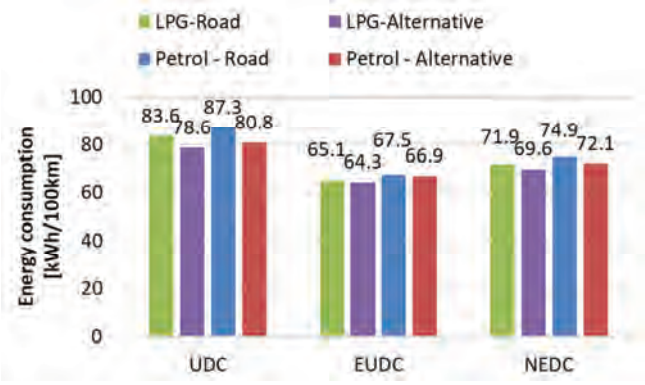

Fig. 16. Impact of resistance forces on energy consumption

In particular, an increase in engine efficiency is seen for the EUDC cycle, during which the car is moving at higher speeds and higher drag forces are acting on it. The differences in average engine efficiency values for the EUDC phase were higher by about 8–10% than for the UDC urban phase. The efficiency of the engine fueled with LPG was also marginally higher than that of the engine fueled with gasoline.

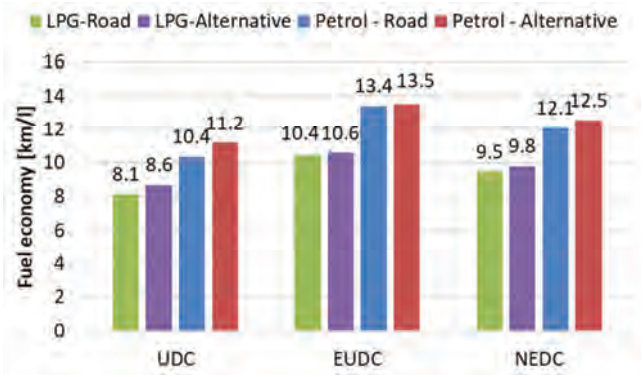

Fig. 17. Impact of resistance forces on fuel economy

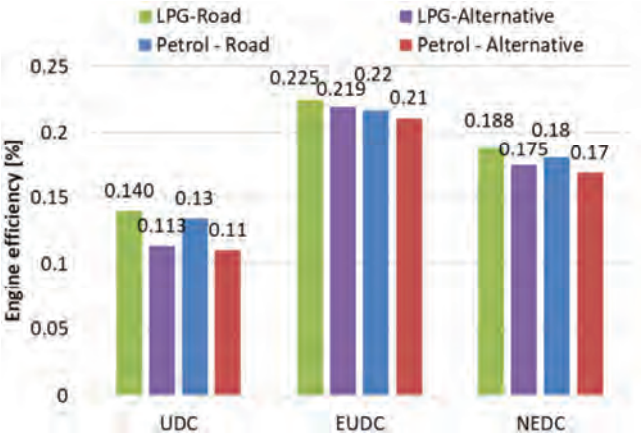

Fig. 18. Impact of resistance forces on average engine efficiency

4. Conclusions

The study showed that due to CO_2 emissions and energy (fuel) consumption, it is important to determine the coefficients of resistance to motion on the basis of road tests. Thanks to that, the results obtained during dynamometer tests are close to the values in the real car operation conditions.

In the case of the other pollutants tested (THC, CO, NO_x), the values of the emission factors do not depend unequivocally on the traffic resistance and may be both lower and higher.

The results of the tests confirmed also the higher values of the engine efficiency at LPG fuelling in relation to petrol fuelling. Also the average engine efficiency is higher for the traffic resistance determined by the road method.

Acknowledgements

This work was supported by The Ministry of Infrastructure and Development under the Eastern Poland Development Operational Program including European Regional Development Fund, which financed the research instruments.

Nomenclature

AT	ambient temperature
CO	carbon monoxide
CO_2	carbon dioxide
CVS	constant volume sampler
EUDC	extra urban driving cycle
LPG	liquefied petroleum gas
NEDC	new European driving cycle
NMHC	non-methane hydrocarbons
NOx	nitrogen oxides
OBD	on-board diagnostics
PEMS	portable emissions measurement systems
PM	particulate matter
RDE	real driving emissions
SI	spark ignition
THC	total hydrocarbons
UDC	urban driving cycle

Bibliography

[1] ANDRZEJEWSKI, M. Wpływ stylu jazdy kierowcy na zużycie paliwa i emisję substancji szkodliwych w spalinach. *Praca doktorska*. Wydział Maszyn Roboczych i Transportu. Politechnika Poznańska. Poznań 2013.

[2] ARCZYŃSKI, S. Mechanika ruchu samochodu. *WNT*. Warszawa, 1993.

[3] AVL AMA i60 Exhaust Measurement System Specification. *AVL* 2013.

[4] BARLOW, T.J., LATHAM, S., MCCARE, I.S. et al. A reference book of driving cycles for use in the measurement of road vehicle emissions. Project report PPR354. *Transport Research Laboratory*. https://assets.publishing.service.gov.uk/government/uploads/system/uploads/attachment_data/file/4247/ppr-354.pdf

[5] BIELACZYC, P., WOODBURN, J., SZCZOTKA, A. Exhaust emissions of gaseous and solid pollutants measured over the NEDC, FTP-75 and WLTC chassis dynamometer driving cycles. *SAE Technical Paper* 2016-01-1008. 2016. https://doi.org/10.4271/2016-01-1008

[6] CHARYUNG, K., HYUNWOO, L., YONGSUNG, P. et al. Study on the criteria for the determination of the road load correlation for automobiles and an analysis of key factors. *Energies*. 2016, **9**(8), 575. https://doi.org/10.3390/en9080575

[7] CHŁOPEK, Z., BIEDRZYCKI, J., LASOCKI, J. et al. Comparative examination of pollutant emission from an automotive internal combustion engine with the use of vehicle driving tests. *Combustion Engines*. 2016, **164**(1), 56-64. https://doi.org/10.19206/CE-116490

[8] CUBITO, C., MILLO, F., BOCCARDO, G. et al. Impact of different driving cycles and operating conditions on CO_2 emissions and energy management strategies of a Euro-6 hybrid electric vehicle. *Energies*. 2017, **10**, 1590. https://doi.org/10.3390/en10101590

[9] DUARTE, G., GONÇALVES, G., FARIAS, T. Analysis of fuel consumption and pollutant emissions of regulated and alternative driving cycles based on real-world measurements. *Transportation Research Part D: Transport and Environment*. 2016, **44**, 43-54. https://doi.org/10.1016/j.trd.2016.02.009

[10] FONTARAS, G., ZACHAROF, N.-G., CIUFFO, B. Fuel consumption and CO_2 emissions from passenger cars in Europe - Laboratory versus real-world emissions. *Progress in Energy and Combustion Science*. 2017, **60**. https://doi.org/10.1016/j.pecs.2016.12.004

[11] GOŁĘBIEWSKI, W. Relacje pomiędzy właściwościami trakcyjnymi pojazdu a zużyciem paliwa. Rozprawa doktorska. Zachodniopomorski Uniwersytet Technologiczny w Szczecinie. *Wydział Inżynierii Mechanicznej i Mechatroniki*. Szczecin 2014.

[12] JAWORSKI A. Odwzorowanie oporów ruchu samochodu podczas badań emisji zanieczyszczeń w spalinach na hamowni podwoziowej. Monografia: Systemy i środki transportu: konstrukcja i badania: wybrane zagadnienia. Nr 21. *Oficyna Wydawnicza Politechniki Rzeszowskiej*. Rzeszów 2020.

[13] JAWORSKI, A. Problematyka wyznaczania współczynników oporów ruchu samochodów do badań emisji zanieczyszczeń spalin w warunkach symulowanych na hamowni podwoziowej. *Вісник Національного Транспортного Університету*. 2019, **3**(45), 52-58, Kijów.

[14] JAWORSKI, A., BOICHENKO, S., MADZIEL, M. et al. Comparative assessment of CO_2 emissions and fuel consumption in a stationary test of the passenger car running on various fuels. *Наукоємні технології*. 2020, **3**(47). https://doi.org/10.18372/2310-5461.47.14936

[15] JAWORSKI, A., MĄDZIEL, M., KUSZEWSKI, H. et al. The impact of driving resistances on the emission of exhaust pollutants from vehicles with the spark ignition engine fuelled with petrol and LPG. *SAE Technical Paper* 2020-01-2206. 2020. https://doi.org/10.4271/2020-01-2206

[16] JAWORSKI, A., LEJDA, K., MĄDZIEL, M. Assessment of the emission of harmful car exhaust components in real traffic conditions. IOP Conferences Series: *Materials Science and Engineering*. 2018, **421**, 042031. https://doi.org/10.1088/1757-899X/421/4/042031

[17] JAWORSKI, A., KUSZEWSKI, H., USTRZYCKI, A. et al. Analysis of the repeatability of exhaust pollutans emission research for cold and hot starts under controlled driving cycle conditions. *Environmental Science and Pollution Research*. 2018, **25**, 17862-17877. https://doi.org/10.1007/s11356-018-1983-5

[18] JAWORSKI, A., KUSZEWSKI, H., USTRZYCKI, A. Wyznaczanie współczynników symulacji oporów ruchu w badaniach na hamowni podwoziowej. *Logistyka*. 2015, **4**.

[19] JAWORSKI, A., MĄDZIEL, M., LEJDA, K. Creating an emission model based on portable emission measurement system for the purpose of a roundabout. *Environmental Science and Pollution Research*. 2019, **26**(21), 21641-21654. https://doi.org/10.1007/s11356-019-05264-1

[20] JAWORSKI, A., MĄDZIEL, M., KUSZEWSKI, H. et al. Analysis of cold start emission from light duty vehicles fueled with gasoline and LPG for selected ambient temperatures. *SAE Technical Papers* 2020-01-2207. 2020. https://doi.org/10.4271/2020-01-2207

[21] JIMÉNEZ, J.L., MCLINTOCK, P.M., MCRAE, G.J. et al. Vehicle specific power: a useful parameter for remote sensing and emissions studies. Ninth CRC On-Road Vehicle Emissions Workshop. San Diego, California, 04.1999. http://cires.colorado.edu/~jjose/Papers/Jimenez_VSP_9thCRC_99_final.pdf

[22] LEJDA, K., JAWORSKI, A., MĄDZIEL, M. et al. Assessment of petrol and natural gas vehicle carbon oxides emissions in the laboratory and on-road tests. *Energies*. 2021, **14**(6), 1631. https://doi.org/10.3390/en14061631

[23] KADIJK, G., LIGTERINK, N. Road load determination of passenger cars. 2012, Report TNO. 04.2019. https://www.tno.nl/media/1971/road_load_determination_passenger_cars_tno_r10237.pdf

[24] KÜHLWEIN, J. The impact of official versus real-world road loads on CO_2 emissions and fuel consumption of European passenger cars. *The International Council On A Clean Transportation*. 2016. https://www.theicct.org/sites/default/files/publications/ICCT_Coastdowns-EU_201605.pdf (accessed on 12.04.2019)

[25] MERKISZ, J., PIELECHA, J., JASIŃSKI, R. Ekologiczna ocena samochodów osobowych w drogowych testach emisyjnych. *Technika Transportu Szynowego*. 2015, **12**.

[26] MERKISZ, J., PIELECHA, J., JASIŃSKI, R. Ocena emisji spalin pojazdów kategorii Euro 6 w testach drogowych. *Prace Naukowe Politechniki Warszawskiej*. 2017, **115**.

[27] MERKISZ, J., PIELECHA, J., GIS, W. Gasoline and LPG vehicle emission factors in a road test. *SAE Technical Paper* 2009-01-0937. 2009. https://doi.org/10.4271/2009-01-0937

[28] MERKISZ, J., PIELECHA, J., BIELACZYC, P. et al. Analysis of emission factors in RDE tests as well as in NEDC and WLTC chassis dynamometer tests. *SAE Technical Paper* 2016-01-0980. 2016. https://doi.org/10.4271/2016-01-0980

[29] MERKISZ, J., PIELECHA, J., BIELACZYC, P. et al. A comparison of tailpipe gaseous emissions from the RDE an WLTP test procedures on a hybrid passenger car. *SAE Technical Papers* 2020-01-2217. 2020. https://doi.org/10.4271/2020-01-2217

[30] MERKISZ, J., RYMANIAK, Ł. The assessment of vehicle exhaust emissions referred to CO_2 based on the investigations of city buses under actual conditions of operation. *Eksploatacja i Niezawodnosc – Maintenance and Reliability.* 2017, **19**(4), 522-529. https://doi.org/10.17531/ein.2017.4.5

[31] MERKISZ-GURANOWSKA, A., PIELECHA, J. Emisja zanieczyszczeń z pojazdów samochodowych a parametry ruchu drogowego. *Oficyna Wydawnicza Politechniki Warszawskiej*. Warszawa 2014.

[32] PELKMANS, L., DEBAL, P. Comparison of on-road emissions with emissions measured on chassis dynamometer test cycles, *Transportation Research Part D: Transport and Environment*. 2006, **11**(4), 233-241. https://doi.org/10.1016/j.trd.2006.04.001

[33] PIELECHA, J., MERKISZ, J., KURTYKA, K. et al. Cold start emissions of passenger cars with gasoline and diesel engines in real driving emissions tests. *Combustion Engines*. 2019, **179**(4), 160-168. https://doi.org/10.19206/CE-2019-427

[34] Regulation No 101 of the Economic Commission for Europe of the United Nations (UN/ECE) — Uniform provisions concerning the approval of passenger cars equipped with an internal combustion engine with regard to the measurement of the emission of carbon dioxide and fuel consumption and of categories M1 and N1 vehicles equipped with an electric power train with regard to the measurement of electric energy consumption and range (accessed on 2.11.2020) https://op.europa.eu/en/publication-detail/-/publication/12faf0c9-6266-4af2-97e4-6a67b5fbaf44

[35] Šarkan, B., Skrúcaný, T., Semanová, Š., Madleňák, R. et al. Vehicle coast-down method as a tool for calculating total resistance for the purposes of type-approval fuel consumption. *Scientific Journal of Silesian University of Technology*. Series Transport. 2018, **98**. https://doi.org/10.20858/sjsutst.2018.98.15

[36] Service Manual 2014 AVL- ROADSIM 48".

[37] Statistics Poland. Transport and Communication. Vehicles by Age Groups. https://bdl.stat.gov.pl/BDL/dane/podgrup/temat/8/239/2825

[38] STOJECKI, A. Badania wpływu topografii terenu na emisję związków szkodliwych spalin samochodów osobowych. *Rozprawa doktorska*. Wydział Maszyn Roboczych i Transportu. Politechnika Poznańska. Poznań 2015.

[39] SYNÁK, F., RIEVAJ, V. The impact of driving resistances of a vehicle on global pollution. *17th International Scientific Conference Globalization and Its Socio-Economic Consequences*. University of Zilina (accessed on 14.06.2021). https://www.researchgate.net/publication/326990879_THE_IMPACT_OF_DRIVING_RESISTANCES_OF_A_VEHICLE_ON_GLOBAL_POLLUTION

[40] SZCZOTKA, A., PUCHAŁKA, B., BIELACZYC, P. et al. Influence of the chassis dynamometer regulation on the exhaust emission results. *AUTOBUSY – Technika, Eksploatacja, Systemy Transportowe.* 2019, **24**(6), 280-285. https://doi.org/10.24136/atest.2019.164

[41] TIETGE, U., ZACHAROF, N., MOCK, P. et al. From laboratory to road – a 2015 update of official and "real-world" fuel consumption and CO_2 values for passenger cars in Europe. *International Council on Clean Transportation*. 2015. https://theicct.org/sites/default/files/publications/ICCT_LaboratoryToRoad_2015_Report_English.pdf

[42] TSIAKMAKIS, S., FONTARAS, G., CUBITO, C. et al. From NEDC to WLTP: effect on the type-approval CO_2 emissions of light-duty vehicles. EUR 28724 EN. *Publications Office of the European Union*. Luxembourg 2017. https://doi.org/10.2760/93419

[43] UNECE. Regulamin nr 83 Europejskiej Komisji Gospodarczej Organizacji Narodów Zjednoczonych (EKG ONZ) – Jednolite przepisy dotyczące homologacji pojazdów w zakresie emisji zanieczyszczeń w zależności od paliwa zasilającego silnik. https://eur-lex.europa.eu/legal-content/PL/TXT/PDF/?uri=CELEX:42012X0215(01)&from=EN

[44] ZACHAROF, N., FONTARAS, G., CIUFFO, B. et al. Review of in use factors affecting the fuel consumption and CO_2 emissions of passenger cars. *Euro Commission*. Luxembourg 2016. https://core.ac.uk/download/pdf/81684802.pdf

Artur Jaworski, DEng. – Faculty of Mechanical Engineering and Aeronautics, Rzeszow University of Technology.
e-mail: *ajaworsk@prz.edu.pl*

Prof. Kazimierz Lejda, DSc., DEng. – Faculty of Mechanical Engineering and Aeronautics, Rzeszow University of Technology.
e-mail: *klejda@prz.edu.pl*

Maciej Bilski, DEng. – Faculty of Architecture, Poznan University of Technology.
e-mail: *maciej.bilski@put.poznan.pl*

Article citation info:
SZWAJA, S., SZYMKOWIAK, M. The Szymkowiak's over-expanded cycle in the rocker engine with the variable compression ratio – kinematics. *Combustion Engines*. 2022, **189**(2), 68-72. https://doi.org/10.19206/CE-143157

Stanisław SZWAJA
Mirosław SZYMKOWIAK

Combustion Engines
Polish Scientific Society of Combustion Engines

The Szymkowiak's over-expanded cycle in the rocker engine with the variable compression ratio – kinematics

ARTICLE INFO

Received: 10 August 2021
Revised: 31 August 2021
Accepted: 18 October 2021
Available online: 30 October 2021

The article discusses the innovative concept of the over-expanded thermodynamic cycle, the author of which is the Polish engineer-designer Mirosław Szymkowiak. This cycle is realized on the basis of a new and innovative, previously unknown design, of a piston-crankshaft linkage mechanism with the aid of an additional element known as a rocker arm. Additionally, the proposed mechanism allows for a smooth change of the compression/expansion ratio of the engine during its operation. In the beginning, the earlier conceptions of the rocker engine developed by Szymkowiak were presented, and then the main construction assumptions and kinematic calculations were described. It was confirmed, that the developed linkage has big potential in improving the engine's thermal efficiency by approximately 12% relative. Additionally, it significantly reduces the exhaust gas pressure, when the exhaust valve is opened, therefore, contributes to the reduction of the noise emitted by the engine.

Key words: *rocker, engine, linkage, over-expanded cycle, variable expansion/compression ratio*

1. Introduction

Several intensive measures have been taken focusing on issues related to combustion and engine design. Research is conducted on the improvement of the engine overall efficiency and reduction of exhaust emissions. It is carried out on various levels, including the search for new kinematic solutions that enable the variable compression ratio and over-expanded cycle implementations into the engine. As a result, several solutions were invented to convert the reciprocating motion of the piston into the rotary motion of the crankshaft [1–3].

One of these kinematic mechanisms is presented in the article. Its inventor is the Polish engineer Mirosław Szymkowiak. Szymkowiak has been working on his solutions for years [3] and as a result, he has achieved several improvements. The main feature of the developed mechanism is the rocker arm that connects two connecting rods: the first one is located between the piston and the rocker arm, the second one - between the rocker arm and the crankshaft, respectively. In the past (1950s and 1960s) the engine equipped with a rocker arm and two connecting rods was the Commer TS3 2-stroke diesel engine built by Tilling-Stevens in the Rootes group [1, 2]. Each cylinder contained two pistons positioned horizontally opposite each other and moving opposite each other as depicted in Fig. 1. This engine was launched into mass production and installed in trucks.

The concept of applying the rocker as the element for combining combustion forces from 4 pistons into a single crank of the crankshaft was the main idea of this design (Fig. 3 and 4). Hence, the mechanism examined in the paper is novel work and is under intellectual protection. Unlike the two-stroke Commer engine, the rocker engine presented in the paper is four-stroke one. The mechanism provides possibilities of obtaining various mean piston speeds at constant crankshaft rotational speed because the piston stroke is independent of the crank length. Additionally, the mechanism provides possibility of change in both the compression and expansion ratio. This concept refers to the solution presented by Rychter and Teodorczyk [4, 5]. The mechanism VR/VL, which they proposed, applies a variable ratio of the length of the crank to the connecting rod in order to change the compression ratio.

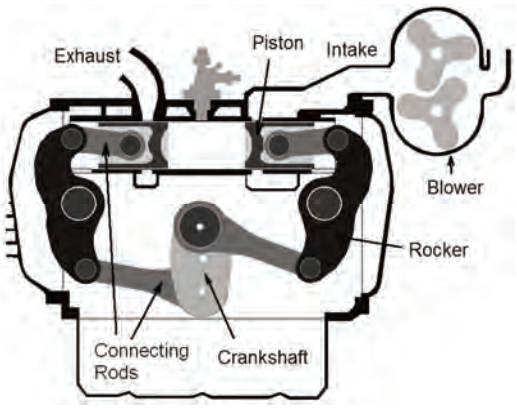

Fig. 1. Kinematic linkage in the rocker Commer engine [1, 2]

As depicted in Fig. 2 the rocker in this conception connects a piston and transfers motion with aid of the main connecting rod into the crankshaft. In further analysis the rocker is equipped with four pins separately connecting each piston to the rocker as shown in Fig. 3 and 4.

Kozak [6] presented a closer qualitative analysis of a crank-and-rocker piston mechanism. In comparison to a conventional piston assembly, this mechanism is composed of additional elements called rockers. A higher number of elements allows better functional flexibility of the mechanism, particularly in terms of the piston motion. As discussed by Kozak, this feature can be used to control the course of the engine torque, the heat losses to the cooling system, the reduction of the piston pressure on the cylinder liners (friction and mechanical losses) as well as variation of the compression ratio easily performed during engine

operation. As Magryta recommended [7], the finite element methods and analytical kinematics analysis can be successfully applied into the motion and stress analysis for the piston-conrod-crankshaft mechanism.

The first conception of the rocker engine invented by M. Szymkowiak is depicted in Fig. 2.

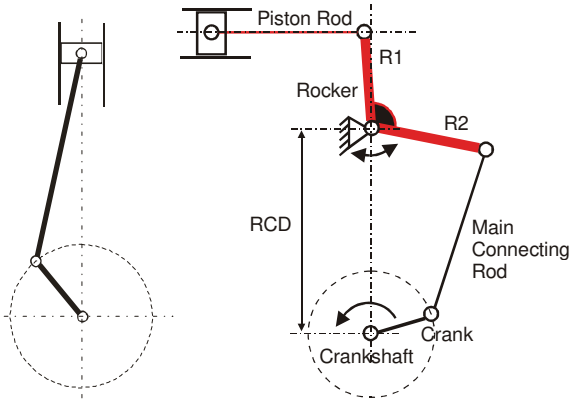

Fig. 2. Kinematic diagram of a) classic linkage, b) first conception of the rocker engine

On the basis of the construction presented in Fig. 2, Mr. Szymkowiak worked out the multi-cylinder engine with kinematic linkage presented in Fig. 3 and its 3-D presentation in Fig. 4. As seen in Fig. 4, the 8-cylinder engine features its compactness and relatively short crankshaft length.

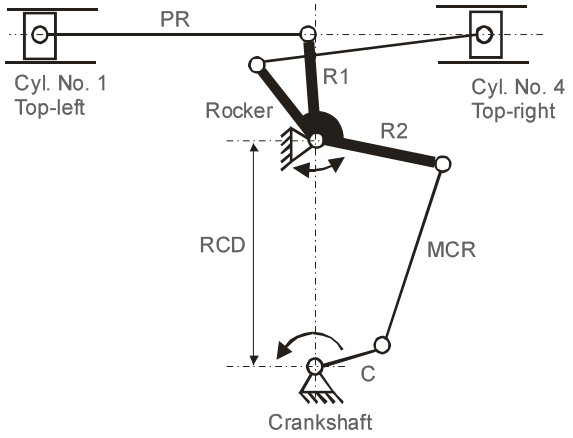

Fig. 3. Kinematic diagram of the 2-cylinder rocker engine

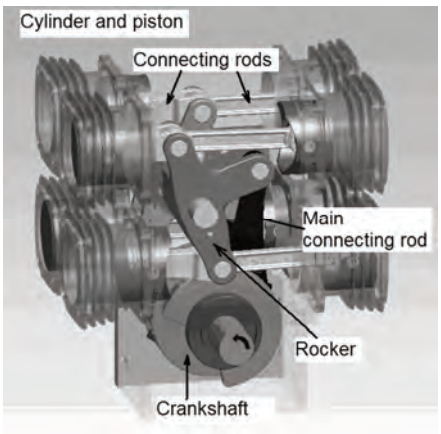

Fig. 4. Conception of the 8-cylinder rocker engine

Next modifications were done towards cylinders' positions. From their horizontally oriented locations the cylinders were oriented vertically as depicted in Fig. 5a.

a)

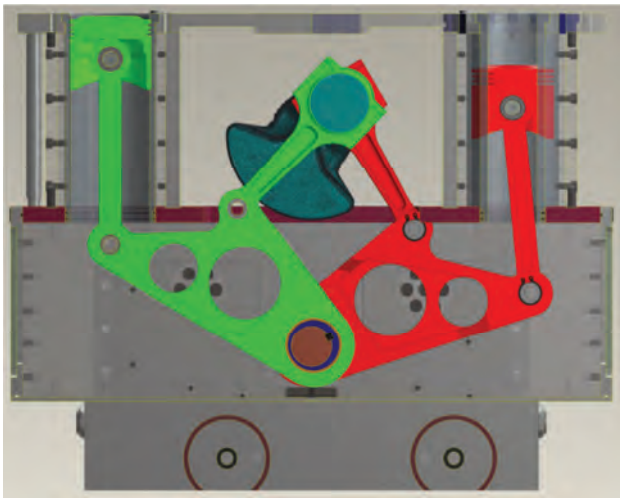

b)

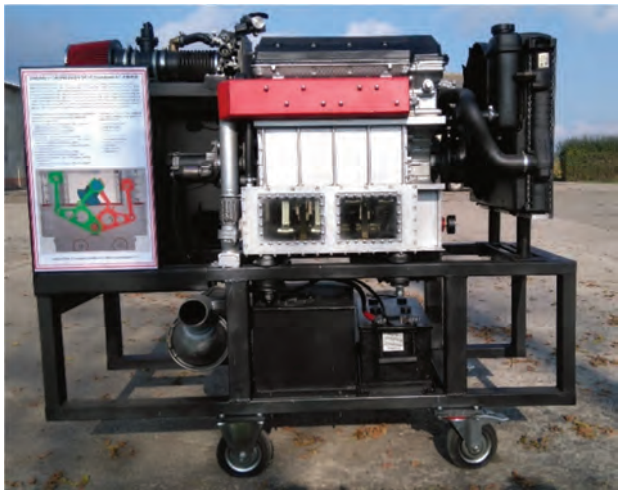

Fig. 5. a) Model and b) prototype of the 8-cylinder rocker engine

Based on this conception the 8-cylinder engine was built (Fig. 5b) and tested. During the engine preliminary tests, the proper engine work without any malfunction was confirmed. The design of the rocker crank mechanism allows to obtain benefits as follows:

- change of the compression and expansion ratio in a simple way during operation of the engine,
- significant reduction in fuel consumption,
- the possibility of using various fuels,
- the asymmetry in compression and expansion,
- significant increase in torque from the beginning of the expansion process,
- non-zero torque at the TDC,
- piston-cylinder sleeve force is several times lower in comparison to the classic solutions, that leads to a decrease in friction wear, so increases overall efficiency, and increases the life of the piston and cylinder,

– excellent ratio of mass to the engine swept volume,
– a significant reduction of height in the marine engine (a slider is an unnecessary item).

The proposed construction makes building the long-stroke engine without drawbacks associated with the classic solution.

A characteristic feature of the engine is an innovative way to transfer the reciprocating motion of the pistons to the rotary motion of the crankshaft. The crankshaft in combination with its innovative location between the cylinder rows allows for features inaccessible to traditional solutions. The design is very flexible and anyone has a much greater amount of slack variables than in traditional solutions and can use them to achieve the required parameters. It is worth of emphasizing that the proposed linkages would be particularly useful for engines with long strokes working at relatively high loads (CHP units, marine engines, harvesting machines, mining machinery, train engine as well as lorries, off-road military vehicles etc.).

2. Engine with variable compression ratio and over-expanded cycle – the conception

Several studies realized by Mr. M. Szymkowiak occurred fruitful in working out the conception and finally the engine, which characterizes by both variable compression ratio and over-expanded cycle. The schematic diagram is shown in Fig. 6. As depicted, the mechanism consists of the following parts:

– piston (1),
– connecting rods (2) and (5),
– rocker (3),
– eccentricity – eccentric crank (4),
– crankshaft (6).

A specific feature of this linkage is the eccentric crank, which rotates in the same direction as the crankshaft rotates, but with a speed twice lower than the engine crankshaft speed n_s. The eccentricity notion, used in further discussion, is the length of this eccentric crank. The rocker is swingingly mounted to this crank.

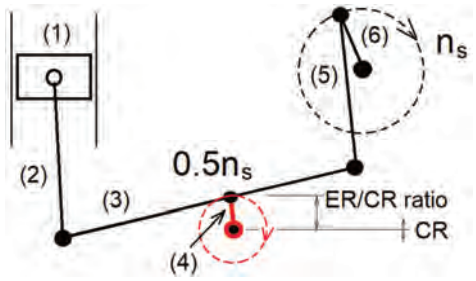

Fig. 6. Piston-crankshaft linkage of the new conception of the rocker engine

The main dimensions of the linkage and the engine are as follows:

– rocker (3) length: 220 mm,
– connecting rod (2) length: 162.5 mm,
– connecting rod (5) length: 143 mm,
– eccentric crank (4) length: varied from 0 till 20 mm,
– crank length (6): 32.9 mm,
– single cylinder displacement: 376 ccm,
– cylinder bore: 60 mm,
– maximum piston stroke: 133.2 mm,
– compression ratio: 9.5,
– proposed fuel: regular gasoline.

As shown in Fig. 6, the compression and expansion ratios can be changed by changing the vertical position of the eccentric crank rotational axis. The construction of the proposed mechanism allows change of this parameter under engine work. The compression ratio can vary from 7 to 14.

The CAD model of this engine is presented in Fig. 7. Among others, horizontal lines mark TDC and BDC of the pistons.

a)

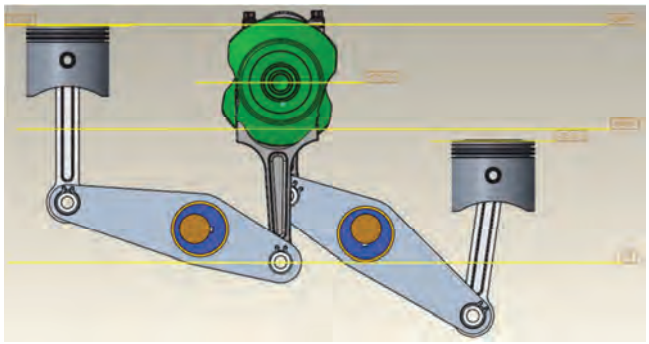

b)

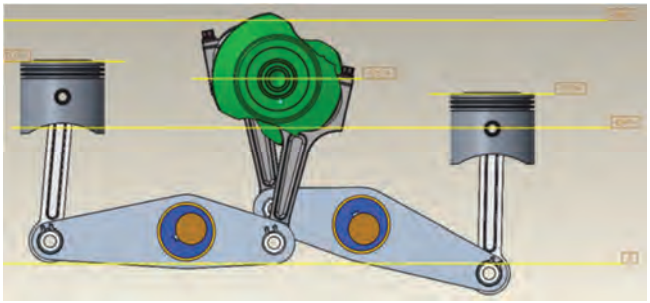

c)

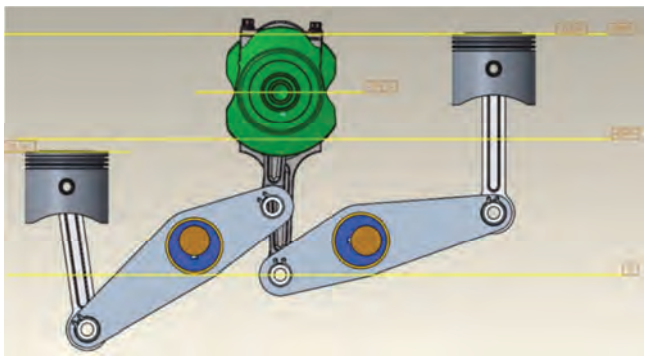

Fig. 7. New conception in various crankshaft angular positions: a) 0 CA deg, b) 120 CA deg, c) 180 CA deg

3. Results and discussion

Kinematic analysis was realized with the aid of Matlab/Simulink software. Hence, the kinematic linkage was directly simulated in this computational environment without any mathematical models. Figure 8 shows the piston dis-

tance profile over the crank angle for a 4-stroke engine. The idea for realizing the over-expanded thermodynamic cycle is based on variable piston stroke, which is shorter at the compression process (denoted as the compression stroke in Fig. 8), and longer at the expansion one. As seen, the compression stroke expressed in crank angle is around 159 CA deg, while the expansion stroke is 213 CA deg. Hence, additional expansion work is generated, that creates additional power benefit on the engine crankshaft. Piston position at 0 mm corresponds to its TDC location. The negative numbers result from positioning of piston motion in the coordinating system in the Matlab modelling software. The piston profile was determined for the eccentricity of 15 mm. Other piston distance profiles vs. crank angle for various eccentricities are depicted in Fig. 9.

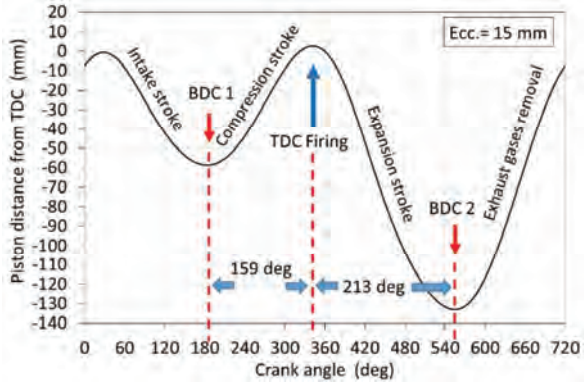

Fig. 8. Piston distance from TDC

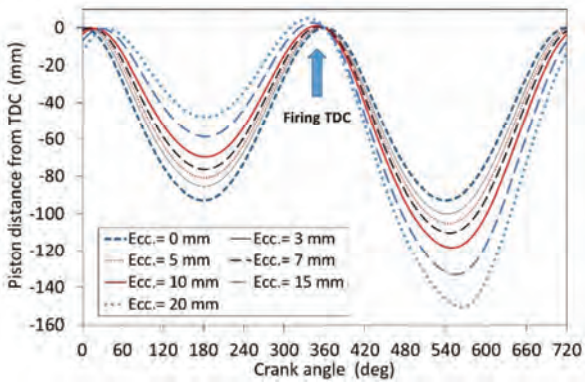

Fig. 9. Piston distance from TDC for various eccentricities

As concluded from Fig. 9, higher eccentricity makes the compression stroke shorter and lengthens the expansion stroke. Thus, both the expansion and the compression ratio vs. eccentricity are depicted in Fig. 10. Based on preliminary studies, it was assumed that eccentricity may be subject to changes in the range from 0 to 15 mm, denoted in Figure 10 as the useful range for engine operation, where the compression stroke does not differ significantly from its initial value, that is important as regards combustion process and any abnormal combustion known as knock.

To show potential benefit from the over-expanded cycles, the expansion/compression ratio was introduced. As one can conclude from Fig. 11, the expansion to compression ratio (ER/CR) increases with increase in the eccentricity.

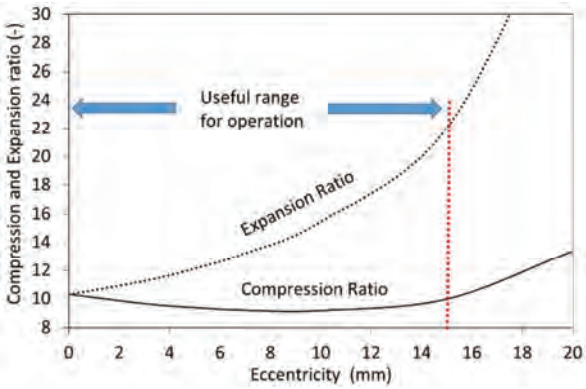

Fig. 10. Expansion and compression ratio vs. eccentricity

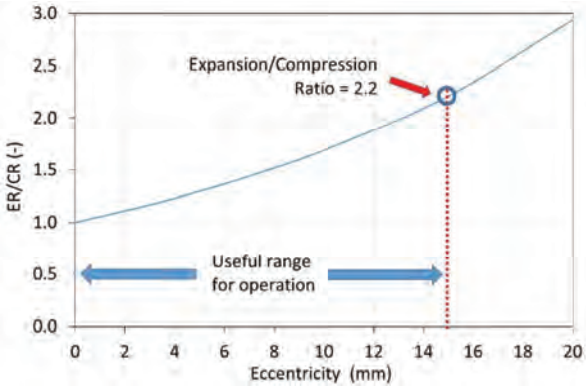

Fig. 11. Expansion to compression ratio vs. eccentricity

The maximum for the eccentricity is limited by the power drop generated by the engine. As shown in Fig. 12, additional power generated by the engine increases with increase in eccentricity and indirectly with increase in expansion/compression ratio. As analyzed, the maximum limit for the ER/CR is 2.2, that corresponds to the eccentricity of approximately 15 mm.

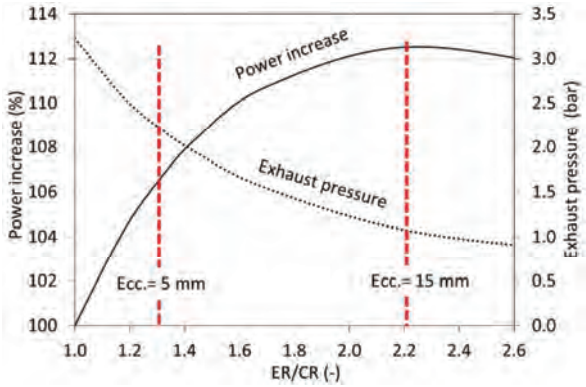

Fig. 12. Power increase and exhaust gas pressure at the end of the expansion stroke

As analyzed plots in Fig. 12, the remarkably low exhaust pressure of approximately 1 bar is observed at the end of the expansion stroke when the exhaust valve gets open for ER/CR of 2.2. This is the additional benefit from applying the over-expanded cycle. The exhaust pressure close to ambient pressure at the exhaust valve opening does not generate a pressure wave in the exhaust manifold, and fur-

ther, in the exhaust pipeline. Hence, one can conclude that the engine equipped with the over-expanded cycle by Szymkowiak does not require a silencer for dumping exhaust acoustic noise.

4. Conclusion

The proposed linkage mechanism invented by Miroslaw Szymkowiak is characterized by the following features:

- expansion/compression ratio (ER/CR) of the engine can be higher 1, which indicates the over-expanded thermodynamic cycle in the engine,
- the maximum of the expansion/compression ratio is 2.2, which provides the maximum benefit for the engine power,
- by changing the vertical location of the axis of rotation of the eccentric crank, both the expansion and compression ratio can be changed. It can be realized under engine work.

Nomenclature

BDC	bottom dead center	ER	expansion ratio
CA	crank angle	DI	direct injection
CR	compression ratio	TDC	top dead center

Bibliography

[1] PatOP: Single-crankshaft opposed-piston engine http://www.pattakon.com/patop/CommerTS.gif

[2] HILLMAN CAR CLUB OF SOUTH AUSTRALIA INC. https://www.sa.hillman.org.au/TS3.htm

[3] SZYMKOWIAK, M., SZWAJA, S. New concept of a rocker engine – kinematic analysis. *Journal of Kones*. 2012, **19**, 443-449. https://doi.org/10.5604/12314005.1138160

[4] RYCHTER, T.J., TEODORCZYK, A., STONE, C.R. A theoretical study of a variable compression ratio turbocharged diesel engine. *Proceedings of the Institution of Mechanical Engineers, Part A: Journal of Power and Energy*. 1992, **206**(4), 227-238. https://doi.org/10.1243/PIME_PROC_1992_206_039_02

[5] RYCHTER, T.J., TEODORCZYK, A. VR/LE engine with variable R/L during a single cycle. *SAE Technical Paper* 850206. 1985. https://doi.org/10.4271/850206

[6] KOZAK, W. Crank and rocker piston assembly. *Combustion Engines*. 2013, **152(1)**, 10-27. https://doi.org/10.19206/CE-117009

[7] MAGRYTA, P., PIETRYKOWSKI, K., BIAŁY, M. et al. The influence of load distribution in kinematic constraints of connecting rod on the results of the stress simulation. *Combustion Engines*. 2017, **170**(3), 84-87. https://doi.org/10.19206/CE-2017-313

Prof. Stanisław Szwaja, DSc., DEng. – Mechanical Engineering and Computer Science Faculty, Czestochowa University of Technology.
e-mail: *szwaja@imc.pcz.pl*

Mirosław Szymkowiak, MSc. – alumnus from AGH – University of Science and Technology. Engineer in his own enterprise.
e-mail: *lfp-ztg@lfp-ztg.pl*

Article citation info:
CIEŚLIK, W., SZWAJCA, F., WISŁOCKI, K. Reverse engineering of research engine cylinder-head. *Combustion Engines*. 2022, **189**(2), 73-82. https://doi.org/10.19206/CE-143481

Wojciech CIEŚLIK
Filip SZWAJCA
Krzysztof WISŁOCKI

Combustion Engines
Polish Scientific Society of Combustion Engines

Reverse engineering of research engine cylinder-head

ARTICLE INFO

Received: 16 September 2021
Revised: 27 October 2021
Accepted: 29 October 2021
Available online: 2 November 2021

The pursuit of increasing the efficiency of internal combustion engines is an ongoing engineering task that requires numerous research efforts. New concepts of injection or combustion systems require preliminary investigation work using research engines. These engines, usually single-cylinder, make it possible to isolate a single variable in a complex combustion mixture preparation process, thus enabling analysis of the changes being made. However, these engines are relatively expensive and their designs are offered by a limited number of manufacturers. The authors of this paper have successfully undertaken the engineering task of modifying an existing research engine cylinder head in such a way as to implement an electronically controlled variable valve timing system of the intake system. The process of reverse engineering, together with design assumptions that finally contributed to the construction of the assumed solution has been described in this paper.

Key words: *reverse engineering, research engine, 3D measuring system, tomographic measurement, variable valve timing*

1. Introduction

Human activity towards continuous economic development causes, among others, a significant expansion of the transportation network across the planet. Despite the passage of decades, the primary source of mechanical energy is still constituted by various types of internal combustion engines (ICEs), which are estimated to be approximately 2 billion in total worldwide [1]. Restrictions applied to internal combustion engines, which are the dominant source of propulsion, resulting in a preference for alternative propulsion systems. Considering the size of the ICE share, it is difficult to talk about a complete shift away from this type of energy source in support of battery electric vehicles. Additionally, no solution could replace ICE in such a wide range as Automotive, Marine, Aviation or Electric production. Increased research on combustion systems and exhaust gas aftertreatment systems applied in many solutions implemented in series production, resulting in a significant rise in energy conversion efficiency and reduction of toxic emissions. The mentioned effect led to an improvement in the attractiveness of ICE and a significant reduction in its environmental impact [2].

The outlook for further development of internal combustion engines based on the automotive industry is related to the necessity of meeting future emission standards, especially CO_2 limits [3, 4]. In order to meet future standards, efforts are being made, leading to the electrification of powertrains. Parallel work is being carried out to improve the ICE. Figure 1 shows the evolution of the propulsion system, whose priority in the initial phase of development was low cost and high reliability (ICE 1.0) to technologically advanced hybrid systems (ICE 4.0) based on the close cooperation of the internal combustion engine with the electric system [5].

Developing an internal combustion engine involves the experimental research carried out on model test stands such as constant volume chambers or rapid compression machines and real single or multi-cylinder engines [6]. The process of a hierarchical approach to engine testing presented by Kyrtatos et al. [7] combines the analysis of fundamental aspects and the application of the tested technical solution in a closed application-fundamentals-application cycle. For this purpose, simulations and experiments performed with modern tools are used. The experimental part includes the study of fundamental phenomena carried out using a constant volume chamber with optical access, optical testing on a single cycle RCEM machine using assumed geometry and finally on a single cylinder research engine close to the production engine.

Fig. 1. Passenger car powertrain system development [5]

The engine research results are the implementation of new highly advanced systems that reduce fuel consumption, which translates directly into lower GHG emissions [8]. Engine manufacturers indicate the possibility of fuel efficiency improvement in the range of 20–30% by implementing, e.g. variable compression ratio VCR, cylinder deactivation or application of unconventional work cycles of Atkinson/Miller engine in the hybrid drive system. Also, the combustion of lean mixtures, decreasing the combustion temperature, and spark-assisted compression ignition system are attractive [9].

The introduction of a new solution to large-scale production is a complex process requiring considerable time and financial resources. Figure 2 presents the state of advancement of selected systems for increasing the efficiency of an internal combustion engine. It is worth noting that there are systems not introduced to mass production (Full

Authority Cylinder Deactivation) and those commonly used (Variable Valve Timing). The continuous modernization of ICE requires new test benches or upgrades to existing ones. Hence the need to take into account in the development of further improvements, e.g. the presence of variable valve timing.

Boosted Engines	Intro Year	Variable Valve Timing (VVT)	Integrated Exhaust Manifold	High Geometric CR	Friction Reduction	Higher Stroke/Bore Ratio	Boosting Technology	Cooled EGR	Variable Valve Lift	Miller Cycle	VNT/VGT Turbo	Partial Discrete Cyl. Deac.	Full Authority Cylinder Deac.	Variable Compression Ratio	Gasoline SPCCI/Lean modes
Ford EcoBoost 1.6L	2010														
Ford EcoBoost 2.7L	2015														
Honda L15B7 1.5L	2016														
Mazda SKYACTIVE-G 2.5L	2016						4				4				
VW EA888-3B 2.0L	2018														
VW EA211 EVO 1.5L	2019							3							
VW/Audi EA839 3.0L V6	2018				3										
Nissan MR20 DDT VCR 2.1L	2018			+	3		3	3							3
Mazda SKYACTIVE-X SPCCI 2.0L[1]	2019			+	3						NA				
EPA/Ricardo EGRB24 1.2L[2]	N/A														

yellow – early implementation *light & dark green – nearing maturity* *red – technology not present*

1 – Supercharged, **2** – EPA Draft TAR, **3** – Not known at time of writing, **4** – Mazda accomplish equivalent of VNT/VGT using novel valving system

Fig. 2. Combustion engines technology upgrades and implementation status [10]

The Institute of Combustion Engines and Powertrains of Poznan University of Technology has a single-cylinder research engine AVL 5804, part of a dynamometer bench. It allows for advanced development work in the field of mixture formation and combustion systems. Due to its high operational value, this test stand is subject to the continuous modernization in line with current trends. Originally the engine worked as a diesel with a direct fuel injection system based on an electronic rotary distributor pump. Subsequently, it was modified in several ways, including applying the common rail system and system for co-combustion of liquid and gaseous fuels (dual fuel). Finally, the design in which the spark-jet ignition system (TJI) was applied and was introduced for using gaseous fuels [11–13].

2. Main goal of the project

The desire to conduct further research related to the development of low-emission combustion systems forced us to carry out another significant modification of the engine head construction so that it was possible to implement a smooth change of intake camshaft position in relation to the crankshaft position. In order to do so, a new head with a modified construction was made, in which an electrically controlled variable valve timing system was implemented.

For that purpose it was decided to implement the reverse engineering method while a new cylinder head with adequate variable valve timing was at that time neither available nor financially essential. For casting of the new and adequately modified cylinder head the knowledge of the internal structure and geometry was essential as well. To achieve the appropriate geometric mapping the 3D-scanning technology has been implemented and on this way the full 3D-project has been generated. It was the basis for casting, modifications and final turning and milling post processing.

The production process of the new cylinder-head, including the design, manufacture and start-up phases has been presented in this paper.

3. Features and significant of Research engines

In the development of internal combustion engines, it is essential to carry out experiments on test benches that reproduce the real engine's continuous operation as closely as possible. For this purpose, single or multi-cylinder experimental engines are used (Fig. 3). The use of TSCE engines is particularly attractive due to the possibility of analyzing the basic engine systems and processes during operation from cycle to cycle. Compared to multi-cylinder MCE engines, single-cylinder TSCEs reduce the cost of test equipment and greatly increase diagnostic availability. Single cylinder TSCE and OSCE engines are currently widely used for primary research types. For development projects, the implementation of single cylinder engines must be carefully considered [14].

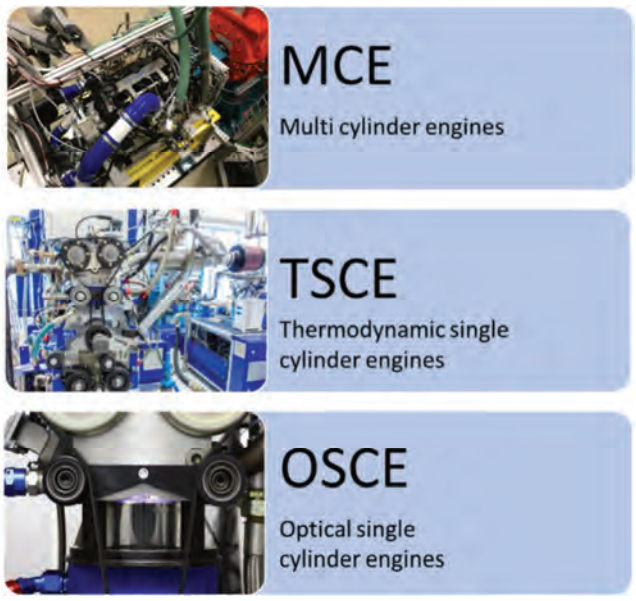

Fig. 3. Research engines types [14, 22, 32, 33]

Single cylinder optical engines are engines constructed to allow optical access to the working volume. The beginnings of implementing optical research on a running engine dates to 1920's and early 1930's [15]. The breakthrough came in 1961 when Bowditch [16] published a new design of research engine, assuming optical access through the crown of a specially designed expanded piston. This concept was initiated with the implementation of overhead valve engines and is still being developed today.

The advantage of using optical engines is the possibility of visualising in-cylinder processes using advanced measurement techniques [15]. It is particularly applicable in validating CFD models and exploring the knowledge of charge movement, combustion, and combustion product formation. However, it is worth noting the requirements for optical access design. For laser methods, at least two sight glasses are required.

Although optical engines have some advantages, they have significant limitations in terms of speed and load. The use of a transparent cylinder, most often made of quartz or sapphire, substantially affects the design of the piston-cylinder gasket. Unconventional sealing systems made of polyamide or graphite are used for this purpose. As a result, it is possible to eliminate a lubricating medium that adversely affects the quality of the obtained image. In addition, modification of the piston design involves additional mass, significantly increasing the inertia forces [17].

Johansson et al. [18] when carrying out a study on the effect of supercharging on the combustion and emissions of SGDI engine, used fully transparent optical engine and TSCE also called full metal engine with a displacement of 475 cm^3. The tests were conducted at 5 points with a maximum engine speed of 2000 rpm and a load of 4 bar BMEP. A problem was observed in the use of the optical engine due to the impossibility of obtaining steady-state conditions because of the short time available for adjusting the control parameters. The mentioned engine should be operated for a short time to minimize the risk of mechanical damage. Therefore, the advantages of both engines were combined, and TSCE engine was used for emission measurements and the OSCE engine for visualization of the combustion process.

In another study [19], a light-duty full metal engine was compared with an optical engine allowing optical access to the combustion chamber from the piston crown side under the same operating conditions. In these studies, special attention was paid to the thermodynamic aspect related to the significant differences in thermal conductivity of the materials used [20]. The results indicate a significant effect of using different materials on the heat flow characteristics. Measurements of the piston bottom temperature near the TDC by laser-induced phosphorescence indicate about 110°C higher temperature for the optical piston at 2 bar IMEP. Differences in the thermal state of the system result in different thermodynamic parameters in the cylinder. The authors point out the requirement to control the thermodynamic state of the combustion chamber walls to increase the convergence of results with full metal engines.

The considerable difficulties associated with the use of optical engines have resulted in thermodynamic engines in a wide range of applications. Current commercial sales of single cylinder research engines, among others, include AVL, Ricardo and FEV. AVL points to developing benches equipped with large single cylinder research engines in a modular approach that provides great flexibility. Outlining four basic platforms allow for engines with cylinder diameters of 150–520 mm [21]. In terms of smaller engines [22] three series are offered: 540 dedicated to passenger cars, 580 for Light duty engines and 530 for heavy duty engines. Ricardo, on the other hand, offers four engine types for different purposes [23]. Starting with the Hydra model for passenger car applications, the Proteus 300 for HD engines, the Atlas II for marine off-highway and power generation applications, and the last one, the Prometheus, with a piston diameter of 200–300 mm and maximum stroke of 1500 mm. FEV also offers designs with a wide range of cylinder diameters (65 to 530 mm) [24].

A relatively easy way to modify the single cylinder research engine that this paper uses is an effective tool for advanced engine research [25]. For example, for the study of knocking combustion phenomena, an AVL 5402 research engine originally operating as CI mode with a centrally located injector was modified. As a result, the engine was converted to SI mode with a PFI injection system and a circular ring was placed under the cylinder head equipped with four spark plugs and four pressure sensors mounted radially [26]. Subsequently, the Ricardo Hydra engine was modified for HCCI Combustion. This research used rebreathe style camshaft, piston coating and heat flux probes assembled in cylinder head [27]. Grabner et al. redesigned the AVL 5403 engine to compare two central and side injector placement positions during E85 and gasoline combustion [28]. It is also popular to modify research engines to burn gaseous fuels in a mono fuel or dual fuel configuration [29, 30].

4. Modernization concept

The primary responsibility for proper engine operation is the charge exchange system, i.e. intake and exhaust valve lift and timing. Proper control of the opening/closing of the inlet and exhaust system directly influences the internal combustion engine parameters such as power, torque, fuel consumption, and exhaust emissions. The first systems enabling optimization of the charge exchange process were developed in the early 1980s. Subsequent generations of these systems have concerned the use of both inlet and outlet valve opening control.

In this project it was decided to use a less popular system of variable valve timing control, which is used in Lexus vehicles. In order to implement variable intake valve timing in a single-cylinder research engine, an electric motor with a ±20º control range (total control range is 40º) was implemented. The VVT-iE (Variable Valve Timing-intelligent Electric) system allows smooth adjustment of the inlet valve opening using only an electric signal for control. The use of an electric motor (instead of a hydraulic or mechanical system) allows the system to operate effectively both at low temperatures and at low engine speeds with low oil pressure. The adopted Lexus solution uses a second generation actuator combined with a planetary gearbox (Fig. 4).

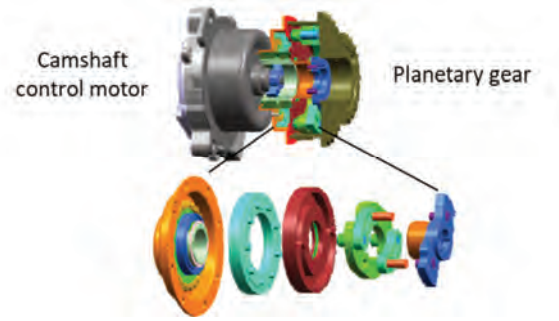

Fig. 4. Elements of the applied variable phase execution system [31]

An additional advantage of using electrical variable camshaft phasing control is the relatively small upgrade to the current timing system of the test engine. The scheme of acceleration and deceleration of the timing phases in the applied system is shown in Fig. 5.

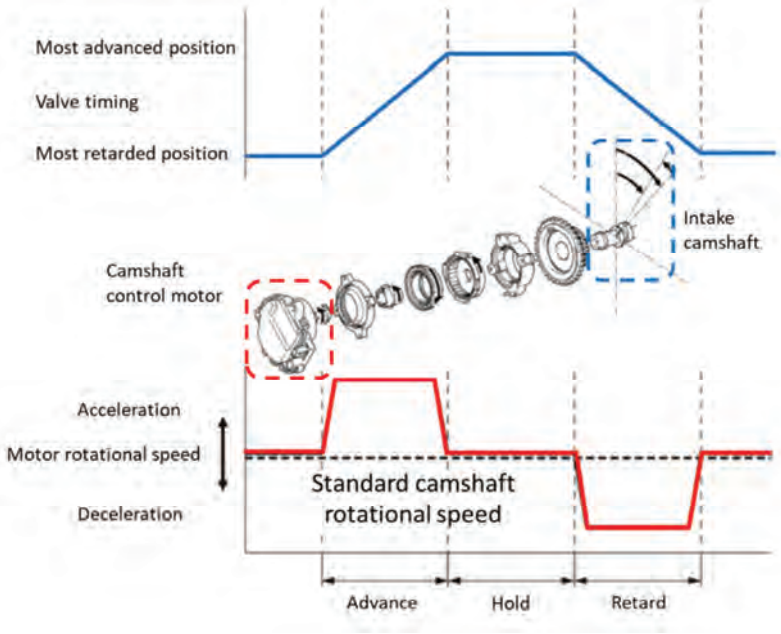

Fig. 5. Relationship between electric motor speed and advance and retard timing [34]

The camshaft control motor consists of a motor that operates the camshaft control actuator in the advance or retard direction, an EDU that controls the rotational condition of the motor and a Hall IC type rotational sensor that detects the current shaft speed. The motor is a brushless type DC motor installed in the engine front cover in front of the camshaft control actuator. The axis of the electric motor coincides with the axis of the intake shaft (Fig. 5). In accordance with the target intake shaft position, the ECM transmits the motor rotational speed instruction signals and the motor rotational direction instruction signals to the EDU. The EDU drives the motor to rotate the intake camshaft in advance or retard direction based on these signals. To advance, the electric motor speed becomes faster than the camshaft speed. To retard, the motor rotational speed becomes slower than the camshaft rotational speed. Depending on the operating condition of the internal combustion engine, the electric motor can operate in two directions. As the advance signals from the ECM cause the motor to operate at a higher speed than the camshaft, the camshaft gear rotates in the direction shown in the illustration via the reduction unit. This rotation causes the intake camshaft coupled with the camshaft gear to rotate in the advanced direction. As the retard signals from the ECM cause the motor to run slower than the camshaft, the camshaft gear rotates in the direction shown in the illustration via the reduction unit. This rotation causes the intake camshaft coupled with the camshaft gear to rotate in the retard direction.

The ability to independently control the timing phases using an electric motor creates opportunities for new research on the presented experimental engine.

5. Recovery of OEM cylinder head geometry

5.1. Optical scanning

Due to the modernization of the research engine in operation, it was necessary to make a 3D model of the research engine cylinder head equipped with a spark jet ignition system [35, 36] using only non-destructive methods. Therefore, two non-contact measurement methods were used. The first stage consisted of optical scanning of the outer planes using the ATOS II Triple Scan measurement system. Due to its accuracy and versatility, this system is used in industry and scientific institutions [37]. Using the laser triangulation method (used in the discussed cylinder-head reconstruction method), the measuring system consists of a laser light source displayed as a line, the measuring object, and a camera as a photosensitive element. Working with an overhead projector, stereoscopic cameras capture three views of an object within a single measurement. This technology requires fewer scans, providing higher quality data even when scanning shiny surfaces or complex geometric figures. Optical scans were realized both for the manufactured test engine cylinder head and the individual components mounted in the system (Fig. 6 and 7) and the location of the cylinder head on the engine (Fig. 8).

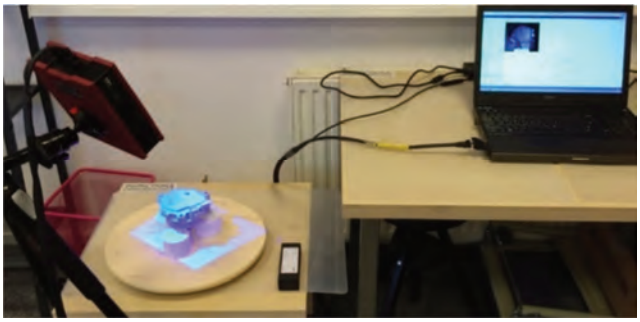

Fig. 6. Optical scanning process of an camshaft control motor using GOM's ATOS Core

The ATOS measuring system uses the measurement and projection method developed by Gesellschaft für Optische Messtechnik (GOM). The use of blue light technology makes it possible to carry out measurements regardless of

the lighting conditions. The two CCD cameras used realise approx. five million measuring points in an interval of a few seconds. The projector of the measurement head projects the sequence of stripes on the measured object (Fig. 9), while the CCD cameras record their course. By solving the optical transformation equations, the system calculates the coordinates for each camera pixel with high accuracy. The result of a single measurement is a point cloud that unambiguously reflects the scanned surface. The measurement is saved in STL (Standard Triangle Language) format, which needs to be converted into a 3D project.

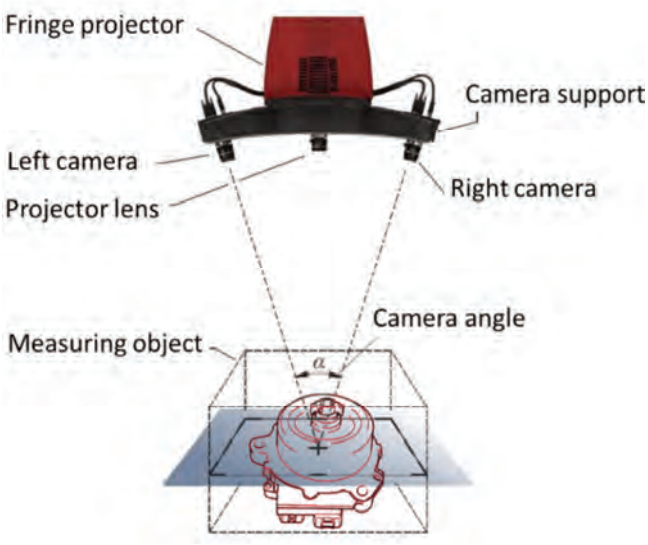

Fig. 7. Scanning process diagram

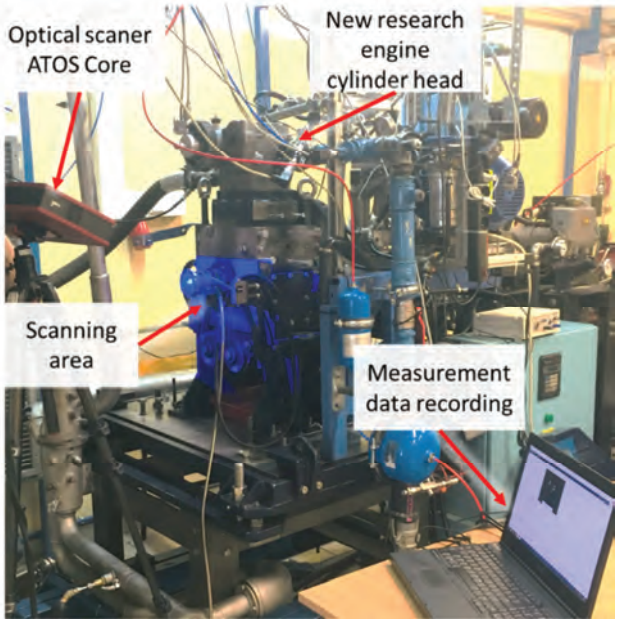

Fig. 8. Optical scanning process of area of driveline

5.2. Tomographic scanning

The single cylinder test engine whose cylinder head has been modified is equipped with a closed cooling system. It is possible to control the temperature of the cooling liquid on the test bench. The previous step of optical scanning of the cylinder head does not provide information about the structure's internal spaces, the completion of which is crucial to ensure the correct operation of the system. In order to determine the internal areas of the cooling channels as well as the inlet and outlet channels, a CT scan was performed.

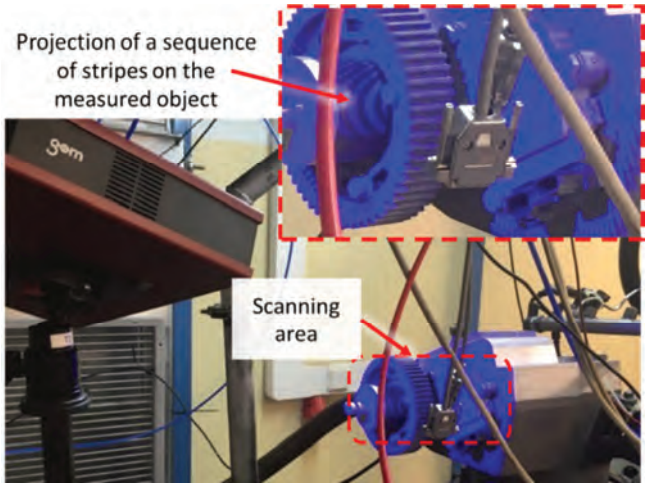

Fig. 9. Projection of a sequence of stripes on the measured object

Computed tomography is one of the noninvasive diagnostic methods to obtain a cross-section through a component. Several tomographic techniques are known [38]:

- x-rays,
- two-dimensional ultrasonography (USG 2D),
- computed tomography(CT),
- magnetic resonance tomography (MRT, NMR – nuclear magnetic resonance),
- positron emission tomography (PET),
- single photon emission tomography (SPECT),
- optical coherent tomography (OCT).

In the diagnostic technique, mainly computed tomography is used to obtain spatial images (3D) while scanning the object from different directions. Figure 10 shows the cylinder head of a GE Phoenix CT scanner. The v/Tome/x m 300 type tomograph with a maximum lamp power of 500 W with 300 kV enables high accuracy examinations up to 0.5 µm using a 180 kV lamp. Mass of tested elements cannot exceed 50 kg. The maximum dimensions of tested detail are 500 × 500 × 600 mm.

In order to reconstruct the image, it is necessary to use the analytical method. This method gives the best measurement results but requires large computational capacities. The two-dimensional Fourier analysis method uses a fast Fourier transform to describe the absorption profiles obtained. Each projection is transformed to obtain the absorption coefficient in each voxel. The absorption coefficients are converted into CT numbers, also called Hounsfield HU units [35].

$$1\ \mathrm{HU} = \mathrm{K}\frac{\mu_\mathrm{p}-\mu_\mathrm{w}}{\mu_\mathrm{w}} \tag{1}$$

where: K – image gain constant (individual for each CT scanner), µp – pixel absorption coefficient, µw – water absorption coefficient (reference value).

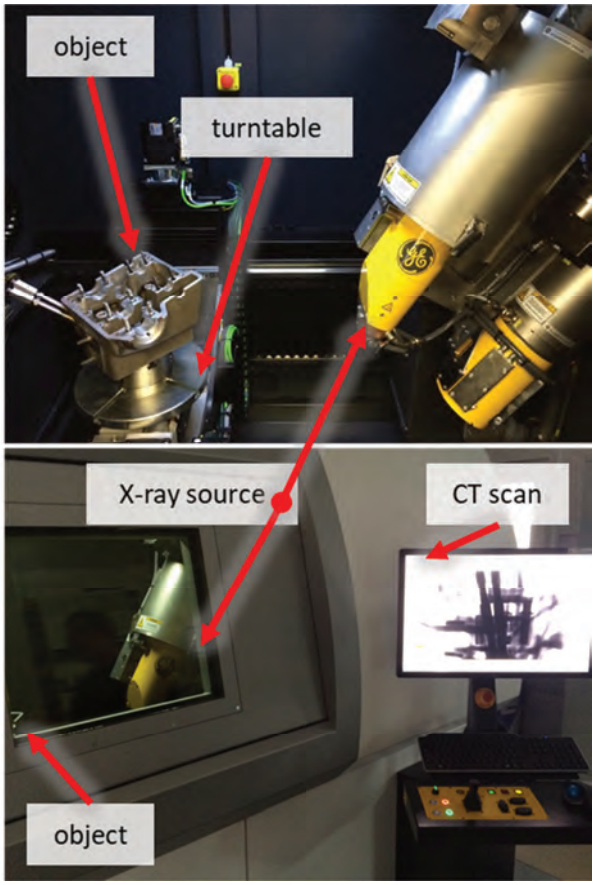

Fig. 10. Location of the research engine head in a GE tomographic scanner model V/Tome/x m

The range of Hounsfield units for CT is –1000 to +4000, and it allows the image to be represented in shades of grey. Only 256 gray levels are used in practice, which is a selected slice of the CT number value. It makes it possible to observe the image with high contrast, thus enabling the interpretation of the measurement result (Fig. 11).

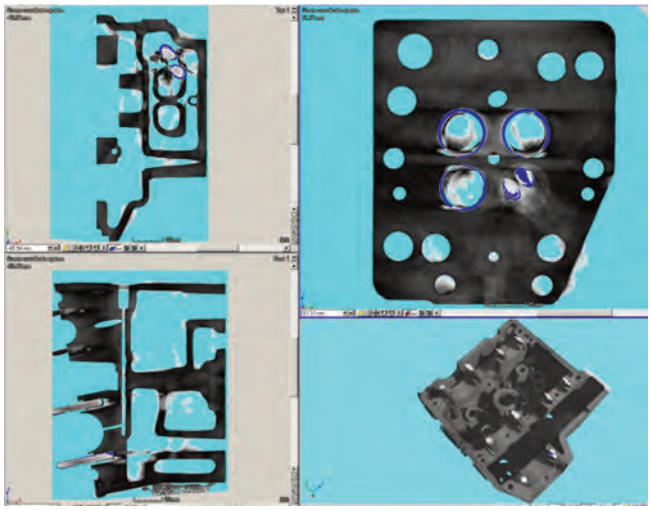

Fig. 11. View of the test engine headspace during tomographic examination

In order to reproduce structural elements, high accuracy of the internal structure of the object is required. To increase the measuring accuracy, the method with a linear detector is used (Fig. 10 and 12). This method consists in reducing the radiation beam by means of an aperture to a flat beam. Using a linear detector and rotating 360º, a flat X-ray image of a single slice of the test object is obtained. In order to obtain a spatial image of the entire workpiece, it is necessary to move the object in the vertical plane additionally. During measurements of the cylinder head, the measurement resolution was 2 mm in the Y-axis, allowing recognition of the geometries necessary for the design of the cylinder head internal volumes (Fig. 13).

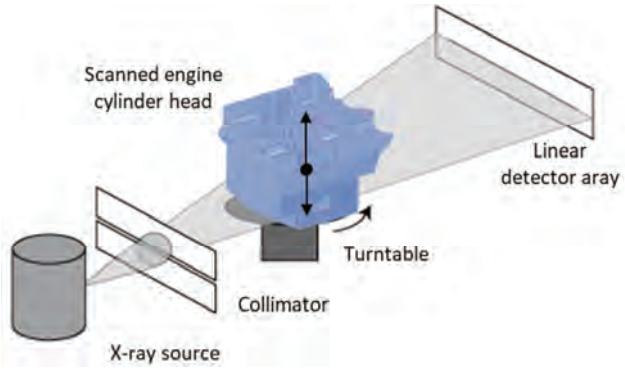

Fig. 12. Methodology tomographic inspection with linear detector

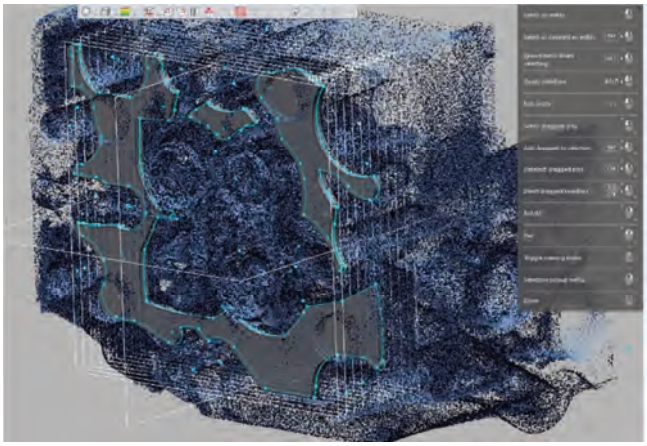

Fig. 13. Design of the internal spaces of the cooling system – view of the measurement point cloud obtained from the tomographic scanning process

6. Reverse modeling and modernization

The performed measurements (described in sections 5.1 and 5.2) allowed making a 3D model of the test engine's reference cylinder head. The finished model was compared with the measurement file, and deviations were determined (Fig. 14).

The use of the VVT-iE system resulted in an extension of the cylinder head housing by 99.6 mm towards the valve train (Fig. 15). As a result, design changes were made to the dry belt drive of the valve train. In order to avoid unfavourable changes in the force distribution on the main bearings of the crankshaft, it was decided to produce an aluminium box equipped with an intermediate shaft (Fig. 16), avoided locating the gear on the extended part of the crankshaft. It could lead to excessive wear of the main sliding bearings and crankshaft fatigue wear.

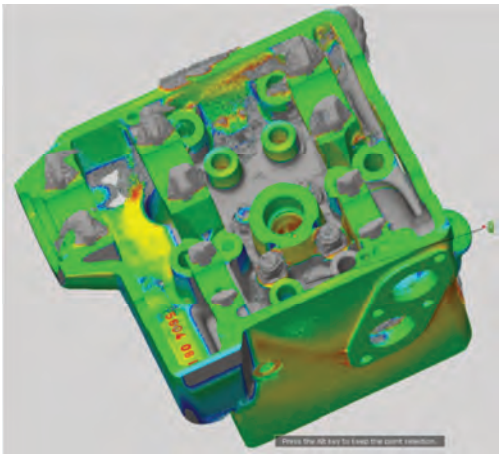

Fig. 14. Comparison of the developed model with the image obtained by scanning along with the specified deviations

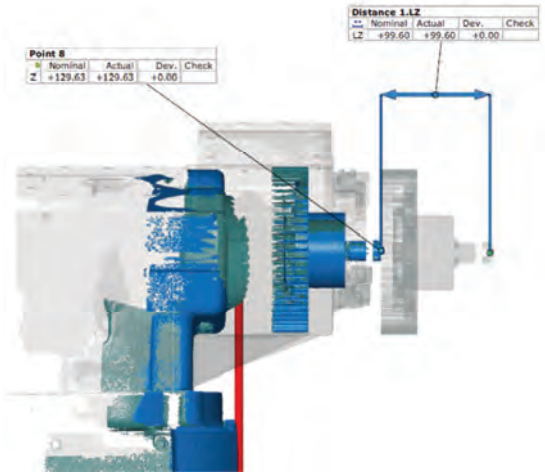

Fig. 15. Visualization of reference and modified cylinder head length comparison based on optical scan results

The design of the new valve train is based on the use of two timing belts instead of one with no change in the timing ratio. Drive is transmitted from crankshaft to intermediate shaft, which in turn drives the exhaust camshaft. The intermediate shaft is supported on both sides by ball roller bearings. Both belts are equipped with an independent tensioning roller system. The view of the intermediate shaft assembled is shown in Fig. 16, and the location on the engine is shown in Fig. 17.

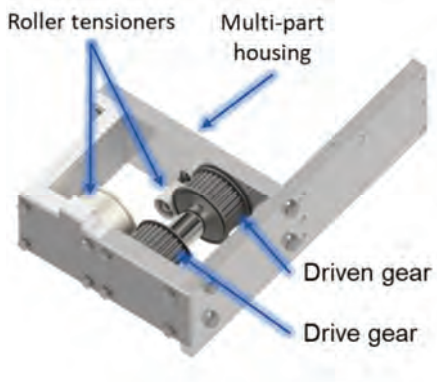

Fig. 16. View of intermediate shaft box

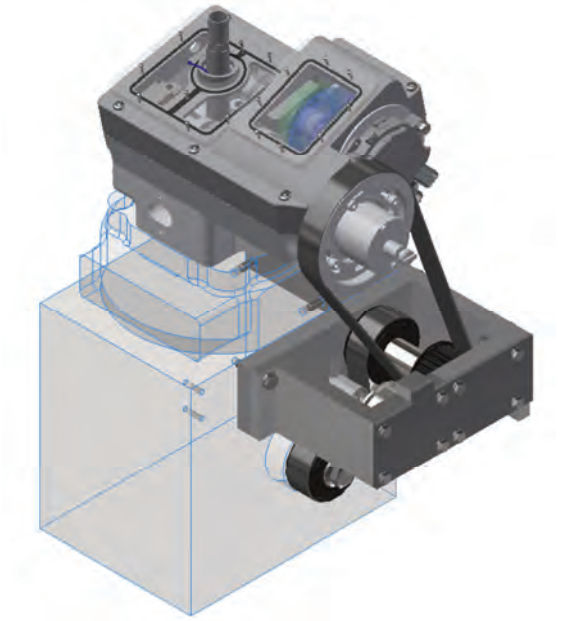

Fig. 17. The CAD model of modified cylinder head and the valve train system

7. Cylinder head validation and future research steps

The new components were mounted on a test bench. The cylinder head was subsequently subjected to a leak test. The coolant and oil were forced to flow using an independently controlled AVL 577 system. The fluids were gradually heated up to a temperature of 90°C.

In the next step of the process, the valve timing diagram was created, taking into account two extreme positions of the intake camshaft (Fig. 18 and 19). The valve timing diagram shows the delay and advanced phase of intake combined with a control range of 47°CA and valves opening length of 203°CA. In addition, the position of the exhaust shaft is fixed. The graph also shows the duration of the opening of the inlet and outlet valves. Moreover, the overlapping duration has been pointed. The opening characteristics of the valves will be individually adjusted at a later stage to the specifics of the tests performed.

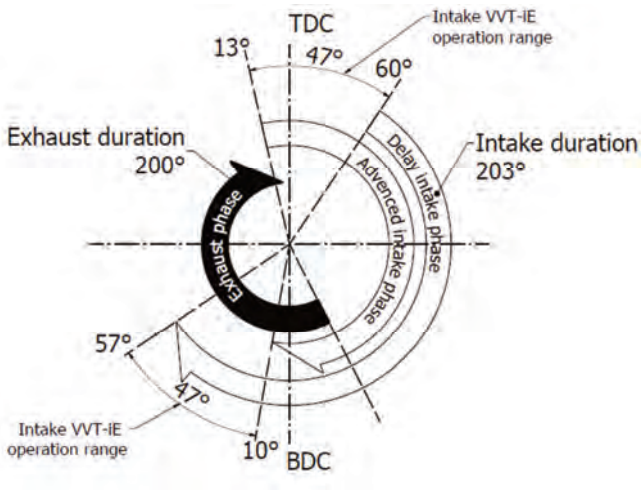

Fig. 18. Valve timing diagram after cylinder head modification

The last step was to run the engine in motored cycles with a fuel cut. The engine was run at 1500 rpm engine speed, during which the cylinder pressure was recorded for two extreme positions of the intake camshaft (Fig. 19). Position 1 is the maximum intake valve opening advance, while position 2 is the maximum retardation. It resulted in higher peak pressure values for the first intake position due to higher cylinder filling. The readings of the airflow meter located in the intake system per mass of air in the cylinder are 318 mg of air per cycle for position 1 and 302 mg for position 2. The repeatability of the engine's operation from cycle to cycle is satisfactory in both cases COV_{pp} (pp – peak pressure) does not exceed 0.3% of 1000 cycles, which eliminates any irregularities.

The development and implementation of the cylinder head equipped with the described system of electronically controlled valve timing phases allow conducting cycle-by-cycle research for precise analysis of transients. Recording the combustion process during a controlled change of the cylinder filling strategy will allow more accurate identification of combustion systems dedicated to hybrid powertrains.

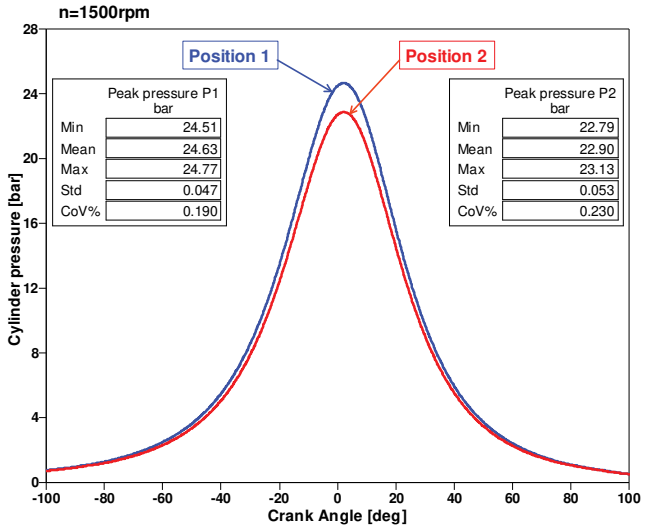

Fig. 19. Cylinder pressure curves for two different intake camshaft modes

Figure 20 shows the waterfall diagram of the cylinder pressure waveform for 15 cycles of engine operation. The position of the inlet camshaft relative to the crankshaft was changed between extreme positions. It should be noted that the repositioning process occurs over several cycles, during which combustion parameters can be monitored.

The content presented in this paper deals with the manufacturing process of an AVL 5804 engine cylinder head modified for research purposes. The manufacturing process included:

- making structural assumptions,
- reconstruction of the original cylinder head geometry using advanced measurement techniques,
- carrying out the design phase,
- manufacture of the cylinder head with equipment,
- starting the modified engine.

The result of the work is a modified engine design that allows research on low-emission combustion systems using the VVT-iE technology. In the future, the test stand will be used for comprehensive analysis of the combustion process and validation of computer simulations, the course of which is presented in Fig. 21.

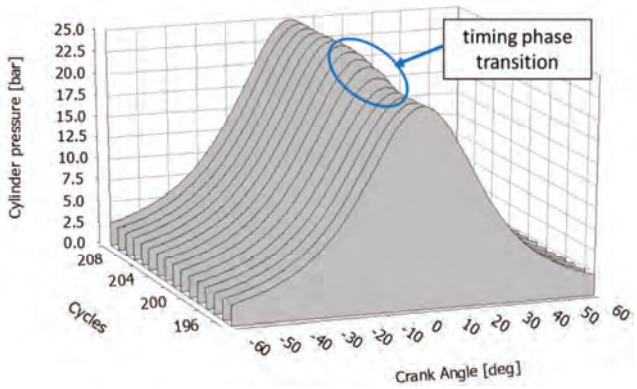

Fig. 20. Waterfall diagram showing the change in compression pressure during changes in the timing system adjustment

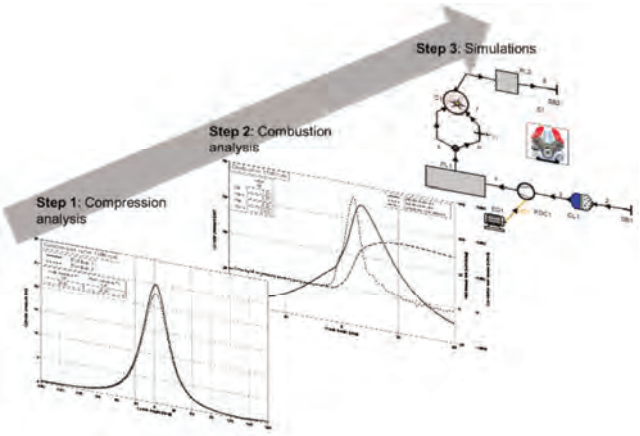

Fig. 21. Graphical representation of the proceedings related to the further development of the test bench.

8. Conclusion

The main aims of the performed studies and work described in this paper were to enhance the research possibilities of the 1-cylinder test engine for its operation with variable valve timing and to study the possibilities and restrictions of reverse engineering methodology in modernisation of real engine. Both tasks are successfully fulfilled and completed.

It was proven that 3D-scanning technology makes it possible to generate the fully useful geometrical and constructional project even than when the internal structure of the engine part is very complicated and completely unknown. The generated in this way the construction drawings of cylinder head made it possible to conduct redesigning of it, prepare for the casting process and to final mechanical turning and milling post processing. In this way this methodology has been positively verified.

Finally, the new cylinder head, modernised, equipped with variable valve timing and ready to operate on the 1-cylinder research engine has been delivered, proved and validated.

The examined methodology of reverse engineering has been proven for cylinder head with very complicated internal structure. This method can be then satisfactory applied in reconstructing of engines or machines parts or elements when the construction documentation is not available and other method of non-destructive recognition of its structure is not available.

Acknowledgements

This work was supported by the EU – Horizon 2020 [grant number 652816]. The authors of this paper would also like to acknowledge all the people who supported the various stages of designing the prototype cylinder head, especially the employees of the companies and institutions:

– 3D Team – company providing optical scans
– ITWL – Air Force Institute of Technology – cooperation in performing CT scans
– 4p Engineering Office – the company responsible for the cylinder head casting
– Kazimieruk Precision Parts – company realizing the cylinder head machining
– Świątek – Polish manufacturer of camshafts – maker of prototype camshafts
– FNS Special Tools Factory
– Parawowscy AMP – Engine parts producer – valve manufacturer
– Jacek Tomaszewski – The company responsible for fitting valve seats

Additional information

Further information and videos from our research are available on YouTube channel: **PUT Powertrain Lab**

Indexes

BDC	bottom dead center
BMEP	brake mean effective pressure
CAD	computer aided design
CCD	charge-coupled device
CFD	computational fluid dynamics
CT	computed tomography
CoV	coefficient of variation
GHG	greenhouse gas
HCCI	homogeneous charge compression ignition
HD	heavy duty
ICE	internal combustion engine
IMEP	indicated mean effective pressure
RCEM	rapid compression expansion machine
MCE	multi cylinder engines
OSCE	optical single cylinder engines
PFI	port fuel injection
SGDI	spray guided direct injection
SI	spark ignition
STL	standard triangle language
TJI	turbulent jet ignition
TSCE	thermodynamic single cylinder engine
TDC	top dead center
VCR	variable compression ratio
VVT-iE	variable valve timing-intelligent electric

Bibliography

[1] SHERRY, C. Internal combustion engine – the road ahead. *Efficient Manufacturing*. 2019, **10**. https://issuu.com/publishi/docs/em_jan_2019

[2] REITZ, R.D., OGAWA, H., PAYRI, R. et al. IJER Editorial: The future of the internal combustion engine. *International Journal of Engine Research*. 2020, **21**(1), 3-10. https://doi.org/10.1177/1468087419877990

[3] NAPOLITANO, P., FRAIOLI, V., GUIDO, F. et al. Assessment of optimized calibrations in minimizing GHG emissions from a dual fuel NG/diesel automotive engine. *Fuel*. 2019, **258**, 115997. https://doi.org/10.1016/j.fuel.2019.115997

[4] ZACHAROF, N., DOULGERIS, S., MYRSINIAS, I. et al. A methodology for monitoring on-road CO_2 emissions compliance in passenger vehicles. *SAE Technical Paper* 2020-37-0034. 2020. https://doi.org/10.4271/2020-37-0034

[5] FRIEDL, H., FRAIDL, G., KAPUS, P. Highest efficiency and ultra low emission – internal combustion engine 4.0. *Combustion Engines*. 2020, **180**(1), 8-16. https://doi.org/10.19206/CE-2020-102

[6] LIU, H., ZHANG, H., SHI, Z. et al. Performance characterization and auto-ignition performance of a rapid compression machine. *Energies*. 2014, **7**, 6083-6104. https://doi.org/10.3390/en7096083

[7] KYRTATOS, P., BOLLA, M., BENEKOS, S. et al. Advanced methods for gas-prechamber combustion research and model development. *16th Conference The Working Process of the Internal Combustion Engine*. Graz 2017.

[8] ELGOWAINY, A., HAN, J., WARD, J. et al. Current and future United States light-duty vehicle pathways: cradle-to-grave lifecycle greenhouse gas emissions and economic assessment. *Environmental Science & Technology*. 2018, **52**(4), 2392-2399. https://doi.org/10.1021/ acs.est.7b06006

[9] JOSHI, A. review of vehicle engine efficiency and emissions. *SAE International Journal of Advances and Current Practices in Mobility*. 2019, **1**(2), 734-761. https://doi.org/10.4271/2019-01-0314

[10] STUHLDREHER, M., KARGUL, J., BARBA, D. et al. Benchmarking a 2016 Honda Civic 1.5-liter L15B7 turbocharged engine and evaluating the future efficiency potential of turbocharged engines. *SAE International Journal of Engines*. 2018, **11**(6), 1273-1305. https://doi.org/10.4271/2018-01-0319

[11] WISŁOCKI, K. Endoscopic observations of flame propagation in combustion chamber of an DI Diesel engine with mixture partial homogenisation. *Combustion Engines*. 2007, **128**(1), 43-58. https://doi.org/10.19206/CE-117332

[12] PIELECHA, I., WISŁOCKI, K., CIEŚLIK, W. et al. Analysis of a dual-fuel combustion engine fueled with diesel fuel and CNG in transient operating conditions. *SAE Technical Paper* 2016-01-2305. 2016. https://doi.org/10.4271/2016-01-2305

[13] BUESCHKE, W., SZWAJCA, F., WISLOCKI, K. Experimental study on ignitability of lean CNG/air mixture in the multi-stage cascade engine combustion system. *SAE Technical Paper* 2020-01-2084. 2020. https://doi.org/10.4271/2020-01-2084
[14] WINKELHOFER, E., HOPFNER, W. Optical single cylinder engines in engine research and development. *Combustion Engines*. 2013, **152**(1), 71-78. https://doi.org/10.19206/CE-117014
[15] MITTAL, M., MEHTA, P. Design features of optically accessible engines for flow and combustion studies – a review. *SAE Technical Paper* 2018-01-1775. 2018. https://doi.org/10.4271/2018-01-1775
[16] BOWDITCH, F.W. A new tool for combustion research – a quartz piston engine. *SAE Technical Paper* 610002. 1961. https://doi.org/10.4271/610002
[17] CLASÉN, K., DAHL, A. Development of next generation optical engines concept design and validation by numerical methods. *Chalmers University of Technology*. Göteborg 2016. https://odr.chalmers.se/bitstream/20.500.12380/247265/1/247265.pdf
[18] JOHANSSON, A., DAHLANDER, P. Experimental investigation of the influence of boost on combustion and particulate emissions in optical and metal SGDI-engines operated in stratified mode. *SAE International Journal of Engines*. 2016, **9**(2), 807-818. https://doi.org/10.4271/2016-01-0714
[19] KASHDAN, J., THIROUARD, B. A comparison of combustion and emissions behaviour in optical and metal single-cylinder diesel engines. *SAE International Journal of Engines*. 2009, **2**(1), 1857-1872. https://doi.org/10.4271/2009-01-1963
[20] RICHMAN, R., REYNOLDS, W. The development of a transparent cylinder engine for piston engine fluid mechanics research. *SAE Technical Paper* 840379. 1984. https://doi.org/10.4271/840379
[21] KÖGL, R., RUSTLER, M., HIRSCHL, G. New single-cylinder engine generation from AVL. *MTZ industrial*. 2018, **8**, 38-43. https://doi.org/10.1007/s40353-018-0010-0
[22] AVL Single Cylinder Research Engines – AVL product description. Graz 2020.
[23] Ricardo Single-Cylinder Research Engines. Combustion research and mechanical testing of engine parts for diesel, gasoline and alternative fuels. https://automotive.ricardo.com/engines/single-cylinder-research-engines
[24] One cylinder, a hundred applications. https://magazine.fev.com/en/fev-single-cylinder-engines-important-development-tools-combustion-optimization/
[25] MENZEL, F., SEIDEL, T., SCHMIDT, W. et al. Single-cylinder engine as a tool for developing new combustion processes. *MTZ Worldwide*. 2006, **67**, 6-9. https://doi.org/10.1007/BF03227827
[26] SHI, H., UDDEEN, K., AN, Y. et al. Experimental study on knock mechanism with multiple spark plugs and multiple pressure sensors. *SAE Technical Paper* 2020-01-2055. 2020. https://doi.org/10.4271/2020-01-2055
[27] MOSER, S., O'DONNELL, R., HOFFMAN, M. et al. Experimental investigation of low cost, low thermal conductivity thermal barrier coating on HCCI combustion, efficiency, and emissions. *SAE Technical Paper* 2020-01-1140. 2020. https://doi.org/10.4271/2020-01-1140
[28] GRABNER, P., EICHLSEDER, H., ECKHARD, G. Potential of E85 direct injection for passenger car application. *SAE Technical Paper* 2010-01-2086. 2010. https://doi.org/10.4271/2010-01-2086
[29] SZWAJCA, F., WISŁOCKI, K. Thermodynamic cycles variability of TJI gas engine with different mixture preparation systems. *Combustion Engines*. 2020, **181**(2), 46-52. https://doi.org/10.19206/CE-2020-207
[30] PIELECHA, I., WISŁOCKI, K., CIEŚLIK, W. et al. Application of IMEP and MBF50 indexes for controlling combustion in dual-fuel reciprocating engine. *Applied Thermal Engineering*. 2018, **132**, 188-195. https://doi.org/10.1016/ j.applthermaleng.2017.12.089
[31] HATTORI, M., INOUE, T., MASHIKI, Z. et al. Development of variable valve timing system controlled by electric motor. *SAE International Journal of Engines*. 2009, **1**(1), 985-990. https://doi.org/10.4271/2008-01-1358
[32] BACH, C. Record efficiency for a gas engine. https://www.empa.ch/web/s604/gason
[33] Reactive Flows and Diagnostics. https://www.rsm.tu-darmstadt.de/home_rsm/members_rsm/members_details_162688.en.jsp
[34] Camshaft control actuator. https://mytechdoc.toyota-europe.com (accessed on 01.03.2020).
[35] BUESCHKE, W., SKOWRON, M., SZWAJCA, F. et al. Flame propagation velocity in 2-stage gas combustion system applied in SI engine. *IOP Conference Series: Materials Science and Engineering*. 2018, **421**. https://doi.org/10.1088/1757-899X/421/4/042009
[36] BUESCHKE, W., SKOWRON, M., WISŁOCKI, K. et al. Comparative study on combustion characteristics of lean premixed CH_4/air mixtures in RCM using spark ignition and turbulent jet ignition in terms of orifices angular position change. *Combustion Engines*. 2019, **176**(1), 36-41. https://doi.org/10.19206/CE-2019-105
[37] Reverse engineering. https://reversesolutions.pl/inzy-nieria-odwrotna/ (accessed on 07.09.2021)
[38] KUŁASZKA, A., CHALIMONIUK, M., WIECZOROWSKI, M. The assessment of defects and discontinuities in weldings by means of computed tomography. *Przegląd spawalnictwa*. 2015, **87**(12). http://www.pspaw.pl/index.php/pspaw/article/view/541/546

Wojciech Cieślik, DEng. – Faculty of Civil and Transport Engineering, Poznan University of Technology
e-mail: *wojcich.cieslik@put.poznan.pl*

Filip Szwajca, MEng. – Faculty of Civil and Transport Engineering, Poznan University of Technology.
e-mail: *filip.szwajca@put.poznan.pl*

Prof. Krzysztof Wisłocki, DSc., DEng. – Faculty of Civil and Transport Engineering, Poznan University of Technology.
e-mail: *krzysztof.wislocki@put.poznan.pl*

Article citation info:
ZACHAREWICZ, M., KNIAZIEWICZ, T. Model tests of a marine diesel engine powered by a fuel-alcohol mixture. *Combustion Engines*. 2022, **189**(2), 83-88. https://doi.org/10.19206/CE-143486

Marcin ZACHAREWICZ
Tomasz KNIAZIEWICZ

Combustion Engines
Polish Scientific Society of Combustion Engines

Model tests of a marine diesel engine powered by a fuel-alcohol mixture

ARTICLE INFO

Received: 13 July 2021
Revised: 29 October 2021
Accepted: 30 October 2021
Available online: 2 November 2021

The paper presents the results of model and empirical tests conducted for a marine diesel engine fueled by a blend of n-butanol and diesel oil. The research were aimed at assessing the usefulness of the proprietary diesel engine model in conducting research on marine engines powered by alternative fuels to fossil fuels. The authors defined the measures of adequacy. On their basis, they assessed the adequacy of the mathematical model used.

The analysis of the results of the conducted research showed that the developed mathematical model is sufficiently adequate. Therefore, both the mathematical model and the computer program based on it will be used in further work on supplying marine engines with mixtures of diesel oil and biocomponents.

Key words: *model tests, diesel engine, model adequacy assessment, alternative fuels, diagnostics*

1. Introduction

In recent years, a lot of emphasis has been put on the issue of air pollution with toxic compounds, and significant carbon dioxide emissions. It is reflected in the increasingly restrictive regulations on the emission of toxic compounds in transport.

Another important issue is the limited availability of fossil fuels. It can be expected that their prices will rise in the foreseeable future. This will result in an increase in the cost of people, and goods transportation.

One of the key modes of transportation is sea transport. This is mainly due to its versatility (practically any type of cargo, and the possibility of transporting bulky goods), and relatively low costs. For watercraft dedicated to the transport of people, and goods, the average lifetime is 29 years [15]. It follows, that most of the ships used in the world are equipped with reciprocating engines that do not meet the current stringent emission standards for toxic compounds. In most cases, these are two-stroke reciprocating engines adapted to run on light, and residual fuel. This results in the need to search for methods to reduce the emission of toxic compounds, and greenhouse resulting from the combustion of fossil fuels that are hydrocarbons. One of the methods of reducing the combustion of fossil fuels is the use of mixtures of the above-mentioned fuels, and broadly understood biocomponents. One of such biocomponents is n-butyl alcohol.

The paper presents the results of empirical, and model tests of a ship engine powered by a mixture of diesel oil, and n-butyl alcohol with volume fractions of 5, 10, and 15% n-butyl alcohol and 95, 90, and 85% diesel oil, respectively. The authors did not focus on residual fuels due to increasing restrictions on their use. This is mainly due to the fact that they are contaminated with sulfur compounds. The results of the research were presented in a statistical analysis, the purpose of which was, among others, to verify the proprietary engine model in relation to the real object. Positive verification should allow the model to be used in further work on alternative methods of powering marine engines. This will significantly reduce the research time, and cost.

The issue of the use of biocomponents in fuels is dealt with by many centers, both in Poland and abroad. Most of the research concerns fuels used in motor transport. For which the use of mixtures of fossil fuels and biocomponents has been the norm for many years [16, 18]. A large part of the research concerns their use in automotive spark ignition engines [2, 5]. Research has also been carried out on the use of mixtures to power compression ignition engines [6, 9]. Considerable interest (reflected in the number of publications) in the use of biocomponents in fuels used in road and rail transport results from European and national regulations [15, 16]. However, there are few publications on the use of mixtures of fossil fuels and biocomponents in shipbuilding. Research on reducing the emission of toxic and greenhouse compounds (resulting from the combustion of fossil fuels) in the shipbuilding industry is enforced by the IMO (the so-called Sulfur Directive) and the European Union regulations, which impose restrictive sulfur oxide emission limits [4, 14].

2. Research methodology

The first stage of research was to develop a program for their implementation. It was presented in the form of an algorithm containing all the anticipated stages of the research [3, 11, 17] (Fig. 1).

3. Model of the reciprocating diesel engine

According to the research implementation program presented (Fig. 1), the first stage of the research was to develop a model of a reciprocating diesel engine [10, 11]. It was decided to use the model developed by the authors for the needs of diagnostic tests. It allows for the implementation of tests for a four-stroke reciprocating diesel engine. It is possible to conduct tests for both supercharged, and undercharged engines powered by virtually, any fuel containing hydrogen, carbon, nitrogen, oxygen, and sulfur. The engine may have a V-shaped, or linear arrangement of cylinders, and may contain from 1 to 8 cylinders. The model allows for any modification of the geometrical dimensions of the piston-crank system, i.e. cylinder diameter, connecting rod length, crankshaft crank length, and combustion chamber height. Moreover, it is possible to modify its structure in-

fluencing the parameters of heat exchange between the medium inside the cylinder, and the cooling liquid and air. In addition, it is possible to modify the injection advance angle, the number and diameter of the injector holes, the opening and closing angles of the intake, and exhaust valves, their cross-sectional areas, and a number of other engine operating parameters.

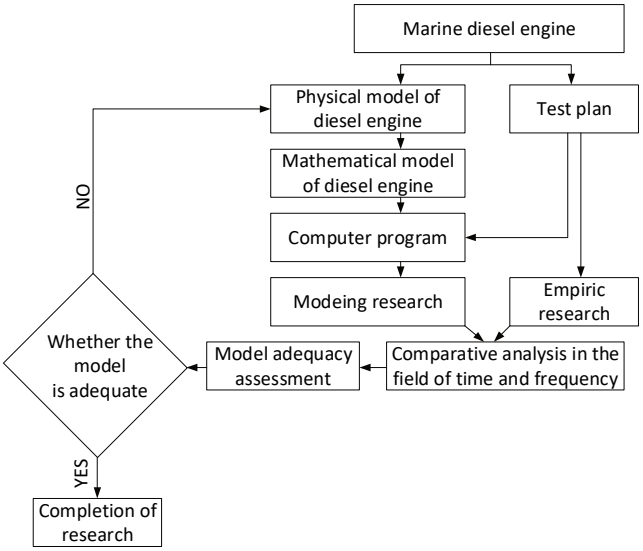

Fig. 1. Research program

The mathematical model of the marine engine, adopted for the purpose of the research, was assessed for adequacy during its development. The adequacy assessment consisted in conducting a comparative analysis of the selected measures for the modeled engine, and the real object. It was carried out in relation to laboratory engines installed in the Laboratory of the Engine Room Explitation – Sulzer engine type 6AL 20/24, and in the Laboratory of Marine Electrical Equipment – engine licensed from Leyland, type 6SW400. All tests were carried out on standard diesel fuel with mass fractions of 87% carbon, and 13% hydrogen. As a result of the research, it was found that the model is qualitatively, and quantitatively adequate [11, 13].

4. Research plan

According to the algorithm presented in Fig. 1, a research plan was developed. It included the test conditions, determined the engine operating parameters that were measured and recorded, and the concentration of the mixture of diesel oil and alcohol (n-butanol). It was assumed that the tests will be carried out on the SULZER 6Al 20/24 marine engine installed in the Laboratory of the Engine Room Exploitation. The engine is loaded with a drag torque by means of a Froude water brake Napier C045/C. The test conditions included the values of the angular velocity of the crankshaft, and the values of the engine load with the torque. It was assumed that tests will be carried out for the following rotational speed of the crankshaft: 600, 675 and 750 rpm. The adopted torque values are: 1, 2.80, 4.65 kNm. It has been assumed, that the measurements for each of the torque, and rotational speed values will be performed for the following mass concentration values of the fuel F75, and alcohol (n-butanol):

- 100% fuel, and 0% alcohol (mass fractions: 87% carbon, and 13% hydrogen),
- 85% fuel, and 15% alcohol (mass fractions: carbon 83.67%, hydrogen 13.09%, and oxygen 3.24%),
- 70% fuel, and 30% alcohol (mass fractions: carbon 80.34%, hydrogen 13.18%, and oxygen 6.48%).

It was assumed, that the following engine energy parameters will be measured during the tests:

- indicated pressure,
- crankshaft rotational speed,
- hourly fuel consumption,
- concentrations of: carbon monoxide, carbon dioxide, nitrogen oxides, and oxygen,
- location of the engine fuel rail,
- turbo speed,
- boost pressure,
- exhaust gas temperature at the exit from the engine cylinders, at the entrance, and exit of the turbine of the turbocompressor,
- cylinder supply air temperature (downstream of the water cooler),
- air volume flow supplied the engine.

Measurements of all the above-mentioned parameters, except for the indicated pressure, were carried out with the sampling frequency of 1 Hz, and a resolution of 12 bit. The indicated pressure was measured with a frequency of 10 kHz, and a resolution of 12 bits. On the basis of the indicated pressure measurement, the following were calculated: average indicated pressure, maximum combustion pressure, compression pressure, indicated power. The research plan is presented in Table 1.

Table 1. Research plan

Number of measure	600 rpm	1	2	3	4	5	6	7	8	9
	675 rpm	10	11	12	13	14	15	16	17	18
	750 rpm	19	20	21	22	23	24	25	26	27
n-butyl content [%]		0	13	26	0	13	26	0	13	26
Torque [kNm]		1			2.80			4.65		

An original device developed at the Polish Naval Academy was used to measure the indicated pressure. It uses the KISTLER type 7613B transducer. The crankshaft speed is measured with an inductive sensor (the model tests used the rotational speed of the crankshaft calculated on the basis of the indicated pressure measurements). Hourly fuel consumption was measured with a weighing device. The TESTO 350-Maritime analyzer was used to measure the concentration of carbon monoxide, carbon dioxide, nitrogen oxides, and oxygen. The measurement of the position of the engine's fuel rail was carried out using a proprietary device based on a linear potentiometer. The rotational speed of the turbocharger was measured with a magnetoelectric device. A strain gauge transducer was used to measure the boost pressure. Temperature measurements were made using thermocouples. The list of measured parameters, measuring ranges of the instruments used and the measurement accuracy are grouped in Table 2.

Table 2. Parameters of the measuring system of the SULZER engine, type 6AL 20/24

Parameter	Scope of measure.	Measuring accuracy [%]	Sampling frequency [Hz]	Converter type
Indicated pressure	25 MPa	0.1	20 000	piezoelectric
Crankshaft rotational speed	8 000 min^{-1}	0.1	1	inductive
Hourly fuel consumption	100 kg/h	1	[–]	gravimetric
Concentrations of toxic compounds	According to the specification of the TESTO 350-MARITIME device (all measurements meet the MARPOL Annex VI standard)			
Location of the fuel rail	100 mm	1	1	potentiometric
Turbocharger rotation speed	40 000 min^{-1}	0.5	1	magnetoelectric
The boost pressure	0.25 MPa	1	1	strain gauge
Exhaust gas temperatures	873 K	0.3	1	thermocouple
Air temperature	373 K	0.3	1	resistance
Air volume flow	2 600 m^3	1.5	1	Von Karman effect

5. Findings

In accordance with the proposed research program, both empirical, and model research were carried out in accordance with the described research plan. In the case of model tests, the number of parameters used to assess its adequacy was reduced (in relation to the measured parameters) to [11]: the value of the indicated pressure, and derivative parameters, as well as the excess air coefficient. On the other hand, indicated power, rotational speed, and boost pressure were input parameters to the mathematical model.

The adequacy of the mathematical model was assessed with the selection of the input parameters of the model, so that they correspond to the parameters of the modeled engine:

- connecting rod length,
- length of the crank,
- combustion chamber volume,
- cylinder diameter,
- material parameters used to calculate heat transfer,
- the mass of individual elements performing reciprocating and rotary motion,
- opening and closing angles of intake and exhaust valves,
- injection advance angle, ignition delay angle,
- the number and diameter of the injector holes,
- supercharging parameters.

Then, the measures used to assess the model adequacy were selected. As in the case of previous diagnostic tests [11, 12], these were:

- excess air factor λ,
- hourly fuel consumption Ge,
- measure K characterizing the similarity of indicated pressure courses, as a function of the crankshaft rotation angle [16].

Based on the experience obtained as a result of model, and empirical research (research for diagnostic purposes), it was assumed that the relative values of the measures should not exceed:

- 20% for the excess air ratio λ,
- 10% for hourly fuel consumption Ge.

On the other hand, the measure K should not reach a value greater than 10.

The value of the K measure was defined as [11, 12]:

$$K = 1 - \frac{S_1}{S_2} \tag{1}$$

where: $S_1 = \int_0^{720} p_{SCmodel}(\alpha)d\alpha$, $S_2 = \int_0^{720} p_{SCmeasure}(\alpha)d\alpha$
where: $S_1 = f(\alpha)$ – area under the diagram of the averaged pressure course indicated as a function of the crankshaft rotation angle for a real object, $S_2 = f(\alpha)$ – area under the indicated pressure graph as a function of the crankshaft rotation angle for the model.

The value of the K parameter is a function of the crankshaft rotation angle. It is used for analysis within a limited range of angles corresponding to the highest pressure values (including combustion pressure), i.e. from the injection opening angle to the exhaust valve opening angle.

After selecting the input parameters of the model, simulations, and empirical tests were carried out for the load, and the nominal rotational speed when the engine was powered with diesel oil without alcohol addition. After verifying, that the empirical, and model-based results meet the adequacy requirements, further research was started. Figure 2 shows the course of the indicated pressure as a function of the angle of rotation of the engine crankshaft obtained during the described tests. The course of the integral curves of the indicated pressure for model and empirical tests is shown in Fig. 3. The course of changes in K parameter is shown in Fig. 4. The test results are presented in Table 3. Table 4 summarizes the relative values of the engine model adequacy measures for the conducted test.

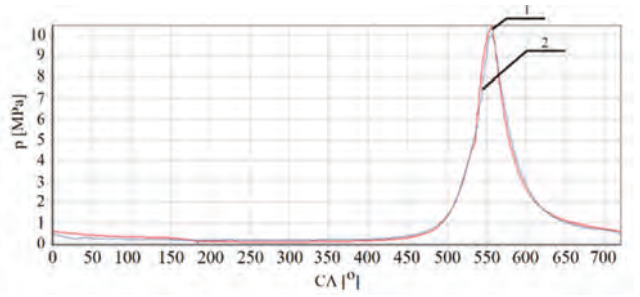

Fig. 2. The course of the indicated pressure obtained as a result of model tests – 1, and empirical tests – 2 as a function of the angle of rotation of the crankshaft

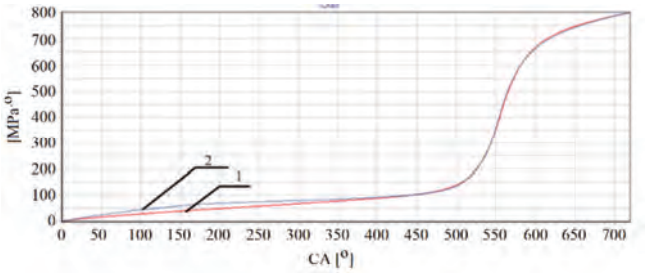

Fig. 3. The course of the indicated pressure integral curves obtained as a result of model tests – 1 and empirical tests – 2 as a function of the angle of rotation of the crankshaft

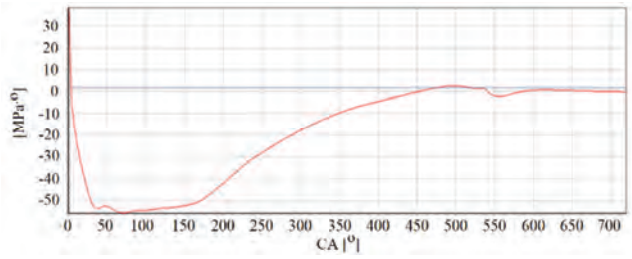

Fig. 4. Course of K measure

Table 3. Summary of the results obtained as a result of model, and empirical tests for an engine operating at a rotational speed of 750 rpm and a load of 5.12 kNm

	Indicated power	Indicated maximum pressure	Hourly fuel consumption	The air excess factor
	[kW]	[MPa]	[kg/h]	[–]
Model research	438.1	10.02	1397	1.42
Empirical research	438	10.11	1487	1.42

Table 4. Relative values of measures of model adequacy for an efficient engine

	Indicated power	Hourly fuel consumption	The air excess factor	K measure
	[%]	[%]	[%]	[–]
The values of the measures of adequacy	0.02	0.89	6.4	2.17

The analysis of the results of the study included in Table 3, and the measures of adequacy in Table 4 allowed for the transition to the next stage. It consists in assessing the adequacy of the mathematical model of a ship engine when it is powered by a mixture of diesel oil, and n-butyl alcohol.

The next step was to assess the adequacy of the mathematical model of the marine engine powered by mixtures of diesel fuel with n-butanol. The research was conducted in accordance with the adopted research plan contained in Table 1. The results of the measurements are grouped in Table 5. The values of the adequacy measures for the model are presented in Table 6. In Table 5, the results obtained as a result of empirical tests are marked in gray. However, the results obtained as a result of model tests are marked in blue. The values of rotational speed and indicated power (calculated on the basis of the analysis of the measured indicated pressure) are marked in gray in Table 5. They are input parameters to the mathematical model.

The results of model and empirical tests presented in Table 5, and the values of adequacy measures contained in Table 6 allowed for the recognition of the model as adequate in the entire scope of the research conducted. Earlier studies (conducted for the purpose of developing a diagnostic method) showed that the model is inadequate in terms of rotational speeds of up to 600 rpm and no-load operation) [10]. This allows the conclusion that also in the case of the currently conducted tests, the model may be inadequate for low torque loads and for low rotational speeds.

In the case of previously conducted tests, it was shown that the inadequacy was most likely due to the simplifications used in the model, and the fact that the marine engine (fuel dose and injection advance angle) was adjusted for nominal loads and rotational speeds of its crankshaft.

Table 5. Results of the conducted research

Torque [kNm]	Alcohol [%]		750 rpm				675 rpm				600 rpm		
			Ge [kg/h]	λ [–]	n/Ni [rpm]/[kW]		Ge [kg/h]	λ [–]	n/Ni [rpm]/[kW]		Ge [kg/h]	λ [–]	n/Ni [rpm]/[kW]
0.98	23%	Point 9	74.04	1.90	608/307	Point 18	83.16	1.99	681/346	Point 27	88.68	2.12	746/370
			76.88	1.85			78.66	1.87			83.54	2.01	
	13%	Point 8	74.04	1.86	608/325	Point 17	81.84	1.98	680/367	Point 26	89.94	2.08	751/397
			68.01	1.86			77.96	1.81			87.55	1.94	
	0%	Point 7	72.06	2.06	605/309	4Point 16	81.06	1.94	681/359	Point 25	88.38	2.06	750/338
			65.05	1.94			77.68	1.80			82.82	1.93	
2.81	23%	Point 6	49.38	2.21	606/213	Point 15	54.06	1.20	675/237	Point 24	60.66	2.26	748/253
			44.68	2.01			59.27	2.26			59.17	2.31	
	13%	Point 5	48.36	2.03	602/209	Point 14	52.56	2.14	674/226	Point 23	59.46	2.50	746/253
			45.02	1.96			56.40	2.13			58.21	2.27	
	0%	Point 4	48.90	2.04	609/220	Point 13	49.86	2.16	675/233	Point 22	58.86	2.22	755/260
			45.76	1.94			53.11	2.11			58.06	2.28	
4.65	23%	Point 3	24.90	2.67	602/108	Point 12	28.56	2.69	675/123	Point 21	32.28	2.68	749/136
			26.38	2.50			27.48	2.91			34.80	2.91	
	13%	Point 2	24.72	2.60	604/110	Point 11	29.76	2.68	673/124	Point 20	32.22	2.67	747/132
			25.95	2.44			29.35	2.90			34.52	2.83	
	0%	Point 1	26.22	2.53	598/112	Point 10	30.06	2.58	647/129	Point 19	32.40	2.62	748/138
			24.97	2.41			31.55	2.81			33.78	2.80	

Table 6. Values of measures of adequacy of the mathematical model

Torque [kNm]	Alcohol concentration	750 rpm				675 rpm					600 rpm		
		Point 1	K [–]	Ge [%]	λ [%]		K [–]	Ge [%]	λ [%]		K [–]	Ge [%]	λ [%]
0.98	23%	Point 9	3.12	3.84	3.95	Point 18	8.84	5.41	6.03	Point 27	6.55	5.79	5.32
	13%	Point 8	3.01	8.02	2.15	Point 17	8.38	4.74	8.08	Point 26	5.87	2.66	6.73
	0%	Point 7	3.44	9.72	5.82	Point 16	8.36	4.17	7.22	Point 25	5.38	6.28	6.31
2.81	23%	Point 6	3.33	9.51	9.05	Point 15	6.60	9.63	3.24	Point 24	4.88	2.45	2.21
	13%	Point 5	3.24	6.90	3.50	Point 14	1.70	7.31	0.47	Point 23	4.87	2.10	9.20
	0%	Point 4	4.95	6.42	4.41	Point 13	3.95	6.52	2.09	Point 22	4.36	7.37	2.70
4.65	23%	Point 3	2.48	5.94	3.38	Point 12	8.34	3.77	7.52	Point 21	5.03	7.08	8.58
	13%	Point 2	8.29	7.97	6.15	Point 11	7.12	1.37	8.21	Point 20	6.54	6.33	5.99
	0%	Point 1	4.73	4.77	4.74	Point 10	2.61	4.95	8.91	Point 189	2.54	4.26	6.87

The conducted research has shown that when the engine is running idle, there are very large discrepancies between maximum pressures in individual engine cylinders. They may also result from the applied methodology of indicated pressure measurement. The measurement was carried out individually for each cylinder. This could result in a change in the engine operating conditions during the measurement (fluctuations in the rotational speed of the crankshaft and the engine load with the water brake). This phenomenon was illustrated by presenting a diagram of the maximum pressure for individual cylinders of the engine operating at a rotational speed of 450 rpm, and a torque load of 0.42 kNm (Fig. 5). On the other hand, Fig. 6 shows the values of the maximum pressure for the engine operating at a rotational speed of 750 rpm, and a load of 4.65 kNm.

The discrepancies between the values of the measured and modeled parameters, and what is the result, and the discrepancies in the values of the measures of adequacy, visible in the test results (Table 5) and in the values of the adequacy measures (Table 6):

– the excess air coefficient varies from 0.47 to 9.20%,
– hourly fuel consumption in the range from 1.37 to 9.72%,
– K measure from 1.70 to 8.84%.

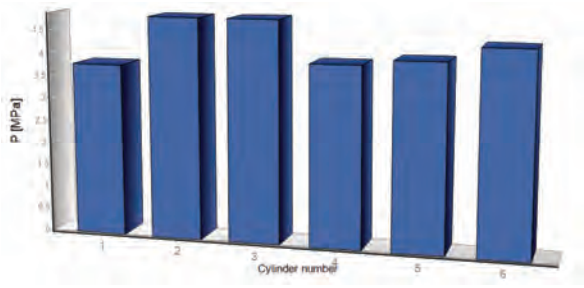

Fig. 5. The values of the maximum indicated pressure for the engine working with the crankshaft rotational speed of 450 rpm, and the load of 0.42 kNm (diesel oil)

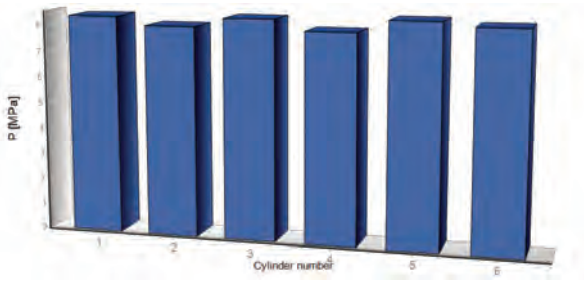

Fig. 6. The values of the maximum indicated pressure for the engine working with the crankshaft rotational speed of 750 rpm and the load of 4.65 kNm (diesel oil)

These fluctuations are randomly distributed and are probably the result of:

– the uniqueness of the processes taking place in the engine cylinders,
– slight influence of the fuel-alcohol mixture used on the measured engine operation parameters,
– the uniqueness of the test conditions for different concentrations of the fuel mixture (inaccuracy of the water brake setting and rotational speed fluctuations introduced by the engine speed controller),
– inaccuracies in indicated pressure measurements caused by wave phenomena occurring in the channels of indicator valves,
– low accuracy of measuring hourly fuel consumption with a weighing instrument (the accuracy of the scale used was 1g, the measurement was carried out within 60 s),
– high inertia of the excess air factor measurement (large length of the measuring channel).

Despite the mentioned sources of measurement errors, it can be observed (in most cases) that the use of different concentrations of the mixture of diesel oil and n-butanol has a noticeable effect on the measured engine operating parameters (Table 5):

– an increase in n-butanol concentration causes an increase in the excess air ratio,
– an increase in the n-butyl alcohol content in the mixture increases the hourly fuel consumption.

Similar relationships can be observed when analyzing the results of empirical research.

6. Conclusions

The results of model and empirical research conducted by the authors and presented have confirmed the adequacy (both qualitative and quantitative) of the developed mathematical model. This justifies its use in research on the use of mixtures of fossil fuels with biocomponents. The use of a mathematical model and a computer program based on it should significantly reduce the amount of empirical research performed. This translates into shortening the time of research and reducing their costs.

Nevertheless, the authors noticed the need to increase the adequacy of the mathematical model (the results of the research are, admittedly, within the adopted ranges of the adequacy measures), which results from the relatively low impact of the use of mixtures of diesel fuel with alcohol. Further research should include:

- applying a smaller calculation step (currently all parameters are counted every 0.1 crankshaft rotation),
- clarification of the heat transfer calculations between the medium and the cylinder walls (now the heat transfer is being modeled. The use of Woschni [7, 8] and Bulaty [1] dependencies in the case of the conducted research resulted in significant errors,
- development of an analytical method for calculating the ignition delay for the mixtures used. The applied method of calculating the release of heat (the heat flux is supplied to the cylinder along with the injected fuel) does not take into account the delay in ignition of the fuel-air mixture (for the needs of the model, this parameter was selected on the basis of empirical tests),
- increasing the repeatability of the test conditions (repeatability of the torque load and rotational speed of the crankshaft).

Nomenclature

Ge	hourly fuel consumption	S	surface area
K	measure of similarity	λ	excess air factor

Bibliography

[1] BULATY, T. Beitrag zur Berechnung des Wärmeüberganges, insbesondere in längsgespülten, Langhubigen Dieselmotoren. *Motortechnische Zeitschrift*. 1985, **46**(2).

[2] ELFASAKHANY, A. State of art of using biofuels in spark ignition engines. *Energies.* 2021, **14**, 779, 1-26. https://doi.org/10.3390/en14030779

[3] KNIAZIEWICZ, T., ZACHAREWICZ, M. A physical model of energetic processes in a diesel marine generator set. *Combustion Engines*. 2018, **57**(4), 10-17. https://doi.org/10.19206/CE-2018-402

[4] MURUGESANA, A., UMARANIB, C., SUBRAMANIANC, R. et al. Bio-diesel as an alternative fuel for diesel engines – a review. *Renewable and Sustainable Energy Reviews.* 2009, **13**(3), 653-662. https://doi.org/10.1016/j.rser.2007.10.007

[5] PAGLIUSO, J. Biofuels for spark-ignition engines. *Advanced Direct Injection Combustion Engine Technologies and Development, Gasoline and Gas Engines.* 2010, 229-259. https://doi.org/10.1533/9781845697327.229

[6] SATISH, K., HYUN, C.J., JAEDEUK, P. Advances in diesel-alcohol blends and their effects on the performance and emissions of diesel engines. *Renewable and Sustainable Energy Reviews*. 2013, **22**, 46-72. https://doi.org/10.1016/j.rser.2013.01.017

[7] WOSCHNI, G. A universally applicable equation for the instantaneous heat transfer coefficient in internal combustion engines. *SAE Technical Paper* 670931, 1967. https://doi.org/10.4271/670931

[8] WOSCHNI, G., KLAUS, B., ZEILIGER, K. Untersuchung des Wärmetransportes zwischen Kolben, Kolbenringen und Zylinderbüchse. *Motortechnische Zeitschrift*. 1998, **59**(9).

[9] YOUNG NO, S. Application of biobutanol in advanced CI engines – a review. *Fuel*. 2016, **183**, 641-658. https://doi.org/10.1016/j.fuel.2016.06.121

[10] ZACHAREWICZ, M. Możliwości oceny stanu okrętowego silnika spalinowego o podatności diagnostycznej. *AMW*. Gdynia 2019.

[11] ZACHAREWICZ, M., KNIAZIEWICZ, T. Mathematical modelling malfunctions of marine diesel engine. *MATEC Web of Conferences*. 2017, **118**, 1-5. https://doi.org/10.1051/matecconf/201711800001

[12] ZACHAREWICZ, M., KNIAZIEWICZ, T. Method of evaluation of the technical condition of the Diesel-electric unit. *Diagnostyka.* 2019, **20**(2), 113-119. https://doi.org/10.29354/diag/109669

[13] ZACHAREWICZ, M., KNIAZIEWICZ, T., BOGDANOWICZ, A. The use of mathematical model of marine diesel engine in computer program, *New Trends in Production Engineering*. 2018, 487-493. https://doi.org/10.2478/ntpe-2018-0056

[14] Międzynarodowa konwencja o zapobieganiu zanieczyszczaniu morza przez statki (konwencja MARPOL, tekst jednolity: Dz. U. z 2016 r. poz. 761, z późn. zm.)

[15] Raport: Specjalistyczne badania statystyczne w przemyśle stoczniowym. Stan na 31.12.2019 roku. CTO S.A.

[16] Rozporządzenie ministra gospodarki z dnia 17 grudnia 2010 r. w sprawie wymagań jakościowych dla biokomponentów, metod badań jakości biokomponentów oraz sposobu pobierania próbek biokomponentów. Dz. U. 2017.506 t.j.

[17] Rozporządzenie Ministra Infrastruktury i Rozwoju z dnia 7 października 2015 r. w sprawie wymagań dotyczących zawartości siarki w paliwie żeglugowym, w tym sposobu jej oznaczania (Dz. U. poz.1665).

[18] Ustawa z dnia 25 sierpnia 2006r. o biokomponentach i biopaliwach ciekłych. Dz. U. 2020.1233 t.j.

Marcin Zacharewicz, DSc. DEng. – Faculty of Mechanical and Electrical Engineering, Polish Naval Academy.

e-mail: *M.Zacharewicz@amw.gdynia.pl*

Prof. Tomasz Kniaziewicz, DSc., DEng. – Faculty of Mechanical and Electrical Engineering, Polish Naval Academy.

e-mail: *T.Kniaziewicz@amw.gdynia.pl*

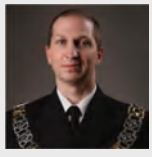

Article citation info:
KAŹMIERCZAK, A.R., MATLA, J. Method of verifying the emission level of the exhaust components of a special vehicle in relation to EURO III standard in road conditions. *Combustion Engines*. 2022, **189**(2), 89-93. https://doi.org/10.19206/CE-143485

Andrzej R. KAŹMIERCZAK
Jędrzej MATLA

Combustion Engines
Polish Scientific Society of Combustion Engines

Method of verifying the emission level of the exhaust components of a special vehicle in relation to EURO III standard in road conditions

ARTICLE INFO

Received: 16 September 2021
Revised: 19 October 2021
Accepted: 30 October 2021
Available online: 2 November 2021

The following article presents the method of verification of EURO III standard in real conditions for special vehicles. The test object qualified as a special vehicle was tested in road conditions along a defined route, and then the obtained measurement results were compared to the exhaust emission standard (EURO III) applicable for this vehicle. A method of comparing the emission factors in road conditions with the indicators obtained on the engine dynamometer was proposed. An AVL mobile exhaust gas analyzers PEMS dedicated for RDE road tests were used in the research.

Key words: *emissions verification method, PEMS, special vehicle, RDE, exhaust components*

1. Introduction

Air pollution, and in consequence the health problem gains greater importance every year. The subsequent EURO standards, which describes the allowable limits of exhaust gases emission are even more stringent [1, 2]. It was found that nowadays real-world emissions exceed the level achieved in the laboratory tests, especially the emission of nitrogen oxides emitted by diesel engines. Therefore, the usability of the road test is proposed [1, 3–5].

The vehicles are investigated according to accurate methods using a variety of sophisticated devices. One of the most common and accurate methods of exhaust gases verification is Portable Emission Measurement System (PEMS). The models developed based on PEMS measurements are widely used to predict the pollution in an urban area which helps to select the perfect location of urban facilities such as, for example pedestrian crossings [5]. It was also determined that the most hazardous emission is generated while accelerating from 0 to 80 km/h [6].

In general, PEMS methodology is predominantly applicable for gaseous emission only. Lately, it was also introduced to the heavy-duty vehicle due to the implementation of solid particle number (PN). The performance of the heavy-duty vehicles was verified and the result was described in [7]. It appeared that the results are within 40–65% of the laboratory standards with only minor robustness issues, which makes them suitable for in-service conformity regulation.

The EURO III standard requires the performance of an experiment in a strict regime, mostly with the aid of a dynamometer. In consequence to verify the compliance of and existing vehicle with this standard, it is required to dismount the engine and perform investigations. The PEMS systems provide the possibility to perform the euro test in real-time driving. All parameters of the exhaust gases are gathered during road tests [5]. However, in the case of road test the reliable and repeatable conditions are much more difficult to achieve. The style of driving can affect the measurements. As it was proven in [8] the emission characteristic depends on the type of traffic flow. Therefore, the change in driving behaviour, or driving gear selection leads to a significant increase of emission factor. Moreover, the traffic is a determining factor in creating NO_x pollutants [9]. It was also found that the emission factor depends not only on the driving operational intensity but also on the duration and frequencies of individual maneuver states. Another important factor in the emission problems is the aging of vehicles. It appears that even fivefold growth of CO and HC was determined for vehicles older than 15 years [1].

Since the year 2020 the conformity factor for new vehicles is 1.5. No matter the difficulty to provide repeatable test results, it is planned to implement the RDE with PEMS measurements for legislation approval [10]. However, the vast amount of factors affecting the RDE test (e.g. traffic, driving behaviour, moisture, ambient pressure and temperature, etc.) should be taken into account. It is speculated that this should be overcome by focusing on the most frequently driven operating conditions [11, 12].

This paper provides an overview of the possibility to implement the PEMS measurement for heavy-duty special vehicle compliance with EURO III standards. The authors are aware of the inaccuracy of the method, which in its assumptions does not use the OBD system, but their main goal was to propose a method suitable for use on a military vehicle in road conditions without connection to diagnostic systems.

2. Methodology

2.1. Test vehicle

Vehicle that was an object of investigation (Fig. 1) was classified as N3G group according to the EU type approval system. It is dedicated to carrying goods for military purposes in off-road conditions, thus it is treated as a special purpose vehicle and it is not obliged to fulfill corresponding emissions requirements for commercial heavy-duty trucks.

Due to the limited maximum speed of the test vehicle (Table 1), it was impossible to implement an ETC chassis dynamometer test suitable for the EURO III engine, where the average speed of the motorway part is set at a level of

88 km/h. Moreover, the design of the vehicle with three driving axles makes it practically impossible to test on a standard chassis dynamometer.

Fig. 1. Test vehicle

Table 1. Selected parameters of the test vehicle

Category	N3G
Mileage	321 km
Engine type	Compression ignition, turbocharged
Engine displacement	10300 ccm
Max. power	316 kW at 2100 RPM
Max. velocity	85 km/h
Emissions standard	EURO III
Vehicle curb weight	12200 kg
Permissible gross weight	27000 kg
Tires	14 R20 A/T

2.2. Measuring equipment

Vehicle tailpipe emissions measurement was conducted with an AVL PEMS system dedicated to RDE testing consisting of the following components:

- GAS module equipped with two channel FID enabling simultaneous measurement of THC and CH_4, NIDR analyzer for CO_2 and CO reading, NDUV unit for NO_x measurement and paramagnetic analyzer for O_2 measurement,
- PM module composed of measuring unit equipped with a laser NDIR meter capable of continuous measurement of PM quantity and gravimetric filter for recording particulate mass,
- EFM device based on Pitot tubes enabling exhaust gases flow measurement even in case of relatively strong pulsations while the engine is idle or highly loaded. For purposes of the following research, a 4 inches diameter flowmeter was used,
- SC module dedicated to recording and processing of all signals with 2 Hz frequency,
- GPS unit for measuring vehicle ground velocity independently from its instruments, capable of connecting with up to 12 satellites at the same time,
- weather station collecting data about ambient pressure and temperature,
- batteries providing independent source of power for all measuring devices,
- generator being a backup source of energy in case of batteries failure.

2.3. Testing procedure

Due to the fact that the tested vehicle was designed to carry loads, most of the measuring devices were installed on the cargo area on its back as shown in Fig. 2. The weather station, as well as GPS unit were placed on the roof to increase the accuracy of the measurements. The full test should consist of at least two runs, first without payload and second with 50 to 60% of the maximum vehicle payload. Such requirements result from differences in driving characteristics of an off-road vehicle [13].

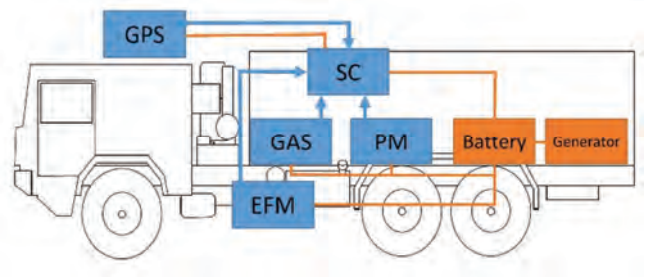

Fig. 2. Scheme of equipment setup

Before the test tire pressure was adjusted according to the manufacturer's data and a test drive was conducted to achieve the operating temperature of an engine and check all the readings.

The tests were carried out on a route defined by the Military Technological Guide developed in compliance with the Polish Defense Department requirements. The test circuit was established over a total distance of 22.5 km in both directions.

Fig. 3. Test route

The test route was established to minimize the influence of congestion and ambient conditions on the test results.

2.4. Method description

Before calculating vehicle energy demand, a fuel sample needs to be tested to determine the calorific value necessary for further analysis. The calorific value of the fuel sample is determined according to the reference method described by the norm PN-Z-15008-4:1993. Then the engine emission factors of the vehicle are calculated from the actual values during the test. The total fuel consumption for the test was calculated using the airflow and air to fuel ratio measurement method described in detail by the formulas in section 8.4.1.6 of Annex 4 to UN/ECE Regulation No 49.

Thanks to the PEMS SC unit, this part of the research was automated, so the total masses of particular components and the fuel consumed were known.

The mentioned method being similar to the carbon balance method, is based on the assumption that the total mass of carbon in the fuel consumed is equal to the total carbon mass in the exhaust gases. Today fuels are composed almost only of saturated hydrocarbons; thus during the combustion process all carbon molecules are emitted in exhaust gases.

To estimate the total carbon mass of exhaust gases the concentrations of CO, CO_2 and THC have to be measured. Moreover, an air to fuel ratio measurement equipment such as a zirconia type sensor is used for the measurement of the excess air ratio.

The selection of airflow and air to fuel ratio measurement method over the carbon balance method resulted from the fact that it does not require any of the ECU readings, making it more objective and suitable to use when an engine is not equipped with any sensors.

The next step of the evaluation method proposed by the authors is the calculation of the total energy consumption in the road test, which is done according to formula 1.

$$E_T = m_f * c_f \tag{1}$$

where: E_T – is total energy consumption in test, [MJ], m_f – is total mass of fuel consumed, [kg], c_f – is fuel calorific value, [MJ/kg].

Since energy consumption can be straightforwardly converted into kWh unit the emission per km for any exhaust component may now be calculated.

$$m_x = m_{xT}/E_T \tag{2}$$

where: m_x – is specific emission of component, [g/kWh], m_{xT} – is total mass of component emitted in test, [g], E_T – is total energy consumption in test, [kWh].

The last step in the assessment of vehicle emissions is the comparison of the values obtained with the emission limits specified by the EURO III standard. Due to the experiment character, limits for transient testing should be applied. They are presented in the Table 2.

Table 2. Emission limits for heavy-duty CI engines – transient testing [14]

Exhaust component	Limit	
CO	5.45	g/kWh
NMHC	0.78	g/kWh
CH_4	1.60	g/kWh
NO_x	5.00	g/kWh
PM	0.16	g/kWh

3. Results

The road test was conducted under moderate traffic conditions. The average ambient temperature during the test was 20.8°C with a relative humidity of 46%. The duration of the test was about 36 minutes with an average velocity of 37.05 km/h.

The course of the speed profile clearly shows that the route will be driven in both directions at a similar speed.

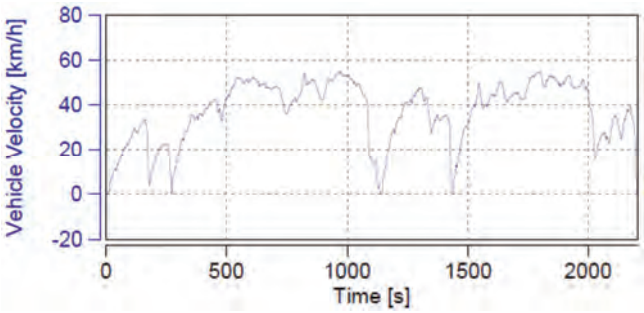

Fig. 4. Road test velocity profile of the vehicle

The concentrations of the selected exhaust components in the road test were recorded and presented in a graphical form.

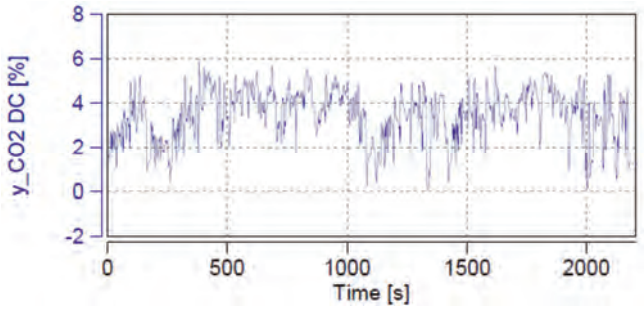

Fig. 5. Carbon dioxide concentration during the test

In the case of the course of carbon dioxide emission, a clear correlation was observed with the vehicle speed profile during the test. At the same time, it was discovered that the oxygen concentration curve is an inverse of the carbon dioxide curve, which was expected.

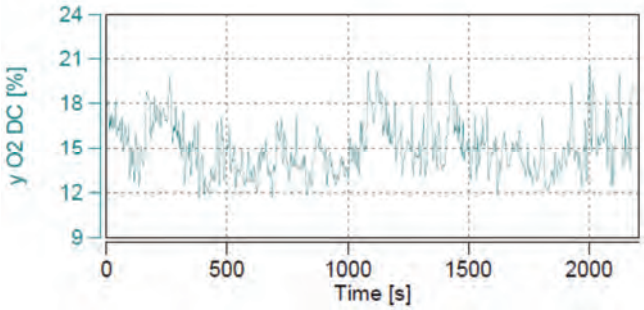

Fig. 6. Oxygen concentration during the test

The concentration of oxygen in the exhaust gas reaches its highest values during stops and engine braking.

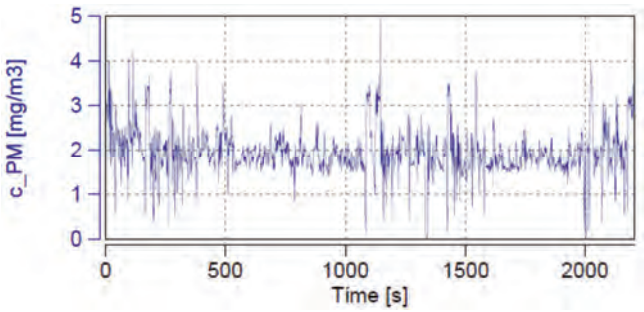

Fig. 7. Particulate matter concentration during the test

The highest concentration of particulate matter during the test was observed during the acceleration of the vehicle. It was connected with an increase in fuel consumption under those conditions resulting from a rapid increase in engine load.

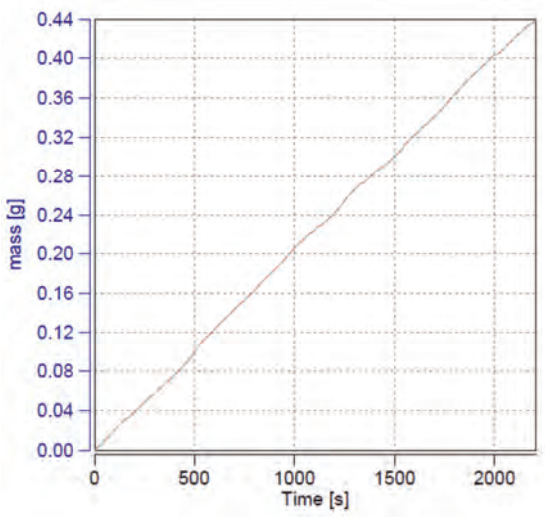

Fig. 8. Particulate mass during the test

The progression of the total amount of particulate mass, similar to the linear one, proves that the test was performed correctly and the route was properly selected.

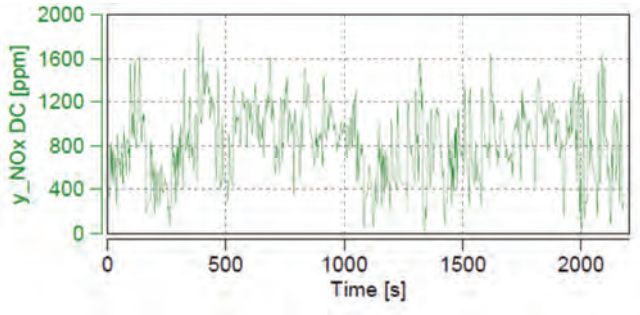

Fig. 9. Nitrogen oxides concentration during the test

The highest concentration of nitrogen oxides was observed during engine load, as is the case with carbon dioxide. The increase in the amount of nitrogen oxides is related to the increase in the temperature of the combustion process; therefore, it proves that the engine was working properly.

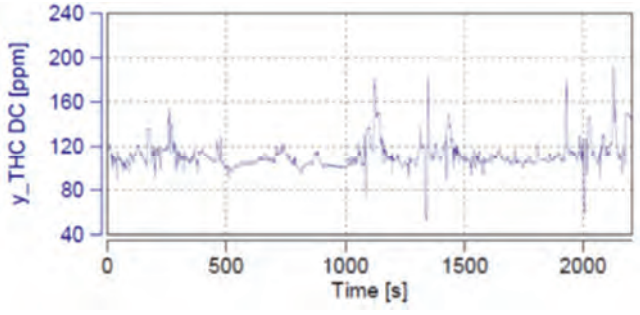

Fig. 10. Total hydrocarbons concentration during the test

For most of the test, the hydrocarbon concentration fluctuated around a constant value of 100 ppm. Visible peaks were observed while the vehicle decelerated. The increase in hydrocarbons during engine braking is a natural symptom of its work.

All of the courses obtained did not differ from the expected values. The characteristics of the concentrations of the individual components did not show any abnormalities in the engine operation during the test and were used for further analysis.

The calorific value of the fuel was determined (Table 3) and the calculated mass of the fuel consumed was referred to its calorific value, thus obtaining the total energy consumption in the test.

Table 3. Road test data

Duration	2205	s
Distance	22.8	km
Average velocity	37.2245	km/h
Consumed fuel mass	5.24	kg
Fuel calorific value	47.57	MJ/kg
Total energy consumption	249.267	MJ
Specific energy consumption	10.9328	MJ/km

The total emitted mass of the compounds was calculated and then the emission factors were obtained by relating the mass of the compounds to the distance traveled.

Table 4. Selected engine emission factors in test

Exhaust component	Total mass emitted in test		Emission per km		Emission per kWh	
THC	15.58	g	0.68	g/km	0.225	g/kWh
NMHC	15.27	g	0.67	g/km	0.220	g/kWh
CH_4	0.36	g	0.02	g/km	0.005	g/kWh
CO_2	16352.80	g	717.23	g/km	235.984	g/kWh
NO	370.01	g	16.23	g/km	5.340	g/kWh
NO_2	25.12	g	1.10	g/km	0.362	g/kWh
NO_x	395.13	g	17.33	g/km	5.707	g/kWh
PM	4.38	g	0.19	g/km	0.063	g/kWh

4. Discussion

The results obtained (Table 4) in relation to the emission limits (Table 2) indicate that the EURO III standard was met in relation to non-methane hydrocarbons, methane and particulate mass. In the case of nitrogen oxides, the limit was exceeded, thus further testing with payload was stopped.

As it was mentioned in paragraph 2.4, the undoubted advantage of the presented method is its versatility and the possibility of testing independently from the sensors in the vehicle. The methodology presented in this article, in relation to the reference method for the verification of EURO III emission factors, allows the vehicle to be tested in conditions similar to its natural road operation. For further verification of the method, consecutive tests are required with the vehicle operating in terrain conditions.

The test route should be selected in such a way that it is possible to achieve an average speed approximately 50% of the maximum speed of the vehicle. The complete test should consist of a route in both directions to minimize the influence of congestion and ambient conditions on the test results.

Acknowledgements

Testing equipment used in the presented research was purchased by Wrocław University of Science and Technology as a part of the "Complex GEO-3EM ENERGY ECOLOGY EDUCATION" financed by the European Regional Development Fund within the Regional Operational Program of the Lower Silesian Voivodship for the years 2014-2020.

Nomenclature

AVL	Anstalt für Verbrennungskraftmaschinen List
ECE	Economic Commission for Europe
ECU	engine control unit
EFM	electronic flow meter
ETC	European transient cycle
EU	European Union
FID	flame ionization detector
GPS	global positioning system
NDIR	nondispersive infrared
NDUV	non-dispersive ultra violet spectroscopy
NMHC	non-methane hydrocarbons
PEMS	portable emission measuring system
PM	particulate mass
PN	particulate number
RDE	real driving emissions
SC	system control
THC	total hydrocarbons
UN	United Nations

Bibliography

[1] HASSANI, A., SAFAVI, S.R., HOSSEINI, V. A comparison of light-duty vehicles' high emitters fractions obtained from an emission remote sensing campaign and emission inspection program for policy recommendation. *Environmental Pollution*. 2021, **286**, 117396. https://doi.org/10.1016/j.envpol.2021.117396

[2] PUŠKÁR, M., KOPAS, M. System based on thermal control of the HCCI technology developed for reduction of the vehicle NO_x emissions in order to fulfil the future standard Euro 7. *Science of the Total Environment*. 2018, **643**, 674-680. https://doi.org/10.1016/j.scitotenv.2018.06.082

[3] LUJÁN, J., BERMÚDEZ, V., DOLZ, V. et al. An assessment of the real-world driving gaseous emissions from a Euro 6 light-duty diesel vehicle using a portable emissions measurement system (PEMS). *Atmospheric Environment*. 2018, **174**, 112-121. https://doi.org/10.1016/j.atmosenv.2017.11.056

[4] KO, J., JIN, D., JANG, W. et al. Comparative investigation of NO_x emission characteristics from a Euro 6-compliant diesel passenger car over the NEDC and WLTC at various ambient temperatures. *Applied Energy*. 2017, **187**, 652-662. https://doi.org/10.1016/j.apenergy.2016.11.105

[5] JAWORSKI, A., MĄDZIEL, M., LEJDA, K. Creating an emission model based on portable emission measurement system for the purpose of a roundabout. *Environmental Science and Pollution Research*. 2019, **26**. https://doi.org/10.1007/s11356-019-05264-1

[6] SÖDERENA, P., LAURIKKO, J., WEBER, C. et al. Monitoring Euro 6 diesel passenger cars NO_x emissions for one year in various ambient conditions with PEMS and NO_x sensors. *Science of the Total Environment*. 2020, **746**, 140971. https://doi.org/10.1016/j.scitotenv.2020.140971

[7] GIECHASKIEL, B., SCHWELBERGER, M., DELACROIX, C. et al. Experimental assessment of solid particle number Portable Emissions Measurement Systems (PEMS) for heavy-duty vehicles applications. *Journal of Aerosol Science*. 2018, **123**, 161-170. https://doi.org/10.1016/j.jaerosci.2018.06.014

[8] YU, Q., YANG, Y., XIONG, X. et al. Assessing the impact of multi-dimensional driving behaviors on link-level emissions based on a Portable Emission Measurement System (PEMS). *Atmospheric Pollution Research*. 2021, **12**(1), 414-424. https://doi.org/10.1016/j.apr.2020.09.022

[9] GÓMEZ, A., FERNÁNDEZ-YÁÑEZ, P., SORIANO, J.A. et al. Comparison of real driving emissions from Euro VI buses with diesel and compressed natural gas fuels. *Fuel*. 2021, **289**, 119836. https://doi.org/10.1016/j.fuel.2020.119836

[10] OLABI, A.G., MAIZAK, D., WILBERFORCE, T. Review of the regulations and techniques to eliminate toxic emissions from diesel engine cars. *Science of the Total Environment*. 2020, **748**, 141249. https://doi.org/10.1016/J.SCITOTENV.2020.141249

[11] LEE, T., PARK, J., KWON, S. et al. Variability in operation-based NO(x) emission factors with different test routes, and its effects on the real-driving emissions of light diesel vehicles. *The Science of the Total Environment*. 2013, **461-462**, 377-385. https://doi.org/10.1016/j.scitotenv.2013.05.015

[12] MERKISZ, J., RYMANIAK, Ł., ZIÓŁKOWSKI, A. et al. The analysis of the emission level from a heavy-duty truck in city traffic. *Combustion Engines*. 2012, **150**(3), 80-88. https://doi.org/10.19206/CE-117033

[13] MERKISZ, J., PIELECHA, J., STOJECKI, A. et al. The influence of terrain topography on vehicle energy intensity and engine operating conditions. *Combustion Engines*. 2015, **162**(3), 341-349.

[14] Directive 1999/96/EC of the European Parliament and of the Council.

Prof. Andrzej R. Kaźmierczak, DSc., DEng. – Faculty of Mechanical Engineering, Wrocław University of Science and Technology.
e-mail: *andrzej.kazmierczak@pwr.edu.pl*

Jędrzej Matla, MEng. – PhD student, Wrocław University of Science and Technology.
e-mail: *jedrzej.matla@pwr.edu.pl*

Article citation info:
KNEBA, Z., STEPANENKO, D., RUDNICKI, J. Numerical methodology for evaluation the combustion and emissions characteristics on WLTP in the light duty dual-fuel diesel vehicle. *Combustion Engines*. 2022, **189**(2), 94-102. https://doi.org/10.19206/CE-143334

Zbigniew KNEBA
Denys STEPANENKO
Jacek RUDNICKI

Combustion Engines
Polish Scientific Society of Combustion Engines

Numerical methodology for evaluation the combustion and emissions characteristics on WLTP in the light duty dual-fuel diesel vehicle

ARTICLE INFO

Received: 13 July 2021
Revised: 21 October 2021
Accepted: 25 October 2021
Available online: 22 November 2021

The worldwide aim of reducing environmental impact from internal combustion engines bring more and more stringent emission regulations. In 2017 by EU has been adopted new harmonized test procedure called WLTP. In general terms this test was designed for determining the levels of harmful emissions and fuel consumption of traditional and hybrid cars. This procedure contains specific driving scenarios which representing real-life driving patterns. Test cycles contain vehicle velocity versus time profiles and directly in powertrain analysis on the test benches cannot be used. In order to back calculate drive cycles to engine rpm versus torque profiles a simple longitudinal vehicle dynamics method was used in this paper. Moreover, in order to determine most representative engine operation points during WLTP a density based grid clustering method was implemented. The experimental part of the study focuses on the comparative evaluation of the effect of various diesel to LPG substitution ratios (0% LPG, 10% LPG, 20% LPG and 30% LPG) on combustion and emission characteristics of dual-fuel diesel engine.

Key words: *dual-fuel engine, drive cycle simulation, internal combustion engine, emission reduction, alternative fuels, WLTP*

1. Introduction

The worldwide environmental considerations provide to increasing the stringent regulations that are aimed to lowering the harmful emissions (HC, CO, PM and NO_x) in the exhaust gases of the internal combustion engines. In 2017 the Worldwide Harmonized Light Vehicles Test Procedure has been adopted as the new test procedure in the European type-approval system and replaces the New European Driving Cycle. While the NEDC was based on theoretical driving scenarios, the WLTP was developed using real-driving data with the aims to provide real-life driving conditions. Moreover, WLTP includes several test cycles (called WLTC) applicable to vehicle categories of different rated power to curb mass ratio. In general, WLTP driving cycles is divided into four parts with different average speeds: urban driving (low), suburban driving (medium), extra-urban driving (high), and a highway zone (extra high) (Table 1). Each part contains a variety of driving phases (varying vehicle velocity within time) shown in Fig. 1.

Table 1. WLTC test cycles for conventional vehicles [17]

Vehicle category	PMR [W/kg]	V_{max} [km/h]	Driving phases
1	22 ≤ PMR	–	Low + Medium + Low
2	22 < PMR ≤ 34	–	Low + Medium + High + Extra High
3a	PMR >34	< 120	Low + Medium + High + Extra High
3b		≥ 120	Low + Medium + High + Extra High

Driving cycles are used to gain a quantitative understanding of fuel consumption and emissions for traditional and hybrid cars during either development phase or homologation process under specific driving scenarios. Moreover, these driving cycles allows to perform powertrain analysis during real-life driving or during investigations on the test benches. In order to use driving patterns in test bench investigations they must be back calculated from vehicle velocity versus time profiles to engine rpm vs. torque profiles. This objective can be achieved by the longitudinal vehicle dynamics approach. Longitudinal dynamics approach is a low time consumption method that makes use of as limited information as possible referring mainly to already available data sources in combination with empirical models, while allows to, provide simulation with required accuracy.

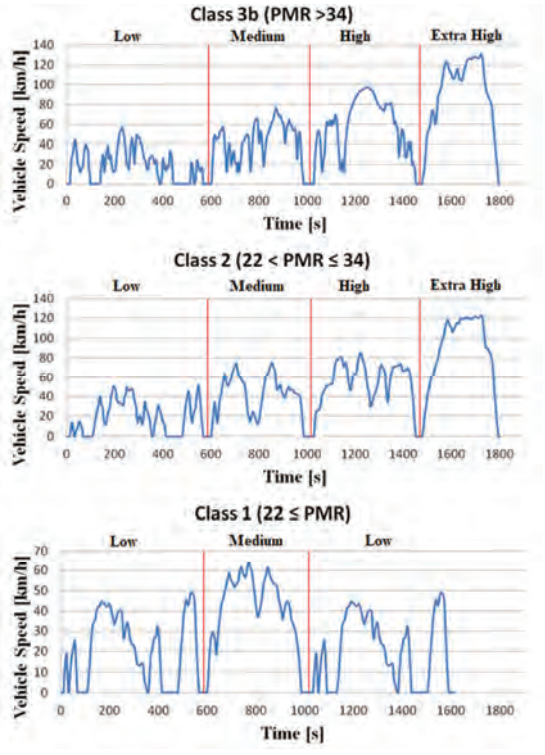

Fig. 1. Speed vs. time traces of the WLTC driving cycle for all vehicle classes [17]

The current work presents simple longitudinal dynamics method in combination with WLTP gear-shifting rules and density based grid clustering method for assessing the introduction of Worldwide Harmonized Light Vehicles Test Procedure in the light duty dual-fuel diesel vehicle (using the example a Golf IV car). Moreover, combustion and emission characteristics of various diesel fuel to LPG substitution ratios (0% LPG, 10% LPG, 20% LPG and 30% LPG) in the most representative operation points during the WLTP are evaluated in this article.

2. Methodology

In this work, fuel effect on engine performance and emissions has been evaluated under Worldwide Harmonized Light Vehicles Test Procedure. In order to back calculate specific drive patterns to engine rpm and torque, was selected commercial FWD passenger vehicle Golf IV, made by Volkswagen factory, technical specifications are presented in Table 2 and Fig. 2.

Depending on the rated power to curb mass ratio of Golf IV 3b test scenario (time-based profile of vehicle speed) (Fig. 1) has been selected.

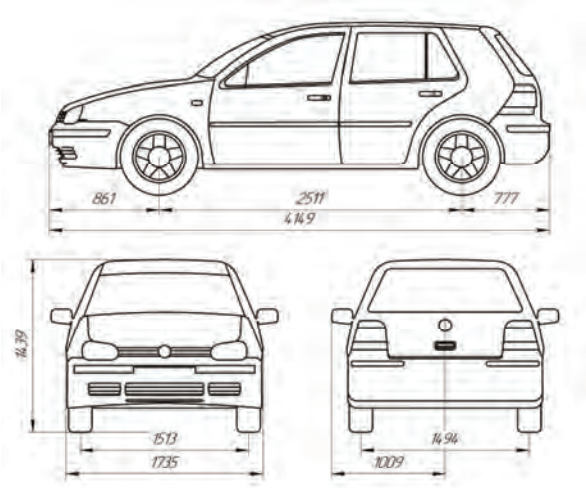

Fig. 2. Volkswagen Golf IV dimensions [19]

Table 2. Volkswagen Golf IV technical specifications [19]

Parameter	Unit	Value
Brand, Model & Generation	–	Volkswagen Golf IV
Production	year	2000
Maximum speed	km/h	195
Vehicle curb weight	kg	1237
Vehicle gross weight	kg	1300
Vehicle total weight	kg	1780
Tires	–	195/65 R15
Gearbox	–	Manual 6-Gear

2.1. Longitudinal dynamic method description

Longitudinal dynamic model implements a one degree-of-freedom rigid vehicle body with constant mass undergoing longitudinal motion. The vehicle axles are parallel and form a plane. The longitudinal direction lies in the parallel plane and is perpendicular to the axles. If the vehicle is traveling on a slope, the normal direction is not parallel to gravity but is always perpendicular to the axle-longitudinal plane (MathWorks, n.d.).

All forces acting on the vehicle during the motion shown in Fig. 3.

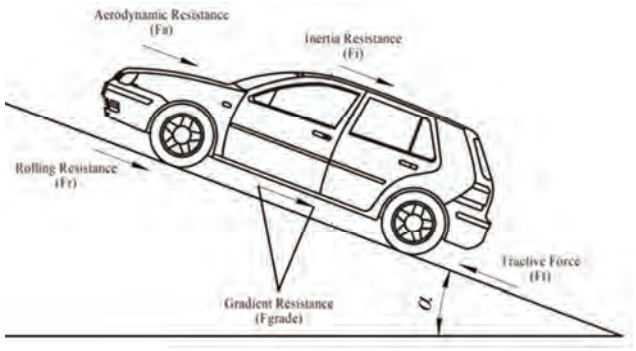

Fig. 3. Forces distribution under longitudinal motion

In general term, to ensure vehicle motion a provided torque from powertrain system on a driving wheels, must allow to obtain a force exceeding the motion resistance forces. Figure 4 illustrates a simplified version of the engine powertrain system.

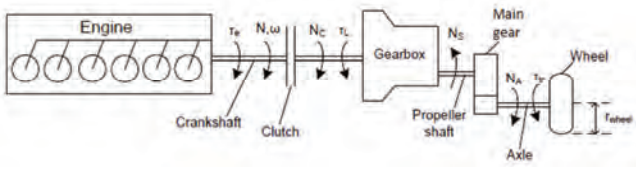

Fig. 4. Conceptual illustration of powertrain system [5]

2.2. Powertrain analysis

In this analysis we assume that the road surface is to be flat and vehicle will behave according to Newton's second law. The basic equation can be expressed as

$$\sum \mathrm{Ft} = \sum \mathrm{Ftr} \tag{1}$$

The powertrain model includes the various sub-modules vehicle dynamics model, wheel dynamics model and gear shifting strategy. Application of the below-described sub-models is necessary so as to convert the vehicle speed vs. time profile (Fig. 1), into engine torque vs. speed profile (Fig. 7). After that, the grid clustering method followed by experimental analysis can be applied.

2.3. Vehicle dynamics model

The first step of the calculation is to derive all resistance forces acting on car during motion. The four resistance forces experienced by a vehicle during the motion are the aerodynamic resistance, tire rolling resistance, gradient resistance and inertia resistance. Total traction resistance is given by

$$\sum \mathrm{Ftr} = \mathrm{Fr} + \mathrm{Fa} + \mathrm{Fi} + \mathrm{Fgrade} \tag{2}$$

2.3.1. Aerodynamic resistance

The component of exerted force that acts on moving object by the air in opposite direction relative to their motion called aerodynamic resistance. This resistance can be approximated as [2, 3, 5, 8]:

$$Fa = 0.5 \times \rho \times Cd \times Af \times V^2 \quad (3)$$

where

$$Af = 0.9 \times H \times B \quad (4)$$

The aerodynamic drag coefficient varies according to the vehicle shape. The most common values for this coefficient shown in Fig. 5.

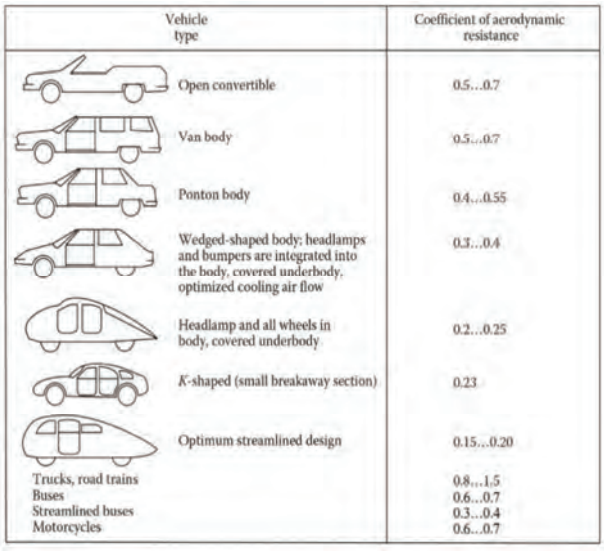

Fig. 5. Aerodynamic drag coefficient for different vehicle types [3]

2.3.2. Tire rolling resistance

The tire rolling resistance is a force applied to each wheel with a dynamic radius with opposite direction to the car's motion. This force is calculated from equation (5) [2, 8]:

$$Fr = m_v \times g \times Crr \times \cos\alpha \quad (5)$$

The rolling resistance coefficient depends on the road surface and determined experimentally. The typical values of the rolling resistance coefficient given in Table 3.

Table 3. Rolling resistance coefficient [6]

Road and pavement condition	Value
Very good concrete	0.008–0.01
Very good tarmac	0.01–0.0125
Average concrete	0.01–0.015
Very good pavement	0.015
Very good macadam	0.013–0.016
Average tarmac	0.018
Concrete in poor condition	0.02

2.3.3. Gradient resistance

If the car moves on a sloping road, weight of the vehicle produces a component of gravitational force, which acts on the vehicle center of gravity and always directed downward. This force is usually called gradient resistance. Generally, in standard tests assumed flat road surface therefore [5, 8]:

$$Fgrade = 0 \quad (6)$$

However, gradient resistance can be calculated from this equation [2, 8]:

$$Fgrade = m_v \times g \times \sin\alpha \quad (7)$$

2.3.4. Inertia resistance

During the car motion with acceleration, an inertial force is produces, which acts on the center of the vehicle mass in opposite direction to its motion. This force usually called inertia resistance and can be calculated from this equation [2, 6]:

$$Fi = m_i \times \frac{dV}{dt} \quad (8)$$

2.3.5. Vehicle inertia mass

The inertia mass is a total mass of the vehicle increased by the mass factor [1, 7]:

$$m_i = m_v \times \delta \quad (9)$$

Mass factor can be approximated from the equation below [2, 8]:

$$\delta = d_1 + d_2 \times i_g^2 \quad (9)$$

where

$$d_1 = \frac{1+\sum J_w}{r_d^2 \times m_v} \quad (11)$$

$$d_2 = \frac{J_p \times \eta_t \times i_0^2}{r_d^2 \times m_v} \quad (12)$$

If mass moments of inertia of the rotating parts associated to the powertrain system are not known, the mass factor, for a passenger car can be estimated from the following empirical equation:

$$\delta = 1.04 + 0.024 \times i_g^2 \quad (13)$$

2.4. Wheel dynamics model

In this block as described in the equations below are calculated:

1. Wheel rotating speed from the velocity profile

$$V = \frac{\pi \times N_c \times r_d}{30 \times i_g \times i_0} \quad (14)$$

2. Tractive force, as a result of engine torque transmitted on the driven wheels, from vehicle powertrain system, as described in the equation below [5, 19, 21]

$$Ft = \frac{T_e \times i_g \times i_0 \times \eta_t}{r_d} \quad (15)$$

where

$$r_d = 0.97 \times (h + r) \quad (16)$$

2.5. Gearshift strategy

In this step specific shifting points are predicted, via gear shifting strategy for vehicles with manual transmission introduced in (UNECE, 2021). WLTP gear selection algorithm taking into account the different powertrain configurations and was designed in a way to emulate the gear shifting strategy from the real-life driving. The gear shifting process influencing on powertrain inertia and engine output speed, which as a result affects on the vehicle acceleration performance and fuel consumption. Hereby, to represent real-life driving patterns proper calculation of the gear shifting sequence is an important event during the back calculation phase. In order to determine required gears and shifting points the following boundary conditions and data are needed in gear selection algorithm:

1. Boundary conditions that shall not be less or greater (minimum and maximum engine speed, maximum rated engine power and the corresponding rated engine speed, number of forward gears, vehicle velocity limits and others).
2. Full load power curve versus engine speed profile: the engine power demand at the resulting engine speed cannot exceed the full-load output power curve of the engine.

In general term, the calculated gear in WLTP is the gear that ensure that the engine speed is lie between a defined minimum and maximum value while providing the necessary traction power with simultaneous fulfillment of additional requirements described in [17] (i.e. avoidance instabilities in gear shifting, ensuring drive ability and others).

The generated gear shifting sequence with final engine torque vs. time profile for diesel vehicle Volkswagen Golf IV illustrated in Fig. 6 and Fig. 7.

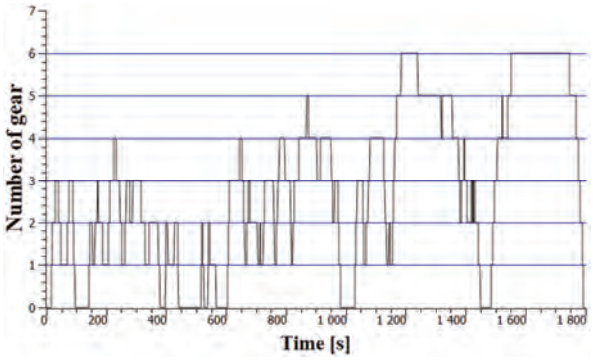

Fig. 6. Calculated gear gearshift strategies

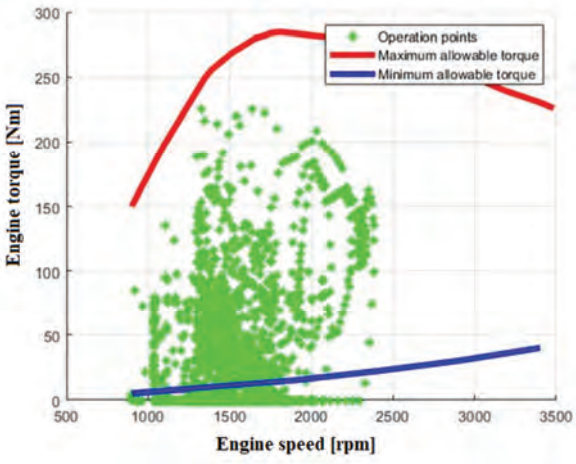

Fig. 7. Calculated engine torque vs. time profile under WLTC 3b

In Figure 7 presented covered speed/power region for selected diesel vehicle during WLTC 3b. Moreover, Fig. 7 shows two curves. Red one represents maximum torque curve presented in (Volkswagen, n.d.). Blue one represents minimum available torque that the engine can obtain. Minimum torque curve is a result of the characteristics of the hydraulic dynamometer (The hydraulic dynamometer always is under load conditions, therefore engine cannot obtain a torque under its minimum).

3. Grid clustering method

In this step we assume that the OP below minimum torque curve (blue line in Fig. 7) does not taken into account during the calculating phase. Calculation of the weighted operation points was performed with a simple grid clustering approach. There are, many different types of Grid Based Clustering Algorithms (CLIQUE (CLUSTERING IN QUEST), STING (A Statistical Information Grid Approach to spatial Data Mining), Wave Cluster and others) that are described in many scientific works such as [10, 12, 20] and others. In general, summarizing the information presented in the above publication, the grid-based clustering algorithm has a features described below. A major advantage of this method is fast processing of the data. The computational complexity depends on the number of cells in the spatial area. The basic concept of a grid clustering method is to organize data, by collecting points that falls within prescribed boundaries (rectangular blocks) into groups. The purpose of clustering is to reduce the amount of data being stored while still producing a set of operation points that represent the overall driving cycle.

A simple density based grid clustering algorithm consists of the following calculation steps:

1. Initialization phase: During this phase user defines the grid size as a step along the X axis and the Y axis.
2. Creation of the grid structure (The quantized space is divided into predetermined (in first step) number of cells to form grid structure).
3. Calculation of the density (amount of OP) for each cluster in the grid structure.
4. Identifying the average values along X and Y axis for each cluster.
5. Selection the operation point (for each cluster) with parameters closest to the average values (X and Y position).
6. Setting the diameter of the OP corresponds to the number of engine operating points in the cluster.

The result of the grid clustering binning is presented in Fig. 8.

To assess the combustion and emission characteristics in a light-duty diesel engine under WLTC a seven steady-state operating points was chosen (Table 4) in the range of engine operating points (Fig. 8). Note that the variations of torque and engine speed within test matrix are the same of the area were the majority of the operation points lie.

Table 4. Selected operation points

OP N°	Engine speed [rpm]	Torque [Nm]	Sampling frequency [kHz]	Share in test[%]
p1	1315	22	72	14.54
p2	1350	56	73	22.28
p3	1375	92	75	6.8
p4	1650	23	90	13.03
p5	1690	71	92	12.74
p6	1726	91	94	7.74
p7	2280	145	124	5.28

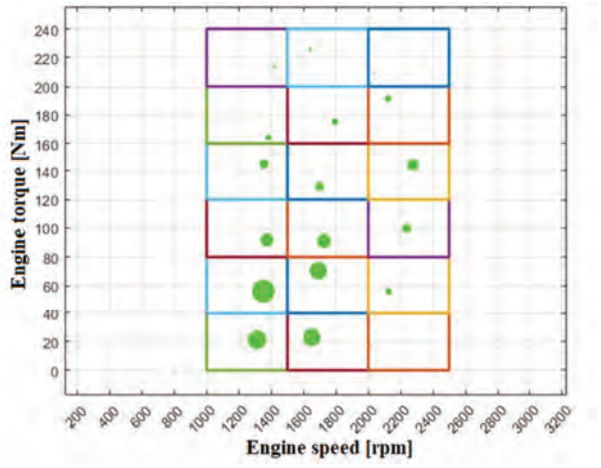

Fig. 8. Binned engine operation points under WLTC 3b

4. Experimental setup

Experiments at seven OP were conducted on a commercial direct injection turbocharged diesel engine AJM 1.9 TDI, made by Volkswagen factory, which is a four stroke, four-cylinder, water-cooled engine. Main characteristics of the base engine are presented in Table 5.

The schematic diagram of the test bench is showed in Fig. 9. Diesel engine has been properly adapted by Ska-Tech company to work under dual-fuel mode (diesel fuel and LPG). In this operation mode LPG in gaseous form inducted directly into the inlet manifold to form homogeneous mixtures with intake air. This fuel mixture ignited by the pilot quantity of diesel fuel directly injected in the cylinder. Dual-fuel mode is a proven solution that allows slightly reduce harmful compounds in exhaust gases. Moreover, dual-fuel adaptation is inexpensive and requires minimum installation of additional components. No additional modifications in EGR rate, engine tuning, i.e. injection timing of the pilot fuel and others does not applying.

In-cylinder pressure is acquired with AutoPSI-S fiber optics-based cylinder pressure sensor made by Optrand Inc. The crankshaft position was measured with a digital shaft encoder type CKQH-58 made LIKA. In order to analyze the in-cylinder pressure and net heat release rate the pressure and crankshaft angle data of 150 consecutive cycles are sampled and recorded. Data acquisition were carried out using the module USB-6212 manufactured by National Instruments that was connected to a PC via USB interface. Sampling frequency of data acquisition module for seven OP was calculated according to the Nyquist–Shannon sampling theorem and presented in Table 4. This theorem states that to accurately reconstruct the waveform of the signal the rate of sampling frequency must be greater more than twice the highest frequency of the signal.

In particular, for the continuous measurement of toxic emissions, the exhaust gas analyzer KIGAZ-310 by KIMO was employed. This gas detector used for measuring oxides of nitrogen (NO_x), carbon monoxide (CO), carbon dioxide (CO_2) and oxygen (O_2) concentration in the exhaust gas.

The net heat release rate (NHRR) is calculated by applying the first law of thermodynamics. The main equation to determine the apparent NHRR for the ICE can be expressed as

$$\frac{dQ}{d\varphi} = \frac{\gamma}{\gamma-1} \times p\frac{dV_c}{d\varphi} + \frac{1}{\gamma-1} \times V_c\frac{dp}{d\varphi} \tag{17}$$

where

$$\gamma = \frac{C_p}{C_v} \tag{18}$$

The consumption of LPG and diesel fuel are measured by an electronic scales made by AWO firm. All the signals from the measuring devices and instruments were fed to a PC via USB interface.

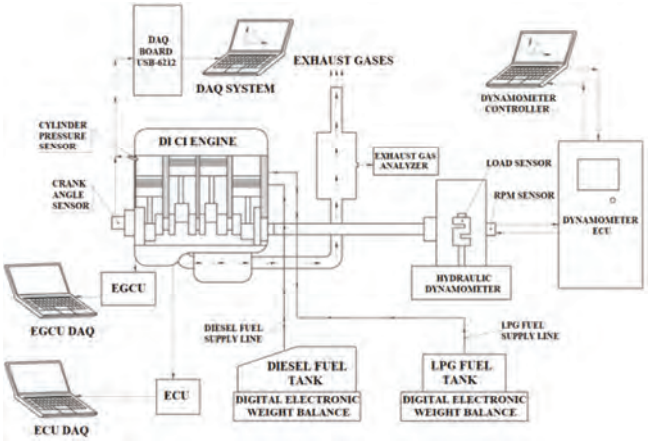

Fig. 9. Test bench schema

Table 5. Base engine specifications

Parameter	Unit	Value
Displacement	[cm^3]	1896
Diesel fuel injector type	–	pump and nozzle unit
Gas fuel injector type	–	4-cylinder LPG/CNG injection rail BARRACUDA
Number of cylinders	–	4
Number of valves per cylinder	–	2
Bore	[mm]	79.5
Stroke	[mm]	95.5
Compression ratio	–	18.0:1
Maximum speed	[rpm]	4000
Rated power	[kW]	85
Maximum torque at 1900 rpm	[Nm]	285

The effects of LPG proportion on combustion and emissions under selected OP are investigated. The test fuel is DF100, DF90, DF80 and DF70, which include 0% LPG, 10% LPG, 20% LPG and 30% LPG on an energy basis respectively. The physic-chemical properties of LPG and diesel fuel are shown in Table 6.

To present the percentage of LPG in the blended fuel on an energy basis, the following equation is used,

$$SR = \frac{\dot{m}_G \times LHV_G}{\dot{m}_D \times LHV_D + \dot{m}_G \times LHV_G} \times 100\% \tag{19}$$

Increasing gaseous fuel quantity means changing the air fuel ratio. In order to ensure an equivalence engine performance for both the normal diesel mode and the dual-fuel mode AFR must be at the same level (or need to be in this range). Obtaining similar AFR for an engine running in single- or dual-fuel mode required calibrations of the

EGCU lookup tables. The calibration process is described in sufficient detail in the previous work [14].

AFR was calculated according to simple equation [7]:

$$\lambda = \frac{21}{21+O_2} \tag{20}$$

where O_2 value presented in Fig. 14.

Table 6. Properties of diesel fuel and LPG [11, 14]

Parameter	Unit	Diesel fuel	LPG (60% butane and 40% propane)
Molecular weight	[g/mol]	96	≈ 52.5
Liquid density at 20°C	[kg/m^3]	800–840	≈ 566
Vapor pressure at 25°C	[bar]	–	≈ 5
Cetane number		40–55	≈ 4
Lower heating value	[MJ/kg]	≈ 42.91	≈ 46
Latent heat of evaporation	[kJ/kg]	250	≈ 405
Stoichiometric air to fuel ratio	[kg/kg]	14.6	≈ 15.2

5. Results and discussion

5.1. The combustion characteristics

Received pressure data was averaging and calculated pressure curves were positioned as a function of crank angle, the results shown in figure below. The effect of various LPG to diesel fuel blends on in-cylinder pressure and net heat release rate in three OP (p1 – 1315 rpm, 22 Nm, p5 – 1690 rpm, 71 Nm, p7 – 2280 rpm, 145 Nm) are shown in Fig. 10. Note, that all motored pressure traces were measured under zero load conditions. It is clearly seen from Fig. 10, that the higher LPG percentage produces lower pressure rise rate compared to diesel fuel. This may refer to the reduction in volumetric efficiency, poor in cylinder mixing quality of fuels (LPG to Diesel), an abundant presence of residual gases and incomplete combustion of the fuel mixture.

It is found that the net heat release rate has same tendency as pressure traces and for diesel NHRR is higher than the other LPG/diesel fuel blends. Lower NHRR except the reasons described above, may informs about low-temperature flames during the combustion. Low temperature leads to a slower reaction rate, which influence on the concentration of NO_x, HC and CO in the exhaust gases. It is also seen that as the load and speed increases, the NHRR increases too. This may refer to a faster reaction rate and better flame propagation with an increase in cylinder pressure.

Furthermore, the reduction in the amount of liquid fuel used to initiate the combustion has adverse effects on the quality of liquid fuel spray. This produces poor liquid fuel preparation and atomization due to a slow development of fine droplets which affects the mixture combustion process [15].

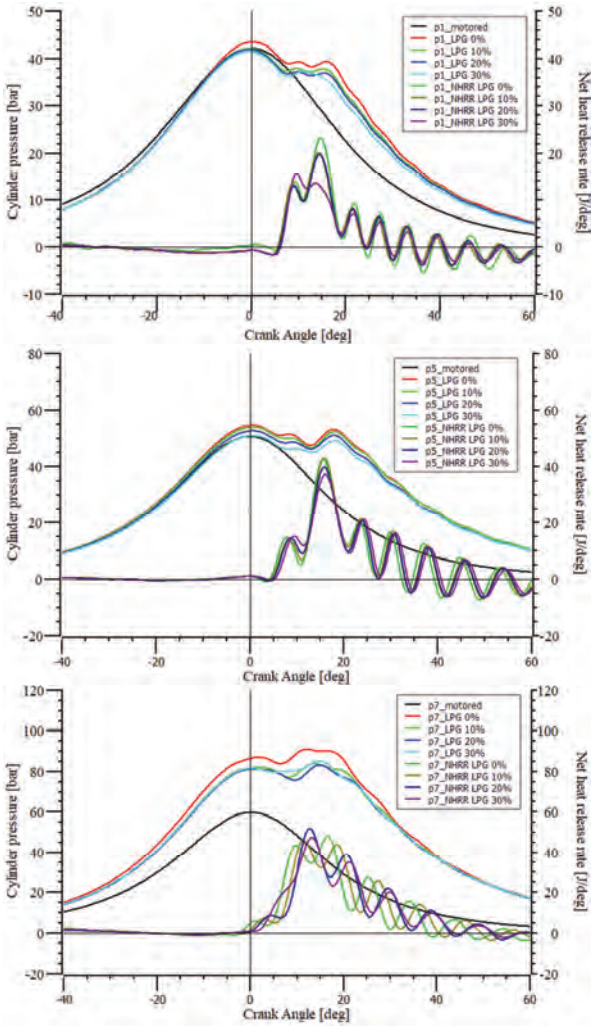

Fig. 10. Cylinder pressure and net heat release rate variations

5.2. Emission characteristics

After averaging the emissions data, the results has been presented in figures below. NO_x is one of the main pollutants emitted by diesel engines, which is toxic and the main precursor to photochemical smog. Nitrogen Oxides (NO_x) are products of burning of hydrocarbon fuels under high pressure and temperature conditions in the cylinder. Figure 11 shows the effect of LPG proportion on NO_x emissions. With the increase of load and engine speed, NO_x emissions increase too due to the higher in-cylinder temperature. Higher LPG proportion in fuel mixture leads to a simultaneous reduction in NO_x emissions. The reasons, to explain this can be:

1. As the LPG proportion increases the quantity of fed diesel simultaneously decreases.
2. The temperature drop of the mixture due to heat absorption during LPG vaporization (as a result of higher latent heat value of LPG).

However, temperature drop can lead to incomplete combustion which results in increasing the content of HC and CO.

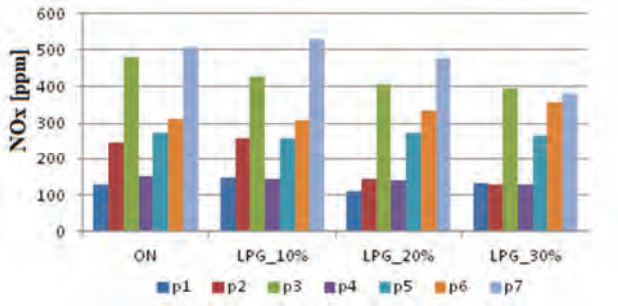

Fig. 11. The comparison of NO_x emissions

Figures 12 and 13 show comparative values of CO and CO_2 in the exhaust gasses. It can be seen that CO emissions are higher under dual- fuel mode than those in single- fuel. The main reason is a low cylinder gas temperature due to temperature drop. In addition CO concentration in exhaust gases possibly increases due to low cetane number of LPG and problems associated with mixing air and gaseous fuel [15]. Carbon monoxide (CO) is a product of incomplete combustion due to limited oxygen supply or an excess of carbon. The higher CO concentration in exhaust gases can be overcome by varying factors i.e. pilot fuel quantity, injection timing. According to the author [3], the CO emissions could be reduced with an earlier injection period, which would promote a better rate of CO emissions decomposition and oxidation. Rise of CO when the LPG proportion increases is caused by not optimal injection timing for dual fuel mode [9].

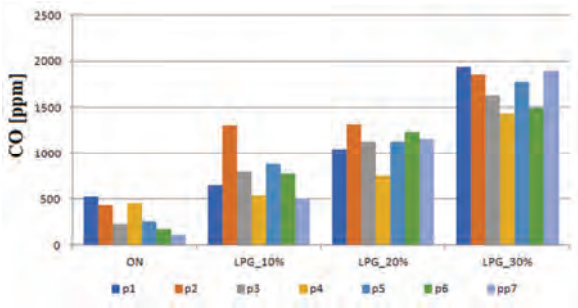

Fig. 12. The comparison of CO emissions

CO_2 as shown in Fig. 13 regardless to LPG proportion is on the same level. This can be explained by the fact that the same AFR (which is confirmed by the content of O_2 in exhaust gases shown in Fig. 14) was maintained at all operational points.

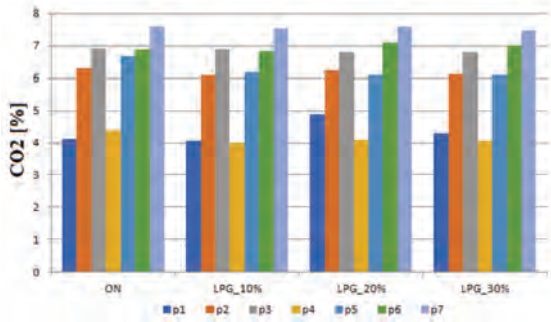

Fig. 13. The comparison of CO_2 emissions

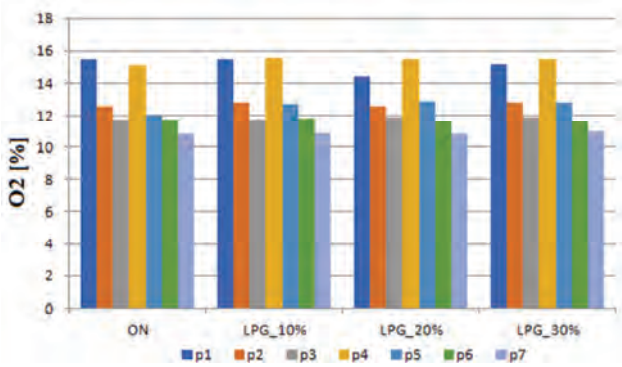

Fig. 14. The comparison of O_2 emissions

6. Summary and conclusions

The present paper collates the outcomes of a wide research activity devoted to evaluating the effect of various LPG proportion on combustion and emissions under WLTC, in a four-cylinder dual-fuel direct injection turbocharged diesel engine AJM 1.9 TDI. Summing up the paper and the results of the research, the main conclusions drawn are:

1. Back calculate methodology was proposed to estimate engine speed and torque during the WLTC driving cycle. The procedure is based on the simple longitudinal dynamics approach.
2. In order to determine OP's, density based grid clustering method was proposed and implemented.
3. The effects of various LPG proportion on combustion and emissions characteristics reveals that, in the tested operating points, the use of LPG offers a reduction of NO_x compared to the diesel fuel. The drawbacks concerning to the LPG use are associated with incomplete combustion, lower pressure rise rate with respect to original ones (diesel fuel) and an increment of unburned hydrocarbons that leads to a strong increment of carbon dioxide emissions. In addition by the fact that the AFR in single- and dual-fuel mode was at the same level, CO_2 emissions under all OP's are similar.

It seems that LPG dual-fuel combustion mode is a promising technique for controlling NO_x emissions [1] especially on existing diesel engines with slight modification to the engine structure. Overall, the proper adaptation and optimization of the diesel engine operating conditions including the injection strategy as well as ECU operation algorithms need to be done in order to obtain the improved performance and engine out emissions in dual-fuel operation mode. For Euro 6 and higher engines, the addition of LPG will worsen the emission factors.

The publication focuses on the preparation of a methodology for testing a dual-fuel engine on an engine dynamometer. Although the diesel and LPG fueled engine was tested, the methodology is being prepared for other synthetic fuels that will be used in the future.

Acknowledgements

The authors wish to express their deep thanks to the Ski-Tech company (street Franciszka Okroja 22, 80-297 Miszewo) for the LPG fuel supply system.

Nomenclature

AFR	air fuel ratio
DAQ	data acquisition system
DF	diesel fuel
ECU	electronic control unit
EGCU	electronic gas control unit
EGR	exhaust gas recirculation
FWD	front wheel drive
LPG	liquefied petroleum gas
NEDC	new European driving cycle
NHRR	net heat release rate
OP	operation point
PMR	power to curb mass ratio
SR	substitution ratio
WLTC	worldwide harmonized light vehicles test cycles
WLTP	worldwide harmonized light vehicles test procedure
Af	cross-sectional area of the vehicle
B	vehicle width
Cd	aerodynamic drag coefficient
C_p	specific heat at constant pressure
Crr	rolling resistance coefficient
C_v	specific heat at constant volume
d_1	mass factor of the engine
d_2	mass factor of the wheel
Fa	aerodynamic resistance
Fgrade	gradient resistance
Fi	inertia resistance
Fr	rolling resistance
Ft	traction force
Ftr	total traction resistance
g	gravitational acceleration
h	tire height
H	vehicle height
i_0	gear ratio of the final drive
i_g	gear ratio of the transmission for selected gear
J_p	moment of inertia of the rotating components associated with the power unit
J_w	wheel moment of inertia
L_{HVG}, L_{HVD}	lower heating values of gaseous and diesel fuel
m_G, m_D	mass flow rates of gaseous and diesel fuel
m_i	vehicle mass of inertia
m_v	total mass of the vehicle, represent mass of the base vehicle unit plus driver and all on-board systems associated with the power train system
N, N_A, N_C, N_S	represent the engine, wheel, clutch, propeller shaft, rotating speed respectively
p	in-cylinder pressure
Q	total amount of in-cylinder heat
r	rim radius
r_d	dynamic radius of the tire
T_e, T_L, T_{tr}	represent the engine, powertrain resistance, traction, torques respectively
Vc	in-cylinder volume
V	velocity of the vehicle
α	slope angle of the road
γ	ratio of the specific heats
δ	mass factor
η_t	driveline overall efficiency
λ	air fuel ratio
ρ	air density
φ	crank angle

Bibliography

[1] ASHOK, B., ASHOK DENIS, S., RAMESH KUMAR, C. LPG diesel dual fuel engine – a critical review. *Alexandria Engineering Journal.* 2015, **54**(2), 105-126. https://doi.org/10.1016/j.aej.2015.03.002

[2] DĘBICKI, M. Teoria samochodu: teoria napędu. *Wydawnictwa Naukowo-Techniczne*, Warszawa 1976.

[3] ECKERT, J.E., SANTICIOLLI, F.M., COSTA, E.S. et al. Vehicle gear shifting co-simulation to optimize performance and fuel consumption in the brazilian standard urban driving cycle. *Blucher Engineering Proceedings.* 2014, **1**(2), 615-631. https://doi.org/10.5151/engpro-simea2014-81

[4] GENG, P., CAO, E., TAN, Q. et al. Effects of alternative fuels on the combustion characteristics and emission products from diesel engines: A review. *Renewable and Sustainable Energy Reviews.* 2017, **71**, 523-534. https://doi.org/10.1016/j.rser.2016.12.080

[5] GIAKOUMIS, E.G., ZACHIOTIS, A.T. Investigation of a Diesel-engined vehicle's performance and emissions during the WLTC driving cycle – comparison with the NEDC. *Energies*. 2017, **10**, 1-19. https://doi.org/10.3390/en10020240

[6] JAZAR, R. Vehicle Dynamics: Theory and Application: Third Edition. *Springer.* Cham 2017. https://doi.org/10.1007/978-3-319-53441-1

[7] KIMO Kigaz. Combustion gas analyser. User manual. 1-24, 2010.

[8] KROPIWNICKI, J. Modelowanie układów napędowych pojazdów z silnikami spalinowymi. *Wydawnictwo AGNI.* Pruszcz Gdański 2016.

[9] LUFT, S. A dual-fuel compression ignition engine – distinctive features. *Combustion Engines*. 2010, **141**(2), 33-39. https://doi.org/10.19206/CE-117144

[10] GAN, G., MA, C., WU, J. Data Clustering: Theory, Algorithms, and Applications. *ASASIAM Series on Statistics and Applied Probability*. 2007. https://doi.org/10.1137/1.9780898718348

[11] MATHWORKS. Vehicle Body 1DOF Longitudinal. Retrieved from https://www.mathworks.com/help/autoblks/ref/vehiclebody1doflongitudinal.html

[12] MR, I., MOHAN, D. A survey of grid based clustering algorithms. *International Journal of Engineering Science and Technology.* 2010, **2**, 3441-3446.

[13] PARK, S.H., LEE, C.S. Applicability of dimethyl ether (DME) in a compression ignition engine as an alternative fuel. *Energy Conversion and Management*. 2014, **86**, 848-863. https://doi.org/10.1016/j.enconman.2014.06.051

[14] STEPANENKO, D., KNEBA, Z. ECU calibration for gaseous dual fuel supply system in compression ignition engines. *Combustion Engines*. 2020, **182**(3), 33-37. https://doi.org/10.19206/CE-2020-306

[15] TIRA, H.S., HERREROS, J.M., TSOLAKIS, A. et al. Characteristics of LPG-diesel dual fuelled engine operated with rapeseed methyl ester and gas-to-liquid diesel fuels. *Energy.* 2012, **47**(1), 620-629. https://doi.org/10.1016/j.energy.2012.09.046

[16] TUKIMAN, M.M., OSMAN, S.A., FAWZI, M. et al. Effect of performance and exhaust emission using liquid phase LPG sequential injection as an alternative fuel in spark ignition engine. *International Journal of Integrated Engineering*. 2018, **10**(8), 223-230. https://doi.org/10.30880/ijie.2018.10.08.032
[17] UNECE Worldwide Harmonized Light Vehicles Test Procedure (WLTP). 2021.
[18] VOLKSWAGEN. The Self-Study Programme 209 1.9-ltr TDI Engine with pump injection system. Retrived from http://www.volkspage.net/technik/ssp/ssp/SSP_209.pdf
[19] VWGolf.pl. Dane techniczne Volkswagen Golf 4. Retrived from https://www.vwgolf.pl/dane-techniczne/vw-golf-mk4/
[20] WANG, L., LI, H. Clustering algorithm based on grid and density for data stream. *AIP Conference Proceedings*. 2017, **1839**, 020202. https://doi.org/10.1063/1.4982567
[21] WARCZEK, J. Metoda pomiaru promienia dynamicznego koła samochodowego. *Zeszyty Naukowe Politechniki Śląskiej*. 2010, 7, 97-103.

Zbigniew Kneba, DSc., DEng. – Faculty of Mechanical Engineering and Ship Technology, Gdansk University of Technology.
e-mail: *zkneba@pg.edu.pl*

Denys Stepanenko, MEng., PhD student – Faculty of Mechanical Engineering and Ship Technology, Gdansk University of Technology.
e-mail: *denstepa@pg.edu.pl*

Jacek Rudnicki, DEng. – Faculty of Mechanical Engineering and Ship Technology, Gdansk University of Technology.
e-mail: *jacekrud@pg.edu.pl*

Article citation info:
JAROŃ, A., BORUCKA, A., SOBECKI, G. Assessment of the possibility of using nanomaterials as fuel additives in combustion engines. *Combustion Engines*. 2022, **189**(2), 103-112. https://doi.org/ 10.19206/CE-143824

Agata JAROŃ
Anna BORUCKA
Grzegorz SOBECKI

Combustion Engines
Polish Scientific Society of Combustion Engines

Assessment of the possibility of using nanomaterials as fuel additives in combustion engines

ARTICLE INFO

Received: 26 September 2021
Revised: 30 October 2021
Accepted: 9 November 2021
Available online: 5 December 2021

Nanomaterials are a new group that has quickly found a wide range of applications in medicine, cosmetology, the food, weapons or automotive industry. They are also used as a fuel additive. This paper reviews the literature and assesses the current state of knowledge regarding the use of nanoparticles in automotive engine fuels. The results obtained so far are presented and further research directions in this field are identified.

Key words: *internal combustion engines, diesel fuel, fuel additives, emission of pollutants, engine operation*

1. Introduction

Road transport is the most prevalent mode of transportation. Internal combustion engines are invariably the most popular form of propulsion and diesel is the dominant fuel. This results in high environmental pollution, mainly due to emission of harmful substances such as carbon monoxide, particulate matter, unsaturated hydrocarbons and nitrogen oxides into the atmosphere, which contribute to the formation of smog. The pollution produced poses a threat not only to the ecosystem, but also to human health and life. In order to reduce the problem resulting from the use of internal combustion engines, a number of researches are being conducted in a variety of areas related to efficient combustion, fuel cleaning technology, catalytic technology, particulate filters, and the use of alternative fuels. Strict regulations related to the limitation of pollutant emissions force both scientists and entrepreneurs to look for alternatives to fossil fuels (e.g. biodiesel, dimethyl ether, alcohols, natural gas, dimethyl carbonate or hydrogen [9]). In addition, additives are used to reduce harmful emissions. These include calcium-, phosphorus-, silicate-, alcohol-based products, tertiary additives like nitromethane, nitroethane, methyl ester, nano additives [4, 7]. These are very rapidly growing areas. In this article, the authors have undertaken to analyze and evaluate current developments in the area related to the use of fuel additives, limiting the review study conducted to nanomaterials. The aim of the paper is to present the possibility of their application as fuel additives, to show potential benefits resulting from their use and to justify the necessity of conducting further research, especially in view of their so far marginal application in the automotive industry, estimated (in relation to other branches of industry) at about 1% [13]. The authors hypothesized (research hypothesis) that the use of nanomaterials as fuel additives is an important element in the development of the automotive industry in line with the sustainable transport paradigm because it contributes to the reduction of harmful emissions to the atmosphere through chemical mechanisms and the presence of functional groups capable of improving fuel combustion quality.

2. Characteristics of nanomaterials

Nanomaterials are a group of materials both naturally occurring and synthesized, of any dimension, but having structure at the nanoscale i.e. 1 to 100 nm [3]. Nanomaterials are characterized by very good mechanical, electrical, optical and thermal properties. Nanomaterials find wide applications in automotive industry, including production of paints, coatings, lubricants, materials for electrical and electronic devices, sensors, etc. They are also produced as a lightweight material with high strength as well as corrosion and heat resistance, used in structural components [1]. However, the authors would like to pay special attention to their use as a fuel additive. According to available research in this area, nanoparticles are effective in reducing emissions and improving engine performance [17]. The use of additives can change parameters such as density, volatility or sulfur content [17]. In addition, it affects ignition time, ignition delay, friction, and emissions of harmful pollutants such as nitrogen oxides, carbon monoxide, carbon dioxide, unburned hydrocarbons, smoke.

The most popular nanomaterials include cerium oxide, carbon nanotubes, aluminum oxide, titanium oxide, graphene oxide, aluminum oxide, iron oxide, copper oxide, and zinc oxide. Their chemical and physical properties are presented later in this article.

2.1. Physical and chemical properties of nanomaterials

Carbon nanotubes

Carbon nanotubes are allotropic varieties of carbon, long, thin, and cylindrical in shape, about 1–3 nm in diameter and hundreds to thousands of nanometers in length [4, 16]. In terms of structure, carbon nanotubes can be divided into: Single-Wall Carbon Nanotubes (SWCNT) and Multi-walled Carbon Nanotubes (MWCNT). Single-wall carbon nanotubes consist of a single graphene sheet with a tube-like structure, while multi-walled ones consist of multiple graphene sheets [2, 16].

Single-wall nanotubes range from 0.4 to 10 nm in diameter while multi-walled ones from 10 to 100 nm [2]. Carbon nanotubes are characterized by their ability to form oxi-

dized forms of CNTs by the action of acids such as nitric, sulfuric, or potassium manganate Oxidized carbon nanotubes dissolve better in water by becoming more polar [21]. Comparing carbon nanotubes to conventional powdered or granular activated carbon, they feature a large active surface area to volume ratio, thus showing a higher potential to remove heavy metals from water, while conventional activated carbon is characterized by a smaller active surface area and activation energy [16].

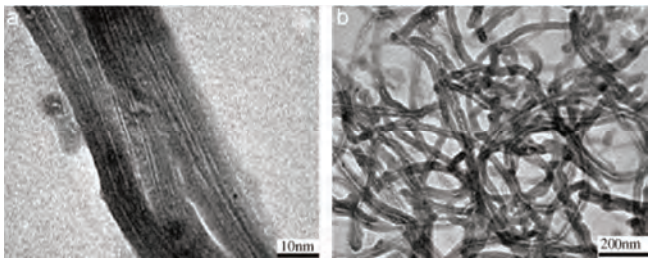

Fig. 1. Shows a) single-wall carbon nanotubes b) multi-walled carbon nanotubes [24]

Metal oxides and non-metal oxides

Metal oxide nanoparticles include mainly TiO_2, Fe_3O_4, SiO_2, Al_2O_3. They are of interest to a wide range of researchers due to their versatile properties, which include environmental friendliness, non-toxicity, high electrical and mechanical conductivity, large specific surface area, ease of synthesis and low manufacturing cost. They find application mainly in sorption or composite formation. Metal oxide composites with porous structures are gaining popularity because they exhibit, due to combining different material properties, higher yield compared to conventional metal oxides [20].

Iron nanoxide

Iron oxide-based nanomaterials exhibit great potential for eliminating pollutants due to their superparamagnetism. They are characterized by low production costs, are easy to obtain, have a large surface-to-volume ratio, and are harmless. Iron nanoxides find vast application in adsorption due to their high SSA (specific surface area) (30–100 gm^{-1}) [22]. They feature reactive surface sites and functional groups, which contributes to the effective adsorption of contaminants.

Iron oxide-based nanoparticles come in various forms, e.g.: nano ovals, nano rings, nano strips and graphene-based complexes for the elimination of heavy metals. In nature, iron oxides occur in several forms such as hematite (α-Fe_2O_3), magnetite (Fe_3O_4), maghemite (γ-Fe_2O_3), goethite (α-FeOOH), lepidocrocite (γ-FeOOH), and hydrous ferric oxide (HFO).) However, hematite, magnetite, and maghemite have found the greatest use in water treatment because they exhibit extraordinary surface charge properties and redox activity, as well as polymorphism that includes a temperature-induced phase transition and unique magnetism [19]. Hematite is a relatively inexpensive adsorbent and is the most stable iron oxide. It is used for adsorption of organic pollutants and heavy metals [19]. Magnetite also has a strong affinity for ions such as Pb(II), Cu(II), Cd(II). Magnetite exhibits a reducing ability that contributes to adsorption. According to [19], γ-Fe_2O_3 reduces Cr(IV) to Cr(III) and causes its immobilization on the surface. It is also an effective adsorbent of As(V) because it shows high affinity between Fe^{3+} and As^{5+} [19].

Iron oxides: Fe_3O_4 and γ-Fe_2O_3 are characterized by strong magnetic properties, which depend on the particle size, composition and shape – when the particle size is 15 nm or 40 nm, they can already obtain supermagnetic properties [19], i.e. that they are attracted by a magnetic field, but do not retain magnetic properties after the field is removed.

Aluminum oxide

They are characterized by low manufacturing cost, significant toxicity, large specific surface area, large pore volume. The following forms can be distinguished: hexagonal, orthorhombic, monoclinic, tetragonal and cubic, core. According to [19], aluminum oxide exhibits a strong affinity for adsorption of arsenic and fluorine. Mesoporous γ-Al_2O_3 show the best adsorption properties for heavy metal removal.

Titanium dioxide

Nano titanium dioxide has a dual application: adsorption and photocatalysis of organic compounds. Photocatalysis does not work in the case of high concentrations of organic pollutants due to poor light transmission. On the other hand, titanium dioxide-based nanomaterials show high adsorption capacity of heavy metal ions like lead, cadmium, tin, nickel and copper. According to [6], there are several mechanisms for adsorption of contaminants on titanium dioxide. The Ti(IV) ion can act as a Lewis acid due to the uncompensated positive charge that coordinates molecules with a free pair of electrons. In contrast, O_2^- is a Lewis base and adsorbs acidic molecules and cations. Other interactions between titanium dioxide and impurities include hydrogen bonding and electrostatic interaction.

Graphene oxide

The oxidized form of graphene is graphene oxide (GO), which is formed by oxidation and exfoliation. Graphene oxide contains an oxygen-containing group. It can be a: phenolic, carboxyl, hydroxyl or epoxy group.

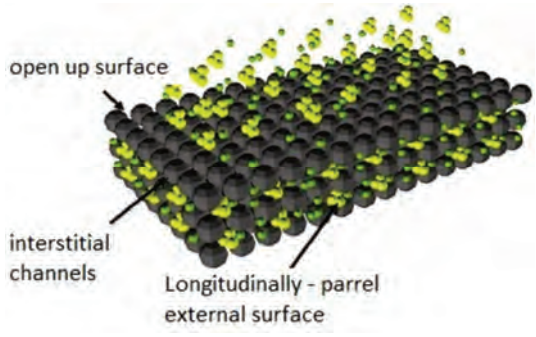

Fig. 2. Structure and adsorption site of graphene sheets [2]

Consequently, the surface has a negative charge and positive ions can be attracted by electrostatic interaction. The adsorption efficiency can be improved by introducing additional oxygen-containing groups from polymer particles, metal oxides or hydroxides. These can include caboxymethyl cellulose, ethylenediaminetetraacetic acid

(EDTA), ZnO, acetylacetone and TiO_2. The reaction occurring between ions and groups depends on the pH value. As pH increases, the oxygen-containing groups are deprotonated and as a consequence the adsorbent surface is more negatively charged – the attraction of positively charged cations increases. However, with a decrease in pH, protonation and the reverse phenomenon occurs [22]. In addition, pH also affects the very form of heavy metal cations that can hydrolyze to hydroperoxides. At high pH, precipitation of cations may occur or negatively charged hydroxides will form, which will electrostatically repel from the adsorbent.

3. Nanoparticles as fuel additives

3.1. Cerium oxide

According to [11], cerium oxide has the ability to catalyze combustion reactions by passing oxygen ions from its lattice structure. The addition of cerium oxide to the fuel aids in the breakdown of unburned hydrocarbons and their residues, thereby reducing toxic vapor emissions while consuming less fuel. The addition of cerium oxide helps to reduce the weight of the fuel in the combustion chamber, which limits the formation of nitrogen oxides and makes ignition reactions more efficient. In [23], tests consisting in adding cerium nanoxide at 100 mg/l to diesel fuel and checking its effect on the performance of a four-stroke diesel engine were carried out. The nanopowders were 25 nm (Ce_{25}) and 50 nm (Ce_{50}) in size. The parameters of nano additives used in the study are summarized in Table 1.

Table 1. Physical characteristics of the materials used [23]

Type	Bulk density [g/cm^3]	Specific surface area [m^2/g]	Size [mm]
Ce_{25}	0.53	30–50	Max 25
Ce_{50}	0.53	30–50	Max 50

Ce_{25}, Ce_{50} were mixed with standard diesel at 40 ppm and then ultrasonically vibrated for two hours to obtain a homogeneous blend. After 24 hours, the mixtures were pumped into a fuel tank at the test stand. Diesel fuel produced by Coryton Advanced Fuels was used as a reference.

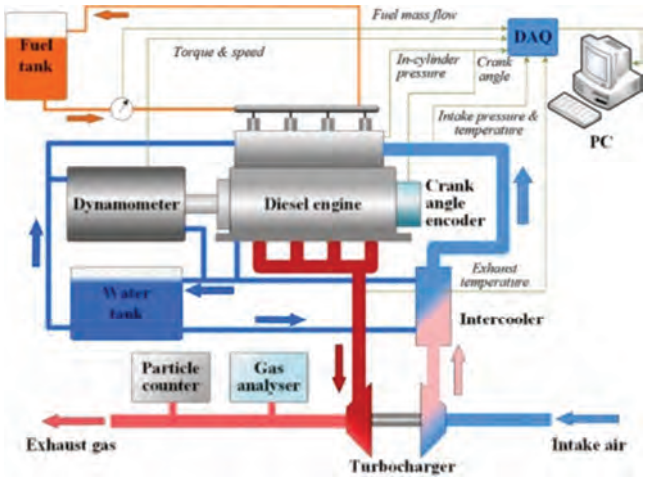

Fig. 3. Measuring station [23]

The study was conducted using a Cummins ISBN four-stroke diesel engine. Fuel was compressed through a common rail and injected through four injector ports. Flow rate was measured with a Coriolis flowmeter, while pressure was controlled in the third cylinder using an AVL QC34C pressure transducer. The gas analyzer detected carbon monoxide, nitrogen oxides, and unburned hydrocarbons.

Fuel was pumped into the fuel tank. The engine was run for 20 min at 1,600 rpm and 25% load to consume all the fuel in the system and warm up the engine. After the experiment was completed with the test fuel, it was drained and the lubricating oil was renewed. The next day, all steps were repeated using a new batch of test fuel. The experimental conditions lasted for two minutes. Pressure, flow rate, and gaseous emissions were recorded. Based on the research conducted, the following conclusions were made in each area [23].

Fuel consumption

The additives used have no significant effect on the diesel engine's fuel consumption. The cerium nanoxide alters only the physicochemical properties resulting from the atomization and reaction rates of the composition and fuel products.

CO emissions

CO emissions are dependent on engine speeds. Emissions increase with increasing engine load because the air-fuel ratio decreases at high load, causing incomplete combustion when oxygen is in short supply.

At certain threshold values, emissions fall and then rise sharply. This is because at high speeds the combustion time is shorter causing more incomplete combustion which accelerates CO production. At high loads, CO emissions are reduced compared to regular diesel.

NO_x emissions

The addition of CeO_2 nanopowders contributes to the reduction of NO_x. The cerium oxide assumes the function of a catalyst that promotes oxidation of unburned fuel compositions. Ce_2O_3 contributes to the deoxidation of oxidation products. NO_x oxides are reduced using the equation [23]:

$$Ce_2O_3 + 2NO \rightarrow 2\,CeO_2 + \frac{1}{2}\,N_2$$

Ce_{25} is characterized by higher specific NO_x emission than Ce_{50}, which is a consequence of the different sizes of CeO_2 nanopowders. As [23] studies have shown, fuels with nano additives produce lower emissions compared to regular diesel.

Emissions of unburned hydrocarbons

Emissions of unburned fuel compositions is favored by incomplete combustion, atomization, as well as high temperature and presence of oxidants. As [23] studies have shown, emissions decrease with increasing load at all speeds. Unburned fuels easily oxidize and form soot – so-called particulates – due to carbonization and dehydrogenation.

The nano additive reduces unburned hydrocarbon emissions, but only at certain speeds in the 1,490–1,855 rpm range. Hydrocarbon emissions decrease at 2,200 rpm as they then spend less time in the combustion chamber where the reaction is limited.

PM emissions

The addition of nano-oxide contributes to lower emissions than for pure diesel, regardless of changing load and speed. This is because cerium oxide oxidizes particulate matter and simultaneously consumes unburned components (particles, elements) of fuels before they can be converted to particulate matter by carbonization and dehydrogenation reactions. However, Ce_{25} particles are characterized by lower specific emissions than Ce_{50} because the small size particles can more easily aggregate unburned fuel particles.

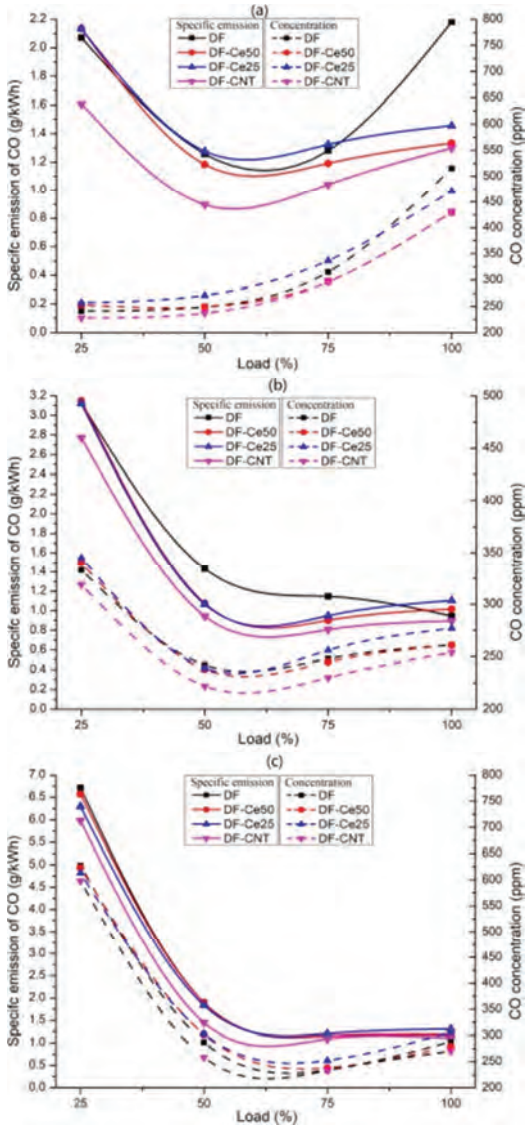

Fig. 4. CO emission from the tested fuels at engine speeds of 1490 rpm (a), 1855 (b), and 2200 rpm (c) [24]

3.2 Carbon nanotubes

A group of particular importance are carbon nanotubes (CNTs), which due to their high magnetic, electrical, optical and thermal conductivity exhibit a significant potential for use as fuel additives to improve performance and reduce emissions of harmful substances. The research conducted in [14] focused on studying the effect of adding multi-walled carbon nanotubes (MWCNTs-COOH) to biodiesel as an admixture to standard diesel fuel. The test was conducted in one cylinder of the engine.

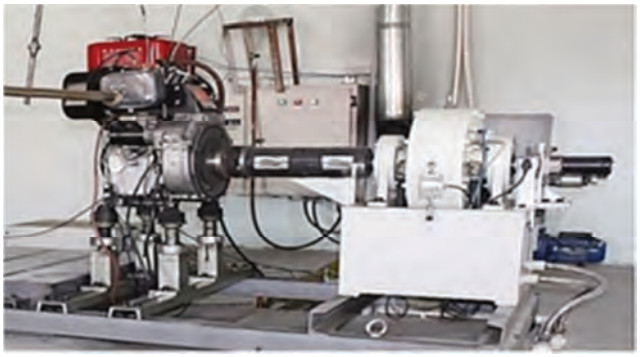

Fig. 5. Engine and dynamometer [14]

As reported by [14] MWCNTs-COOH have amide groups that are able to react with many reagents. Multi-walled carbon nanotubes (MWCNTs-COOH) were mixed at 30, 60, 90 ppm with a solution containing 95% diesel fuel and 5% biodiesel (B5). The fuel was mixed for 30 min in an ultrasonic device to obtain a homogeneous blend.

As reported in [14], a DICOM 50.115/5 model diesel engine was used. An eddy current test bed with remote control (MPA-40 model) was used to measure torque, while an emission tester was used to measure exhaust gas. Physiochemical parameters like dynamic and kinematic viscosity and flash point were determined after blend (fuel) preparation. The tests were conducted for three speeds of 1,800, 2,100 and 2,400 rpm at full engine load. In addition, power, torque, temperature, pressure, and ambient humidity were recorded during each test. The running time of the engine was 10 min. The following results were obtained [14].

Technical performance of the engine

Adding multi-walled carbon nanotubes to the diesel/biodiesel mixture increases torque and braking power, which is defined as the rate of work done by the engine. The fuel mixture of B5 and MWCNTs-COOH at 1,800, 2,100 and 2,400 rpm results in 20.58%, 20% and 7.59% increase in power, respectively. The increase in power and torque is explained by improved combustion quality inside the cylinder (combustion is complete). The functionalized nanotubes have sufficient oxygen amount which contributes to complete combustion. Another reason for the increase in power and torque is the catalytic activity of the nanoparticles, which results in a reduction in ignition delay and fuel combustion time. In addition, MWCNTs-COOHs enhance heat transfer as a result of increase in the surface-to-volume ratio. Moreover, the addition of nanotubes reduces the viscosity of the fuel, resulting in increased power. The specific fuel consumption increases due to the addition of MWCNTs-COOH which is explained by faster combustion, higher heat release and lower combustion delay.

Environmental parameters

Carbon monoxide (CO)

Carbon monoxide is produced by semi-combustion, i.e. with a limited amount of oxygen. Carbon monoxide formation in the combustion process can also be caused by low flame temperatures. Oxygen groups, present in multi-walled carbon nanotubes, help increase the oxygen present in combustion, resulting in improved combustion and lower

emissions of environmentally harmful carbon monoxide. Tests conducted in [14] showed that there was a reduction in CO emissions at all speeds.

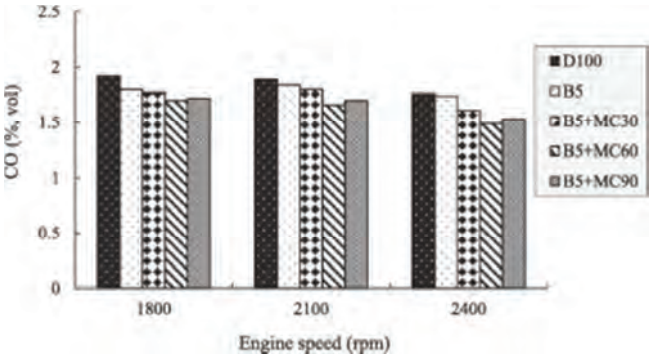

Fig. 6. Effect of the additive on CO emission [14]

Compared to conventional diesel, the blend of B5 fuel and carbon nanotube additive resulted in reductions of 11.45%, 10.05% and 15.34% at 1,800, 2,100 and 2,400 rpm, respectively.

Carbon dioxide (CO_2)

Providing additional oxygen from MWCNTs-COOH additives and converting semi-combustion to complete combustion produces more carbon dioxide on combustion. In a study published by [14], the increase in emissions produced by carbon nanotube fuel blend at 1,800 and 2,100 rpm amounted to 14.28% and 26.92%, respectively.

Unburned hydrocarbons UHC

Unburned hydrocarbons are produced by low temperature combustion and dilution of the fuel mixture. Using carbon nanotubes, the reduction in UHC formation at 1,800 and 2,100 rpm for diesel amounted to 18.91%, 20.58%, and 13.04% and 15.55%, respectively, compared to B5 fuel [14].

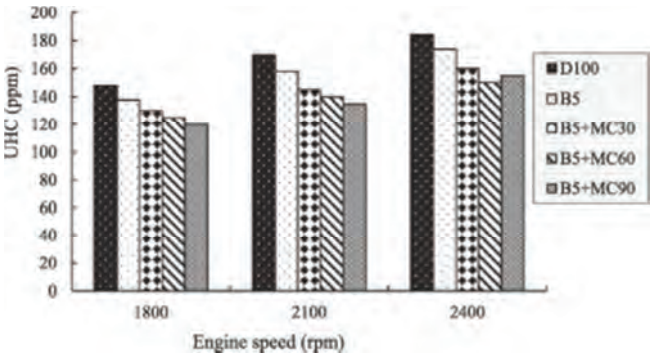

Fig. 7. Effect of the additive on UHC emission [14]

The decrease in emissions is explained similarly to CO and CO_2 by an improvement in combustion quality due to the supply of oxygen. In addition, the use of carbon nanotubes improved atomization and fuel distribution in the chamber by oxidizing hydrocarbons and carbon monoxide.

Nitrogen oxide NO

Combustion temperature is responsible for nitrogen oxide emissions. The higher the temperature, the higher the nitrogen oxide emissions. The combustion temperature depends on the cetane number and the quality of the fuel. According to [14], the addition of carbon nanotubes to fuel increases NO emissions by 0.74% and 0.24% on average compared to diesel and diesel/biodiesel blend.

Aluminum oxide

Aluminum nanoxide has a larger surface area compared to the bulk. Nano Al_2O_3 has a small size so it can be mixed in biodiesels and used in compression ignition engines NO emission problems and performance degradation can be reduced by using some nano additives. A fuel blend of 80% diesel and 20% biodiesel, 100 mg/ml alumina nanoparticles and isopropanol – as a surfactant – which prevented phase separation were used in a study conducted in [12]. The blend was ultrasonically treated to reduce particle agglomeration.

Thermal efficiency of braking:

The addition of aluminum nanoxide to diesel fuel increased the viscosity, which contributed to a decrease in fuel atomization and combustion rate.

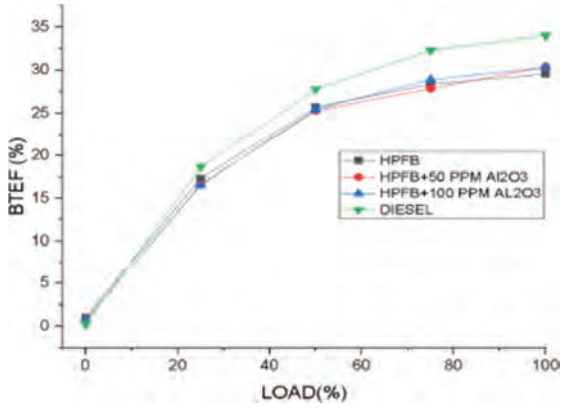

Fig. 8. Effect of the additive on thermal efficiency of braking [12]

There are slight differences in thermal efficiency between the pure diesel tested and the diesel with nano additive. However, the addition of aluminum oxide causes a slight decrease in thermal braking efficiency.

Exhaust temperature

At low engine loads, the exhausts temperatures of both fuels were similar. In contrast, the temperature of both exhausts increases at higher loads. This is explained by the fact that complete combustion occurs at low load. As the viscosity of the fluid increases, the load increases, resulting in a higher exhaust temperature.

According to the relation presented in [12], the addition of aluminum oxide slightly contributes to the increase in exhaust temperature.

Carbon monoxide emissions

As reported by [12, 15] as the workload of the diesel engine increases, CO emissions increase, but the addition of aluminum oxide causes the increase in emissions to be less.

Carbon dioxide emissions

The use of biodiesel as a diesel additive increases CO_2 emissions. In tests conducted in [12], it was shown that the use of aluminum oxide nano-additive in combination with bio-

diesel reduces carbon dioxide emissions, which is, however, still higher than in the case of pure diesel at all engine loads.

Hydrocarbon emissions

Studies in [12, 15] have shown that at all engine loads, nano-oxide results in lower hydrocarbon emissions (similar to carbon dioxide emissions) but hydrocarbon emissions are the lowest in the case of pure diesel.

NO_x emissions

The results obtained in [12] show that at engine loads of 0%, 25% and 100%, the highest emissions are recorded for pure diesel compared to high performance fuel and high performance fuel with 50 and 100 ppm aluminum oxide additives. A mixture with a concentration of 100 ppm oxide gave the lowest toxic NO_x emissions.

Titanium oxide

Titanium oxide nanoparticles have found application primarily as a biodiesel additive. They are able to improve engine performance and reduce harmful emissions. The tests conducted in [8] used a Kirloskar TV1 four-stroke, single-cylinder, vertical, water-cooled engine. The test fuels were fed to the engine under varying load conditions controlled by a dynamometer. Fuel consumption was recorded every 10 seconds. Smoke, hydrocarbon emissions, NO_x, CO, CO_2 were characterized. Brake thermal efficiency, volumetric efficiency, exhaust temperature and specific fuel consumption were also tested.

Specific fuel consumption

Defined as the total amount of fuel burned by an engine per unit of mechanical work or energy, decreases with engine load [8]. The addition of titanium nanoxide results in reduced fuel consumption compared to biodiesel. Both in [8] and [18] studies, fuel consumption decreased with the increase in TiO_2 concentration. However, a nano-additive concentration above 250 ppm is not recommended as the engine will not run satisfactorily.

Thermal efficiency of the brake

It is the ratio between the braking (output) power and the output heat. In other words, the ability to convert an input such as heat into mechanical energy. The addition of titanium oxide at engine efficiencies above > 60% results in better efficiency than for regular biodiesel [8].

Carbon monoxide emissions

The addition of TiO_2 nanoparticles reduces emissions compared to diesel [18]. This can be explained by the higher activation energy of titanium dioxide, which, by acting as an antioxidant, causes complete combustion.

Carbon dioxide emissions

In [8] tests, carbon dioxide emissions for pure biodiesel were the lowest. However, the higher the concentration of titanium oxide in the blend, the lower the emission. At 200 ppm, emissions were already at levels comparable to pure biodiesel.

Unburned hydrocarbons

Unburned hydrocarbons show the extent to which the fuel has not been burned properly. These compounds are the major smog contributors in large cities. In both [8, 18] tests, hydrocarbon emissions were lower in case of titanium oxide fuels. However, tests in [18] have additionally shown that a blend with biodiesel alone produces lower emissions than pure diesel. TiO_2 nanoparticles contribute to complete combustion resulting in lower emissions of environmentally troublesome hydrocarbons. According to [18], as TiO_2 concentration increases, hydrocarbon and carbon monoxide emissions increase. This is explained by increased viscosity, lower heating value and flash point.

Nitrogen oxides (NO_x)

Observing the results obtained in [8, 18] one can see an increase in nitrogen oxide emissions in case of both pure and blended with titanium oxide biodiesel, compared to diesel. The increase in NO_x emissions may be a consequence of increased combustion rates, resulting in higher temperatures and oxygen availability for oxidation. However, tests [8] showed that at a concentration of 200 ppm TiO_2, NO_x emissions are lower compared to biodiesel.

Graphene oxide

Recently, monolayer graphene has gained great popularity. It is non-toxic, features a high surface-to-volume ratio, thermal dissociation and chemical volume.

Graphene has atoms in sp^2 hybridization state and has two-dimensional flat sheets of carbon atoms. Graphene oxide is graphene with oxygen functional groups in its structure. These groups may include: hydroxyl (-OH), epoxy (-C-O-C), carbonyl (C=O) and carboxyl (COOH) groups [5].

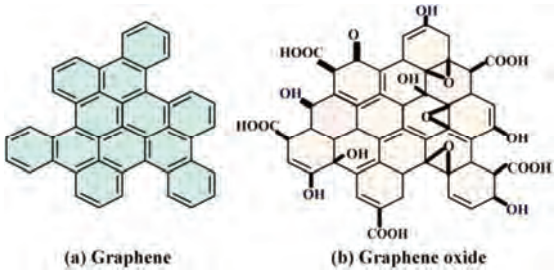

Fig. 9. Chemical structure of graphene and graphene oxide [5]

In the test conducted in [5], a blend of diesel fuel and graphene oxide with different concentrations, i.e: 20, 40, 60 ppm, was used to check the effect of GO additive. The fuel blend was prepared in two stages. First, 1 liter of fuel was mixed with nano additives using a magnetic stirrer at 900 rpm for 20 min. In the second step, the blend was placed in an ultrasonic probe to improve stability. A two-cylinder, four-stroke turbocharged diesel engine was used for the test. The engine was controlled by an electronic control module. The study was conducted with a triple injection sequence. Analytical results obtained

Friction characteristics

According to [5], fuel composition and the presence of additives affect friction – mainly sliding friction – in the fuel injector. The presence of graphene oxide results in reduced friction in all three fuels tested. GO nanoparticles are highly permeable, and when mixed with fuel, they reduce sliding friction between fuel particles and the injector surface.

Ignition delay

The ignition delay is strongly dependent on the cetane number. The presence of GO nanoparticle affected the ignition delay. The greatest reduction was observed at a concentration of 40 ppm. Graphene oxide has functional groups that are able to carry oxygen and facilitate fuel combustion.

Combustion time

The use of the nano additive reduced the combustion time. This is explained by the fact that GO has catalytic activity, where a large surface area increases the rate of combustion. According to [5] the most effective concentration is 40 ppm (not 60 ppm). The GO concentration in the fuel must not be too high because agglomeration of individual particles can occur due to Van der Waals forces. Particle agglomeration can reduce the total surface area, resulting in a weakened performance of the nano additive.

Mass fraction burn

As [5] test results show, the presence of GO contributes to faster fuel burn. The faster combustion rate is explained by the fact that the instantaneous fuel-air reaction zone is charged by the presence of oxygen in the functional groups.

Temperature in cylinder

For pure diesel, a temperature decrease of 31°C was observed at a concentration of 40 ppm GO, while a temperature increase of more than 20°C was observed for the diesel/biodiesel blend, obtaining divergent results. The reduction in temperature is a consequence of the reduction in ignition. Another reason may be the ability of nanoparticles to adsorb heat.

Specific fuel consumption

Biodiesel blends showed higher fuel consumption than base diesel due to the limited heating value. The addition of GO nano additive showed a positive effect on fuel consumption. The reduction in combustion time and ignition delay, as well as the presence of GO (which facilitated carbon oxidation), led to effective fuel combustion.

Thermal efficiency of braking

As the study showed, the presence of GO had little effect on brake heat. Typical GO concentrations for improved engine performance showed a 1.4% increase in efficiency for diesel fuel. For biodiesel, there was also an improvement in performance for the indicated GO concentration.

Smoke emissions

In [5] tests, GO there was a 22.33% reduction in smoke emissions at an optimum concentration of 40 ppm. Other concentrations had less effect on smoke. For biodiesel, adding GO had the same effect. The 40 ppm concentration gave the greatest smoke reduction compared to the 20 and 60 ppm concentrations.

The deterioration of emission reduction for higher concentration is explained by particle agglomeration and reduction of GO surface area.

Emissions of nitrogen oxides

Higher reductions in nitrogen oxide emissions were obtained for graphene nanoparticle than for graphene oxide alone. At a concentration of 40 ppm GO, a reduction of 8.5% was achieved for diesel fuel, while for biodiesel blends it amounted to 10.5% and 8.8%, respectively.

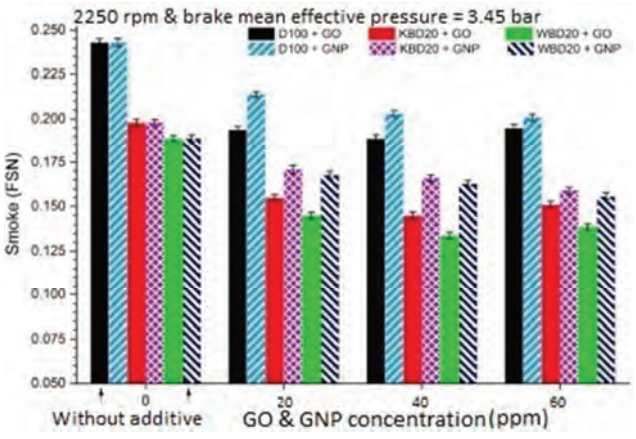

Fig. 10. Variation of smoke emission depending on the concentration GO [5]

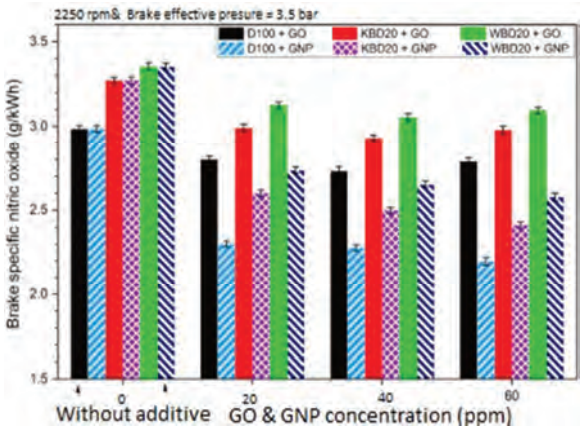

Fig. 11. Variation of NO_x emission depending on the concentration GO [5]

On the other hand, graphene nanoparticle obtained better reduction for diesel, i.e. 26.4%, while for biodiesel blends – 26.3% and 23.1%.

Hydrocarbon emissions

The addition of GO to the fuel contributed to hydrocarbon reduction for all fuels tested (pure diesel and biodiesel blends).

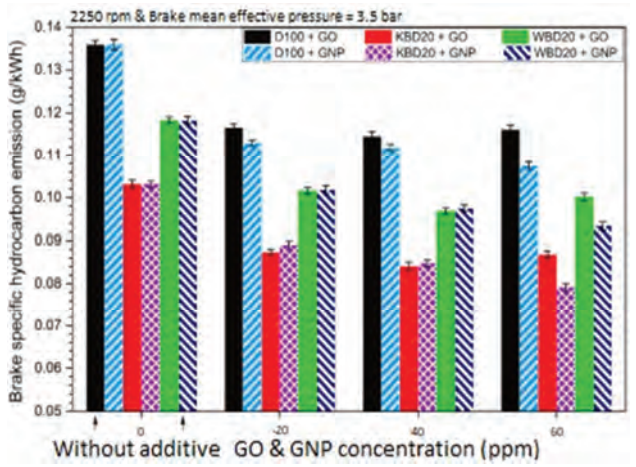

Fig. 12. Variation of HC emission depending on the concentration GO [5]

This phenomenon is explained by the reduced ignition time, which prevents excessive mixing of the fuel and thus results in less unburned hydrocarbons.

Carbon monoxide (CO)

The results of [5] tests showed a reduction in CO emissions under the influence of GO additives in all fuels. The presence of oxygen groups in GO contributes to the oxidation of CO to CO_2.

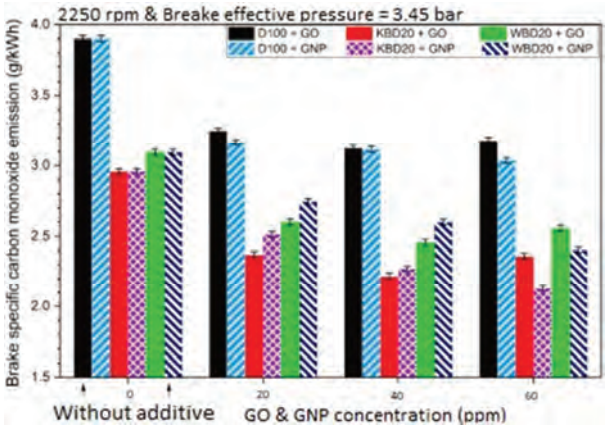

Fig. 13. Variation of CO emission depending on the concentration GO [5]

The maximum reduction reported for 40 ppm GO in the case of diesel is 21.9% while for biodiesel blends it is 27% and 22.7%. Increase in the GO concentration did not cause increase in the reduction, which is explained as in previous results by its ability to agglomerate particles.

Iron oxide and zinc oxide

Adding iron or zinc oxide nanoparticles to the fuel reduces the cohesive forces between the fuel molecules, leading to breakup into smaller droplets. This results in an increase in the momentum of the fuel jet and an increase in fuel penetration into the cylinder. Zinc oxide is non-corrosive, has antioxidant ability, high wear resistance and is inexpensive. In tests conducted by [10], 75% diesel and 25% biodiesel were mixed to form a D75NB25 blend. Iron-zinc nanoxide at 200 ppm was added to the mixture, mixed thoroughly using a magnetic stirrer to form a homogeneous mixture and ultrasonicated. The test was conducted on a two-cylinder diesel engine. A digital contact tachometer was used to measure the engine speed. The test was performed at a constant speed of 1,500 rpm with a variable brake test stand load. Physical properties like density, viscosity and calorific value were tested according to ASTM and IS standard methods. The following results were obtained [10].

Specific fuel consumption during braking

Comparing the results, iron oxide had the greatest effect on fuel consumption. However, the addition of zinc oxide also made a positive contribution to fuel consumption compared to conventional diesel. The reduction in specific fuel consumption is explained by the improved combustion rate and shorter ignition delay time. The addition of nanoparticles contributes to uniform heat distribution during heating, which improves the combustion reaction.

Thermal efficiency of brakes

As reported in [10], the thermal efficiency of brakes increases with increasing load for all fuel samples due to the increase in temperature during combustion. Adding zinc oxide and iron oxide increases the thermal efficiency, which amounts to 35.1% and 34.6% compared to pure diesel where it amounts to 30.12% and 34.23%.

NO_x emissions

Nitrogen oxide emissions were higher for the iron oxide-zinc blends at higher load, while emissions for the biodiesel-diesel blend and pure diesel were lower at higher load compared to the nano additive blends. The higher emission value is a consequence of higher density and higher oxidation capacity.

Emissions of unburned hydrocarbons

The results showed that the unburned hydrocarbon content increases with load. The mixture containing iron-zinc nanoxide had lower emissions than diesel. This phenomenon is explained by a more efficient oxidation reaction. Comparing the two nano additives, iron oxide caused lower emission.

Carbon monoxide emissions

Carbon monoxide emission observations made in [10] are variable over the engine operating load range. Carbon monoxide emissions decrease in the initial range of operation to moderate load. After the moderate value is exceeded, emissions increase. The reduction in CO is due to the poor area of the flame zone and the increase in CO is due to the reduced amount of oxygen available for combustion. Nanoparticles have the ability to catalyze combustion reactions and thus contribute to the reduction of CO emissions.

Smoke emissions

Observations show that iron oxide and zinc oxide nanoparticles contribute to lower smoke emissions compared to diesel. However, iron oxide particles cause the least emissions.

4. Conclusions

Obviously, the analysis presented by the authors does not exhaust the problem, however, the review of literature points to an interesting direction of further research on the possibilities of using nanomaterials as fuel additives. In addition, some discrepancies have been noted regarding the effect of nano-additives, for example, on the reduction of emissions of harmful gases selected pollutants. Selected groups favor this reduction and others do not, or even cause an increase in emissions, such as the use of carbon nanotubes contributes to an increase in emissions of environmentally harmful nitrogen oxides, while the presence of graphene oxide causes their reduction. It is also an interesting observation that groups like titanium oxide and graphene reduce emissions of harmful carbon monoxide by improving fuel combustion from semi-combustion to complete combustion, but in doing so cause an increase in CO_2 emissions, which is in turn a greenhouse gas. The literature analysis also shows that all nanomaterials have a positive effect on the reduction of hydrocarbon emissions, which clearly indicates an improvement in combustion quality and improvement in technical parameters such as specific fuel

consumption, cylinder temperature, exhaust temperature, ignition delay. From the review presented, it can also be seen that most of the studies were conducted on the blends of diesel and biodiesel with the nano additive, and only a few studies show the effect of adding the nanomaterial to pure diesel. Moreover, the literature is dominated by studies on the effects of nanomaterials for diesel fuels, which creates a research gap in the area of gasoline engines and sets a potential direction for further research.

Nomenclature

MWCNTs-COOH	multi-walled carbon nanotubes
CNT	carbon nanotubes
UHC	unburned hydrocarbons
PM	particulate matter
CO	carbon monoxide
CO_2	carbon dioxide
NO_x	nitrogen oxides
TiO_2	titanium dioxide
Ce_2O_3	cerium oxide
Al_2O_3	aluminum oxide

Bibliography

[1] ASMATULU, R., NGUYEN, P., ASMATULU, E. Nanotechnology safety in the automotive industry. *Nanotechnology Safety.* 2013, 57-72. https://doi.org/10.1016/B978-0-444-59438-9.00005-9

[2] AWAD, A.M., JALAB, R., BENAMOR, A. et al. Adsorption of organic pollutants by nanomaterial-based adsorbents: An overview. *Journal of Molecular Liquids*. 2020, **301**, 112335. https://doi.org/10.1016/j.molliq.2019.112335

[3] BOVERHOF, D.R., BRAMANTE, C.M., BUTALA, J.H. et al. Comparative assessment of nanomaterial definitions and safety evaluation considerations. *Regulatory Toxicology and Pharmacology*. 2015, **73**(1), 137-150. https://doi.org/10.1016/j.yrtph.2015.06.001

[4] CAROLL, J.P., FINNAM, J.M. The use of additives and fuel blending to reduce emissions from the combustion of agricultural fuels in small scale boilers. *Biosystems Engineering*. 2015, **129**, 127-133. https://doi.org/10.1016/j.biosystemseng.2014.10.001

[5] CHACKO, N., JEYASEELAN, T. Comparative evaluation of graphene oxide and graphene nanoplatelets as fuel additives on the combustion and emission characteristics of a diesel engine fuelled with diesel and biodiesel blend. *Fuel Processing Technology*. 2020, **204**, 106406. https://doi.org/10.1016/j.fuproc.2020.106406

[6] DAS, R., VECITIS, C.D., SCHULZE, A. et al. Recent advances in nanomaterials for water protection and monitoring. *Chemical Society Reviews*. 2017**, 46**, 6946-7020. https://doi.org/10.1039/C6CS00921B

[7] FAYYAZBAKHSH, A., PIROUZFAR, V. Comprehensive overview on diesel additives to reduce emissions, enhance fuel properties and improve engine performance. *Renewable and Sustainable Energy Reviews*. 2017, **74**, 891-901. https://doi.org/10.1016/j.rser.2017.03.046

[8] JAYARAMAN, J., ISLAMLASKA, I., DEY, K. et al. Investigation on titanium oxide nano particles as additives for operating biodiesel fuelled engine. *Materials Today.* 2021, **44**(5), 3525-3529. https://doi.org/10.1016/j.matpr.2020.09.291

[9] KEGL, T., KRALJ, A.K., KEGL, B. et al. Nanomaterials as fuel additives in diesel engines: A review of current state, opportunities and challenges. *Progress in Energy and Combustion Science*. 2021, **83**, 100897. https://doi.org/10.1016/j.pecs.2020.100897

[10] KHOND, V.W., RAMBHAD, K., RAMBHAD, K. New diesel-neem biodiesel blend (D75NB25) containing nano iron oxide, silicon dioxide and zinc oxide for diesel engine: An experimental investigation *Materials Today*. 2021, **47**(11), 2701-2708. https://doi.org/10.1016/j.matpr.2021.03.004

[11] LOKESH, N., SHAAFI, T. Enhancement of diesel fuel properties: Impact of cerium oxide nano additives on diesel engine performance and emissions. *Materials Today*. https://www.sciencedirect.com/science/article/pii/S2214785320375465

[12] MANOJ, P., KALYAN, B., JAYARAMAN, B. et al. Experimental assessment of alumina nano additives on the performance of C.I. engine fuelled with a high-performance fuel blend. *Materials Today*. 2021, **44**(5), 3544-3549. https://doi.org/10.1016/j.matpr.2020.09.373

[13] FOLTYNOWICZ, Z., CZAJKA, B., MARANDA, A. et al. Aspects of nanomaterials for civil and military applications. Part 2. The use of and concerns arising from infiltration of the natural environment. *Materiały Wysokoenergetyczne/ High Energy Materials*. 2017, **9**, 18-39. https://doi.org/10.22211/matwys/0158 ISSN 2083-0165

[14] GUNDOSHMIAN, T.M., HEIDARI-MALENI, A., JAHANBAKHSHI, A. Evaluation of performance and emission characteristics of a CI engine using functional multi-walled carbon nanotubes (MWCNTs-COOH) additives in biodiesel-diesel blends. *Fuel*. 2021, **287**, 119525. https://doi.org/10.1016/j.fuel.2020.119525

[15] MUVVA, R., SHAAFI, T., ARUNKUMAR, M. Experimental investigation by utilizing nano alumina with waste cooking oil biodiesel fuel in CI engine. *Materials Today*. https://www.sciencedirect.com/science/article/pii/S2214785320377865

[16] SINGH, S., KAPOOR, D., KHASNABIS, S. et al. Mechanism and kinetics of adsorption and removal of heavy metals from wastewater using nanomaterials. *Environmental Chemistry Letters*. 2021, 1-31. https://doi.org/10.1007/s10311-021-01196-w

[17] SOUDAGAR, M.E.M., NIK-GHAZALI, N.N., KALAM, M.A. et al. The effect of nano-additives in diesel-biodiesel fuel blends: A comprehensive review on stability, engine performance and emission characteristics. *Energy Conversion and Management*. 2018, **178**, 146-177. https://doi.org/10.1016/j.enconman.2018.10.019

[18] SUNIL, S., CHANDRA, B.S. Studies on titanium oxide nanoparticles as fuel additive for improving performance and combustion parameters of CI engine fueled with biodiesel blends. *Materials Today*. 2021, **44**(1), 489-499. https://doi.org/10.1016/j.matpr.2020.10.200

[19] WANG, L., SHI, C., WANG, L. et al. Rational design, synthesis, adsorption principles and applications of metal oxide adsorbents: a review. *Nanoscale*. 2020, **12**, 4790-4815. https://doi.org/10.1039/C9NR09274A

[20] WANG, R., LI, X., NIE, Z. et al. Metal/metal oxide nanoparticles-composited porous carbon for high-performance

supercapacitors. *Journal of Energy Storage*. 2021, **38**, 102479. https://doi.org/10.1016/j.est.2021.102479

[21] YU, G., LU, Y., GUO, J. et al. Carbon nanotubes, graphene, and their derivatives for heavy metal removal. *Advanced.* 2018, **1**, 56-78. https://doi.org/10.1007/s42114-017-0004-3

[22] ZHANG, J.J., HAN, L., WANG, J. et al. Graphene-based materials for adsorptive removal of pollutants from water and underlying interaction mechanism. *Advances in Colloid and Interface Science*. 2021, **289**, 102360. https://doi.org/10.1016/j.cis.2021.102360

[23] ZHANG, Z., LU, Y., WANG, Y. et al. Comparative study of using multi-wall carbon nanotube and two different sizes of cerium oxide nanopowders as fuel additives under various diesel engine conditions. *Fuel*. 2019, **256**, 115904. https://doi.org/10.1016/j.fuel.2019.115904

[24] OUYANG, Y., CONG, L.M., CHEN, L. et al. Raman study on single-walled carbon nanotubes and multi-walled carbon nanotubes with different laser excitation energies. *Physica E: Law-dimensional System and Nanostructures.* 2008, **9**, 2386-2389. https://doi.org/10.1016/j.physe.2007.11.008

Agata Jaroń, MEng. – Faculty of New Technologies and Chemistry, Military University of Technology.
e-mail: *a.jaron04@gmail.com*

Grzegorz Sobecki, MEng. – School Battalion, Military University of Technology.
e-mail: *grzegorz.sobecki@wat.edu.pl*

Anna Borucka, DSc., DEng. – Faculty of Safety, Logistics and Management, Military University of Technology.
e-mail: *anna.borucka@wat.edu.pl*

AIR FORCE INSTITUTE OF TECHNOLOGY
INSTYTUT TECHNICZNY WOJSK LOTNICZYCH

ul. Księcia Bolesława 6, 01-494 Warszawa, Poland
tel.: +48 261 851 300; fax: +48 261 851 313
www.itwl.pl e-mail: poczta@itwl.pl

SUPPORTING OPERATIONS & MAINTENANCE OF AERONAUTICAL ENGINEERING:

- tribological diagnostics of lubrication systems in power units and hydraulic systems
- endoscopic examinations of power units
- measurements of operation parameters of power units using one's own and company systems and their analysis

DEVISING AND DEVELOPING NEW DIAGNOSTIC METHODS:

- CT examinations – V/tome/X CT system
- blade vibration measurements using the tip-timing method

NEW TECHNOLOGIES FOR UNMANNED AERIAL VEHICLES:

- technical condition monitoring system of mini jet engine
- hybrid drive of unmanned aerial vehicle

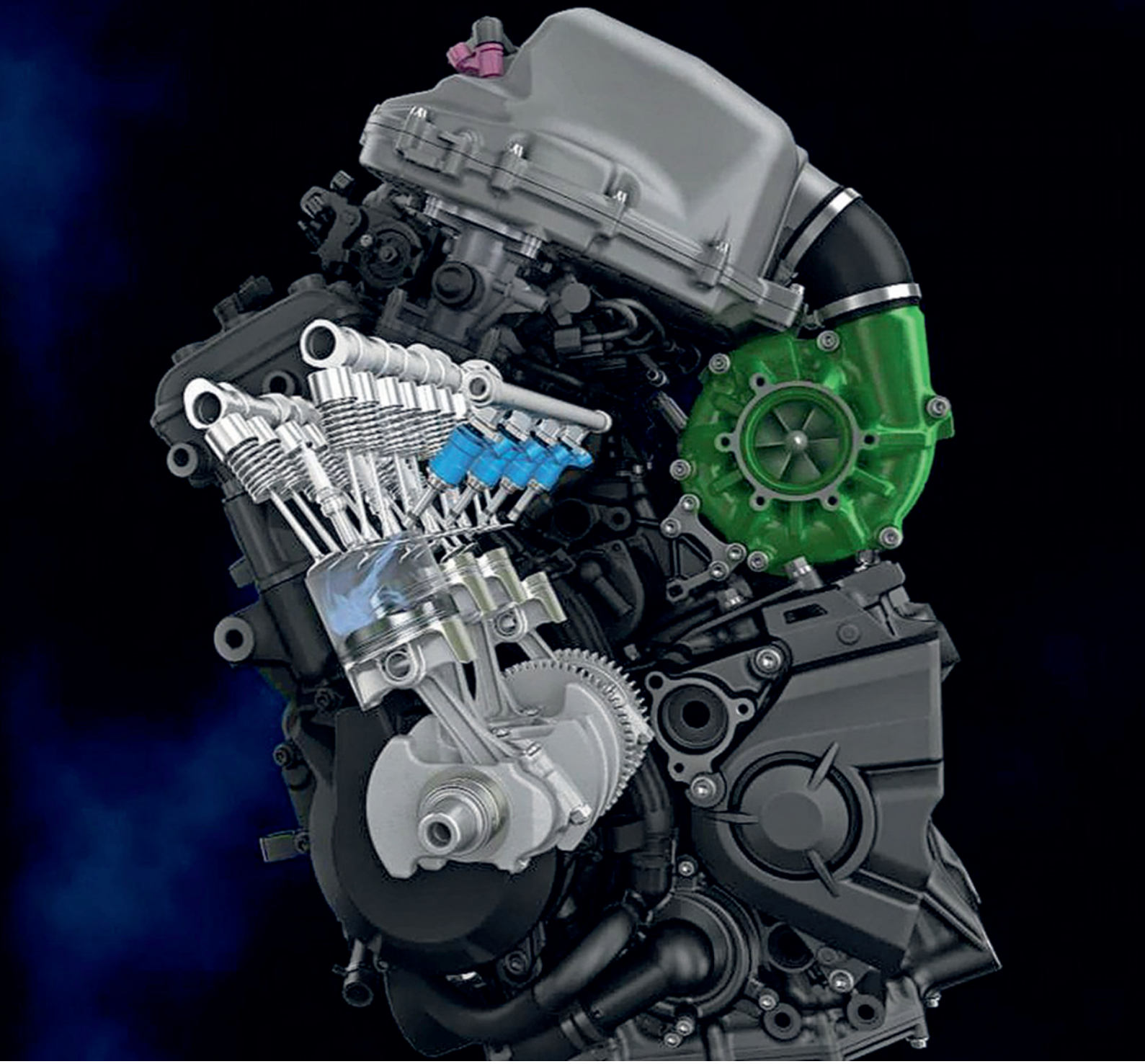

Publisher:

Polish Scientific Society of Combustion Engines

ISSN: 2300-9896
eISSN: 2658-1442

Combustion Engines

Polskie Towarzystwo Naukowe Silników Spalinowych

www.combustion-engines.eu